The Effects of Coarse Aggregate Cleanliness and Moisture Content on Asphalt Concrete Compactability and Moisture Susceptibility

Prepared for

Mississippi Department of Transportation

December 2011

Written and Performed by:

Kevin L. Williams

Isaac L. Howard

L. Allen Cooley, Jr.

Technical Report Documentation Page

1. Report No. FHWA/MS-DOT-RD-11-208	2. Government Accession No.	3. Recipient's Catalog No.	
4. Title and Subtitle The Effects of Coarse Aggregate Cleanliness and Moisture Content on Asphalt Concrete Compactability and Moisture Susceptibility		5. Report Date December 31, 2011	
		6. Performing Organization Code	
7. Author(s) Kevin L. Williams, PE, Staff Materials Engineer, Burns Cooley Dennis, Inc. Isaac L. Howard, PhD, Assistant Professor, Mississippi State University L. Allen Cooley, Jr., PhD, Principal, Burns Cooley Dennis, Inc.		8. Performing Organization Report No.	
9. Performing Organization Name and Address Mississippi State University Burns Cooley Dennis, Inc. Civil and Env. Engineering Dept. 278 Commerce Drive 501 Hardy Road: P O Box 9546 Ridgeland, MS 39157 Mississippi State, MS 39762		10. Work Unit No. (TRAIS)	
		11. Contract or Grant No. SS-208	
12. Sponsoring Agency Name and Address Mississippi Department of Transportation Research Division PO Box 1850 Jackson, MS 39215-1850		13. Type Report and Period Covered Final Report January 11, 2008 to December 31, 2011	
		14. Sponsoring Agency Code	

15. Supplementary Notes: Work performed under Mississippi Department of Transportation (MDOT) State Study 208 titled: *Effects of Coarse Aggregate Cleanliness & Moisture Content on Stripping Susceptibility & Long Term Performance of HMA Mixes*. Mississippi State University (MSU) was the lead institution for the project that was performed under Work Assignment No. MSU 2007-06 and principal investigator Isaac L. Howard. Burns Cooley Dennis, Inc. was a subcontractor to Mississippi State University and performed all field work related to this project.

16. Abstract: Twelve field projects were studied where forty-four locations were evaluated to assess the cause or causes of asphalt concrete that exhibits 'tender zone' characteristics (i.e. instability during compaction) and to investigate the tendency of these mixes to be susceptible to moisture damage over time. Data was collected during construction and samples were taken and used to conduct multiple laboratory tests. All field and laboratory data was used to develop multiple regression equations to predict final in place air voids and moisture susceptibility. The overall conclusion from the research was that compactability appeared to be predicted in a reasonable manner while moisture susceptibility did not. The Methylene Blue test appears promising when used in conjunction with moisture content (cold feed and mix moisture contents were measured) as a means of providing guidance for achieving higher in place density. The tensile strength ratio (TSR) test as performed in this research on laboratory compacted specimens was found to be questionable in terms of its ability to predict field moisture susceptibility.

17. Key Words Stripping, Moisture Damage, Crushed Gravel, TSR, Hamburg, Field Compactability, Accumulated Compaction Pressure, Adhered Fines		18. Distribution Statement Unclassified	
19. Security Classif. (of this report) Unclassified	20. Security Classif. (of this page) Unclassified	21. No. of Pages 158	22. Price

Form DOT F 1700.7 (8-72)   Reproduction of completed page authorized

NOTICE

TABLE OF CONTENTS

LIST OF FIGURES

LIST OF TABLES

ACKNOWLEDGEMENTS

LIST OF VARIABLES

Abs   Water absorption of aggregate by aggregate mass (%)

ACP   Accumulated compaction pressure

ACP_{BD} Percent of the total ACP occurring during breakdown rolling

ACP_i Accumulated compaction pressure to point (i)

ANOVA   Analysis of Variance

APA   Asphalt Pavement Analyzer

a   Regression coefficient for predicting temperature loss

B_i Original dry mass term for adhered fines calculation

BB-1   Bituminous base mixture

b   Regression coefficient for predicting temperature loss

C_i Post washing dry mass for adhered fines calculation

C_1 Slope of accumulated compaction pressure versus V_a plot

C_2 Intercept of accumulated compaction pressure versus V_a plot

CP_{rp} Compaction pressure (pli / contact circular segment)

c   Regression coefficient for predicting temperature loss

D/B   Dust to effective asphalt binder ratio

DOT   Department of Transportation

D_R Dust ration, or actual fines content divided by design fines content

d   Regression coefficient for predicting temperature loss

Δ_8 Gradation difference relative to the maximum density line at the 2.36 mm sieve

ESAL   Equivalent single axle load

ε Random error of multiple regression model

F   Statistic used in ANOVA

FAA   Fine aggregate angularity

F&E   Flat and elongated particles (5:1 length to thickness ratio)

FF   Fractured faces

FF_0 Percentage of particles with 0 fractured faces

FF_1	Percentage of particles with 1 fractured face
FF_2	Percentage of particles with 2 fractured faces
FM	Fineness modulus
G_b	Specific gravity of asphalt binder
GLPA	Gyratory load cell plate assembly
G_{mb}	Bulk specific gravity of a compacted asphalt specimen
G_{mm}	Theoretical maximum specific gravity according to AASHTO T209
% G_{mm}	Percent of theoretical maximum specific gravity achieved
G_{sa}	Apparent specific gravity of aggregate
G_{sb}	Bulk specific gravity of aggregate
G_{se}	Effective specific gravity of aggregate
GVL	Gravel percentage in mixture
HWTD	Hamburg wheel-tracking device
HMA	Hot mixed asphalt
HT	High traffic mixture (e.g. HT 9.5mm); 85 design gyrations
IDT	Indirect tensile test
k	Number of independent variables used in multiple regression
LL	Liquid Limit (AASHTO T89)
LMS	Limestone
LVDT	Linear variable displacement transducer
LWT	Loaded wheel tester
MBV	Methylene blue value
MBV_{SP}	Methylene blue value measured on a gravel stockpile
MBV_{CF}	Methylene blue value measured on a cold feed belt sample
MDOT	Mississippi Department of Transportation
MIST	Moisture Induced Stress Tester
MT	Medium traffic mixture (e.g. MT 9.5 mm): 65 design gyrations
m	Total number of rollers for ACP calculation
NCAT	National Center for Asphalt Technology

NCHRP National Cooperative Highway Research Program

N_{des} Number of design gyrations used in the SGC

NMAS Nominal maximum aggregate size

n Total number of passes of a given roller for ACP calculation

n Number of observations used in multiple regression

p Number of roller passes

p-value Term defining statistical significance

$P_{Adh(\%)-All}$ Adhered fines when entire gradation is considered

$P_{Adh(\%)-5711}$ Adhered fines according to ASTM D5711-95

$P_{Adh(\%)-9.5mm}$ Adhered fines of material greater than 9.5 mm

$P_{Adh(\%)-4.75\,mm}$ Adhered fines of material greater than 4.75 mm but smaller than 9.5 mm

$P_{Adh(\%)-2.36\,mm}$ Adhered fines of material greater than 2.36 mm but smaller than 4.75 mm

$P_{0.075}$ Percent passing 0.075 mm sieve

P_{AC} Total asphalt content based on mix mass (%)

P_b Design asphalt content based on mix mass (%)

$P_{ba(mix)}$ Asphalt absorption based on total mix mass (%)

P_{be} Total effective asphalt binder based on mix mass (%)

$\pm$ PCS Percent above (+) or below (-) the primary control sieve

$P_{F\&E}$ Percentage of flat and elongated particles (%)

PI Plasticity Index

PG Performance grade of asphalt binder

PL Plastic Limit (AASHTO T90)

pli Pounds per linear inch of contact pressure applied by roller

r Type of roller

R^2 Coefficient of determination

R^2_a Adjusted coefficient of determination accounting for *n* and *k*

S Standard Error interpreted as the sample estimate of the standard deviation of ε

SA Total surface area of aggregate (m^2/kg)

SA_8 Surface area of aggregate retained on 2.36 mm (No 8) sieve (m^2/kg)

SC-1	Surface course mixture
SE	Sand equivalency (%)
SEI	Secondary Electron Image
SEM	Scanning Electron Microscope
SGC	Superpave Gyratory Compactor
SIP	Stripping inflection point
SSD	Saturated surface dry
ST	Standard traffic mixture (e.g. ST 9.5mm): 50 design gyrations
S_t	Indirect tensile strength at failure
$S_{t(Dry)}$	Indirect tensile strength at failure of control (i.e. unconditioned) specimen
$S_{t(Wet)}$	Indirect tensile strength at failure of conditioned (i.e. saturated) specimen
t	Thickness of compacted asphalt layer or specimen
T_S	Pavement surface temperature measured with hand held infrared device
T_B	Pavement temperature measured with thermocouple inserted near the bottom of the pavement layer
T_{BD}	Average temperature during breakdown rolling
T_F	Average time of breakdown rolling divided by the recommended cessation time of PaveCool 2.4
T_M	Pavement temperature measured with thermocouple inserted near the middle of the pavement layer
T_U	Pavement temperature measured with thermocouple inserted near the upper portion of the pavement layer
TSR	Tensile strength ratio (%)
V_a	Total air voids of compacted asphalt (%)
$V_{a(P)}$	Percent air voids in laboratory compacted specimens during production
VFA	Voids filled with asphalt
VMA	Voids in mineral aggregate
$w_{CF-\%}$	Cold feed moisture content
$w_{Mix-\%}$	Moisture content of asphalt mixture
WMA	Warm mixed asphalt
x	Time (seconds)

$x_{1..16}$	Independent variables for multiple regression
y	Predicted temperature loss ($^{\circ}$F)
y_p	Dependent or predicted variable from multiple regression
β_0	Constant from multiple regression
$\beta_{1..16}$	Coefficient for independent variables x_1 to x_{16} from multiple regression

CHAPTER 1 – INTRODUCTION

1.1   Introduction and Problem Statement

It has been observed for well over ten years that certain aggregates used in asphalt production, after having been crushed and washed, retain on their surface a very fine coating of what has been described as 'dust' resulting from the crushing operation. It has also been observed that the effects of this 'dust' coating, especially when the aggregates are wet, can be severe enough to cause the asphalt mixture to exhibit 'tender zone' characteristics. These characteristics include instability during the compaction operation (a phenomenon which is normally associated with mix temperature). In these cases, it has been observed that the 'tender zone' characteristics are independent of mix temperature, and that the instability has resulted in air voids over 10% in the field. It is believed that the 'dust' (whether wet or dry) which coats the aggregate prevents adhesion of the hydrated lime and asphalt cement to the aggregate. The result of this lack of adhesion in an asphalt mixture is often durability loss because it will likely have high in-place air voids, and will also be susceptible to premature moisture damage and failure due to the lack of adhesion between the asphalt cement and the aggregate particles.

The Mississippi Department of Transportation (MDOT) sometimes faces the problems discussed in the previous paragraph on a recurring basis, which makes the construction and maintenance of safe, cost effective, and durable pavements a formidable challenge. Aggregate sources and their properties are a key pavements consideration in any state, as aggregate properties are important to the long term durability of paving mixtures. Recent budgetary constraints have only heightened the need for better performing paving materials, which when considered in the context of the aforementioned issues potentially associated with aggregate cleanliness and moisture content form the basis for the research performed in this report.

1.2   Objectives and Scope

The primary objective of this report was to study the cause or causes of tenderness of asphalt mixtures (i.e. instability during compaction) and to investigate the tendency of these mixes to be susceptible to moisture damage over time. To accomplish the primary objective, field and laboratory data were collected that complimented one another and allowed assessment of both tenderness and moisture susceptibility for each project. Field evaluations consisted of monitoring compaction by measuring changes in density and temperature with successive roller passes. Laboratory testing consisted of determining various aggregate blend properties, gravel source properties, and moisture susceptibility of the mixture.

This study evaluated four gravel sources used in asphalt production on a total of twelve paving projects in Mississippi. The asphalt mixtures evaluated consisted of Superpave and Marshall mixtures of various nominal maximum aggregate sizes and were comprised of all gravel or gravel/limestone aggregate blends. Three of the four aggregate

sources were evaluated after rainfall to determine the effects of moisture on compaction. No long term performance data was collected from any of the projects. All assessments made in this report were from samples taken during construction.

CHAPTER 2 - LITERATURE REVIEW

2.1   Overview of Literature Review

This chapter provides a review of past research pertaining to tenderness and moisture susceptibility. Items of particular interest were field compaction data, aggregate tests, causes of moisture related problems, and moisture susceptibility testing.   The review is organized by topic.

2.2   Field Compaction

2.2.1   Fabricio and West (2008)

Research was conducted at the National Center for Asphalt Technology (NCAT) to determine factors that affect hot mixed asphalt (HMA) field compaction and quantify applied compactive effort based on NCAT test track data from 2000 and 2003. Factors identified as affecting HMA field compaction were aggregate type, gradation, environmental conditions, asphalt binder characteristics, compaction equipment, roller operation, and lift thickness.

It was determined that aggregates with rough surface texture, cubical or block shaped particles, and highly angular particles require increased compactive effort. Researchers also determined that in general, asphalt mixtures with higher fines content were more difficult to compact than mixtures with lower fines content.

Environmental conditions that affect HMA field compaction were identified as underlying surface temperature, ambient temperature, and wind speed.   These environmental conditions affect the mixture temperature by controlling the rate of cooling of the HMA layer. The viscosity of the asphalt binder is directly related to mixture temperature. As mixture temperature increases, the asphalt binder viscosity decreases, reducing the required compactive effort. The longer the environmental factors allow the HMA temperature to remain within an optimum compaction temperature range, the more time the construction crew has to achieve required density.

Compaction equipment and roller operation were identified as important factors affecting HMA field compaction. Compaction is accomplished by three basic pieces of equipment: the paver screed, steel wheeled rollers, and pneumatic rollers. The roller type and operational characteristics (mass, dynamic force, wheel load and tire pressure) affect compaction. Roller speed is important in that lower roller speed decreases the shear rate of the mix which allows the aggregate to rearrange into more dense configurations. Earlier passes over hotter HMA will increase the change in density more than later passes at lower temperatures.

The researchers defined Accumulated Compaction Pressure (ACP) to quantify the total compactive effort applied to the HMA mat. ACP was defined as the summation of pressure applied by each pass of each roller in the field compaction process. ACP is calculated using Eq. 2.1, and a summary of the method is provided.

$$ACP = \sum_{r=1}^{m} \sum_{p=1}^{n} CP_{rp} \qquad (2.1)$$

Where,

r = roller type
p = pass number
CP_{rp} = compaction pressure (pli / contact circular segment)

For static steel wheel rollers, pli is the gross weight of the roller divided by the combined width of the drums. For vibratory rollers, pli is the sum of the centrifugal force of the vibrating drums and the gross weight divided by the width of the drums. The compaction pressure for static or vibratory steel wheel rollers is determined by dividing the pli by the small contact circular segment or arc where the drums are in contact with the HMA mat. The contact arc decreases during the first few roller passes, then will be nearly constant after the third pass. For pneumatic rollers, the contact pressure is assumed to be equal to the tire pressure.

ACP was calculated for HMA on the NCAT test track in 2000 and 2003. The total ACP for each mix was analyzed using factors known to affect compaction: gradation type, lift thickness (t), nominal maximum aggregate size (NMAS), t/NMAS, mixture temperature, and asphalt grade. Analysis showed only t/NMAS and mixture temperature had a significant effect on ACP.

2.2.2 Cooley and Williams (2009)

Field research evaluated lift thickness influences on the ability to achieve desirable in-place density with a reasonable compactive effort. Ten paving projects in Mississippi were studied (five with 9.5 mm NMAS and five with 12.5 mm NMAS). Testing included monitoring of HMA compaction by measuring density following each roller pass, measuring temperature at four locations (surface, top, middle, and bottom of the layer) and obtaining compaction equipment and environmental information.

Lift thickness effects on temperature were addressed by normalizing the data to 0 at time 0 and evaluating the change in temperature (decrease in temperature being positive) with the Morgan-Mercer-Flodian (MMF) model shown in Eq 2.2.

$$y = \frac{ab + cx^{d}}{b + x^{d}} \qquad (2.2)$$

Where,

y = predicted temperature loss (^{o}F)
x = time (seconds)
a, b, c, d = regression coefficients

Typical parameters reported using the Eq. 2.2 model were: $a = -0.2892$; $b = 128.03$; $c = 180.44$; $d = 0.7090$; $R^2 = 0.95$. Thicker layers were shown to generally maintain temperature for longer periods compared to thinner layers.

Multiple regression led to the model shown in Eq 2.3. An analysis of variance (ANOVA) was performed and the p-value was 0.000 indicating the model was significant at a 95% confidence level. The coefficient of determination (R^2) of the model was 0.58.

$$\% \, G_{mm} = 7.6e^{-5}(\text{ACP})(P_{0.075}) + 3.4e^{-3}(T_M)(t/\text{NMAS}) + 4.2e^{-2}(V_{a(P)})(\pm \text{PCS}) \qquad (2.3)$$

Where,

$\% \, G_{mm}$ = percent of theoretical maximum specific gravity achieved during compaction
ACP = accumulated compaction pressure defined in Eq. 2.1 with units of psi
$P_{0.075}$ = fines content
T_M = temperature near the middle of the asphalt layer with units of ^{o}F
t/NMAS = layer thickness divided by nominal maximum aggregate size
$V_{a(P)}$ = percent air voids in laboratory compacted specimens during production
$\pm$ PCS = percent above (+ or finer) or below (- or coarser) the primary control sieve

Sensitivity analysis investigated each variable while holding all other variables to their average values. Effects of Eq. 2.3 inputs on $\% \, G_{mm}$ within the range of values considered in the sensitivity analysis are summarized in the following list. All terms but $P_{0.075}$ had a practically meaningful effect on $\% \, G_{mm}$.

- ACP   approximately 2% change in $\% \, G_{mm}$ (higher ACP, higher $\% \, G_{mm}$)
- $P_{0.075}$ approximately 0.2% change in $\% \, G_{mm}$ (higher $P_{0.075}$, higher $\% \, G_{mm}$)
- T_M just under 2% change in $\% \, G_{mm}$ (higher T_M, higher $\% \, G_{mm}$)
- t/NMAS approximately 3% change in $\% \, G_{mm}$ (higher t/NMAS, higher $\% \, G_{mm}$)
- $V_{a(P)}$ just over 2% change in $\% \, G_{mm}$ (higher $V_{a(P)}$, lower $\% \, G_{mm}$)
- $\pm$ PCS   approximately 3.5% change in $\% \, G_{mm}$ (+ or finer mixes, higher $\% \, G_{mm}$)

2.2.3   US Army Corps of Engineers (2000)

Some tender asphalt mixtures exhibit a surface defect known as check cracking. Checking is defined as short transverse cracks, usually 2.5 to 7.6 cm long and 2.5 to 7.6 cm apart, which occur in the pavement surface at some time during the compaction process. If checking is going to occur, it usually occurs when the HMA mat temperature is less than 116°C and additional passes of a vibratory or static steel wheel roller are applied over the mat. Check cracking does not normally occur during compaction with a pneumatic tire roller.

Check cracking is primarily caused by either excessive deflection of the underlying pavement layers due to the compaction equipment or one or more deficiencies in the asphalt mix design. A mixture that exhibits tender characteristics is not internally stable enough to support compaction equipment. Mix design issues are the more

common cause of checking and include excess asphalt cement or moisture in the mixture, too much midsize sand material and too little fine sand material, and a lack of room in the aggregate gradation for the asphalt cement (low voids in mineral aggregate, or VMA).

Checking is detrimental to long-term pavement performance because the tender mix characteristics affect the in-place density. Density can be significantly reduced if compaction is accomplished further back behind the paver when the mix has cooled in an attempt to reduce checking. A mix that contains check cracks will typically lack density and have a reduced pavement life.

2.2.4 Brown et al. (2004)

The authors reported that several studies have reported a t/NMAS ratio of 4 is preferred rather than the most commonly used minimum value of 3. It has been found that the pavement density that can be obtained under normal rolling conditions is clearly related to the t/NMAS ratio. It was recommended that the t/NMAS ratio be at least 3 for fine-graded mixes and at least 4 for coarse-graded mixes. It was reported that ratios less than these suggested values can be used but that the consequence is a greater than normal compactive effort. In most cases, a t/NMAS of 5 does not result in the need for additional compaction to obtain the desired density. It was noted that care must be exercised with lift thicknesses that become too large in the context of achieving adequate density. Rapid cooling of thinner mats was indicated to be one of the reasons for low density of thinner sections.

2.2.5 Brown (1984)

The author describes tenderness as follows. When the asphalt temperature is too high a tender mix will not adequately support compaction equipment without excessive lateral movement, which requires delays while the mix cools. Variable thicknesses are especially problematic in these situations as part of the mix is too hot and part is too cold. Mix temperatures should allow roller support immediately behind the paver. Tender mixes can be caused by high mix temperatures (most popular), poor aggregate gradation, asphalt type, or aggregate type. Experience has shown that most mixtures should be placed at a temperature between 121$^{\mathrm{o}}$C and 149$^{\mathrm{o}}$C, and that temperature adjustments may be needed in the field.

2.2.6 Brown et al. (2000)

The authors reported that tenderness is observed on a small percentage of projects. These mixes tend to move laterally when rolled. Excessive sand in the mix can result in tenderness. Superpave mixes are often coarse graded (below restricted zone). NAPA surveys and contractor feedback resulted in the assessment that approximately 40 percent of coarse-graded Superpave mixes experience some tenderness. The authors reported that most information indicated tender mixes experienced tenderness between 82$^{\mathrm{o}}$C and 116$^{\mathrm{o}}$C and that tender mixes behave normally outside this range. Mixes that are

tender normally move 5.1 to 10.2 mm laterally and can move 30.5 cm laterally in severe tenderness cases. According to the authors, "When tender mixes occur, typically, the mix can be rolled for 1-2 or more passes with a steel wheel roller before the mix begins to move laterally." Tender mixes may be caused by a number of factors, therefore, it is difficult to present a general mechanism describing all cases of tender mixes. Excessive temperature was also reported to cause tenderness in some cases, alongside a host of other factors. If the problem of rubber tire rollers picking up aggregate can be addressed, tender zone problems can be handled very effectively with rubber tire rollers. The authors report that tenderness appears to occur more often with Superpave mixes.

2.2.7   Buchanan and Cooley (2003)

A study of field projects failed to clearly identify one particular reason for the tender zone occurrence. Five projects were evaluated in three southeastern states (one project in Mississippi). The Mississippi project began to push laterally and in front of the roller below approximately 118°C. It was stated the contractor observed this behavior throughout construction. The contractor was able to finish their rolling at approximately 66 to 71°C surface temperatures. Pneumatic rollers were not used due to past material pick up experiences. One observation was each paving project has its own set of weather, mix, and construction characteristics, which in the words of the authors makes determining causes for the tender zone an extremely difficult task. The tender zone generally occurred at approximately 110 to 60°C. No mix parameter could be singled out as directly causing tenderness. Very short haul times and mixture storage times resulted in overasphalted behavior for the high absorption aggregates tested. It was stated that, in general, the mixture should be placed at a temperature as low as possible while still being able to achieve density to achieve stiffness and result in less tenderness.

2.3   Aggregate Properties and Testing

2.3.1   Tarrer and Wagh (1991)

The authors conducted a review of literature and presented several aggregate characteristics that affect asphalt-aggregate bond strength. Included among these factors are: mineralogy, chemical composition, adsorbed coatings, surface texture and porosity, weathering, and surface moisture.

The mineralogical and chemical composition of an aggregate not only influences its surface energy and its chemical reactivity, but also accounts for the presence of adsorbed coatings on the aggregate surface. Surface energy and chemical reactivity dictate whether an aggregate will be hydrophilic or hydrophobic. Adsorbed coatings that have been found on the surface of aggregates such as clay, silt, dust coatings from crushing, ferruginous coatings (on gravel), oil, fatty acids, oxygen and water are related to mineralogical and chemical composition. Some adsorbed coatings such as clay, silt, dust from crushing, and water can be detrimental in regard to moisture susceptibility.

7

Ferruginous coatings, oil, and fatty acids have been found to increase resistance to stripping.

Surface texture and porosity affect the amount of asphalt cement that is absorbed into the aggregate particles. An aggregate with a porous, slightly rough surface will promote adhesion by providing mechanical interlock between the asphalt cement and aggregate surface. Aggregates having large surface pores appear to exhibit stronger bonds with asphalt cement.

Weathered aggregates have been known to exhibit a greater resistance to stripping compared to newly crushed aggregates. This may be due to the outermost layer of adsorbed water molecules being partially replaced or covered by organic contaminants present in the air. These contaminants, such as fatty acids and oils, increase the resistance to stripping.

Aggregates with a dry surface adhere better to asphalt and resist stripping more than damp or wet aggregates. Heating aggregates such that free water and the outermost adsorbed water molecules are removed causes the interfacial tension between the asphalt and the aggregate surface to decrease. This results in a decrease in the stripping potential. Also, asphalt adheres better to hot aggregate as opposed to cold aggregate.

2.3.2   Lee et al. (1990)

A literature review was conducted to determine the state of knowledge with respect to aggregate absorption, including how aggregate properties influence absorption, how absorption can best be determined, and how asphalt properties influence absorption. Asphalt absorption may contribute to premature pavement failure though mechanisms such as moisture damage, accelerated aging, and cracking due to its effects on the remaining effective asphalt film. Asphalt absorption to some degree is thought to improve strength in compacted mixtures due to mechanical interlocking; however, the portion of absorbed asphalt is not available for binding the aggregate particles together. The literature review identified the following conclusions concerning absorption:

1. Asphalt absorption is directly related to aggregate porosity. The total porosity is an indicator for the maximum possible absorption, but the actual pore size determines the rate of absorption.
2. Aggregate particle size and shape has an effect on the rate of absorption, with smaller aggregate particles being filled at a faster rate.
3. The amount of absorption is directly proportional to capillary pressure and time and inversely proportional to viscosity.
4. The amount of absorption has been found to decrease as asphalt viscosity increases.
5. Asphalt absorption is time dependent with the majority occurring during the first ten to thirty days and leveling off at about three months. Percent absorption increases with time at a decreasing rate.

2.3.3   Lee (1969)

Asphalt absorption by aggregates affects, directly and indirectly, mixture design, moisture susceptibility, and the durability of an asphalt mixture film. Among the effects aggregate absorption has on premature pavement failure, the author listed the following:

1. A reduction in asphalt film thickness, resulting in a mixture susceptible to weathering stresses and prone to raveling and cracking.
2. Not enough binder, resulting in a moisture susceptible mixture.
3. Changes to the physical and chemical properties of the effective asphalt binder, possibly resulting in low temperature cracking and premature aging.

A standard test method does not exist which can evaluate, describe, and specify the absorptive characteristics of an aggregate with respect to asphalt. Some methods which indicate aggregate absorption based on water or other fluids do exist. The immersion method can be used to evaluate the potential asphalt absorption. The bulk-impregnated specific gravity method can be used to determine the practical maximum asphalt absorption. The Rice method for theoretical maximum specific gravity can be utilized to determine the practical minimum asphalt absorption. These methods all have disadvantages and limitations.

2.3.4   Aschenbrener (1992)

In this study, seventeen of Colorado's most frequently used aggregate sources were evaluated to identify differences between aggregates as measured by and compared to some European test methods and specifications. The methylene blue test was used to evaluate material passing the 0.075 mm (No. 200) sieve ($P_{0.075}$). The test method and specification used in this study was based upon the International Slurry Surfacing Association, Technical Bulletin No. 145. The purpose of the test is to identify the amount of harmful clays of the smectite group and to provide an indication of the surface activity of the aggregate.

The test results showed that the methylene blue value (MBV) and the sand equivalent tests provided comparable results in characterizing $P_{0.075}$ material as moisture susceptible. Aschenbrener concluded that for tests that fail performance-related moisture susceptibility testing, both the methylene blue and sand equivalent tests are indicators that can provide valuable information for potential improvement of the HMA.

2.3.5   Kandhal et al. (1998)

This study was conducted to determine the best aggregate test method that indicates the presence of detrimental plastic fines in fine aggregate, which may lead to stripping in hot mix asphalt. Ten fine aggregate sources were evaluated by sand equivalent value, plasticity index (PI), and MBV. Ten mixtures containing each fine aggregate source blended with a common limestone coarse aggregate were evaluated for

moisture susceptibility based upon tensile strength ratio (AASHTO T 283) and the Hamburg wheel-tracking device. Statistical analysis showed that tensile strength ratio (TSR) and stripping inflection point (SIP) results were best related to log MBV. Eq. 2.4 shows the regression equation presented by the authors (R^2=0.63, p-value=0.006).

$$TSR = 70.277 - 6.84(Log\ MBV) \tag{2.4}$$

2.3.6 Kandhal and Parker (1998)

The authors conducted an extensive literature review to identify HMA performance parameters affected by aggregate properties. The following performance parameters were identified as being affected by aggregate properties:

1. Permanent deformation (rutting or moisture damage)
2. Degradation (raveling, popouts, or potholing);
3. Fatigue cracking; and
4. Frictional resistance.

Included in the literature review was an evaluation of how aggregate properties affect HMA performance parameters. The following are aggregate properties identified as having influence on HMA performance:

1. Gradation size;
2. Particle shape, angularity, and surface texture;
3. Porosity or absorption;
4. Cleanliness and deleterious materials;
5. Toughness and abrasion resistance;
6. Durability and soundness;
7. Expansive characteristics;
8. Polish and frictional characteristics;
9. Mineralogy and petrography; and
10. Chemical properties.

Laboratory testing was conducted on nine coarse and nine fine aggregate sources to evaluate the aggregate properties identified above. The researchers recommended the following nine aggregate tests for evaluating aggregates for use in HMA pavement:

1. Sieve Analysis of Aggregates for Determining Gradation and Size (permanent deformation and fatigue cracking);
2. Uncompacted Void Content of Coarse Aggregate (permanent deformation and fatigue cracking);
3. Flat or Elongated Particles (2:1 ratio) in Coarse Aggregate (permanent deformation and fatigue cracking);
4. Uncompacted Void Content of Fine Aggregate (permanent deformation);

5. Methylene Blue test – performed on $P_{0.075}$ from parent rock (permanent deformation resulting from stripping);
6. Methylene Blue test – performed on $P_{0.075}$ from baghouse fines and fillers (permanent deformation resulting from stripping);
7. Gradation of $P_{0.075}$ Material – particle size in microns corresponding to 60 and 10 percent passing (permanent deformation resulting from traffic loads as well as stripping);
8. Micro-Deval test (raveling, popouts, or potholes); and
9. Magnesium Sulfate Soundness test (raveling, popouts, or potholes).

2.3.7   White et al. (2006)

Research was conducted to validate aggregate tests identified in NCHRP Report 405 as being related to and predictors of HMA performance. One of the nine tests evaluated in this study was the methylene blue test. Five mixtures were prepared utilizing one coarse aggregate source and five fine aggregate sources. Methylene blue testing was conducted on the $P_{0.075}$ material from the aggregate blends. MBV values obtained from the blends ranged from 0.5 to 8.0. Results were compared to TSR results of pavement cores tested in accordance with AASHTO T283 with one freeze-thaw cycle. The researchers concluded there was somewhat of a relationship between MBV and TSR, but the relationship was not strong and appeared to be affected by the amount of $P_{0.075}$ material in the mixture.

2.4   Hamburg Wheel Tracking Device

2.4.1   Aschenbrener (1995)

The Hamburg wheel-tracking device (HWTD) was evaluated to determine factors influencing test results. Twenty asphalt mixtures representing field performance ranging from good to those that failed within one year of service were evaluated. Two HMA slabs measuring 25.9 cm wide, 32.0 cm long, and 4.1 cm thick were tested simultaneously. The slabs were compacted to 7 ± 1 percent air voids and submerged under water at 50˚C. A 4.7 cm wide steel wheel loaded at 71.7 kg passed over the specimens at a rate of 50 passes per minute. Each specimen was loaded for 20,000 passes or until 20 mm of rut depth occurred.

The city of Hamburg, Germany, where the HWTD is manufactured, specifies a maximum rut depth of 4 mm after 20,000 passes. Previous research in Colorado found the Hamburg specification to be severe for pavements in that state and proposed that a rut depth of less than 10 mm after 20,000 passes would be more reasonable.

Test results produced by the HWTD include creep slope, stripping slope, and stripping inflection point. Creep slope is defined as the inverse of the rate of deformation in the linear region of the deformation curve, after post compaction and prior to stripping. Creep slope relates to rutting due to plastic flow. Stripping slope is defined as the inverse of the rate of deformation in the linear region of the deformation curve, after stripping

begins until completion of the test. Stripping slope is related to the severity of moisture damage. Stripping inflection point is the number of passes at the intersection of the creep slope and stripping slope. Stripping inflection point is related to resistance of the HMA to moisture damage.

Mixtures of known field performance were tested in the HWTD. The resulting stripping inflection point was found to correlate well with known field performance. Pavements categorized as good performers had stripping inflection points greater than 10,000 passes. High maintenance pavements had stripping inflection points between 5,000 and 10,000 passes. Poor performing pavements had stripping inflection points less than 3,000 passes. The HWTD was found to have the potential to discriminate between pavements of varying field stripping performance.

Laboratory tests were conducted on aggregates utilized in the mixtures to determine the presence of clay as identified by the Methylene blue test, dust to asphalt binder ratio, and adherent fines content of material retained on the 4.75 mm sieve. Researchers found that materials that passed all three tests had good performance in the field and in the HWTD. Materials that failed two of the three tests were unlikely to have good performance in the field or the HWTD.

Researchers also concluded that the HWTD is sensitive to: asphalt binder stiffness (performance grade, or PG), test temperature, amount of short-term aging, refining process and crude oil source, use of liquid anti-stripping agent in some cases, use of hydrated lime, and compaction temperature.

2.4.2   Izzo and Tahunoressi (1999)

This study was conducted to evaluate the HWTD and its potential use in assessing HMA moisture susceptibility. The study included a test device repeatability evaluation, comparison of rectangular slab specimens versus cylindrical specimens compacted in the Superpave gyratory compactor (SGC), and an inter-laboratory evaluation of the effects of temperature and anti-stripping additives.

Researchers determined that the HWTD was repeatable among test replicates. Repeatability of test results was not affected by different compaction methods or HMA type. It was concluded that specimens molded in the SGC could be used for moisture evaluation with the HWTD in the comparative evaluation of one material to another. A correlation could not be developed between rectangular slab specimens and cylindrical specimens due to variability of the test results. Therefore, rectangular slab specimens should not be directly compared to cylindrical specimens.

2.4.3   Cooley et al. (2000)

A literature review was conducted to provide information on loaded wheel testers (LWT) used in the United States in which key test parameters found to affect LWT test results were discussed. A review of operating specifications revealed that air voids and test temperatures are two test parameters that are always specified. These parameters were found to have the greatest effect on test results, in particular rut depth. Several

studies have shown that as air voids and test temperatures increase, rut depths also increase. Sample type and compaction method (cylindrical versus beam/slab) can significantly affect test results, though the two sample types have been found to rank mixes similarly. Other parameters reported to affect test results are short-term aging time, conditioning time prior to testing, and the magnitude of loading.

2.4.4 Manandhar et al. (2011)

In this study, researchers evaluated the HWTD and the Asphalt Pavement Analyzer (APA) to determine a rapid test method for evaluating moisture susceptibility. Six plant mixtures were obtained and evaluated in the HWTD and the APA (submerged). The HWTD results showed more stripping in mixtures without antistripping additives compared to those with additives. The HWTD was better than the APA at indicating stripping potential when an antistripping agent was added.

The HWTD was then evaluated at various test temperatures and wheel loading. Six 12.5mm NMAS mixtures were tested at 50°C and 60°C at loads of 71.7, 76.2, 80.7, 85.3 and 89.8 kg. Cylindrical specimens were prepared using the SGC and tested in the HWTD. Prediction models were developed for the six mixtures using HWTD results and the LIFEREG procedure (statistical analysis based on a Newton-Raphson algorithm). Roadway cores were obtained from three projects from which plant produced mix was obtained. The cores were tested in the HWTD and results were compared to the prediction models. The HWTD showed good consistency between the pavement cores and the prediction models when a higher test temperature of 60°C and load levels of 71.7, 76.2 and 80.7 kg were used. It was concluded that the test duration of the HWTD could be reduced from approximately six hours to two hours or less using accelerated mix testing (statistical) models for Superpave mixtures of 12.5 mm NMAS and a binder grade of PG 64-22.

2.4.5 Yildirim and Stokoe (2006)

This research project was conducted to determine the correlation of asphalt pavement field performance to HWTD test results. Three mix design methods and three aggregate types were utilized for a total of nine mixtures. Test sections were placed with each mixture on Interstate Highway 20. Visual inspections were conducted and performance data were gathered over a five year period. For this study pavement cores were tested in the HWTD at 50°C for up to 20,000 passes or a rut depth of 12.5 mm. The HWTD results were correlated to ESALs/mm and compared to field rut data using the dipstick profilometer.

No moisture induced damage was observed in the pavement cores tested in the HWTD. Since there were no measured stripping inflection point or stripping slope, mixtures were evaluated based upon post compaction points (generally the rut depth at 1,000 passes), rut depths at various points, and creep slope. The HWTD results were confirmed by no moisture induced damage being observed in the test sections during the five year observation period. Therefore, researchers concluded that similar types of

deformation patterns could be assumed for both field test sections and lab specimens tested in the HWTD. It was found that rutting observed in the field test sections was minor compared to rutting observed from the HWTD.

2.5   Moisture Sensitivity

2.5.1   Little and Jones (2003)

The authors defined moisture damage as the loss of strength and durability in asphalt mixtures due to the effects of moisture. Moisture damage can occur due to a loss of bond between the asphalt cement or mastic and the fine and coarse aggregate. Moisture damage also occurs due to moisture which permeates and weakens the mastic, making it more susceptible to moisture during cyclic loading.

2.5.2   Hicks et al. (2003)

The authors identified several factors that contribute to moisture sensitivity problems in asphalt pavements. These factors include: moisture-sensitive aggregates, asphalt binder sensitivity, presence of water and traffic, pavement design considerations, material issues, and construction issues. Aggregates can influence moisture sensitivity due to their surface chemistry and the presence of clay fines, which affect the adhesive bond between the aggregate and asphalt binder. The chemistry, stiffness, and processing techniques of asphalt binder influence adhesion with the aggregate and cohesive strength. Moisture and traffic provide the energy required to break the adhesive bonds and cause cohesive failures. Some pavement design flaws trap moisture in the pavement layers. Material production issues such as asphalt binder refining methods, aggregate cleanliness, moisture content and hardness, and mixture handling can influence moisture sensitivity. Weather conditions, segregation, joint construction, compaction, and control of additives were identified as construction issues that may affect moisture sensitivity.

2.5.3   Kandhal (1992)

Excessive dust coating on aggregate was identified as being one of several external factors responsible for inducing premature stripping. The asphalt cement coats the fine dust particles and is not in contact with the aggregate surface. It has also been hypothesized that some very fine clayey material may cause stripping by emulsifying the asphalt cement binder in the presence of water, but this appears to be an insignificant and uncommon factor. One project was referenced on which stripping occurred by hydraulic scouring. The aggregate used on the project was one which had excessive amounts of dust coating. The stripping problem was resolved by washing the aggregate at the quarry.

2.6   Moisture Susceptibility Testing

2.6.1   Kandhal (1992)

Factors which induce stripping in HMA pavements were discussed. The study recommended an investigative methodology to establish stripping as a problem on a specific HMA project or over a broad area. A review of practices for specifying antistripping agents, test methods and acceptance criteria was presented.

A review of the boiling water test method (ASTM D3625) which is similar to MDOT MT-59 to determine the percentage of retained asphalt binder after boiling by visual inspection was presented. Advantages of the test method were listed as: useful for initial screening, minimum amount of equipment required, can be used to test additive effectiveness, may be used for quality control, and can use laboratory or plant produced mix. Some disadvantages of the test method include: subjective analysis, test performed on uncompacted mix, water purity can affect coating retention, assessment of stripping in fines is difficult, highly dependent on asphalt viscosity, does not coincide with field experience, and generally favors liquid antistripping agents over lime.

A review of ASTM D4867 Indirect Tensile Test with Tunnicliff and Root Conditioning was presented, which is similar to MDOT MT-63. Advantages of this test method include: laboratory or plant produced mix or cores from existing pavements can be tested, may evaluate mixtures with or without additives, time required is moderate, initial indications showed good correlation based on 80 percent retained strength. The disadvantages of this test method include: may require trial specimens to obtain air void level or degree of saturation, may not be severe enough (major limitation).

Other test methods reviewed include Lottman (NCHRP 246), Modified Lottman (AASHTO T283) and Immersion-Compression (AASHTO T165). A wide range of test methods were stated to be used by various agencies. However, no one laboratory test procedure has been proven to be "superior" and able to identify moisture susceptible mixtures in all cases.

2.6.2   Parker and Gharaybeh (1988)

In this study, an evaluation of the boil, indirect tensile, and stress pedestal tests were evaluated using surface and base-binder course mixtures. The boil test was performed in accordance with ASTM D3625. Two indirect tensile procedures were performed, one similar to the Tunnicliff-Root procedure and the other similar to the Modified Lottman procedure. The stress pedestal test was an adaptation of a test proposed by Laramie Energy Technology Center and performed in accordance to procedures recommended by Kennedy et al. (1982). Aggregate materials used were selected based on historical field performance ranging from good to poor.

It was concluded that a pass-fail criterion, according to which all reported moisture susceptible mixes fail and all reported moisture resistant mixes pass, could not be developed for any of the methods evaluated. The test methods correctly identified only three of the five mixtures evaluated according to reported field performance. It was

determined that either the tests may not be valid indicators of stripping, or the subjectively reported field performance may not have been valid for specific mixtures. Variability in gradation, asphalt content, drying, mixing, and compaction may significantly affect the potential for a mixture to strip. Laboratory tests on carefully controlled samples may not be sufficiently severe. It was also determined that base-binder mixtures are more susceptible to moisture damage than surface mixtures utilizing the same constituents due to reduced asphalt content (film thickness) and the nature of air voids due to gradation.

2.6.3 Kennedy and Huber (1985)

A series of field experiments were conducted to evaluate the engineering properties of HMA produced with a range of stockpile moisture contents and a range of mixing temperatures utilizing both batch and drum plants. The study was conducted at four asphalt plants utilizing three mix designs composed of limestone and sandstone aggregates. Stockpile moisture contents were categorized as dry, wet, or saturated. The plant mixing temperatures ranged from 79.4°C to 162.8°C. HMA samples were obtained from haul trucks at the plant site and tested to determine moisture content utilizing a convection oven at a temperature of 121°C. Specimens were compacted in the field laboratory that were made from the aforementioned samples. Three different compaction procedures were utilized to produce test specimens including: compaction at 121°C, compaction at the plant mixing temperature, and compaction at the plant mixing temperature targeting 7 percent air voids. Compacted specimens were tested to determine Hveem stability, tensile strength, resilient modulus, and moisture susceptibility characteristics.

Researchers found that the HMA moisture content was influenced by the stockpile moisture content, the mixing temperature, and the aggregate porosity. The moisture data showed that for mixing temperatures of 79.4°C, 107.2°C, and 121.1°C, the HMA moisture content was greatly affected by stockpile moisture content and mixing temperature in both the batch and drum plants. At mixing temperatures of 135°C and 162.8°C, both the batch and drum plants were effective in drying most or all of the moisture from the stockpile aggregates although drying resulted in higher fuel cost and lower production.

Researchers found compactive effort to have the most significant affect on tensile strength test results. The researchers determined that TSR increased slightly with increasing stockpile moisture content. However, observations of TSR data seem to indicate that the authors' findings were influenced greatly by compactive effort, compaction temperature (possible loss of moisture while heating to compaction temperature), and test variability.

The retained asphalt, as quantified by the Texas boiling test, was found to increase as stockpile moisture increased indicating a higher resistance to moisture damage. There was also an indication from the boiling test that resistance to moisture damaged improved as mixing temperature increased.

2.6.4 Huber et al. (2002)

Research was conducted to determine if the tender mix behavior exhibited particularly by some coarse-graded Superpave mixtures was related to moisture content and to develop procedures to accurately measure HMA moisture content. The initial research included an evaluation of various sample containers for storing the HMA and the evaluation of moisture determination methods. The researchers concluded that sealed 1 gallon aluminum paint cans were most effective in retaining moisture when compared with paper grocery bags and plastic oven bags. Conventional oven drying at 110°C was found to be an acceptable alternative to the standard distillation procedure (ASTM D1461) for measuring HMA moisture content. The conventional oven and microwave oven methods were found to give similar results.

Researchers developed a procedure to mix HMA laboratory samples with retained moisture using a bucket mixer and a propane torch. Samples were produced with moisture and compacted at temperatures of 78.9°C and 137.8°C in the SGC utilizing the Gyratory Load Cell Plate Assembly (GLPA). The GLPA is a device which measures the shear forces imparted to the HMA specimen during compaction. The GLPA was believed to be capable of indicating the presence of unstable mixtures by detecting a reduction in the measured frictional resistance during compaction in the SGC. The GLPA indicated no substantial difference in compaction properties of specimens with retained moisture and those utilizing dry aggregates. The researchers concluded that (a) the mixture may not be susceptible to tender mix behavior in the field, (b) the retained moisture content of the wet specimens were too low for differences in compaction properties to be detected, or (c) the GLPA was incapable of identifying tender mix behavior in the SGC mold during compaction.

2.6.5 Buchanan and Moore (2005)

A laboratory study was conducted to determine the ability of the Moisture Induced Stress Tester (MIST) to predict HMA stripping and to develop test protocols for its use. The MIST was designed to detect stripping of laboratory prepared loose or compacted HMA specimens or field cores. Test specimens were subjected to warm water and pressure in the MIST to simulate mechanisms that cause stripping. Turbidity and pH were measured and evaluated as potential indicators of stripping.

The initial phase of testing included comparing TSR values of samples conditioned using the MIST to specimens conditioned according to AASHTO T283. Tensile strength data from the MIST did not follow the same trend as results from AASHTO T283. It was determined that test specimens deformed during conditioning in the MIST, which led to inaccurate results. Therefore, it was determined that loose mix specimens should be evaluated. The boil test was conducted on twelve mixtures in accordance with MT-59. All mixtures evaluated retained an asphalt binder coating greater than ninety-five percent. It was determined that MT-59 is not an accurate method for identifying stripping of HMA mixtures.

Results of specimens tested in accordance with MT-63 were found to be highly variable due to specified allowable saturation and air void levels. MT-63 test data trends included: 1) addition of polymer to the asphalt binder increases the TSR and 2) addition of hydrated lime and hydrated lime plus liquid antistripping additive increases TSR for PG 67-22 mixtures. It was determined that SMA mixtures had a greater resistance to stripping, likely due to the use of modified binder and stabilizing fibers.

It was determined that the MIST demonstrated the potential to measure stripping of HMA. The change in turbidity ratio indicated that some form of stripping occurred during the test. Modifications to the MIST were suggested and further research was recommended prior to selection of test parameters.

2.6.6   Azari (2010)

An evaluation of AASHTO T 283 was conducted during NCHRP 9-26A to provide guidance on precision statements for the test. Limestone and sandstone aggregates were tested alongside SGC and Marshall compaction methods. Forty laboratories participated in the "round robin" test program. The result of the study was that "AASHTO T 283 is, in general, very variable and may provide erroneous results". Results were that the acceptable range of TSR values within one laboratory is approximately 9 percent, while acceptable TSR values between two laboratories is approximately 25 percent.

CHAPTER 3 – EXPERIMENTAL PROGRAM

3.1   Overview of Experimental Program

The experimental program included field and laboratory components as shown in Figure 3.1. Four crushed gravel aggregate sources were selected to represent a range of adherent fines and water absorption values based upon MDOT experience and an initial evaluation performed by the researchers.   Thereafter, twelve asphalt paving projects were evaluated that used these aggregate sources. Five of the asphalt mixtures evaluated were 9.5mm NMAS designs, five were 12.5mm NMAS designs, one was an SC-1 (Type 8 Marshall mixture), and one was a BB-1 (Type 6 Marshall mixture).

```
┌───────────────────────────────────────────────┐
│   Evaluate Gravel Aggregate Sources - Select Four │
└───────────────────────────────────────────────┘
┌───────────────────────────────────────────────┐
│   -Four Gravel Aggregate Sources                 │
│   -Three Field Projects per Aggregate Source     │
│   -Three or Four Sample Locations per Project    │
│   -Twelve Projects and Forty-Four Sample Locations │
└───────────────────────────────────────────────┘
         ┌──────────────┐        ┌──────────────┐
         │  Aggregates  │        │   Asphalt    │
         │              │        │   Concrete   │
         └──────────────┘        └──────────────┘
   ┌────────────┐  ┌────────────┐  ┌──────────┐  ┌──────────────┐
   │ Stockpile  │  │ Cold Feed  │  │ Sampled  │  │  Sampled on  │
   │  Samples   │  │  Samples   │  │ at Plant │  │   Roadway    │
   └────────────┘  └────────────┘  └──────────┘  └──────────────┘
```

Aggregate Tests:

-Gradations

-Methylene Blue

-Adhered Fines

-SEM Images

Aggregate Tests:

-Gradations

-Methylene Blue

-Adhered Fines

-Moisture Content

-Atterberg Limits

-Consensus Properties

Mix Tests:

-Moisture % (microwave)

-G_{mm}

-Extracted Gradation

-Asphalt Content

-TSR

-Boil Test

-Hamburg Wheel Tracking

Mix Tests From Cores:

-G_{mb}

-G_{mm}

-TSR

-Asphalt Content

-Extracted Gradation

Field Monitoring:

-Site Conditions

-Moisture % (microwave)

-Compaction Equipment

-Roller Passes & Timing

-Temperature of Mat w/ Depth

-Nuclear Density vs. Compaction

Figure 3.1. Research Experimental Program

For each of the twelve field projects, aggregate stockpile and cold feed belt materials were obtained. Laboratory testing performed on gravel stockpile materials (17 stockpiles) included gradation, adherent fines, methylene blue, and microscopic evaluation. One cold feed belt sample was obtained to represent each asphalt mixture and to provide material for determining moisture content, gradation, adherent fines, Atterberg limits, methylene blue, and Superpave consensus properties.

Plant produced mix was sampled from three or four haul trucks per project at the production facility to reasonably represent the aggregate blend obtained from the cold feed belt. For each truck sampled, mix was obtained for moisture content determination and placed in a sealed metal container. Additional mix was obtained for evaluating fundamental mixture properties and moisture susceptibility testing in the laboratory.

Each truck sampled was followed to the roadway test location representing that mix. Prior to placement, mix was obtained from the paver or transfer vehicle and placed in a sealed metal container for moisture content determination. At each location, field compaction was monitored since it is believed to be an important parameter related to moisture susceptibility. Rollers used, pavement temperature, and pavement density between roller passes were recorded. Cores were cut to determine in-place density (G_{mb}), tensile strength ratio (TSR), theoretical maximum specific gravity (G_{mm}), extracted aggregate gradation, and asphalt content (P_{AC}).

3.2 Materials Tested

3.2.1 Aggregate Sources Tested

Seven gravel aggregate sources were investigated in the initial stages of the project. Four of these seven sources were tested in this project based on MDOT experience and initial investigation by the researchers. Fundamental properties of the four gravel aggregate sources investigated in this project are presented in Table 3.1.

Table 3.1. Initial Properties of Selected Crushed Gravel Sources

Aggregate Source	Green Brothers	Baldwin Gravel	APAC	Hammett Gravel
Location	Crystal Springs	Hazlehurst	Scribner	Zeiglerville
County	Copiah	Copiah	Monroe	Yazoo
Size	< 12.5 mm	< 12.5 mm	< 12.5 mm	< 12.5 mm
Material Type	Crushed Gravel	Crushed Gravel	Crushed Gravel	Crushed Gravel
Sieve Size	Percent Passing			
19.0 mm	100.0	100.0	100.0	100.0
12.5 mm	100.0	100.0	100.0	99.9
9.5 mm	91.6	91.8	94.4	93.6
4.75 mm	41.2	50.1	49.2	56.7
2.36 mm	22.0	29.4	26.6	32.3
1.18 mm	13.4	18.7	16.0	19.4
0.60 mm	8.8	12.8	11.0	12.4
0.30 mm	6.1	9.2	8.5	8.2
0.15 mm	4.5	6.8	6.8	5.4
0.075 mm	3.6	5.3	5.6	4.0
G_{sb}	2.486	2.460	2.388	2.567
G_{sa}	2.635	2.628	2.605	2.643
Abs	2.27	2.60	3.50	1.16

3.2.2 Asphalt Mixtures Tested

The twelve field projects included in this study involved six different asphalt production facilities and a variety of typical asphalt mixtures utilized in Mississippi roadways. Mixtures evaluated included five 9.5mm and five 12.5mm NMAS Superpave mixtures. Also, included were one SC-1 (Type 8) and one BB-1 (Type 6) Marshall mix designs placed as surface and base mixtures, respectively. Projects 1 and 8 utilized the same mix design, as did projects 3 and 4, as well as projects 5 and 7. Job mix formulas and pertinent mix design parameters for mixtures evaluated are presented in Tables 3.2 and 3.3; the values shown were taken from the mix designs. Projects 10 and 11 did not contain hydrated lime, while all other projects had 1% hydrated lime.

Table 3.2. Design Properties of Asphalt Mixtures for Projects 1 to 6

Project		1	2	3	4	5	6
Gravel Source		Scribner	Zeiglerville	Hazlehurst	Hazlehurst	Zeiglerville	Crystal Springs
Type Blend		GVL/LMS	GVL	GVL	GVL	GVL/LMS	GVL/LMS
Gravel (%)		37	69	74	74	52	54
N_{MAS}		9.5mm	12.5mm	12.5mm	12.5mm	9.5mm	12.5mm
Design Level		MT	MT	HT	HT	HT	HT
N_{des}		65	65	85	85	85	85
Marshall Blows		---	---	---	---	---	---
Binder Grade		PG 67-22	PG 67-22	PG 76-22	PG 76-22	PG 67-22	PG 67-22
Mixing Temp (C)		160	154	163	163	154	154
WMA		---	---	---	---	---	Foam
Percent Passing	37.5 mm	100	100	100	100	100	100
	25.0 mm	100	100	100	100	100	100
	19.0 mm	100	100	100	100	100	100
	12.5 mm	100	96	95	95	100	90
	9.5 mm	95	88	85	85	94	74
	4.75 mm	58	62	56	56	55	45
	2.36 mm	36	44	36	36	37	27
	1.18 mm	25	32	26	26	28	19
	0.60 mm	19	24	19	19	21	15
	0.30 mm	12	12	11	11	11	9
	0.15 mm	8	9	8	8	7	7
	0.075 mm	6.0	6.1	5.2	5.2	5.3	5.1
G_{sb}		2.518	2.546	2.521	2.521	2.589	2.543
G_{sa}		2.658	2.642	2.646	2.646	2.680	2.657
Abs		2.08	1.42	1.87	1.87	1.32	1.68
FF (% 2 Faces)		95.5	92.0	90.6	90.6	95.1	94.9
FAA		44.2	43.2	---	---	44.4	44.1
P_b (%)		6.00	5.30	5.40	5.40	5.20	5.30
$P_{ba(mix)}$ (%)		0.72	0.56	0.92	0.92	0.32	0.78
P_{be} (%)		5.28	4.74	4.48	4.48	4.88	4.52
G_{mm}		2.358	2.394	2.388	2.388	2.420	2.404
G_{se}		2.566	2.584	2.582	2.582	2.611	2.595
VMA (%)		15.5	14.5	14.0	14.0	15.0	14.0
VFA (%)		74.2	72.4	71.1	71.1	73.3	71.4
D/B		1.13	1.29	1.16	1.16	1.09	1.13
TSR		94.5	112.8	86.0	86.0	91.7	91.1

Table 3.3. Design Properties of Asphalt Mixtures for Projects 7 to 12

Project		7	8	9	10	11	12
Gravel Source		Zeiglerville	Scribner	Scribner	Crystal Springs	Crystal Springs	Hazlehurst
Type Blend		GVL/LMS	GVL/LMS	GVL/LMS	GVL	GVL/LMS	GVL
Gravel (%)		52	37	37	65	50	72
NMAS		9.5mm	9.5mm	9.5mm	19mm	9.5mm	12.5mm
Design Level		HT	MT	ST	---	---	ST
N_{des}		85	65	50	---	---	50
Marshall Blows		---	---	---	75	75	---
Binder Grade		PG 67-22	PG 67-22	PG 67-22	PG 67-22	PG 67-22	PG 67-22
Mixing Temp (C)		154	160[a]	160	b	c	163
WMA		---	Foam	---	---	Foam	---
Percent Passing	37.5 mm	100	100	100	100	100	100
	25.0 mm	100	100	100	99	100	100
	19.0 mm	100	100	100	94	100	100
	12.5 mm	100	100	100	80	100	97
	9.5 mm	94	95	95	71	97	88
	4.75 mm	55	58	58	49	69	57
	2.36 mm	37	36	36	34	48	39
	1.18 mm	28	25	25	27	34	29
	0.60 mm	21	19	19	20	27	22
	0.30 mm	11	12	12	9	14	11
	0.15 mm	7	8	8	5	8	7
	0.075 mm	5.3	6.0	6.0	3.1	5.8	5.3
G_{sb}		2.589	2.518	2.515	2.509	2.544	2.495
G_{sa}		2.680	2.658	2.653	2.643	2.652	2.648
Abs		1.32	2.08	2.07	1.65	1.61	2.31
FF (% 2 Faces)		95.1	95.5	95.4	70.8	91.7	90.8
FAA		44.4	44.2	43.8	---	---	---
P_b (%)		5.20	6.00	6.20	4.70	6.10	5.35
$P_{ba(mix)}$ (%)		0.32	0.72	0.73	0.89	0.70	0.77
P_{be} (%)		4.88	5.28	5.47	3.81	5.40	4.58
G_{mm}		2.420	2.358	2.350	2.400	2.374	2.360
G_{se}		2.611	2.566	2.564	2.568	2.594	2.546
VMA (%)		15.0	15.5	15.8	12.4	15.9	14.1
VFA (%)		73.3	74.2	74.9	67.7	74.8	71.6
D/B		1.09	1.13	1.09	0.81	1.07	1.15
TSR		91.7	94.5	92.6	90.1	90.9	88.1

a: mix design temperature was 160 C, but mix was produced warm with estimated temperature of 140 C.
b: mixing temperature was not on design.
c: mixing temperature was not on design, but design was warm mix.

3.3   Field Sampling and Data Collection

Aggregate stockpile and cold feed belt samples obtained at the asphalt plant were placed in sealed plastic containers for laboratory testing. Moisture content of cold feed belt material was determined using a convection oven and was performed prior to subsequent testing. Stockpile and additional cold feed belt materials were also dried prior to reducing the material to the appropriate testing size using a sample splitter.

Asphalt mixture obtained at each asphalt plant and roadway test location was placed in sealed metal containers for laboratory testing. Specimens for determining asphalt moisture content were heated in the sealed container in a convection oven for

approximately 10 minutes at 149°C to loosen the mixture prior to testing in the microwave oven. Asphalt mixture was also obtained for evaluating fundamental properties and moisture susceptibility. Mixture samples were reheated in a convection oven prior to reducing the sample to the appropriate mass for each test conducted.

Figure 3.2 summarizes key data collection attributes at the roadway; site conditions (ambient temperature, base temperature, weather) were also recorded. A paint mark was made 0.6 to 0.9 m from the mat edge, and was the reference point for all testing at that location. At each test location, a hand held infrared temperature device was used to obtain pavement surface temperature (T_S). Pavement temperature was also measured using thermocouples inserted into the pavement at the bottom (T_B), middle (T_M), and upper (T_U) portions of the layer. Pavement temperature was recorded at each test location immediately behind the paver until finish rolling was completed.

Pavement density and roller types were monitored during construction at each test location; density was monitored with a nuclear gauge that is shown in Figure 3.2. Mat density was initially obtained behind the paver prior to the initial pass of the breakdown roller. Subsequent density measurements were obtained after each roller pass. A pass was defined as crossing one location one time. Passes were recorded that were over the paint mark (Figure 3.2) being monitored at each location. Passes that did not occur over the paint mark were not recorded. Compaction time was recorded from when mix was placed until finish rolling was completed. After compaction, cores were cut from each location that were dried in the laboratory under fans at room temperature.
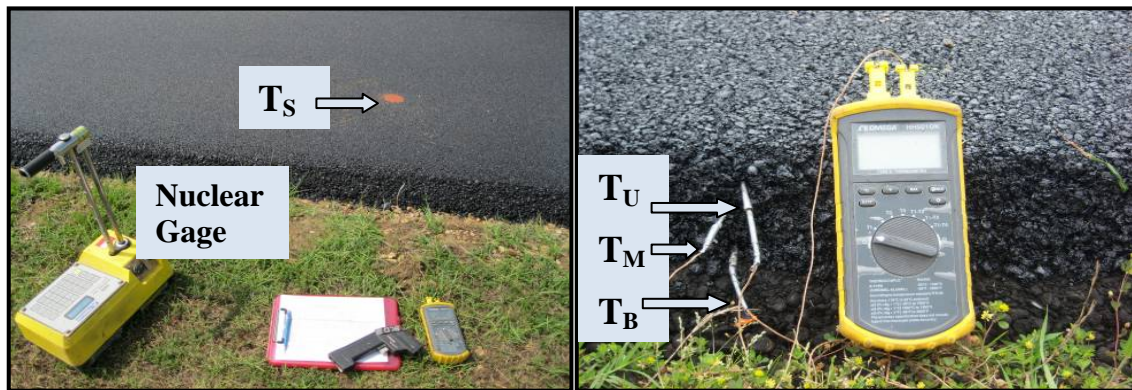
Figure 3.2. Field Data Collection Methods

3.4   Test Methods

3.4.1   Fundamental Aggregate Properties

Aggregate moisture content of cold feed belt samples was determined using a convection oven in accordance with AASHTO T265. Moisture content samples were not reduced prior to testing due to the need to dry the material for further testing. Samples were removed from the sealed plastic containers and the initial mass of each sample was determined. Samples were allowed to dry to a constant mass at a

temperature of 110°C. The dry mass of the material was determined and moisture content was calculated.

Course aggregate particle shape was determined in accordance with ASTM D4791. Testing was conducted on coarse aggregate retained on the 9.5 mm sieve, in accordance with MDOT specifications, on samples obtained from the cold feed belt. Coarse aggregate particles were measured using a proportional caliper device to determine the percentage of flat and elongated (F&E) particles (length to thickness) greater than 5:1 as shown in Figure 3.3.

Figure 3.3. Fundamental Aggregate Properties Testing Equipment

Coarse aggregate surface texture of cold feed belt material was evaluated in accordance with ASTM D5821. Testing was conducted on material coarser than the 4.75 mm sieve in accordance with MDOT requirements. Individual aggregate particles were visually inspected to determine the number of fractured faces each possessed.

Plasticity index was determined to measure the degree of plasticity of fines. The liquid limit of fine aggregate passing the 0.425 mm (No 40) sieve was determined in accordance with AASHTO T89. Plastic limit (PL) was determined in accordance with AASHTO T90. Plasticity index (PI) of fines is defined as the difference between the liquid limit (LL) and the plastic limit.

Fine aggregate bulk specific gravity (G_{sb}) was determined on cold feed belt samples utilizing a modified AASHTO T84 procedure. The test was conducted on washed material passing the 4.75 mm sieve. The fine aggregate was allowed to dry on a metal, flat bottom pan. Saturated surface dry (SSD) condition was determined when the aggregate surface did not change color with stirring and when no moisture was visible on the pan surface when tilted and material moved freely across the pan.

Fine aggregate shape and surface texture was evaluated in accordance with ASTM C1252. Testing was conducted on a standard graded sample (Method A) of cold feed belt material. Each sample was washed, dried, sieved, and combined according to the specified proportions. The test specimen was placed in a funnel, and then allowed to flow freely into a calibrated cylindrical measure. The percentage of uncompacted voids was calculated based on the volume of the cylindrical measure, mass of fine aggregate in

the measure, and G_{sb} of the fine aggregate. Uncompacted voids are referred to as fine aggregate angularity, or FAA. The testing apparatus is shown in Figure 3.3.

The sand equivalent test was conducted on cold feed belt samples in accordance with AASHTO T176 to determine the relative portions of fine dust or claylike material. Fine aggregate passing the 4.75 mm sieve was placed in a graduated, transparent cylinder which is filled with a mixture of water and a flocculating agent. The cylinder was filled with 1.02 cm of solution. Each test specimen was poured into the cylinder and allowed to soak for 10 minutes. The cylinder was then placed on a mechanical shaker for 45 seconds. The cylinder was then filled with solution and allowed to stand for 20 minutes. Sand separated from the flocculated clay, and heights of the sand and clay in the cylinder were measured following the 20 minute period. Sand equivalent value is the ratio of the height of sand to the height of clay multiplied by 100. Higher sand equivalent values will typically be obtained for cleaner fine aggregate.

Gradations were performed according to AASHTO T11 and T27. Washed gradations were reported for gravel sources and cold feed samples. Washed gradations determined the particle size distribution above the 0.075 mm sieve and the material passing the 0.075 mm sieve referred to as fines content or $P_{0.075}$.

3.4.2   Adhered Fines and Scanning Electron Microscope Imaging

Five approaches were used during the project to provide a measure of the adherent fines in the gravel sources and the cold feed samples. The Scanning Electron Microscope (SEM) was also used to visually assess adhered fines. The remainder of this section describes test methods and terminology associated with adhered fines and SEM evaluation.

The first adhered fines measure used T27 dry gradations performed on gravel stockpiles or cold feed materials prior to washing by mechanically shaking the material for approximately 10 minutes. The cumulative mass retained on each sieve after shaking was recorded, alongside the amount passing the 0.075 mm sieve. The materials retained on sieves were then washed according to T11 to determine the amount of material passing the 0.075 mm sieve after mechanical shaking. The fines content removed by washing after mechanical shaking was deemed adhered and is referred to hereafter as $P_{Adh(\%)-All}$ since the entire gradation was considered.

The second through fifth adhered fines measures evaluated all gravel coarse aggregate stockpiles (seventeen total) from all twelve field projects. Samples were denoted 1 to 17 (Table 3.4) and were typically on the order of 4 to 5 kg. Each individual sample was remixed in the lab and halved with a splitter. Each half was sufficient to provide approximately 1,600 g of pre-dried material for adhered fines testing and to provide additional material for SEM evaluation. The halved portions of the sample reduced to approximately 1,600 g were referred to as Sub-sample I and Sub-sample II, while the material taken from the halves and re-combined for SEM evaluation was referred to as Sub-sample III. Sub-samples I to III were then oven dried.

Table 3.4. Coarse Aggregate Stockpile Adhered Fines Sample Identification

Aggregate Source	Sample ID	Project ID	NMAS (mm)
Crystal Springs	9	6	12.5
	13	10	Washed
	14	10	12.5
	15	10	12.5-25.0
	16	11	12.5
Hazlehurst	4	3	19.0
	5	3	12.5
	6	4	19.0
	7	4	12.5
	17	12	12.5
Scribner	1	1	12.5
	11	8	12.5
	12	9	12.5
Zeiglerville	2	2	12.5
	3	2	19.0
	8	5	12.5
	10	7	12.5

Sub-sample I was used to perform ASTM D5711-95: Standard Test Method for Adherent Fines. The result of the test method is termed Percent Adherent Fines, which is given the designation $P_{Adh(\%)-5711}$ in this report. Key terms are the oven dry mass of material coarser than the 4.75 mm sieve after 3 min $\pm$ 15 sec of shaking before washing (B) and after washing (C).

Sub-sample II was used to perform a modified version of ASTM D 5711-95. In the modified approach, the 9.5 mm, 4.75 mm, and 2.36 m sieves were used and aggregate shaken for 3 min $\pm$ 15 sec. The material retained on each sieve was not re-combined, rather was evaluated individually using Eq. 3.1.

$$P_{Adh(\%)-i} = \frac{B_i - C_i}{B_i}$$
(3.1)

Where,

$P_{Adh(\%)-i}$ = Percent adhered fines retained on sieve i but passing sieves greater than i
B_i = Original dry mass of material retained on sieve i but passing sieves greater than i
C_i = Dry material mass retained on sieve i but passing sieves greater than i after washing
i = sieve size: 9.5 mm, 4.75 mm, or 2.36 mm

Sub-sample III was shaken for 3 min $\pm$ 15 sec with 9.5 mm and 4.75 mm sieves. After shaking, aggregates were taken off each sieve of interest to represent that stockpile for evaluation with the scanning electron microscope (SEM). Sample 1 was evaluated in

more detail than the other samples to provide a broader range of data to select a more condensed evaluation protocol for the other samples. Five sample 1 aggregates retained on the 9.5 mm and 4.75 mm sieves were viewed at 30x, 100x, 500x, 1000x, 5000x, and 10000x magnifications. Samples 2 through 17 were investigated with 30x and 500x magnification with the description bar visible for five aggregates retained on the 4.75 mm sieve. Low magnification provides better depth perception in many cases.

Four of the samples (numbers 4, 6, 7, and 8) were further investigated as they represent the four aggregate sources tested. Five aggregates retained on the 4.75 mm sieve were thoroughly washed with warm water and a clean brush to remove all fine particles. The particles were oven dried and then viewed at 30x and 500x magnification. Washed samples were denoted sample 4a, 6a, 7a, and 8a.

The five aggregates of each sieve size and sample (arbitrarily labeled A to E) were prepared and tested in the following manner. Hot melt glue and carbon paste were used to bond specimens to the plate that was inserted into the SEM. Each plate contained five stubs, and one aggregate was placed in each stub. Carbon paste was used to ground the specimens as this is required for proper operation of the microscope. Gold palladium (Au/Pd) was used to make the specimens conductive. Aggregates were coated with a $\approx 60e^{-9}$ meter thick Au/Pd layer. Figure 3.4 is a photograph of the mounting plate, alongside coated and uncoated aggregates.
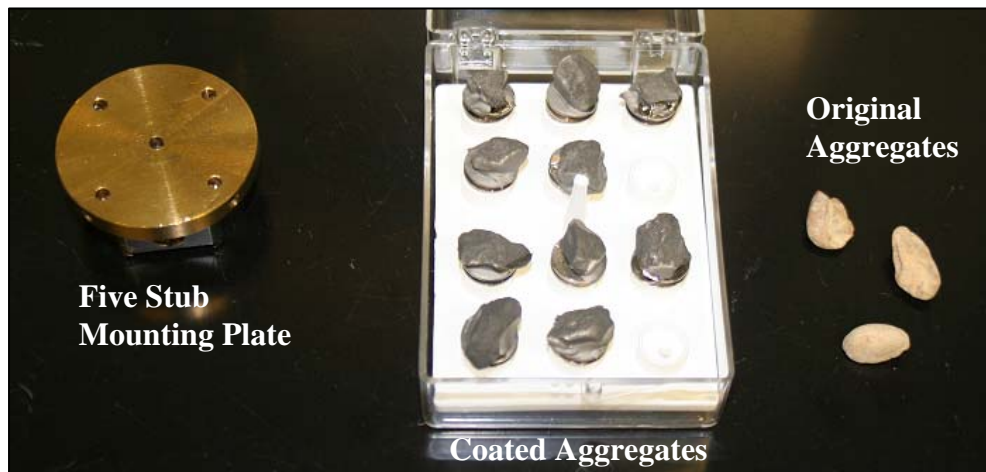
Figure 3.4. Representative Plate of Aggregates Tested with SEM

A model JSM 6500F scanning electron microscope was used. The SEM uses secondary electron imaging and uses electrons rather than light to make specimens visible. An example SEM photo with term descriptions is provided in Figure 3.5. The accelerating voltage used is a typical value. The Secondary Electron Image (SEI) is a higher quality image; back scatter was not used with the images. The working distance is from the bottom of the column to the specimen. The center of the photo was held constant between the 30x and 500x images for samples 2 through 17.
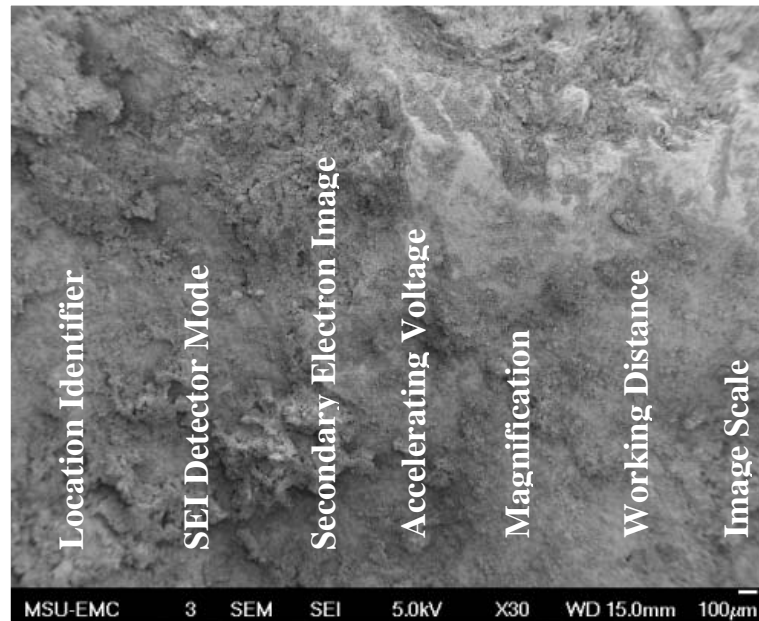
Figure 3.5. Example SEM Image

3.4.3 Methylene Blue

The methylene blue test was conducted to quantify the amount of harmful clays of the smectite (montmorillonite) group and organic matter present in fine aggregate. Testing was conducted according to AASHTO TP57. This test was performed on $P_{0.075}$ material, taken from the wash portion of a representative sample of the stockpile and cold feed belt material. Excess water was decanted and the sample was allowed to dry. Dried material was mixed thoroughly and a 10 g test specimen was placed in a 500 mL Griffin beaker. Slurry was made by adding 30 mL of distilled water and stirring with a magnetic mixer. Methylene blue solution was added to the continuously mixed slurry in 0.5 mL increments. After addition of methylene blue, the sample was allowed to stir for one minute prior to applying one drop of slurry to filter paper using a glass stirring rod. The appearance of the drop on the filter paper was visually inspected (Figures 3.6*a* and 3.6*b*). The endpoint of the test was determined by the formation of a light blue halo around the drop. Aschenbrener (1992) developed the Table 3.5 relationship of methylene blue values and anticipated hot mix asphalt pavement performance as related to moisture susceptibility.

Table 3.5. Expected Performance of Methylene Blue

Methylene Blue (mg/g)	Expected Performance
5-6	Excellent
7-12	Marginally acceptable
13-19	Problems or possible failures
20+	Failure
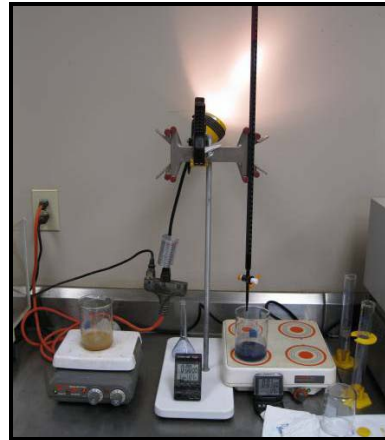
a) *Methylene Blue Testing*   b) *Methylene Blue Equipment*

Figure 3.6. Methylene Blue Apparatus

3.4.4 Fundamental Asphalt Mixture Properties

Plant produced mix and pavement cores were evaluated to determine the G_{mm} in accordance with AASHTO T 209. The vacuum apparatus shown in Figure 3.7 was used to saturate test specimens. One test specimen was obtained from plant produced mixture. Cores from the TSR control subset were heated to remove sawn particle edges and combined to obtain one additional loose test specimen.

Figure 3.7. Fundamental Asphalt Mixture Test Equipment

Bulk specific gravity (G_{mb}) of laboratory produced specimens compacted in the SGC shown in Figure 3.7 and pavement cores were determined in accordance with AASHTO T166. The air void content (V_a) of each specimen was determined in accordance with AASHTO T269 utilizing G_{mb} and G_{mm}.

Asphalt content (P_{AC}) of plant produced mixture and pavement cores was determined in accordance with AASHTO T308 (Method A – Internal Balance). Plant mixture was heated to obtain loose mixture for testing. Asphalt content of pavement cores was determined on specimens utilized to determine G_{mm} after oven drying.

Asphalt content was reported as the uncorrected calibrated asphalt content from the automatic printout.

Plant produced mixture and pavement core gradations were determined as per AASHTO T30. Gradations of the plant produced mixture and pavement cores were performed after determining the asphalt content by the ignition method.

3.4.5 Asphalt Moisture Content

Moisture content of plant produced mixture was determined in accordance with MDOT MT-76 (microwave method). A power control setting was established by heating water in the microwave oven for five minutes as required in MT-76. A power level of 22 produced a difference in water temperature in the range of 20 to 30°C as specified. To determine mixture moisture content, sealed cans containing mix obtained from each project were placed in a conventional oven at a temperature of 149°C for a period of approximately ten minutes to loosen the material. A minimum of 500 g of material was placed in a Pyrex bowl and the initial mass of the sample was recorded (Figure 3.8a). The sample was dried in a microwave oven (Figure 3.8b) at 15 minute intervals using the established power control setting until it reached constant mass.

a) Moisture Specimen   *b) Moisture Specimen in Microwave*

Figure 3.8. Microwave Method for Determining Mixture Moisture

3.4.6 Tensile Strength Ratio

Plant produced mix was tested in accordance with MT-63 (vacuum saturation method). Asphalt mixture was reheated and compacted in the SGC to a 95 mm height to obtain 7 ± 1 percent air voids. Four specimens were compacted and separated into two subsets (control and conditioned) so that the average air voids of the two subsets were approximately equal. Control specimens were placed in a water bath at 25°C for thirty minutes prior to determining the indirect tensile strength ($S_{t(Dry)}$) using the Marshall stability tester at a loading rate of 50 mm/ min in the indirect tensile test (IDT).

Conditioned specimens were vacuum saturated at 525 mm Hg partial pressure for 5 to 10 minutes in the vacuum apparatus previously shown in Figure 3.7. The degree of saturation was between 55 and 80 percent for all specimens, with 65 percent

saturation targeted for all mixes. After conditioning, specimens were placed in a water bath at 60˚C for 24 hours. Specimens were then removed and placed in a water bath at 25˚C for 2 hours $\pm$ 30 minutes prior to determining the wet or conditioned indirect tensile strength $S_{t(Wet)}$. The Marshall Stability tester and hot water bath utilized are shown in Figure 3.9. The tensile strength ratio (TSR) was calculated by dividing $S_{t(Wet)}$ by $S_{t(Dry)}$. After specimens were tested, they were broken in half and visually evaluated for stripping. A minimum TSR of 85 percent with 95 percent retained asphalt coating is specified in the Mississippi Standard Specifications for Road and Bridge Construction (2004 Edition). Eq. 3.2 was used to calculate $S_{t(Dry)}$ and $S_{t(Wet)}$.

$$S_t = \frac{4.9(P)(D)}{V}$$
(3.2)

Where,

S_t = indirect tensile strength at failure
P = applied load at failure (kg)
D = specimen diameter (mm)
V = specimen volume; when conditioned-vol. after 24 hr and 2 hr conditioning periods

Pavement cores were also tested in accordance with MDOT MT - 63, with the exception that only two cores were tested. One core was selected for the control set and one was selected for the conditioned set. The cores were tested as described above.

Figure 3.9. Marshall Stability Tester

3.4.7   Boil Test

Loose plant mix specimens were tested in accordance with MDOT MT - 59 (boiling water test). A glass beaker was filled with 1000 mL of distilled water and brought to a boil using a gas burner. Approximately 200 g of mixture was transferred into the boiling water and allowed to boil for 10 minutes as shown in Figure 3.10*a*. The specimen was removed from the heat and the water decanted. Contents of the beaker were emptied onto a white paper towel and allowed to dry as shown in Figure 3.10*b*. The extent of stripping is determined by visual observation. The maximum stripping allowed by MDOT is 5 percent or 95 percent retained asphalt binder.

| a) Boil Test | b) Specimen after Boiling |
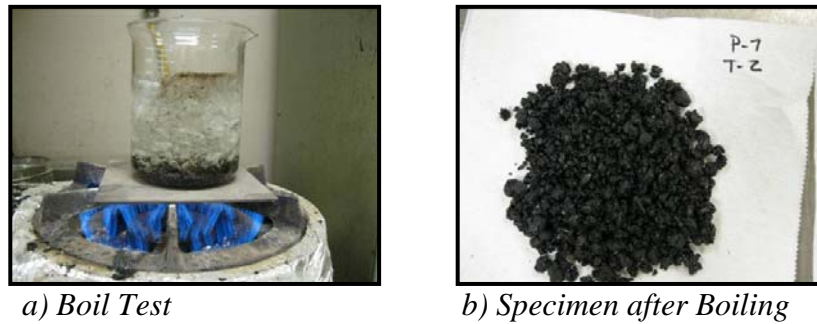
Figure 3.10. Boil Test

3.4.8   Hamburg Wheel-Tracking Device

Moisture susceptibility of compacted asphalt specimens was evaluated with the Asphalt Pavement Analyzer (APA) junior utilizing Hamburg wheel tracking device (HWTD) parameters.   The HWTD measures combined effects of rutting and moisture damage by tracking a loaded steel wheel back and forth across the surface of compacted asphalt specimens that are submerged in 50 $^{\circ}$C water.   The test was conducted in accordance with AASHTO T324.

Plant produced asphalt mixture was reheated and compacted to 63 mm in the SGC to produce samples with 7 ± 2 percent air voids. Four specimens were produced at the appropriate air void level and sawn so that two specimens would fit together in the testing molds to produce two replicate tests.   Two replicate specimens were tested simultaneously using two reciprocating 20.3 cm diameter, 4.7 cm wide steel wheels as shown in Figure 3.11*a*. Each wheel applied a load of 71.7 kg while reciprocating over the specimens, with position varying sinusoidally over time, at a rate of approximately 50 passes per minute. The maximum wheel speed was approximately 30.5 cm/s and was reached at the midpoint of the specimen.

Deformation was measured at the midpoint of the specimen with each pass off the wheel using an LVDT device.   The test was conducted for 20,000 passes or a maximum deformation of 14 mm. An automatic computer control system was utilized for conducting the test and acquiring deformation versus passes data such as number of passes, deformation, and plot of deformation versus number of passes. Figure 3.11*b* shows the HWTD apparatus and computer.

a) HWTD Testing   *b) APA Jr. with Computer*

Figure 3.11. Hamburg Wheel-Tracking Device

CHAPTER 4 – FIELD TEST RESULTS

4.1   Overview of Field Test Results

The field data collected as part of this project is discussed in this chapter, and results are presented and observations made for the field data without regard for the entire data set. This data is analyzed in conjunction with all project data (field and laboratory) in chapter 6. The analysis was performed in this manner due to the large amount and diverse types of data collected in this study.

4.2   Field Data Collected

This section provides the field data collected in tabular form that is interpreted in subsequent sections of this chapter. Table 4.1 summarizes site conditions for all twelve field projects and the corresponding forty-four test locations; the ID is interpreted project-location (e.g. 1-2 is project 1 and location 2). Table 4.2 summarizes the compaction equipment used, and as seen several types of compaction equipment were used during construction of the projects studied.

Table 4.3 provides behind the screed temperatures measured at four locations as discussed in Section 3.3. The data in Table 4.3 occurs at time $t_s = 0$ min with respect to the compaction process. The remainder of the data presented in this section is with respect to the behind the screed time. For example, $t_s = 15$ min is 15 min from when the screed first passed over the location of interest.

Tables 4.4 through 4.7 summarize compactive effort, temperature, and timing construction data organized by gravel source. These tables have data for breakdown, intermediate, and finish rolling. The number and type of passes of each roller in Table 4.2 are shown alongside the time from when the screed first passed over the location. Also provided in Tables 4.4 through 4.7 are the measured temperature ranges during the compaction times shown. Figure 4.1 is an example plot for project 1-1 showing all temperature data collected at that location, which was used to develop Tables 4.3 to 4.7.
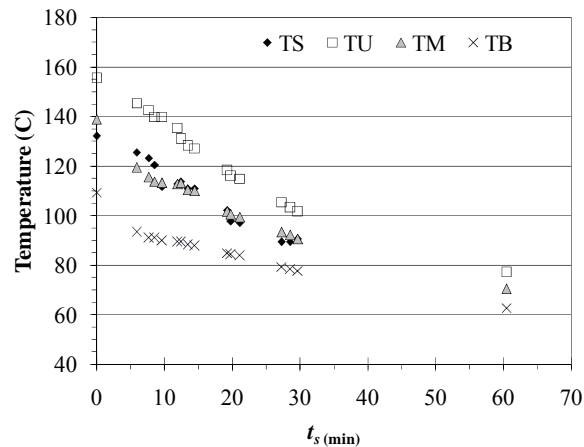
Figure 4.1. Measured Asphalt Temperature Profile at Project 1, Location 1

Table 4.1. Field Data Collection Site Conditions

ID	Ambient Temperature (C)	Base Temperature (C)	Underlying Material (---)	Wind Speed (km/hr)	Weather Conditions
1-1	18.3	33.3	Asphalt	0-8	Mostly Cloudy
1-2	22.2	44.4	Asphalt	8-16	Partly Cloudy
1-3	18.3	33.3	Asphalt	0-8	Partly Cloudy
1-4	18.3	33.3	Asphalt	0-8	Partly Cloudy
2-1	35.0	37.8	Asphalt	Calm	Mostly Cloudy
2-2	35.0	47.8	Asphalt	Calm	Mostly Cloudy
2-3	28.3	36.1	Asphalt	3.2-8	Partly Cloudy
2-4	28.3	36.1	Asphalt	0-8	Partly Cloudy
3-1	24.4	36.7	Asphalt	0-8	Clear and Sunny
3-2	25.6	47.2	Asphalt	0-8	Sunny
3-3	30.0	47.8	Asphalt	0-8	Sunny
3-4	30.0	48.3	Asphalt	0-8	Sunny
4-1	22.2	38.9	Asphalt	0-16.1	Mostly Sunny
4-2	23.3	44.4	Asphalt	0-8	Mostly Sunny
4-3	26.1	44.4	Asphalt	0-8	Mostly Sunny
4-4	28.9	41.1	Asphalt	0-8	Mostly Sunny
5-1	27.2	36.1	Asphalt	Calm	Cloudy & Humid
5-2	30.0	41.7	Asphalt	Calm	Mostly Cloudy
5-3	32.8	45.0	Asphalt	Calm	Mostly Cloudy
6-1	28.3	38.9	Asphalt	0-8	Mostly Cloudy
6-2	30.0	42.2	Asphalt	0-8	Mostly Cloudy
6-3	32.2	46.1	Asphalt	0-8	Mostly Cloudy
6-4	31.1	43.3	Asphalt	0-8	Sunny
7-1	28.3	32.2	Asphalt	0	Cloudy
7-2	32.8	41.7	Asphalt	Calm	Mostly Cloudy
7-3	33.9	43.3	Asphalt	Calm	Mostly Cloudy
7-4	34.4	47.8	Asphalt	Calm	Mostly Sunny
8-1	29.4	39.4	Asphalt	3.2-8	Sunny
8-2	33.3	54.4	Asphalt	Calm	Sunny
8-3	32.2	50.0	Asphalt	0-8	Sunny
9-1	21.1	26.7	Asphalt	Calm	Sunny
9-2	21.7	25.0	Asphalt	0-8	Sunny
9-3	18.9	24.4	Asphalt	Calm	Sunny
9-4	21.1	26.7	Asphalt	Calm	Sunny
10-1	7.2	5.6	Dry Subgrade Soil	Calm	Cloudy
10-2	13.3	10.0	Dry Subgrade Soil	Calm	Cloudy
10-3	12.8	9.4	Dry Subgrade Soil	Calm	Cloudy
11-1	22.8	22.8	Asphalt	8	Partly Sunny
11-2	24.4	22.8	Asphalt	0-8	Partly Sunny
11-3	27.2	32.8	Asphalt	0-8,Gusts 16-24	Mostly Sunny
11-4	26.1	32.8	Asphalt	0-8	Sunny
12-1	16.1	18.3	Asphalt	Calm	Sunny
12-2	13.3	22.8	Wet Subgrade Soil	Calm	Sunny
12-3	25.0	37.8	Asphalt	0-3.2	Sunny

Table 4.2. Compaction Equipment Summary

Proj.	Loc.	Breakdown	Intermediate	Finish
1	1	Hypac C784, Hypac C778B	SP 1118	Hypac C778B
	2	Hypac C784	SP 1118	Hypac C778B
	3	Hypac C784	SP 1118	Hypac C778B
	4	Hypac C784	SP 1118	Hypac C778B
2	1	Ingersoll Rand DD118	---	---
	2	Ingersoll Rand DD118	---	---
	3	Ingersoll Rand DD118	---	---
	4	Ingersoll Rand DD118	---	---
3	1	CAT CB64	---	Ingersoll Rand DD125
	2	CAT CB64	---	Ingersoll Rand DD125
	3	CAT CB64	---	Ingersoll Rand DD125
	4	CAT CB64	---	Ingersoll Rand DD125
4	1	CAT CB64	---	Ingersoll Rand DD125
	2	CAT CB64	---	Ingersoll Rand DD125
	3	CAT CB64	---	Ingersoll Rand DD125
	4	CAT CB64	---	Ingersoll Rand DD125
5	1	Ingersoll Rand DD 110 HF	Sakai GW750-2	Ingersoll Rand DD110
	2	Ingersoll Rand DD 110 HF	Sakai GW750-2	Ingersoll Rand DD110
	3	Ingersoll Rand DD 110 HF	Sakai GW750-2	Ingersoll Rand DD110
6	1	CAT CB564 D	Ingersoll Rand PT125R	CAT CB634D
	2	CAT CB564 D	Ingersoll Rand PT125R	CAT CB564D
	3	CAT CB564 D	Ingersoll Rand PT125R	Bomag 284 AD
	4	CAT CB564 D	Ingersoll Rand PT125R	Bomag BW 284 AD
7	1	Ingersoll Rand DD110 HF	Sakai GW750-2	Ingersoll Rand DD110
	2	Ingersoll Rand DD110 HF	Sakai GW750-2	Ingersoll Rand DD110
	3	Ingersoll Rand DD110 HF	Sakai GW750-2	Ingersoll Rand DD110
	4	Ingersoll Rand DD110 HF	Sakai GW750-2	Ingersoll Rand DD110
8	1	CAT CB64	---	CAT CB-634C
	2	CAT CB64	---	CAT CB-634C
	3	CAT CB64	---	CAT CB-634C
9	1	Volvo DD138 HEA	---	Ingersoll Rand DD138 HFA
	2	Volvo DD138 HEA	---	Ingersoll Rand DD138 HFA
	3	Volvo DD138 HEA	---	Ingersoll Rand DD138 HFA
	4	Volvo DD138 HEA	---	Ingersoll Rand DD138 HFA
10	1	Ingersoll Rand 110 HF	---	Ingersoll Rand 110 HF
	2	Ingersoll Rand 110 HF	---	Ingersoll Rand 110 HF
	3	Ingersoll Rand 110 HF	---	Ingersoll Rand 110 HF
11	1	CAT CB64	Ingersoll Rand PT125R	Ingersoll Rand 110 HF
	2	CAT CB64	Ingersoll Rand PT125R	Ingersoll Rand 110 HF
	3	CAT CB64	Ingersoll Rand PT125R	Ingersoll Rand 110 HF
	4	CAT CB64	Ingersoll Rand PT125R	Ingersoll Rand 110 HF
12	1	Ingersoll Rand DD118 HA	---	Sakai TW 502
	2	Ingersoll Rand DD118 HA	---	Sakai TW 502
	3	Ingersoll Rand DD118 HA	---	Sakai TW 502

Table 4.3. Pavement Temperatures Behind Screed (t_s = 0 min)

Project	Location	T_S (C)	T_U (C)	T_M (C)	T_B (C)
1	1	132	156	139	109
	2	119	132	129	99
	3	---	132	98	88
	4	---	137	116	102
2	1	154	169	172	168
	2	139	157	156	154
	3	139	154	154	152
	4	149	139	160	150
3	1	133	141	140	139
	2	135	139	138	133
	3	141	149	150	148
	4	139	149	148	149
4	1	131	144	138	97
	2	137	148	146	146
	3	143	149	147	146
	4	133	144	144	145
5	1	139	---	155	158
	2	137	138	154	128
	3	156	156	161	129
6	1	128	130	129	131
	2	116	---	133	92
	3	153	168	166	131
	4	127	---	---	---
7	1	154	167	161	154
	2	160	129	159	163
	3	166	134	149	171
	4	167	131	178	179
8	1	105	92	123	126
	2	117	93	121	123
	3	112	118	108	74
9	1	129	142	129	102
	2	141	---	---	---
	3	143	154	153	131
	4	127	131	131	113
10	1	133	148	149	140
	2	144	82	144	139
	3	127	125	91	127
11	1	136	152	147	123
	2	118	128	136	118
	3	141	147	156	135
	4	132	139	138	87
12	1	118	126	127	83
	2	136	141	139	59
	3	123	131	134	86

Table 4.4. Compactive Effort, Timing, and Temperature Summary: Crystal Springs

		Breakdown Rolling						Intermediate Rolling						Finish Rolling					
ID	t (cm)	Comp (---)	Time (min)	T_S (C)	T_U (C)	T_M (C)	T_B (C)	Comp (---)	Time (min)	T_S (C)	T_U (C)	T_M (C)	T_B (C)	Comp (---)	Time (min)	T_S (C)	T_U (C)	T_M (C)	T_B (C)
6-1	3.6	4 Vib 1 St	5 to 8	104 to 88	124 to 109	111 to 107	123 to 114	7 Pn	19 to 23	75 to 69	96 to 89	93 to 88	98 to 92	2 St	39 to 40	57 to 56	72 to 73	74 to 73	76 to 75
6-2	4.9	4 Vib 1 St	2 to 5	107 to 97	--- to 124	131 to 124	100 to 101	9 Pn	13 to 19	97 to 93	109 to 101	107 to 99	93 to 89	1 St	77	69	66	65	66
6-3	7.2	4 Vib 2 St	7 to 11	138 to 131	155 to 144	152 to 142	114 to 108	7 Pn	31 to 36	116 to 111	107 to 101	110 to 104	98 to 96	3 St	43 to 47	108 to 99	94 to 91	97 to 94	92 to 90
6-4	6.0	5 Vib 1 St	3 to 7	119 to 102	---	---	---	6 Pn	16 to 21	98 to 92	---	---	---	1 St	42	73	---	---	---
10-1	10.4	4 Vib	3 to 5	130 to 124	151 to 148	147 to 149	113 to 104	---	---	---	---	---	---	2 St	12 & 26	117 & 107	134 & 111	146 & 127	103 & 91
10-2	9.2	4 Vib	2 to 4	135 to 128	--- to ----	136 to 124	128 to 113	---	---	---	---	---	---	1 St	16	109	---	101	86
10-3	9.4	4 Vib	10 to 14	99 to 94	71 to 66	79 to 72	85 to 79	---	---	---	---	---	---	1 St	44	69	45	46	51
11-1	6.7	5 Vib 1 St	12 to 18	130 to 95	122 to 111	113 to 101	102 to 97	9 Pn	24 to 33	90 to 78	101 to 89	91 to 80	92 to 84	1 St	51	63	74	66	71
11-2	5.6	6 Vib	8 to 14	96 to 82	114 to 99	119 to 103	90 to 83	19 Pn	16 to 37	82 to 56	97 to 69	99 to 67	81 to 64	1 St	54	50	60	57	55
11-3	5.3	5 Vib 1 St	5 to 22	118 to 89	137 to 91	125 to 77	112 to 81	5 Pn	23 to 27	87 to 84	88 to 82	76 to 71	81 to 76	1 St	30	74	78	67	71
11-4	5.0	5 Vib 2 St	5 to 14	111 to 89	116 to 92	119 to 84	81 to 74	9 Pn	16 to 24	88 to 75	89 to 77	82 to 68	74 to 68	2 St	26 & 31	69 & 69	74 & 69	65 & 60	66 & 63

Comp = Compaction   Vib = Vibratory Roller Pass(s)   St = Static Roller Pass(s)   Pn = Pneumatic Roller Pass(s)   Pn-Vib = Vibrating Pneumatic Roller Pass

Table 4.5. Compactive Effort, Timing, and Temperature Summary: Hazlehurst

			Breakdown Rolling					Intermediate Rolling						Finish Rolling					
ID	t	Comp	Time	T_S	T_U	T_M	T_B	Comp	Time	T_S	T_U	T_M	T_B	Comp	Time	T_S	T_U	T_M	T_B
	(cm)	(---)	(min)	(C)	(C)	(C)	(C)	(---)	(min)	(C)	(C)	(C)	(C)	(---)	(min)	(C)	(C)	(C)	(C)
3-1	4.1	4 Vib 1 St	3 to 12	120 to 110	142 to 140	141 to 137	141 to 103	---	---	---	---	---	---	3 St	24 to 32	93 to 92	132 to 126	127 to 120	92 to 87
3-2	6.7	5 Vib	1 to 7	121 to 113	139 to 138	138 to 133	133 to 134	---	---	---	---	---	---	2 St	34 & 39	99 & 95	119 & 116	118 & 115	117 & 113
3-3	5.6	5 Vib	5 to 9	124 to 119	146 to 137	149 to 147	148 to 147	---	---	---	---	---	---	2 St	34 to 38	104 to 101	121 to 116	127 to 123	127 to 124
3-4	4.1	5 Vib	12 to 19	114 to 101	148 to 135	147 to 142	146 to 141	---	---	---	---	---	---	2 St	53 to 56	89 to 88	113 to 112	111 to 109	109 to 107
4-1	4.7	5 Vib	2 to 10	123 to 112	143 to 119	128 to 107	88 to 89	---	---	---	---	---	---	2 St	21 to 23	91 to 88	99 to 98	89 to 88	78 to 78
4-2	5.6	5 Vib 2 St	1 to 20	128 to 114	148 to 141	146 to 139	146 to 134	---	---	---	---	---	---	2 St	24 to 25	114 to 112	139 to 139	136 to 136	130 to 129
4-3	5.9	6 Vib	2 to 11	131 to 114	149 to 134	148 to 139	139 to 115	---	---	---	---	---	---	2 St	17 to 18	107 to 107	141 to 140	128 to 127	106 to 106
4-4	4.6	5 Vib	2 to 7	126 to 116	146 to 144	146 to 144	144 to 135	---	---	---	---	---	---	2 St	17 to 18	104 to 103	138 to 137	132 to 131	120 to 119
12-1	3.8	3 St	1 to 9	107 to 85	123 to 96	121 to 89	79 to 67	---	---	---	---	---	---	2 Pn	7 & 27	91 & 53	100 & 64	93 & 58	68 & 51
12-2	3.1	1 Vib 1 St	11 to 13	87 to 77	105 to 101	94 to 91	62 to 64	---	---	---	---	---	---	2 Pn	21 to 22	60 to 58	80 to 78	70 to 68	57 to 56
12-3	3.4	3 St	4 to 9	97 to 79	129 to 99	99 to 82	78 to 74	---	---	---	---	---	---	1 Pn	23	54	69	56	61

Comp = Compaction   Vib = Vibratory Roller Pass(s)   St = Static Roller Pass(s)   Pn = Pneumatic Roller Pass(s)   Pn-Vib = Vibrating Pneumatic Roller Pass

Table 4.6. Compactive Effort, Timing, and Temperature Summary: Scribner

			Breakdown Rolling					Intermediate Rolling						Finish Rolling					
ID	t (cm)	Comp (---)	Time (min)	T_S (C)	T_U (C)	T_M (C)	T_B (C)	Comp (---)	Time (min)	T_S (C)	T_U (C)	T_M (C)	T_B (C)	Comp (---)	Time (min)	T_S (C)	T_U (C)	T_M (C)	T_B (C)
1-1	5.8	4 Vib	6 to 10	126 to 112	146 to 140	119 to 113	93 to 90	9 Pn	12 to 29	113 to 89	136 to 103	113 to 92	89 to 78	2 St	30 & 60	91 & ---	102 & 77	91 & 77	78 & 63
1-2	4.6	5 Vib 1 St	4 to 10	110 to 90	118 to 94	114 to 92	91 to 73	22 Pn	11 to 42	89 to 58	89 to 58	88 to 57	73 to 52	2 St	31 & 43	64 & 52	65 & 57	63 & 57	57 & 52
1-3	6.2	4 Vib	1 to 4	--- to ---	125 to 104	94 to 86	86 to 77	15 Pn	6 to 31	--- to ---	89 to 48	78 to 47	73 to 45	1 St	48	---	43	41	39
1-4	6.6	4 Vib	2 to 5	--- to ---	131 to 121	107 to 96	94 to 89	12 Pn	7 to 30	--- to ---	110 to 68	91 to 64	84 to 58	1 St	34	---	63	61	54
8-1	5.8	4 Vib 2 St	3 to 21	105 to 84	92 to 99	123 to 93	126 to 79	---	---	---	---	---	---	3 St	22 to 37	81 to 68	98 to 79	92 to 78	79 to 71
8-2	3.7	4 Vib 1 St	4 to 14	113 to 93	92 to 101	112 to 93	118 to 86	---	---	---	---	---	---	2 St	43 to 45	73 to 73	79 to 78	74 to 74	72 to 71
8-3	4.0	4 Vib 1 St	1 to 7	106 to 92	118 to 103	106 to 96	82 to 87	---	---	---	---	---	---	2 St	15 to 16	84 to ---	88 to 87	84 to 83	79 to 78
9-1	3.0	3 Vib 1 St	2 to 7	128 to 118	139 to 128	129 to 127	99 to 96	---	---	---	---	---	---	2 St	26 to 28	92 to 92	104 to 102	104 to 103	85 to 84
9-2	3.5	3 Vib 1 St	1 to 6	110 to 108	151 to 142	154 to 140	121 to 113	---	---	---	---	---	---	2 St	25 to 26	76 to 74	113 to 112	99 to 98	88 to 88
9-3	5.3	3 Vib 1 St	2 to 5	133 to 127	155 to 151	154 to 150	129 to 127	---	---	---	---	---	---	3 St	15 to 20	110 to 107	132 to 110	127 to 119	109 to 104
9-4	4.5	4 Vib 1 St	1 to 5	122 to 106	131 to 119	131 to 116	111 to 106	---	---	---	---	---	---	3 St	24 to 29	66 to 63	81 to 73	74 to 67	72 to 67

Comp = Compaction   Vib = Vibratory Roller Pass(s)   St = Static Roller Pass(s)   Pn = Pneumatic Roller Pass(s)   Pn-Vib = Vibrating Pneumatic Roller Pass

Table 4.7. Compactive Effort, Timing, and Temperature Summary: Zeiglerville

ID	t (cm)	Breakdown Rolling						Intermediate Rolling						Finish Rolling					
		Comp (---)	Time (min)	T_S (C)	T_U (C)	T_M (C)	T_B (C)	Comp (---)	Time (min)	T_S (C)	T_U (C)	T_M (C)	T_B (C)	Comp (---)	Time (min)	T_S (C)	T_U (C)	T_M (C)	T_B (C)
2-1	5.9	11 Vib	4 to 64	135 to 79	168 to 104	170 to 101	160 to 96	---	---	---	---	---	---	---	---	---	---	---	---
2-2	6.9	6 Vib 2 St	4 to 56	117 to 78	155 to 96	154 to 91	143 to 87	---	---	---	---	---	---	---	---	---	---	---	---
2-3	5.6	5 Vib 1 St	4 to 34	118 to 82	151 to 109	152 to 104	139 to 100	---	---	---	---	---	---	---	---	---	---	---	---
2-4	4.1	7 Vib 2 St	4 to 63	133 to 74	133 to 91	149 to 84	133 to 82	---	---	---	---	---	---	---	---	---	---	---	---
5-1	5.8	6 Vib 2 St	2 to 11	134 to 104	--- to ---	144 to 113	154 to 105	5 Pn-Vib	26 to 29	--- to ---	84 to 83	85 to 82	77 to 74	1 St	32	76	---	77	71
5-2	3.8	5 Vib	10 to 20	108 to 88	109 to 71	114 to 87	121 to 89	5 Pn-Vib	31 to 34	79 to 73	66 to 62	63 to 62	77 to 74	2 St	47 to 49	73 to 73	58 to 58	59 to 56	67 to 66
5-3	4.1	7 Vib	5 to 14	137 to 109	146 to 111	103 to 83	113 to 101	4 Pn-Vib	16 to 20	106 to 99	106 to 96	82 to 84	98 to 94	1 St	35	84	77	69	81
7-1	4.2	6 Vib 1 St	3 to 13	121 to 99	137 to 111	149 to 103	138 to 99	4 Pn-Vib	25 to 27	82 to 74	83 to 79	--- to ---	81 to 79	1 St	35	68	71	---	72
7-2	4.4	7 Vib	5 to 12	136 to 109	124 to 99	142 to 109	148 to 109	5 Pn-Vib	17 to 19	96 to 89	90 to 86	94 to 88	98 to 91	2 St	24 to 25	80 to 80	78 to 78	78 to 78	83 to 81
7-3	4.0	7 Vib	4 to 12	143 to 110	130 to 103	131 to 107	162 to 119	5 Pn-Vib	26 to 29	88 to 78	83 to 80	84 to 81	90 to 86	1 St	33	74	76	77	81
7-4	4.2	6 Vib	7 to 23	139 to 102	122 to 93	155 to 101	162 to 104	4 Pn-Vib	24 to 27	97 to 94	92 to 89	100 to 95	103 to 98	1 St	30	88	87	91	94

Comp = Compaction   Vib = Vibratory Roller Pass(s)   St = Static Roller Pass(s)   Pn = Pneumatic Roller Pass(s)   Pn-Vib = Vibrating Pneumatic Roller Pass

Figure 4.2 plots project 1-1 accumulated compaction pressure versus in place air voids measured by a nuclear density gauge that had been offset using cores cut from each section. A linear trendline was fit to the data and made in the form of Eq. 4.1. All forty-four test locations were evaluated with results presented in Table 4.8. Eq. 4.1 was re-arranged so that C_1 could be represented as a positive number, rather than a negative number as shown in Figure 4.2. The final in place air voids predicted by Eq. 4.1 are denoted $V_{a(ACP)}$ as they occur when ACP_i is maximized (i.e. compaction is complete).

$$V_a = C_2 - C_1(ACP_i) \qquad (4.1)$$

Where,

V_a = in place air voids
ACP_i = accumulated compaction pressure to point (i) calculated using Eq. 2.1
C_1 = slope of ACP_i versus V_a plot
C_2 = intercept of ACP_i versus V_a plot

The intercept of the ACP_i versus V_a plot (C_2) did not typically align with the field measured density prior to compaction (i.e. $ACP_i = 0$). Figure 4.2 did not plot $ACP_i = 0$ as there was usually a significant air void reduction between $ACP_i = 0$ and the first roller pass ($ACP_i > 0$), which is an expected result. Behind the screed air voids (i.e. $ACP_i = 0$) were presented in Table 4.8 alongside C_2. Table 4.8 values are used later in the report to assess field compactability. The wide range of ACP, C_1, and $V_{a(ACP)}$ between and within some projects should be noted.
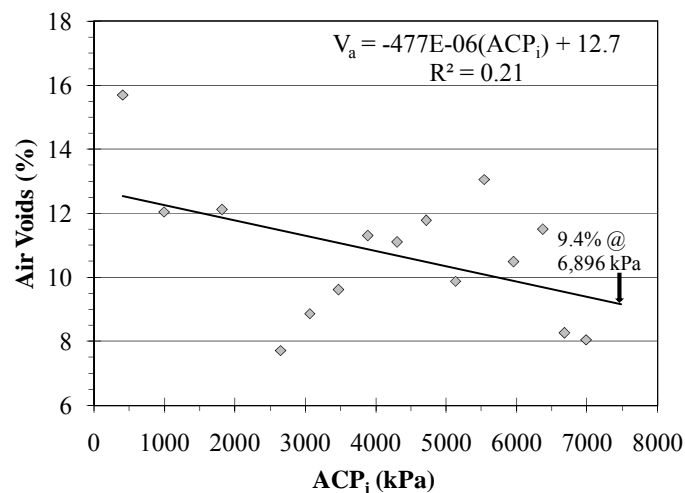
Figure 4.2. Air Voids vs. Compaction Measured in Place for Project 1, Location 1

Table 4.8. ACP Versus Nuclear Density Measured In Place Air Voids

Gravel Source	Proj.	Loc.	ACP (kPa)	C_1 (10^{-6})	C_2 (%)	R^2 (---)	$V_{a(ACP)}$ (%)	V_a ($ACP_i = 0$) (%)	V_a (T 166) (%)
Crystal Springs	6	1	6,155	201	6.0	0.03	4.8	13.2	5.3
		2	6,712	78	5.2	0.01	4.7	16.0	5.5
		3	6,827	770	12.2	0.41	6.9	21.3	5.7
		4	6,004	771	7.6	0.53	3.0	20.4	4.6
	10	1	3,188	1180	8.5	0.66	4.7	13.3	6.6
		2	2,864	-176	4.5	0.01	5.0	10.8	5.0
		3	2,864	1300	9.5	0.86	5.8	13.7	7.1
	11	1	7,676	851	11.3	0.69	4.8	17.9	6.7
		2	12,527	174	8.7	0.12	6.5	15.0	7.0
		3	5,884	653	11.2	0.44	7.4	18.7	7.3
		4	8,340	109	4.6	0.03	3.7	12.0	5.3
Hazlehurst	3	1	4,975	-7	9.8	0.00	9.8	19.0	10.9
		2	4,310	1410	11.1	0.50	5.0	18.0	7.8
		3	4,310	305	7.7	0.35	6.4	16.5	7.5
		4	4,310	911	16.3	0.33	12.4	23.1	12.3
	4	1	3,645	1070	12.0	0.86	8.1	20.0	7.7
		2	4,324	938	8.8	0.27	4.7	12.1	6.9
		3	4,353	195	6.2	0.05	5.4	13.1	6.6
		4	3,645	-46	5.3	0.01	5.5	13.1	7.0
	12	1	1,273	2260	13.7	0.51	10.8	19.6	11.0
		2	1,350	2470	16.8	0.45	13.5	17.4	13.8
		3	1,081	1010	15.4	0.12	14.3	19.1	14.2
Scribner	1	1	6,896	477	12.7	0.21	9.4	25.1	7.3
		2	12,706	299	15.5	0.18	11.7	24.6	8.4
		3	10,130	15	13.0	0.00	12.8	19.8	11.9
		4	8,889	417	16.5	0.38	12.8	24.6	12.9
	8	1	3,460	1420	13.9	0.40	9.0	25.2	10.3
		2	3,121	3010	17.2	0.67	7.8	26.7	10.0
		3	2,510	3760	17.6	0.95	8.2	22.8	7.2
	9	1	4,044	-126	8.0	0.03	8.5	19.5	8.9
		2	2,964	519	6.9	0.12	5.4	17.3	6.9
		3	3,324	1610	12.4	0.64	7.0	16.1	8.1
		4	4,179	1820	15.7	0.77	8.1	21.4	8.6
Zeiglerville	2	1	9,092	407	9.1	0.63	5.4	16.3	6.7
		2	5,345	117	9.4	0.97	8.8	15.6	6.1
		3	4,101	499	11.2	0.85	9.2	18.3	9.4
		4	6,236	400	9.1	0.23	6.6	15.7	8.1
	5	1	6,061	296	12.6	0.12	10.8	24.6	9.9
		2	5,789	-539	9.4	0.06	12.5	18.9	8.9
		3	6,445	468	10.4	0.40	7.4	23.1	8.4
	7	1	6,174	368	7.1	0.23	4.8	13.7	6.3
		2	7,202	559	9.4	0.17	5.4	18.9	4.9
		3	6,879	383	5.6	0.13	3.0	15.7	5.2
		4	5,738	643	9.7	0.29	6.0	18.3	7.0

Note: ID 5-2 showed compaction to noticeably increase air voids.

Table 4.9 compares field core thicknesses to MDOTs supplement to Special Provision No. 907-401-2 dated 06/25/2009 where allowable thicknesses ranges are provided for a given NMAS. Design layer thicknesses are also provided for reference. Projects 9, 10, 11, and 12 were not performed for MDOT.

Table 4.9. Layer Thickness Comparison: Measured to SP 907-401-2 Supplement

Gravel Source	Proj.	Loc.	Design (cm)	907-401-2 Range (cm)	t (cm)	t_R (cm)
Crystal Springs	6	1	3.8	3.8 to 6.4	3.6	-0.2
		2			4.9	0.0
		3			7.2	+0.8
		4			6.0	0.0
	10	1	10.1	5.7 to 8.9	10.4	+1.5
		2			9.2	+0.3
		3			9.4	+0.5
	11	1	5.1	2.5 to 3.8	6.7	+2.9
		2			5.6	+1.8
		3			5.3	+1.5
		4			5.0	+1.2
Hazlehurst	3	1	6.4	3.8 to 6.4	4.1	0.0
		2			6.7	+0.3
		3			5.6	0.0
		4			4.1	0.0
	4	1	6.4	3.8 to 6.4	4.7	0.0
		2			5.6	0.0
		3			5.9	0.0
		4			4.6	0.0
	12	1	3.8	3.8 to 6.4	3.8	0.0
		2			3.1	-0.7
		3			3.4	-0.4
Scribner	1	1	3.8	2.5 to 3.8	5.8	+2.0
		2			4.6	+0.8
		3			6.2	+2.4
		4			6.6	+2.8
	8	1	3.8	2.5 to 3.8	5.8	+2.0
		2			3.7	0.0
		3			4.0	+0.2
	9	1	3.8	2.5 to 3.8	3.0	0.0
		2			3.5	0.0
		3			5.3	+1.5
		4			4.5	+0.7
Zeiglerville	2	1	3.8	3.8 to 6.4	5.9	0.0
		2			6.9	+0.5
		3			5.6	0.0
		4			4.1	0.0
	5	1	3.8	2.5 to 3.8	5.8	+2.0
		2			3.8	0.0
		3			4.1	+0.3
	7	1	3.8	2.5 to 3.8	4.2	+0.4
		2			4.4	+0.6
		3			4.0	+0.2
		4			4.2	+0.4

The term t_R was introduced in Table 4.9 and is the distance in centimeters the average core thickness at a location deviated from the 907-401-2 range for the NMAS used. If the average thickness was within the allowable range, 0 was entered. Negative values indicate core thicknesses below the allowable range and positive values indicate core thicknesses above the allowable range.

Three of the forty-four locations were thinner than the range given in 907-401-2. Project 12 Location 2 was considerably thinner than the 907-401-2 lower bound. Projects 1, 10, and 11 were noticeably thicker than the 907-401-2 range. All four non-MDOT projects were placed outside the 907-401-2 recommended range.

Table 4.10 provides the remaining field data collected. The specified air void content was 8% on all projects where the specification could be located, and mainline paving was the primary case encountered. Rainfall occurred prior to mix production on four of the twelve projects.

Table 4.10. Miscellaneous Construction Data Collected

Project	Rainfall	Specified V_a (%)	Construction Type
1	1 day prior	8	Mainline
2	-	8	Mainline
3	-	8	Shoulder
4	-	8	Mainline
5	1 day prior	8	Mainline
6	-	8	Mainline
7	1 day prior	8	Mainline
8	-	8	Mainline
9	-	8	Mainline
10	-	8	Mainline
11	-	8	Mainline
12	2 days prior (1 production day)	Unknown	Mainline (1,3) Turnout (2)

4.3   Comparison of Measured Field Conditions to PaveCool 2.4

PaveCool 2.4 (Chadboum et al. 1998) was used to account for conditions at each test location to determine if the asphalt mixture under investigation was constructed in a reasonable environment. The goal of this project focused on investigating behaviors of mixes compacted in a manner that gives them a reasonable opportunity to perform well. Environmental or construction practices outside of reasonable expectations are not attributable to the asphalt mixture being used, and as a result, any locations where the conditions were not deemed reasonable should be identified.

All calculations used a latitude of 32^0, and the delivery temperature was taken as the average temperature behind the screed measured with thermocouples (i.e. the average of T_U, T_M, and T_B). In a few instances, air or base temperatures were extrapolated from values measured at other times during the day, and during two

instances, the delivery temperature was taken as T_S when T_U, T_M, and T_B were not available. All simulations were performed with the time set to July 1 at noon since dates and times were not recorded for the projects (dates were recorded but not times). Wind conditions were set to the upper end observed on site. The few assumptions made for PaveCool 2.4 inputs are believed to be reasonable for the intent of the analysis performed.

Appendix A plots PaveCool 2.4 test results for all forty-four test locations alongside measured temperature and timing parameters recorded during construction. Each plot has a solid line representing the cooling curve predicted by PaveCool 2.4, alongside a vertical dashed line at the recommended temperature to cease compaction. The cessation temperature for the project was selected as the default value of 80 $^{\circ}$C for PG 58 and higher binder grades. The researchers do not suggest this default value is correct for all mixtures and conditions; however, the default value was utilized and should be reasonable. Analysis of the data is presented in Chapter 6 where the data presented in Appendix A is interpreted.

Measured temperature and timing parameters that occurred during construction were presented in the Appendix A figures as follows. The average of T_U, T_M, and T_B was plotted versus the beginning and ending time of a given compaction type and denoted with a unique marker. All data necessary to produce the measured values in Appendix A were provided in Tables 4.4 to 4.7. As an example, the two breakdown roller data points in Figure A.1a are (6 min, avg[146 $^{\circ}$C, 119 $^{\circ}$C, 93 $^{\circ}$C]), or (6, 119.3) and (10, 114.3).

CHAPTER 5 – LABORATORY TEST RESULTS

5.1   Overview of Laboratory Test Results

The laboratory data collected as part of this project is discussed in this chapter by topic where results are presented and observations made regarding the data type of interest without regard for the entire data set. This data is analyzed in conjunction with all project data (field and laboratory) in chapter 6. The analysis was performed in this manner due to the large amount and diverse types of data collected in this study.

5.2   Fundamental and Consensus Properties

Tables 5.1 through 5.4 contain fundamental and consensus aggregate property test results for cold feed specimens. Tests conducted include: flat and elongated particles using a 5:1 ratio (ASTM D4791) referred to as $P_{F\&E}$; coarse aggregate angularity (ASTM D5821) referred to by a percentage of a given number (0, 1, or 2) of fractured faces (FF) and referred to as FF_0, FF_1, or FF_2; Atterberg liquid and plastic limits (AASHTO T89 and T90), fine aggregate bulk specific gravity (AASHTO T84), fine aggregate angularity (ASTM C1252), and sand equivalency (AASHTO T176) referred to as SE. Sampling and test procedures were discussed previously.

No meaningful difference was observed with respect to percentage of flat and elongated particles for all test specimens. Coarse aggregate angularity for Crystal Springs gravel was determined to be slightly lower than other gravel sources. Project 10 specimens contained the lowest percentage of fractured particles due to incorporating uncrushed, washed gravel. All cold feed specimens were found to be non-plastic (NP). Fine aggregate angularity was found to range from 38.0 to 46.4. Sand equivalent test results ranged from 34 to 99 with the average of all results being 75. Overall, the lowest sand equivalent values were obtained for Project 7, which are significantly lower than other projects. The average sand equivalent value of 44 for Project 7 would be slightly below most specification requirements of 45.

Table 5.1. Fundamental and Consensus Properties for Crystal Springs

ID	$P_{F\&E}$	FF_0 (%)	FF_1 (%)	FF_2 (%)	PI	G_{sb}	FAA	SE
6-1	0.0	5.7	95.3	84.0	NP	2.514	40.9	79
6-2	0.0	9.3	90.6	83.7	NP	2.510	41.1	99
6-3	0.0	11.7	88.3	77.2	NP	2.519	39.3	84
Avg	*0.0*	*8.9*	*91.4*	*81.6*	*NP*	*2.514*	*40.4*	*87*
10-1	0.0	35.0	65.0	44.2	NP	2.521	38.8	86
10-2	0.0	17.7	82.3	66.5	NP	2.548	39.2	83
10-3	0.0	48.2	51.8	41.8	NP	2.522	38.0	83
Avg	*0.0*	*33.6*	*66.4*	*50.8*	*NP*	*2.530*	*38.6*	*84*
11-1	1.4	5.2	94.8	86.2	NP	2.624	43.5	70
11-2	2.4	7.8	92.0	78.6	NP	2.587	42.6	67
11-3	1.1	6.6	93.4	82.7	NP	2.610	43.9	65
11-4	1.6	8.8	91.2	79.2	NP	2.605	42.7	68
Avg	*1.6*	*7.1*	*92.9*	*81.7*	*NP*	*2.607*	*43.1*	*68*

Table 5.2. Fundamental and Consensus Properties for Hazlehurst

ID	$P_{F\&E}$	FF_0 (%)	FF_1 (%)	FF_2 (%)	PI	G_{sb}	FAA	SE
3-1	0.0	1.4	98.5	94.8	NP	2.380	41.2	78
3-2	0.0	5.2	94.8	94.4	NP	2.323	39.4	87
3-3	0.2	3.9	96.1	91.2	NP	2.350	42.4	80
3-4	0.0	3.6	96.4	92.8	NP	2.325	43.2	84
Avg	*0.1*	*3.5*	*96.4*	*93.3*	*NP*	*2.345*	*41.5*	*83*
4-1	1.5	1.5	98.4	95.1	NP	2.400	42.7	84
4-2	1.0	4.9	95.1	89.0	NP	2.421	41.5	79
4-3	1.1	0.8	99.2	90.3	NP	2.372	42.0	77
4-4	0.0	5.2	94.8	86.6	NP	2.341	41.5	80
Avg	*0.9*	*3.1*	*96.9*	*89.1*	*NP*	*2.384*	*41.9*	*80*
12-1	0.0	0.0	100.0	84.5	NP	2.395	46.4	60
12-2	0.0	1.4	98.6	94.4	NP	2.410	44.8	62
12-3	0.0	1.7	98.3	82.7	NP	2.403	46.0	68
Avg	*0.0*	*1.0*	*99.0*	*87.2*	*NP*	*2.403*	*45.7*	*63*

Table 5.3. Fundamental and Consensus Properties for Scribner

ID	$P_{F\&E}$	FF_0 (%)	FF_1 (%)	FF_2 (%)	PI	G_{sb}	FAA	SE
1-1	0.0	1.2	98.8	97.0	NP	---	42.9[a]	97
1-2	0.0	1.1	98.9	96.3	NP	---	41.9[a]	81
1-3	0.0	0.6	99.4	96.1	NP	---	42.7[a]	92
1-4	0.0	1.8	98.2	96.5	NP	---	40.3[a]	85
Avg	*0.0*	*1.2*	*98.8*	*96.5*	*NP*	*---*	*41.9*	*89*
8-1	0.0	2.7	97.3	92.6	NP	---	41.6[b]	92
8-2	0.5	3.4	96.6	90.5	NP	2.403	41.5	74
8-3	1.0	2.5	97.5	93.2	NP	---	41.3[b]	79
Avg	*0.5*	*2.9*	*97.1*	*92.1*	*NP*	*2.403*[b]	*41.5*	*82*
9-1	1.4	4.8	95.2	89.3	NP	2.401	39.5	73
9-2	0.7	5.6	94.4	89.7	NP	2.411	40.7	86
9-3	1.1	4.8	95.2	88.6	NP	2.400	39.1	75
9-4	1.5	3.0	96.9	90.2	NP	2.414	40.1	60
Avg	*1.2*	*4.6*	*95.4*	*89.5*	*NP*	*2.407*	*39.8*	*74*

a: estimated value based on Project 9 average G_{sb} (same aggregate blend as Project 1)
b: estimated value based on 8-2 G_{sb}.

Table 5.4. Fundamental and Consensus Properties for Zeiglerville

ID	$P_{F\&E}$	FF_0 (%)	FF_1 (%)	FF_2 (%)	PI	G_{sb}	FAA	SE
2-1	0.0	1.5	98.5	97.2	NP	2.428	43.6	77
2-2	0.0	0.9	99.1	99.1	NP	2.386	43.3	75
2-3	0.4	3.0	97.0	97.0	NP	2.401	44.8	82
2-4	0.5	1.0	99.0	99.0	NP	2.383	44.3	76
Avg	*0.2*	*1.6*	*98.4*	*98.1*	*NP*	*2.400*	*44.0*	*78*
5-1	0.0	9.7	90.3	86.1	NP	2.432	41.7[a]	74
5-2	0.0	0.6	99.4	98.1	NP	---	40.9[a]	66
5-3	0.0	13.2	86.9	84.3	NP	2.446	40.6[a]	67
Avg	*0.0*	*7.8*	*92.2*	*89.5*	*NP*	*2.439*	*41.0*	*69*
7-1	0.9	3.8	96.2	89.5	NP	2.422	38.3	46
7-2	1.5	2.7	97.3	92.5	NP	2.379	40.0	50
7-3	1.3	3.6	96.4	92.6	NP	2.458	43.6	44
7-4	1.3	2.2	97.8	93.7	NP	2.431	43.4	34
Avg	*1.3*	*3.1*	*96.9*	*92.1*	*NP*	*2.423*	*41.3*	*44*

a: value based on 5-1 and 5-2 average G_{sb}.

5.3 Adhered Fines and SEM Test Results

Table 5.5 contains adhered fines test results for the stockpile gravel sources. No meaningful differences were observed with the 5711, 9.5 mm, and 4.75 mm test data indicating that particles in this size range could be represented by the 5711 approach that combines 4.75 and 9.5 mm particles. Material between 2.36 and 4.75 mm, however, had more adhered fines than material retained on the 4.75 mm sieve. When the entire gradation was considered, adhered fines increased relative to the material retained on the 2.36 mm sieve, but the magnitude of the increase varied between aggregate sources.

Table 5.5. Adhered Fines Test Results for Coarse Aggregate Gravel Sources

Aggregate Source	Project	$P_{0.075}$	NMAS (mm)	$P_{Adh(\%)}$- All	$P_{Adh(\%)}$- 5711	$P_{Adh(\%)}$- 9.5 mm	$P_{Adh(\%)}$- 4.75 mm	$P_{Adh(\%)}$- 2.36 mm
Crystal Springs	Prelim	3.6	12.5	1.6	---	---	---	---
	6	2.6	12.5	0.8	0.55	0.81	0.49	0.77
	10	---	Washed	---	0.30	0.28	0.23	0.36
	10	2.6	12.5	1.0	0.19	0.18	0.31	0.60
	10	0.8	12.5-25.0	0.4	0.44	0.46	0.63	---
	11	2.9	12.5	2.3	0.53	0.34	0.47	0.80
	Avg^a	*2.5*	*---*	*1.2*	*0.4*	*0.5*	*0.5*	*0.7*
Hazlehurst	Prelim	5.3	12.5	2.3	---	---	---	---
	3	5.4	19.0	2.7	0.84	0.80	0.89	1.50
	3	5.6	12.5	2.9	0.84	0.73	0.85	1.55
	4	4.4	19.0	2.2	0.74	0.73	0.67	1.25
	4	5.2	12.5	2.9	0.86	1.07	0.69	1.36
	12	4.8	12.5	1.9	0.60	0.89	0.55	0.85
	Avg	*5.1*	*---*	*2.5*	*0.8*	*0.8*	*0.7*	*1.3*
Scribner	Prelim	5.6	12.5	2.6	---	---	---	---
	1	3.9	12.5	1.1	0.74	0.50	0.65	1.35
	8	4.5	12.5	1.8	0.66	0.78	0.60	0.86
	9	3.7	12.5	1.3	0.76	0.81	0.67	1.23
	Avg	*4.4*	*---*	*1.7*	*0.7*	*0.7*	*0.6*	*1.2*
Zeiglerville	Prelim	4.0	12.5	1.9	---	---	---	---
	2	3.1	12.5	1.0	0.65	0.53	0.82	1.52
	2	2.6	19.0	1.1	0.77	0.94	0.73	1.07
	5	4.0	12.5	1.7	0.54	---	0.51	0.70
	7	4.0	12.5	1.8	0.72	1.19	0.76	1.71
	Avg	*3.5*	*---*	*1.5*	*0.7*	*0.9*	*0.7*	*1.3*

a: project 10 washed material was not included in the averages.

Hazlehurst had the most adhered fines, Zeiglerville and Scribner had essentially the same amount of adhered fines, and Crystal Springs had the least adhered fines. Total fines content ($P_{0.075}$) followed the same order as adhered fines. Figure 5.1 plots the P_{Adh} to $P_{0.075}$ ratio for the three adhered fines methods deemed most promising earlier in this section. Table 5.6 contains average values for all projects using the Figure 5.1 data.

a) Crystal Springs   b) Hazlehurst

c) Scribner   d) Zeiglerville
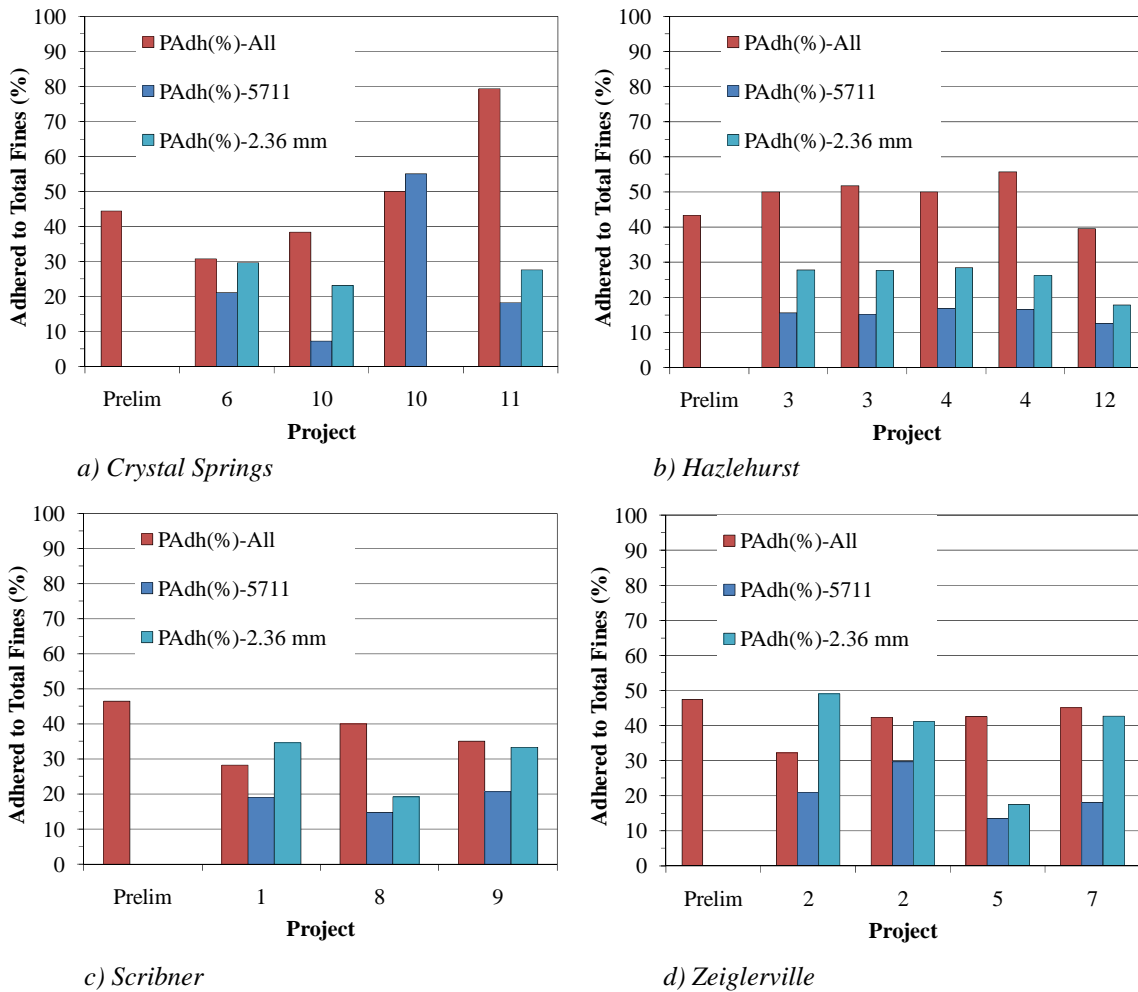
Figure 5.1. Adhered Fines Test Results for Gravel Sources

Table 5.6. Average Adhered to Total Fines Test Results

Gravel Source	$P_{Adh(\%)-All}$	$P_{Adh(\%)-5711}$	$P_{Adh(\%)-2.36 mm}$
Crystal Springs	48.6	25.4	26.8
Hazlehurst	48.4	15.3	25.5
Scribner	37.4	18.1	29.0
Zeiglerville	41.9	20.5	37.6

Table 5.7 contains adhered fines test results from cold feed samples taken at each project. The total fines content for many of the projects appears to be low when compared to design and mixture values, possibly due to sampling error. The research team obtained some of the cold feed samples, while other samples were taken by asphalt plant staff. It appears that a considerable amount of fine particles remained on the cold feed belt after sampling on some projects.

Table 5.7. Adhered Fines Cold Feed Test Results

Gravel Source	Proj.	Loc.	$P_{0.075}$	$P_{Adh(\%)\text{-}All}$
Crystal Springs	6	1	2.1	0.8
		2	2.1	0.8
		3	2.2	1.2
		4	---	---
	10	1	2.2	1.3
		2	2.2	1.2
		3	1.9	0.8
	11	1	8.8	4.9
		2	9.5	5.0
		3	9.5	5.8
		4	8.1	4.2
Hazlehurst	3	1	2.4	1.3
		2	2.6	1.2
		3	2.8	1.3
		4	3.3	1.8
	4	1	2.0	0.9
		2	2.8	1.5
		3	2.1	0.9
		4	1.6	0.7
	12	1	4.0	2.7
		2	3.7	---
		3	3.6	---
Scribner	1	1	2.6	1.2
		2	3.0	1.6
		3	2.2	1.0
		4	5.3	1.8
	8	1	4.3	1.6
		2	3.2	1.5
		3	4.0	1.4
	9	1	5.2	2.9
		2	5.9	2.1
		3	5.1	2.8
		4	5.4	2.5
Zeiglerville	2	1	4.6	2.4
		2	4.4	2.3
		3	3.9	2.1
		4	3.4	1.7
	5	1	3.7	2.0
		2	4.1	2.4
		3	3.4	2.3
	7	1	4.1	2.5
		2	4.1	2.7
		3	4.1	3.0
		4	4.6	2.7

Appendix B contains all SEM images obtained for the project. These images were not intended for stand alone analysis, rather for visual evidence to be used to

support or refute trends observed with other data. The SEM images are used as appropriate in Chapter 6.

5.4   Methylene Blue Test Results

Table 5.8 contains methylene blue test results for gravel stockpiles and cold feed samples. The methylene blue test was conducted in accordance with AASHTO TP 57. Testing was performed on $P_{0.075}$ material, taken from the wash portion of a representative sample of the stockpile or cold feed belt material. Details of the test procedure were previously discussed in Chapter 3. Each result reported in Table 5.1 is based upon the average of two test replicates.

The expected performance of Scribner gravel would be excellent based upon the criteria in Table 3.3. The expected performance of Crystal Springs and Hazlehurst gravels ranged from excellent to marginally acceptable. Zeiglerville gravel would be expected to be problematic or fail.

In most cases, test results from cold feed samples show an improvement when each source is combined with other materials. The greatest improvement was observed with Zeiglerville gravel. Based on cold feed results, excellent performance would be expected for all aggregate blends utilizing Hazlehurst, Scribner, and Zeiglerville gravels. Marginal performance would be expected for aggregate blends utilizing Crystal Springs gravel. Graphical representation of stockpile and average cold feed MBV for each source is presented if Figure 5.2.

Table 5.8. Methylene Blue Value for Gravel Stockpiles and Cold Feed Samples

Aggregate Source	Project	Stockpile NMAS (mm)	MBV	Cold Feed Sample No.	MBV
Crystal Springs	6	19.0	4.00	1	7.00
	6	12.5	4.00	2	6.50
	6	---	---	3	7.00
	10	Washed	---	1	8.50
	10	12.5-25.0	---	2	6.75
	10	12.5	4.50	3	6.25
	11	12.5	9.50	1	8.75
	11	---	---	2	7.75
	11	---	---	3	8.00
	11	---	---	4	8.00
	Avg	**---**	**5.50**	**---**	**7.45**
Hazlehurst	3	19.0	4.00	1	1.75
	3	12.5	4.00	2	1.50
	3	---	---	3	1.75
	3	---	---	4	1.00
	4	19.0	4.00	1	3.00
	4	12.5	4.00	2	6.75
	4	---	---	3	2.75
	4	---	---	4	1.50
	12	19.0	7.75	1	1.00
	12	12.5	5.75	2	1.75
	12	---	---	3	3.00
	Avg	---	**4.92**	---	**2.34**
Scribner	1	12.5	3.50	1	1.00
	1	---	---	2	1.50
	1	---	---	3	1.50
	1	---	---	4	4.50
	8	12.5	3.75	1	1.00
	8	---	---	2	2.75
	8	---	---	3	0.50
	9	12.5	1.00	1	1.00
	9	---	---	2	2.00
	9	---	---	3	0.50
	9	---	---	4	1.50
	Avg	---	**2.75**	**---**	**1.61**
Zeiglerville	2	19.0	>20	1	4.50
	2	12.5	>20	2	3.50
	2	---	---	3	3.50
	2	---	---	4	4.00
	5	12.5	9.00	1	0.50
	5	---	---	2	0.50
	5	---	---	3	0.50
	7	12.5	19.50	1	---
	7	---	---	2	3.25
	7	---	---	3	1.50
	7	---	---	4	1.00
	Avg[a]	---	**17.13**	---	**2.28**

a: values of >20 were assumed to be 20.00 for calculation of average value.

a) Crystal Springs

b) Hazlehurst

c) Scribner

d) Zeiglerville
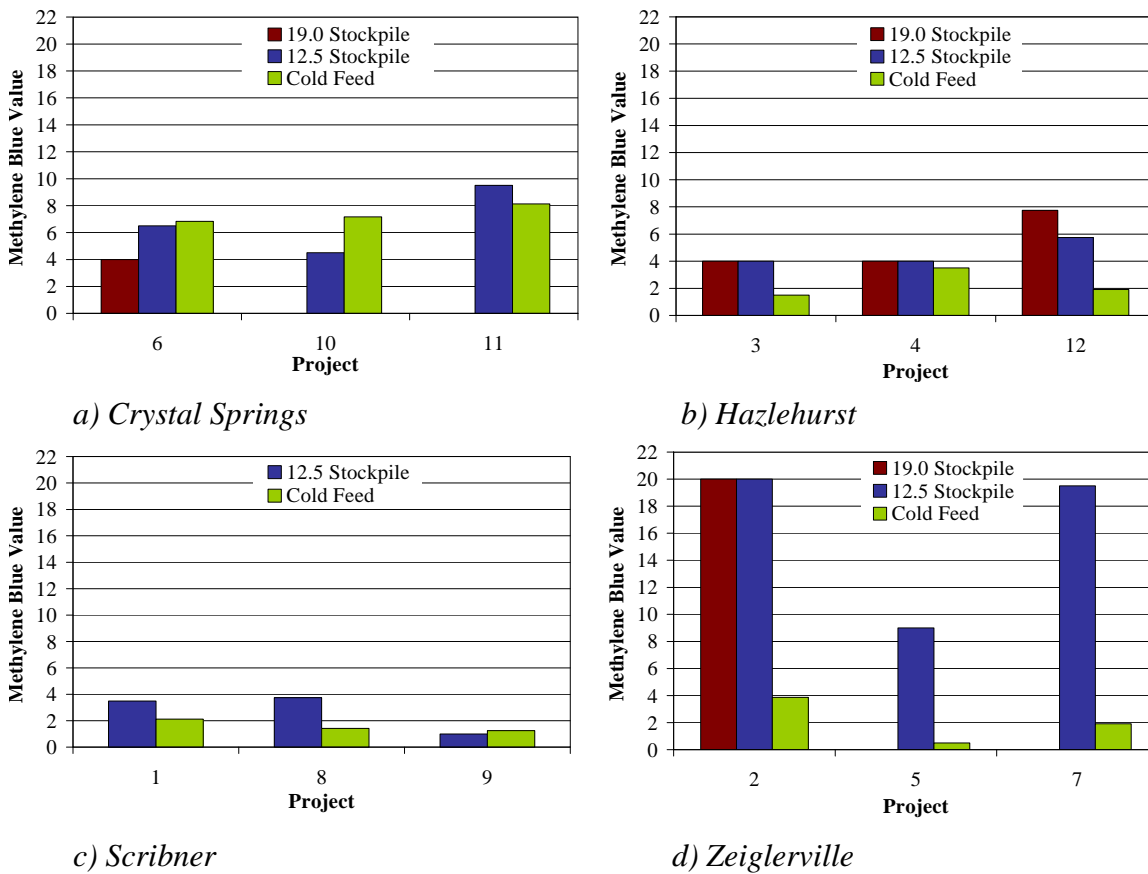
Figure 5.2. Methylene Blue Test Results for Gravel Stockpiles and Cold Feeds

5.5   Gradation Test Results

Tables 5.9 through 5.12 contain gradation test results from cold feed, plant produced mix, and roadway core specimens obtained for each project location. Cold feed gradations were performed in accordance with AASHTO T11 and T27. Plant produced mixture and pavement core gradations were determined as per AASHTO T30 following determination of asphalt content in accordance with AASHTO T308 (Ignition Method). Percentage of aggregate material passing three control sieves (9.5 mm, 2.36 mm, and 0.075 mm) is reported along with the design values for each test location.

The percentage of material passing the 9.5 mm and 2.36 mm sieves for plant mix and roadway cores for each test location appears to be within reasonable tolerance. Both plant mix and roadway cores match design values on the 9.5 mm and 2.36 mm sieves. Percentage passing the 0.075 mm sieve for plant mix and cores did not compare well in many cases. However, both plant mix and core gradations do show that $P_{0.075}$ was low for Project 2 and high for Project 11.

The cold feed fines content for many of the projects appears to be low when compared to design, mixture, and core values, possibly due to sampling error. As

mentioned previously, the research team obtained some of the cold feed samples, while other samples were taken by asphalt plant staff. It appears that a considerable amount of fine particles remained on the cold feed belt after sampling on some projects. Also, cold feed gradations do not include RAP, which was utilized in every mixture included in the research. Therefore, cold feed gradation results should not be compared directly to design target values.

Table 5.9. Gradation (Percent Passing) Test Results: Crystal Springs

ID	9.5 mm				2.36 mm				P$_{0.075}$			
	Mix Design	Cold Feed	Plant Mix	Roadway Core	Mix Design	Cold Feed	Plant Mix	Roadway Core	Mix Design	Cold Feed	Plant Mix	Roadway Core
6-1	74	65	76	---	27	21	32	---	5.1	2.1	5.9	---
6-2	74	59	77	---	27	19	32	---	5.1	2.1	5.7	---
6-3	74	72	74	77	27	30	30	31	5.1	2.2	5.2	4.7
6-4	74	---	76	79	27	---	31	34	5.1	---	5.5	5.2
10-1	71	75	72	78	34	36	37	40	3.1	2.2	2.2	4.3
10-2	71	82	75	71	34	40	41	38	3.1	2.2	1.9	3.8
10-3	71	76	71	67	34	40	36	33	3.1	1.9	1.9	2.9
11-1	97	99	95	95	48	66	52	55	5.8	8.8	7.4	9.1
11-2	97	99	95	92	48	65	53	47	5.8	9.5	7.2	6.9
11-3	97	98	94	93	48	63	53	36	5.8	9.5	5.6	5.6
11-4	97	98	94	95	48	63	53	54	5.8	8.1	7.7	8.9

Table 5.10. Gradation (Percent Passing) Test Results: Hazlehurst

ID	9.5 mm				2.36 mm				P$_{0.075}$			
	Mix Design	Cold Feed	Plant Mix	Roadway Core	Mix Design	Cold Feed	Plant Mix	Roadway Core	Mix Design	Cold Feed	Plant Mix	Roadway Core
3-1	85	88	85	---	36	26	33	---	5.2	2.4	5.4	---
3-2	85	92	90	---	36	50	38	---	5.2	2.6	6.3	---
3-3	85	89	88	90	36	40	36	45	5.2	2.8	6.4	4.9
3-4	85	94	88	---	36	52	36	---	5.2	3.3	5.9	---
4-1	85	87	83	---	36	36	35	---	5.2	2.0	4.8	---
4-2	85	89	89	---	36	37	37	---	5.2	2.8	3.7	---
4-3	85	87	88	---	36	33	39	---	5.2	2.1	5.2	---
4-4	85	87	89	91	36	34	39	41	5.2	1.6	5.6	4.5
12-1	88	89	87	91	39	45	38	39	5.3	4.0	5.1	2.1
12-2	88	85	90	92	39	34	42	44	5.3	3.7	6.5	8.1
12-3	88	85	88	88	39	29	32	39	5.3	3.6	5.1	6.2

Table 5.11. Gradation (Percent Passing) Test Results: Scribner

ID	9.5 mm				2.36 mm				P$_{0.075}$			
	Mix Design	Cold Feed	Plant Mix	Roadway Core	Mix Design	Cold Feed	Plant Mix	Roadway Core	Mix Design	Cold Feed	Plant Mix	Roadway Core
1-1	95	95	94	94	36	31	34	32	6.0	2.6	5.3	6.6
1-2	95	95	93	95	36	30	34	32	6.0	3.0	5.9	6.4
1-3	95	96	96	96	36	29	34	36	6.0	2.2	5.6	6.5
1-4	95	97	95	90	36	35	34	33	6.0	5.3	6.0	5.1
8-1	95	96	96	95	36	28	34	36	6.0	4.3	5.0	7.8
8-2	95	96	95	95	36	20	35	35	6.0	3.2	5.4	6.1
8-3	95	97	94	97	36	23	35	37	6.0	4.0	4.4	6.1
9-1	95	97	96	---	36	41	37	---	6.0	5.2	4.9	---
9-2	95	97	97	---	36	39	38	---	6.0	5.9	5.1	---
9-3	95	97	94	97	36	38	37	37	6.0	5.1	7.0	6.3
9-4	95	96	96	96	36	36	36	35	6.0	5.4	5.3	6.3

Table 5.12. Gradation (Percent Passing) Test Results: Zeiglerville

ID	9.5 mm				2.36 mm				P$_{0.075}$			
	Mix Design	Cold Feed	Plant Mix	Roadway Core	Mix Design	Cold Feed	Plant Mix	Roadway Core	Mix Design	Cold Feed	Plant Mix	Roadway Core
2-1	88	90	86	92	44	45	42	44	6.1	4.6	1.4	5.5
2-2	88	85	87	88	44	38	39	39	6.1	4.4	3.6	3.6
2-3	88	87	89	90	44	39	43	45	6.1	3.9	4.6	4.9
2-4	88	86	91	91	44	40	40	41	6.1	3.4	4.3	4.5
5-1	94	93	93	---	37	33	35	---	5.3	3.7	5.7	---
5-2	94	93	92	---	37	39	35	---	5.3	4.1	5.8	---
5-3	94	93	92	---	37	30	33	---	5.3	3.4	5.6	---
7-1	94	87	93	93	37	30	39	36	5.3	4.1	5.1	5.1
7-2	94	91	92	92	37	32	32	36	5.3	4.1	3.1	5.2
7-3	94	90	93	95	37	31	34	38	5.3	4.1	4.2	5.6
7-4	94	88	92	93	37	27	35	37	5.3	4.6	4.1	5.1

5.6 Moisture Content Test Results

Table 5.13 contains moisture content test results for cold feed and plant produced mixture specimens. Moisture content for cold feed specimens was determined using a convection oven in accordance with AASHTO T265. Mix moisture was determined using the microwave method in accordance with MT-76. Each reported value is based upon a single test result.

The moisture content for all cold feed specimens was found to range between 2.88 and 6.02 percent. Mixture moisture contents were found to range from 0.00 to 0.12 percent. No significant difference was observed between mixture specimens obtained from haul trucks and those obtained from pavers.

Field projects 1, 5, 7, and 12 were conducted one to two days following a rain event. Although it appears rain may have influenced cold feed moisture contents in the case of Projects 1 and 12, it does not appear to have had any effect on mixture moisture content. In general, moisture contents measured for mixtures utilizing Zeiglerville gravel were slightly higher compared to other mixtures.

Table 5.13. Moisture Content of Cold Feed and Mixture Samples

Aggregate Source	ID	Moisture Content, %		
		Cold Feed	Mix - Truck	Mix - Paver
Crystal	6-1	3.25	0.04	0.02
Springs	6-2	3.09	0.02	0.01
	6-3	3.21	0.01	0.01
	6-4	--	0.11	0.05
	Avg	*3.18*	*0.05*	*0.02*
	10-1	3.78	0.06	0.02
	10-2	3.12	0.02	0.02
	10-3	3.36	0.02	0.05
	Avg	*3.42*	*0.03*	*0.03*
	11-1	4.63	0.03	0.03
	11-2	4.72	0.03	0.03
	11-3	4.18	0.05	0.03
	11-4	4.20	0.09	0.03
	Avg	*4.43*	*0.05*	*0.03*
Hazlehurst	3-1	3.74	0.00	0.04
	3-2	4.07	0.00	0.00
	3-3	4.02	0.04	0.00
	3-4	4.16	0.00	0.00
	Avg	*4.00*	*0.01*	*0.01*
	4-1	4.36	0.00	0.00
	4-2	4.13	0.02	0.00
	4-3	4.38	0.02	0.00
	4-4	4.23	0.03	0.02
	Avg	*4.28*	*0.02*	*0.00*
	12-1	5.56	0.01	0.03
	12-2	5.64	0.03	0.03
	12-3	5.61	0.01	0.02
	Avg	*5.60*	*0.02*	*0.02*
Scribner	1-1	6.02	0.00	0.00
	1-2	5.51	0.01	0.04
	1-3	5.40	0.02	0.03
	1-4	5.51	0.03	0.04
	Avg	*5.61*	*0.02*	*0.03*
	8-1	3.01	0.02	0.01
	8-2	3.50	0.06	0.04
	8-3	2.88	0.04	0.02
	Avg	*3.13*	*0.04*	*0.03*
	9-1	3.36	0.02	0.04
	9-2	3.58	0.03	0.02
	9-3	3.45	0.03	0.02
	9-4	3.46	0.02	0.02
	Avg	*3.46*	*0.02*	*0.02*
Zeiglerville	2-1	3.90	0.06	0.09
	2-2	3.50	0.11	0.10
	2-3	3.50	0.10	0.11
	2-4	3.30	0.08	0.11
	Avg	*3.55*	*0.09*	*0.10*
	5-1	3.23	0.11	0.04
	5-2	3.08	0.06	0.03
	5-3	3.17	0.05	0.02
	Avg	*3.13*	*0.07*	*0.03*
	7-1	4.20	0.11	0.10
	7-2	3.80	0.12	0.08
	7-3	4.00	0.08	0.11
	7-4	3.40	0.03	0.08
	Avg	*3.85*	*0.08*	*0.09*

5.7   Plant Mix and Core Mixture Properties

Tables 5.14 through 5.17 contain mix property test results for plant produced mix and pavement cores. Design and measured values presented include asphalt content, G_{mm}, and G_{se}. Core results are based on mixture obtained from combining TSR control specimens. Values presented for asphalt content are based on a single test result performed in accordance with AASHTO T308 (Ignition Method) with no calibration factor or moisture correction applied. The calibration factor for the particular ignition furnace utilized in the research as been found to be insignificant for most aggregate materials tested. Test results for G_{mm} are based upon a single test conducted in accordance with AASHTO T209. G_{se} was calculated using Eq. 5.1.

$$G_{se} = (100-P_{AC}) / [(100/G_{mm}) - (P_{AC}/G_b)] \hspace{2cm} (5.1)$$

Table 5.14 shows a reasonable comparison between plant mix and pavement core properties for mixtures utilizing Crystal Springs gravel. Both asphalt content and G_{mm} are near design values for Projects 6 and 10. However, Project 11 was determined to have an asphalt content below optimum, which was supported by G_{mm} results being higher than the design value.

Table 5.14. Asphalt Mixture Properties for Crystal Springs

ID	Asphalt Content			G_{mm}			G_{se}		
	Design	Mix	Cores	Design	Mix	Cores	Design	Mix	Cores
6-1		4.96	*a*		2.409	2.406		2.588	*a*
6-2		5.11	*a*		2.406	2.395		2.590	*a*
6-3		5.12	5.33		2.416	2.407		2.603	2.600
6-4		5.11	5.24		2.407	2.413		2.591	2.604
Avg	*5.30*	*5.08*	*5.28*	*2.404*	*2.410*	*2.405*	*2.595*	*2.593*	*2.602*
10-1		5.25	5.53		2.402	2.389		2.591	2.586
10-2		5.43	5.12		2.386	2.382		2.579	2.561
10-3		4.85	4.62		2.397	2.413		2.569	2.579
Avg	*4.70*	*5.32*	*5.09*	*2.400*	*2.395*	*2.395*	*2.566*	*2.579*	*2.575*
11-1		5.75	5.92		2.414	2.401		2.627	2.618
11-2		5.27	5.35		2.410	2.409		2.602	2.604
11-3		5.78	5.51		2.405	2.396		2.617	2.594
11-4		5.80	5.73		2.404	2.397		2.616	2.605
Avg	*6.10*	*5.65*	*5.63*	*2.374*	*2.408*	*2.401*	*2.591*	*2.615*	*2.605*

a: cores were damaged/destroyed

Table 5.15 shows plant mix and core properties for mixes utilizing Hazlehurst gravel. Plant mix asphalt content for specimens 3-3, 4-4, 12-2, and 12-3 did not compare well with core results. Core asphalt content for 12-2 appears to be unreasonably high while plant mixture asphalt content for 12-3 appears to be unreasonably low. However, the G_{mm} obtained for each location supports the measured asphalt content. Plant mix G_{mm} for Project 3 is consistently lower than the design value and core G_{mm}. One possible explanation for Project 3 G_{mm} results may be that these tests were the only ones

conducted by the research staff in the producer's quality control laboratory using different equipment than the research laboratory.

Table 5.15. Asphalt Mixture Properties for Hazlehurst

ID	Asphalt Content			G_{mm}			G_{se}		
	Design	Mix	Cores	Design	Mix	Cores	Design	Mix	Cores
3-1		5.23	5.45		2.349	2.378		2.528	2.572
3-2		5.39	5.30		2.350	2.374		2.535	2.561
3-3		5.53	5.15		2.348	2.379		2.538	2.561
3-4		5.35	5.66		2.346	2.371		2.529	2.572
Avg	*5.40*	*5.38*	*5.39*	*2.388*	*2.348*	*2.376*	*2.582*	*2.532*	*2.567*
4-1		5.60	5.89		2.372	2.379		2.571	2.591
4-2		5.77	5.80		2.372	2.371		2.578	2.578
4-3		5.59	5.81		2.383	2.370		2.584	2.577
4-4		5.18	5.81		2.375	2.378		2.557	2.587
Avg	*5.40*	*5.54*	*5.83*	*2.388*	*2.376*	*2.375*	*2.582*	*2.572*	*2.583*
12-1		5.58	5.78		2.378	2.365		2.577	2.569
12-2		5.49	6.55		2.372	2.348		2.566	2.579
12-3		4.21	5.31		2.394	2.369		2.542	2.555
Avg	*5.35*	*5.09*	*5.88*	*2.360*	*2.381*	*2.361*	*2.546*	*2.562*	*2.568*

Mixture properties for mixes utilizing Scribner gravel are given in Table 5.16. In general, plant mix asphalt content and G_{mm} were found to compare well with core results. However, plant mix asphalt content for specimens 1-4 and 9-3 were not found to be similar to core results. Also, plant mix G_{mm} results for specimens 1-1 and 1-3 were not similar to core values. In most cases, G_{mm} results for both plant mix and cores were determined to be higher than design values. This may be due to Scribner gravel having the highest absorption value based on initial source evaluation (Table 3.1). Since tests were conducted on reheated mix, the aggregate may have absorbed more asphalt than during design procedures.

Table 5.16. Asphalt Mixture Properties for Scribner

ID	Asphalt Content			G_{mm}			G_{se}		
	Design	Mix	Cores	Design	Mix	Cores	Design	Mix	Cores
1-1		6.54	6.42		2.376	2.356		2.661	2.580
1-2		6.05	6.33		2.371	2.370		2.584	2.595
1-3		6.05	6.32		2.381	2.355		2.597	2.575
1-4		6.42	5.86		2.381	2.376		2.612	2.583
Avg	*6.00*	*6.27*	*6.23*	*2.358*	*2.377*	*2.364*	*2.566*	*2.601*	*2.583*
8-1		6.13	6.04		2.376	2.373		2.594	2.586
8-2		5.75	5.99		2.383	2.374		2.587	2.586
8-3		5.95	6.09		2.376	2.374		2.587	2.590
Avg	*6.00*	*5.94*	*6.04*	*2.358*	*2.378*	*2.374*	*2.566*	*2.589*	*2.587*
9-1		6.50	*a*		2.379	---		2.613	*a*
9-2		6.07	*a*		2.363	---		2.575	*a*
9-3		6.31	6.97		2.391	2.386		2.621	2.643
9-4		6.21	6.25		2.361	2.386		2.578	2.612
Avg	*6.20*	*6.27*	*6.61*	*2.350*	*2.374*	*2.386*	*2.564*	*2.597*	*2.627*

a: cores were damaged/destroyed

Table 5.17 shows plant mix and core mixture properties for mixes utilizing Zeiglerville gravel. In general, plant mix asphalt content and G_{mm} were determined to compare well with core results and design values. No significant variations were discovered in the test results.

Table 5.17. Asphalt Mixture Properties for Zeiglerville

	Asphalt Content			G_{mm}			G_{se}		
ID	Design	Mix	Cores	Design	Mix	Cores	Design	Mix	Cores
2-1		4.72	4.54		2.417	*a*		2.589	*a*
2-2		5.37	5.30		2.395	2.391		2.589	2.581
2-3		5.12	5.19		2.402	2.417		2.587	2.608
2-4		5.37	5.58		2.398	2.397		2.592	2.600
Avg	*5.30*	*5.15*	*5.15*	*2.394*	*2.403*	*2.402*	*2.584*	*2.589*	*2.596*
5-1		5.05	*a*		2.434	2.447		2.622	*a*
5-2		4.99	*a*		2.436	2.444		2.621	*a*
5-3		5.00	*a*		2.429	2.435		2.613	*a*
Avg	*5.20*	*5.01*	*a*	*2.420*	*2.433*	*2.442*	*2.611*	*2.619*	*a*
7-1		5.36	5.36		2.420	2.426		2.617	2.625
7-2		5.15	5.33		2.428	2.417		2.618	2.612
7-3		5.24	5.34		2.421	2.431		2.614	2.630
7-4		5.15	5.14		2.422	2.424		2.611	2.613
Avg	*5.20*	*5.23*	*5.29*	*2.420*	*2.423*	*2.425*	*2.611*	*2.615*	*2.620*

a: cores were damaged/destroyed

5.8   Tensile Strength Ratio (TSR) Test Results

Plant produced mix was evaluated to determine the resistance to moisture induced damage with MT-63 (vacuum saturation method). Asphalt mixture was reheated and compacted in the SGC to a 95 mm height to obtain 7 ± 1 percent air voids. Four specimens were compacted and separated into two subsets (control and conditioned) so that the average air voids of the two subsets were approximately equal. Control specimens were placed in a 25°C water bath for thirty minutes before measuring indirect tensile strength ($S_{t(Dry)}$) using the Marshall stability tester at a 50 mm/min load rate.

Conditioned specimens were vacuum saturated at 525 mm Hg partial pressure for 5 to 10 minutes in a vacuum apparatus. The degree of saturation was between 55 and 80 percent for all specimens. After conditioning, specimens were placed in a water bath at 60°C for 24 hours. Specimens were then removed and placed in a water bath at 25°C for 2 hours $\pm$ 30 minutes prior to determining the wet or conditioned indirect tensile strength $S_{t(Wet)}$. The tensile strength ratio (TSR) was calculated by dividing $S_{t(Wet)}$ by $S_{t(Dry)}$. After specimens were tested, they were broken in half and visually evaluated for stripping. A minimum TSR of 85 percent with 95 percent retained coating is specified in the Mississippi Standard Specifications for Road and Bridge Construction (2004 Edition).

Pavement cores were also tested in accordance with MDOT MT-63, with the exception that only three cores were tested. Two cores were selected for the control set and one was selected for the conditioned set. The cores were tested as described above.

TSR results for plant produced mix and cores are presented in Table 5.18. TSR was reported for a total of forty sets of plant mix specimens. Twenty-one of the forty sets

of plant mix specimens failed to meet the MDOT minimum TSR requirement of 85 percent.   However, visual observations of thirty-six of the forty plant mix sets revealed that only five sets failed to retain a minimum of 95 percent asphalt coating as required.

A total of thirty-one sets of core specimens were tested. Seventeen sets of core specimens had TSR values below 85 percent, and twelve sets were determined to retain less than 95 percent asphalt coating. All projects had at least one set of plant mix or cores that failed to meet the TSR requirement. However, all conditioned specimens for Projects 1, 5, 6, 7, and 10 retained at least 95 percent asphalt coating.

No relationship between aggregate source and TSR could be concluded based upon TSR results. Visual identification of aggregate coating and the TSR value indicated the same behavior approximately 50% of the time (e.g. 10-2). The remainder of the time visual identification of aggregate coating and the TSR value indicated different behaviors (e.g. 6-3).

Table 5.18. TSR Test Results

Gravel Source	ID	Lab Compacted Plant Mix				Roadway Cores			
		$S_{t(Dry)}$ (kPa)	V_a (%)	TSR (---)	Coating (>95%)	$S_{t(Dry)}$ (kPa)	V_a (%)	TSR (---)	Coating (>95%)
Crystal Springs	6-1	1,185	6.6 to 7.1	NR	Yes	560	5.0 to 5.5	NR	Yes
	6-2	1,154	6.6 to 7.0	NR	Yes	528	5.0 to 5.9	NR	Yes
	6-3	1,473	6.3 to 6.4	75	Yes	577	5.6 to 6.0	NR	Yes
	6-4	1,058	6.1 to 6.7	NR	Yes	776	4.1 to 5.0	NR	Yes
	10-1	1,709	6.2 to 6.9	80	Yes	1,387	4.5 to 4.6	67	Yes
	10-2	1,615	6.3 to 6.7	95	Yes	1,100	4.9 to 5.2	95	Yes
	10-3	1,731	6.6 to 7.0	84	Yes	1,149	6.6 to 7.4	71	Yes
	11-1	1,582	7.0 to 7.3	74	Yes	1,032	6.5 to 6.9	67	Yes
	11-2	1,602	6.9 to 7.2	81	Yes	670	6.9 to 7.1	70	No
	11-3	1,220	7.0 to 7.2	83	No	741	6.9 to 7.7	79	Yes
	11-4	1,217	6.9 to 7.2	84	Yes	936	5.1 to 5.5	79	Yes
Hazlehurst	3-1	1,424	7.4 to 7.5	80	No	581	10.5 to 11.6	77	Yes
	3-2	1,553	7.4 to 7.6	77	No	1,004	7.5 to 8.0	80	Yes
	3-3	1,442	6.9 to 7.1	88	Yes	966	7.3 to 7.8	89	Yes
	3-4	1,299	7.2 to 7.8	88	Yes	545	12.0 to 12.5	89	Yes
	4-1	1,142	7.2 to 8.3	102	Yes	960	7.4 to 8.1	60	No
	4-2	1,267	7.4 to 7.6	VS	Yes	1,030	6.7 to 7.2	62	No
	4-3	1,707	7.7 to 7.8	82	Yes	969	6.5 to 6.7	80	No
	4-4	1,412	7.8	71	No	1,031	6.9 to 7.1	63	No
	12-1	1,486	6.8 to 7.1	87	Yes	630	10.8 to 11.3	95	No
	12-2	1,400	6.9 to 7.1	88	Yes	452	13.0 to 14.2	104	No
	12-3	1,638	7.2 to 7.3	91	Yes	482	14.0 to 14.5	65	No
Scribner	1-1	1,713	6.1 to 6.4	83	Yes	895	7.2 to 7.4	80	Yes
	1-2	1,662	6.1 to 6.2	96	Yes	843	8.3 to 8.4	65	Yes
	1-3	1,503	6.5 to 6.8	84	Yes	562	11.7 to 12.1	85	Yes
	1-4	1,491	6.5 to 6.8	92	Yes	489	12.2 to 13.5	103	Yes
	8-1	1,590	6.9 to 7.0	98	Yes	327	9.6 to 10.8	117[a]	No
	8-2	1,401	6.8 to 7.1	68	Yes	458	8.9 to 11.2	144[a]	No
	8-3	1,415	6.9 to 7.2	71	No	530	7.1 to 7.3	75	No
	9-1	983	6.3 to 6.5	96	Yes	---	8.6 to 9.1	---	---
	9-2	1,291	6.4 to 6.7	68	Yes	---	6.6 to 7.0	---	---
	9-3	1,247	6.5 to 6.7	88	Yes	729	8.0 to 8.4	95	No
	9-4	1,198	6.7 to 6.9	96	Yes	892	7.5 to 7.8	61	Yes
Zeiglerville	2-1	1,376	7.4 to 7.9	78	---	---	5.7 to 7.7	---	---
	2-2	1,285	6.8 to 7.3	97	---	---	5.5 to 6.7	---	---
	2-3	1,137	6.9 to 7.5	97	---	---	8.2 to 10.8	---	---
	2-4	1,332	7.0 to 7.2	95	---	---	7.8 to 8.4	---	---
	5-1	1,318	6.8 to 7.0	80	Yes	740	9.1 to 10.8	NR	Yes
	5-2	1,357	7.0 to 7.5	77	Yes	587	8.4 to 9.3	NR	Yes
	5-3	1,392	6.8 to 7.0	85	Yes	709	8.1 to 8.9	NR	Yes
	7-1	1,585	6.8 to 7.2	76	Yes	782	5.9 to 6.8	104	Yes
	7-2	1,332	6.6 to 7.3	85	Yes	952	4.9	91	Yes
	7-3	1,491	7.0 to 7.2	81	Yes	953	5.0 to 5.4	97	Yes
	7-4	1,401	6.8 to 7.1	90	Yes	841	6.9 to 7.2	96	Yes

NR: test results were not reasonable   VS: vacuum saturation not within specified range
a: test result influenced greatly by one low $S_{t(Dry)}$

5.9   Boil Test Results

Table 5.19 contains MT-59 boil test results for plant produced mixture. Results are reported as a percentage of coated particles above or below 95 percent. All test specimens were estimated to have less than five percent coating loss and no mixture

showed any significant difference compared to other mixtures. Test results indicate all mixtures tested would be resistant to moisture induced damage.

Table 5.19. Boil Test Results for Plant Produced Mixture

Aggregate Source	ID	Binder Grade	Retained Coating Greater than 95% (Yes/No)
Crystal Springs	6-1	67-22	Yes
	6-2	67-22	Yes
	6-3	67-22	Yes
	10-1	67-22	Yes
	10-2	67-22	Yes
	10-3	67-22	Yes
	11-1	67-22	Yes
	11-2	67-22	Yes
	11-3	67-22	Yes
	11-4	67-22	Yes
Hazlehurst	3-1	76-22	Yes
	3-2	76-22	Yes
	3-3	76-22	Yes
	3-4	76-22	Yes
	4-1	76-22	Yes
	4-2	76-22	Yes
	4-3	76-22	Yes
	4-4	76-22	Yes
	12-1	67-22	Yes
	12-2	67-22	Yes
	12-3	67-22	Yes
Scribner	1-1	67-22	Yes
	1-2	67-22	Yes
	1-3	67-22	Yes
	1-4	67-22	Yes
	8-1	67-22	Yes
	8-2	67-22	Yes
	8-3	67-22	Yes
	9-1	67-22	Yes
	9-2	67-22	Yes
	9-3	67-22	Yes
	9-4	67-22	Yes
Zeiglerville	2-1	67-22	Yes
	2-2	67-22	Yes
	2-3	67-22	Yes
	2-4	67-22	Yes
	5-1	67-22	Yes
	5-2	67-22	Yes
	5-3	67-22	Yes
	7-1	67-22	Yes
	7-2	67-22	Yes
	7-3	67-22	Yes
	7-4	67-22	Yes

5.10   Hamburg Test Results

Tables 5.20 through 5.23 contain Hamburg test results for plant produced asphalt mixture. Mix was compacted to a 63 mm height in the SGC to produce four samples per field test location with 7 ± 2 percent air voids. Samples were sawn so that two samples would fit together in the testing mold and produce two replicate test specimens (1 test used two SGC samples). The two test specimens were submerged and tested simultaneously with an applied load of 71.7 kg at a test temperature of 50°C. Testing was conducted in accordance with AASHTO T324 utilizing the APA Jr. The test was conducted for 20,000 passes or a maximum deformation of 14 mm.

The values reported in Tables 5.20 through 5.23 represent the average results of two test specimens. However, single test results are reported for stripping slope and SIP for 11-3 and 11-4. In each of the aforementioned cases, stripping was observed in only one of the two test specimens. Average air voids for all locations ranged from 5.2 to 8.8 percent with an average of 6.6 percent. Post compaction consolidation (measured at 1,000 passes) was found to range from 1.18 mm to 5.26 mm with an average of 2.33 mm. Creep slope ranged from 1,532 to 17,471 passes/mm with an average of 9,486 passes/mm. The measured rut depth after 20,000 passes ranged from 2.85 mm to 11.95 mm with an average of 5.80 mm.

Mixtures showed similar performance when tested in the HWTD with the exception of Project 10 and 11 mixes. In general, most mixtures tested were found to be resistant to stripping in the HWTD. Stripping was only observed in one test specimen from 11-3 and 11-4. Each of those two specimens had a SIP of over 16,500 passes. Project 10 was found to have the highest post compaction consolidation, highest rut depth, and lowest creep slope. The performance of Project 10 mixture is likely due to the use of uncrushed, washed gravel.

Presented in Figure 5.3 are the average Hamburg results for each project. Excluded from Figure 5.3 are results from 10-3 due to both specimens reaching 14 mm depth prior to 20,000 passes. Also excluded from Figure 5.3 are 11-3 and 11-4 due to observed stripping. Figure 5.4 presents single specimen results for those which exhibited stripping (11-3 and 11-4).

Table 5.20. Hamburg Results for Crystal Springs

ID	Avg. V_a	Post Compact., mm	Creep Slope, passes/mm	Stripping Slope, passes/mm	SIP, passes	Passes to 14 mm	Rut Depth at 20,000 passes, mm
6-1	5.2	*2.90*	7,683	NS	NS	TC	6.19
6-2	5.3	*1.55*	9,285	NS	NS	TC	3.71
6-3	5.6	2.09	8,415	NS	NS	TC	5.80
6-4	5.3	1.86	8,382	NS	NS	TC	4.65
Avg	*5.4*	*2.10*	*8,441*	---	---	---	*5.09*
10-1	6.4	2.47	9,158	NS	NS	TC	7.44
10-2	6.1	3.30	3,381	NS	NS	TC	11.16
10-3	6.6	5.26	1,532	NS	NS	12,548	---
Avg	*6.4*	*3.68*	*4,690*	---	---	---	*9.30*
11-1	6.8	2.14	7,271	NS	NS	TC	7.40
11-2	6.7	2.21	8,689	NS	NS	TC	6.86
11-3	6.6	3.91	2,919	803[a]	16,572[a]	18,716[a]	11.95[b]
11-4	6.0	3.17	3,984	1,600[a]	16,826[a]	TC	9.92[b]
Avg	*6.5*	*2.85*	*5,716*	---	---	---	*9.03*

NS: no stripping observed
TC: completed 20,000 passes prior to reaching 14 mm rut depth
a: value reported for one test specimen which exhibited stripping
b: value reported for one test specimen which did not exhibit stripping

Table 5.21. Asphalt Mixture Properties for Hazlehurst

ID	Avg. V_a	Post Compact., mm	Creep Slope, passes/mm	Stripping Slope, passes/mm	SIP, passes	Passes to Failure	Rut Depth at 20,000 passes, mm
3-1	6.2	2.95	10,860	NS	NS	TC	5.38
3-2	7.7	2.88	11,942	NS	NS	TC	5.04
3-3	7.0	3.27	12,945	NS	NS	TC	5.43
3-4	8.5	1.87	12,158	NS	NS	TC	3.59
Avg	*7.4*	*2.74*	*12,226*	---	---	---	*4.86*
4-1	8.8	2.29	12,542	NS	NS	TC	5.08
4-2	8.2	2.48	10,437	NS	NS	TC	5.47
4-3	7.6	1.81	11,437	NS	NS	TC	4.17
4-4	7.5	3.41	15,046	NS	NS	TC	6.36
Avg	*8.0*	*2.50*	*12,365*	---	---	---	*5.27*
12-1	6.6	2.62	8,859	NS	NS	TC	7.19
12-2	6.9	2.43	7,708	NS	NS	TC	8.16
12-3	6.3	1.20	12,265	NS	NS	TC	3.33
Avg	*6.6*	*2.08*	*9,610*	---	---	---	*6.23*

NS: no stripping observed
TC: completed 20,000 passes prior to reaching 14 mm rut depth

Table 5.22. Asphalt Mixture Properties for Scribner

ID	Avg. V_a	Post Compact., mm	Creep Slope, passes/mm	Stripping Slope, passes/mm	SIP, passes	Passes to Failure	Rut Depth at 20,000 passes, mm
1-1	6.9	1.18	9,592	NS	NS	TC	3.58
1-2	5.7	1.84	10,081	NS	NS	TC	5.15
1-3	6.5	1.57	8,225	NS	NS	TC	4.38
1-4	6.2	2.11	7,033	NS	NS	TC	5.45
Avg	*6.3*	*1.67*	*8,733*	*---*	*---*	*---*	*4.64*
8-1	6.5	2.08	8,354	NS	NS	TC	5.70
8-2	6.3	1.61	8,117	NS	NS	TC	4.22
8-3	6.5	2.29	8,874	NS	NS	TC	5.81
Avg	*6.4*	*1.99*	*8,448*	*---*	*---*	*---*	*5.24*
9-1	6.1	1.72	7,689	NS	NS	TC	4.91
9-2	6.2	3.02	8,179	NS	NS	TC	7.76
9-3	6.4	1.63	7,897	NS	NS	TC	4.30
9-4	6.4	2.47	10,426	NS	NS	TC	6.61
Avg	*6.3*	*2.21*	*8,548*	*---*	*---*	*---*	*5.89*

NS: no stripping observed
TC: completed 20,000 passes prior to reaching 14 mm rut depth

Table 5.23. Asphalt Mixture Properties for Zeiglerville

ID	Avg. V_a	Post Compact., mm	Creep Slope, passes/mm	Stripping Slope, passes/mm	SIP, passes	Passes to Failure	Rut Depth at 20,000 passes, mm
2-1	5.5	1.65	17,471	NS	NS	TC	4.54
2-2	6.7	1.67	6,181	NS	NS	TC	5.76
2-3	7.0	1.96	10,834	NS	NS	TC	5.17
2-4	6.3	1.56	6,743	NS	NS	TC	5.20
Avg	*6.3*	*1.71*	*10,307*	*---*	*---*	*---*	*5.17*
5-1	6.6	1.82	15,993	NS	NS	TC	3.62
5-2	6.9	1.60	15,489	NS	NS	TC	2.85
5-3	6.5	2.45	8,572	NS	NS	TC	5.90
Avg	*6.3*	*1.96*	*13,351*	*---*	*---*	*---*	*4.12*
7-1	6.8	1.99	14,118	NS	NS	TC	4.26
7-2	6.6	3.27	12,518	NS	NS	TC	7.27
7-3	6.5	2.24	7,707	NS	NS	TC	6.61
7-4	6.8	2.61	10,380	NS	NS	TC	5.98
Avg	*6.7*	*2.53*	*11,181*	*---*	*---*	*---*	*6.03*

NS: no stripping observed
TC: completed 20,000 passes prior to reaching 14 mm rut depth
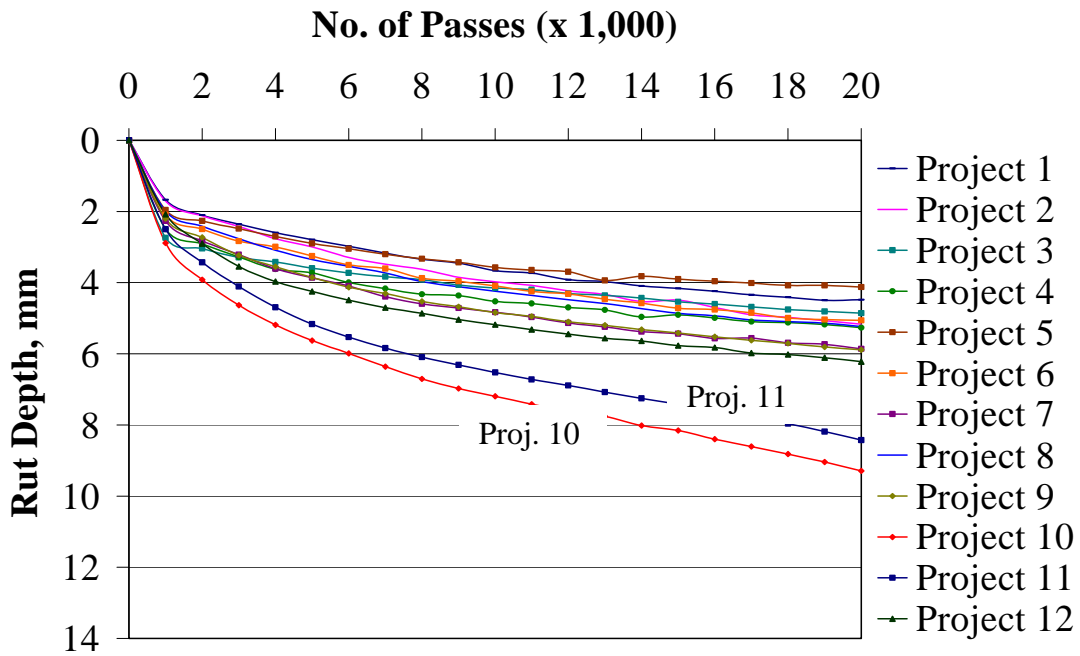
Figure 5.3. Average Hamburg Results for Each Project
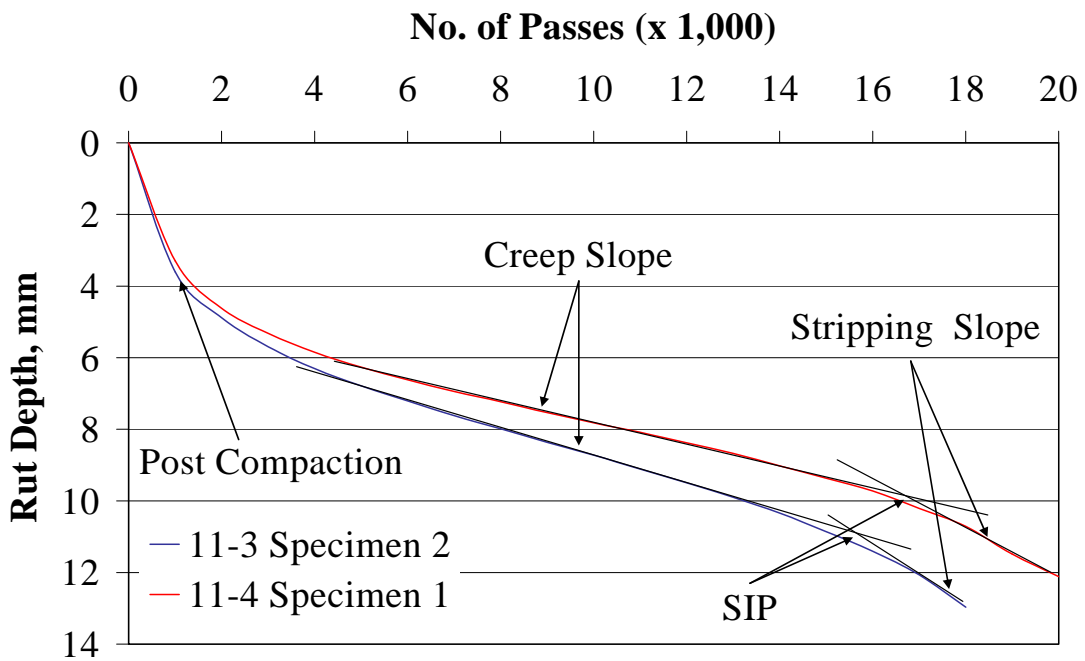
Figure 5.4. Hamburg Results of Specimens which Exhibited Stripping

CHAPTER 6 – ANALYSIS OF LABORATORY AND FIELD DATA

6.1   Overview of Laboratory and Field Data Analysis

The analysis consisted of two primary components. The first was to make observations and look for relevant trends in relation to PaveCool 2.4, SEM images, and recommended practices found in literature or to specification requirements. The second was to use multiple regression techniques to develop prediction equations. Prediction equations were attempted to predict in place air voids and also to predict moisture susceptibility as measured by laboratory tests.

6.2   Observations from Field and Laboratory Data

6.2.1   Comparison of Data Collected to Literature and Specification Requirements

White et al. (2006) and Kandhal et al. (1998) investigated the correlation between TSR and MBV. White et al. (2006) found no significant correlation between TSR and MBV (R^2=0.23). Figure 6.1 plots MBV values obtained from the cold feed belt versus TSR of the laboratory compacted mix alongside the equations presented by White et al. (2006) and Kandhal et al. (1998). It is clear that the equations from literature do not correlate to the data collected, which is highly variable.
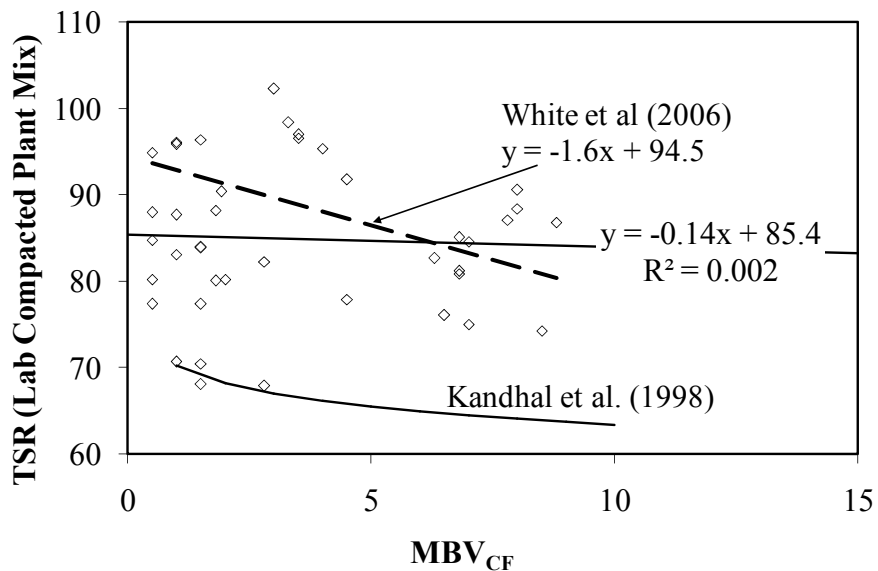
Figure 6.1. Comparison of MBV$_{CF}$ and TSR From Lab Compacted Mix

Mixtures were categorized as being coarse-graded or fine-graded based on the definitions presented in NAPA (2001). Coarse-graded mixtures were used on Projects 1, 3, 4, 5, 6, 7, 8, 9, and 12, whereas fine-graded mixtures were used on Projects 2, 10, and

11. Most asphalt mixtures used in Mississippi are coarse-graded; therefore, the mixtures included in the research are typical of mixtures produced in the state. Of the 33 test locations utilizing coarse-graded mixtures, approximately sixty-seven percent had t/NMAS of 4.0 or greater. Fifty-nine percent of coarse-graded mixtures with t/NMAS of 4.0 or greater had in-place air voids which met specification requirements. Eleven of the coarse-graded mixtures were placed at t/NMAS less than 4.0. Of those eleven mixtures, only about thirty-six percent had in-place air voids which met specification requirements.

As shown in Table 4.9, average field core thicknesses were found to be within MDOT allowable layer thickness ranges at only seventeen of the forty-four test locations. Twenty-four of the average field core thicknesses were found to be greater than the allowable maximum. Core thicknesses at three test locations were found to be thinner than the allowable minimum. Seven of the projects had design thicknesses equal to the maximum allowable layer thickness, while only three were equal to the minimum requirement. Projects 10 and 11 design thicknesses were greater than the allowable layer thickness. Research presented in this report has indicated that thinner sections are, in general, more problematic for density and that excessively thin sections were not prevalent in the data set.

The average field core V_a was found to meet the specified maximum presented in Table 4.10 at twenty-six of the forty-four test locations. Two of the three mixtures placed below the minimum allowable layer thickness failed to achieve acceptable in-place air voids. Nine of the seventeen test locations (53 percent) placed within the allowable layer thickness range met the specified V_a. Sixteen of the twenty-four test locations (67 percent) with layer thicknesses greater than the allowable maximum thickness met the specified V_a. This data agrees with literature cited earlier that thicker layers (within reason) achieve density more easily than thinner layers.

6.2.2 Comparison of Compaction Conditions to PaveCool 2.4

Compaction conditions were evaluated subjectively using the 1 to 5 scale shown below:

5 = Very Favorable   4 = Favorable   3 = Somewhat Favorable
2 = Somewhat Unfavorable   1 = Unfavorable

The evaluation did not consider mix tenderness. Temperature related tenderness was reported in literature at a variety of temperatures and there did not appear to be a reasonable way to compare higher temperatures and relate them to tenderness since the mixes investigated in this study were not the same. The primary component evaluated was the contractor roller pattern in relation to the recommended cessation time predicted by PaveCool 2.4. A cessation temperature of 80 $^\circ$C or reasonably close to 80 $^\circ$C appeared multiple times in literature. The authors used 80 $^\circ$C in this evaluation but it should be noted that some mixes have some level of compactability below 80 $^\circ$C.

Table 6.1 provides the project 1 comparison. All locations were produced in a condition that was at least somewhat favorable. Temperatures were fairly low during parts of the pneumatic rolling, and rolling continued well after the recommended cessation time at three of the four locations.

Table 6.1. Comparison of Project 1 Construction Conditions to PaveCool 2.4

ID	Conditions	Notes
1-1	Very Favorable (5)	1 finish rolling pass (Pn) 25 min after compaction window.
1-2	Somewhat Favorable (3)	15 of the 22 intermediate rolling passes (Pn) and the two finish rolling passes (St) were up to 20 min after compaction window. Temperature was below 60 $^{\circ}$C at conclusion of intermediate rolling.
1-3	Somewhat Favorable (3)	5 of the 15 intermediate rolling passes (Pn) and the finish rolling pass (St) were after compaction window; 13 min after for intermediate rolling and 30 min for finish rolling. Temperature was near 80 and 50 $^{\circ}$C at the beginning and end of intermediate rolling, respectively.
1-4	Favorable (4)	Temperature was near 60 $^{\circ}$C at the end of intermediate rolling.

Table 6.2 provides the project 2 comparison. All compaction occurred over 80 $^{\circ}$C according to measured temperatures. All compaction began while the pavement was above 120 $^{\circ}$C, and ended before the recommended cessation time except for location 4 which was nearly complete by the recommended cessation time. The entire compaction process was performed with one vibratory roller, which should be noted when evaluating this project. Conditions were rated very favorable for all locations, but it should be noted that temperature effects on tenderness were not considered in this evaluation.

Table 6.2. Comparison of Project 2 Construction Conditions to PaveCool 2.4

ID	Conditions	Notes
2-1	Very Favorable (5)	Temperature was relatively high throughout compaction
2-2	Very Favorable (5)	Temperature was relatively high throughout compaction
2-3	Very Favorable (5)	Temperature was relatively high throughout compaction
2-4	Very Favorable (5)	Temperature was relatively high throughout compaction

Table 6.3 provides the project 3 comparison. All compaction was performed prior to the recommended cessation time. Temperatures were relatively high throughout compaction. Conditions were rated very favorable for all locations, but it should be noted that temperature effects on tenderness were not considered in this evaluation. There was a considerable pause between breakdown and finish rolling, but no information is available as to the motivation for the extended pause; no intermediate rolling was performed on the project.

Table 6.3. Comparison of Project 3 Construction Conditions to PaveCool 2.4

ID	Conditions	Notes
3-1	Very Favorable (5)	Temperature was relatively high throughout compaction
3-2	Very Favorable (5)	Temperature was relatively high throughout compaction
3-3	Very Favorable (5)	Temperature was relatively high throughout compaction
3-4	Very Favorable (5)	Temperature was relatively high throughout compaction

Table 6.4 provides the project 4 comparison. All compaction occurred prior to the recommended cessation time of PaveCool 2.4. Temperatures were relatively high throughout compaction for locations 2, 3, and 4.

Table 6.4. Comparison of Project 4 Construction Conditions to PaveCool 2.4

ID	Conditions	Notes
4-1	Very Favorable (5)	Temperature was relatively high throughout compaction
4-2	Very Favorable (5)	Temperature was relatively high throughout compaction
4-3	Very Favorable (5)	Temperature was relatively high throughout compaction
4-4	Very Favorable (5)	Temperature was relatively high throughout compaction

Table 6.5 provides the project 5 comparison. Temperatures dropped below 80 $^{\circ}$C for all locations, and for one location the temperature was considerably below 80 $^{\circ}$C during intermediate rolling. Compaction condition assessments varied, and for location 2 the assessment was the conditions were somewhat unfavorable.

Table 6.5. Comparison of Project 5 Construction Conditions to PaveCool 2.4

ID	Conditions	Notes
5-1	Somewhat Favorable (3)	Temperatures were noticeably below PaveCool 2.4 during intermediate and finish rolling, but were still above to near 80 $^{\circ}$C. Measured temperature decreased very rapidly.
5-2	Somewhat Unfavorable (2)	Temperature was considerably below 80 $^{\circ}$C for all intermediate and finish rolling. Intermediate and finish rolling occurred after the recommended cessation time.
5-3	Favorable (4)	Temperatures were moderate during compaction, but were above 80 $^{\circ}$C for all but finish rolling.

Table 6.6 provides the project 6 comparison. Conditions were favorable to very favorable for all locations. Generally speaking rolling was complete by the recommended cessation time recommended by PaveCool 2.4.

Table 6.6. Comparison of Project 6 Construction Conditions to PaveCool 2.4

ID	Conditions	Notes
6-1	Favorable (4)	Temperatures were moderate during compaction, but were above 80 $^{\circ}$C for all but finish rolling.
6-2	Favorable (4)	Temperatures were moderate during compaction, but were above 80 $^{\circ}$C for all but finish rolling.
6-3	Very Favorable (5)	Temperature was relatively high throughout compaction
6-4	Favorable (4)	Temperature was moderately high throughout compaction with exception of finish rolling which occurred almost an hour after the recommended cessation time when the temperature was just above 60 $^{\circ}$C.

Table 6.7 provides the project 7 comparison. Conditions were generally very favorable. Initial rolling temperatures were fairly high and compaction was complete by the recommended cessation time at all locations.

Table 6.7. Comparison of Project 7 Construction Conditions to PaveCool 2.4

ID	Conditions	Notes
7-1	Favorable (4)	Temperature was fairly high during breakdown rolling but near 80 $^{\circ}$C during intermediate rolling. Temperature was below 80 $^{\circ}$C during finish rolling.
7-2	Very Favorable (5)	Temperatures were fairly high during breakdown rolling and above 80 $^{\circ}$C for intermediate and finish rolling.
7-3	Very Favorable (5)	Temperatures were fairly high during breakdown rolling and at to above 80 $^{\circ}$C for intermediate and finish rolling.
7-4	Very Favorable (5)	Temperature was relatively high throughout compaction.

Table 6.8 provides the project 8 comparison. Conditions were favorable for all three locations. Compaction was essentially complete by the recommended cessation temperature for all three locations.

Table 6.8. Comparison of Project 8 Construction Conditions to PaveCool 2.4

ID	Conditions	Notes
8-1	Favorable (4)	Temperatures were 80 to 120 $^{\circ}$C during compaction.
8-2	Favorable (4)	Temperatures were approximately 75 $^{\circ}$C during finish rolling, while all other parameters were reasonable.
8-3	Favorable (4)	Finish rolling occurred slightly after the cessation time.

Table 6.9 provides the project 9 comparison. Conditions were essentially favorable. Temperatures were moderate to relatively high during breakdown rolling.

Table 6.9. Comparison of Project 9 Construction Conditions to PaveCool 2.4

ID	Conditions	Notes
9-1	Favorable (4)	Temperatures were moderate during compaction, yet well above 80 $^{\circ}$C. Finish rolling occurred several minutes after the recommended cessation temperature.
9-2	Very Favorable (5)	Temperatures were fairly high during breakdown rolling and approximately 100 $^{\circ}$C during finish rolling. All breakdown rolling occurred prior to 120 $^{\circ}$C and all finish rolling occurred after the recommended cessation temperature.
9-3	Very Favorable (5)	Temperature was relatively high throughout compaction. Compaction was complete prior to the asphalt cooling to 120 $^{\circ}$C.
9-4	Favorable (4)	Temperatures were moderate during breakdown rolling and somewhat below 80 $^{\circ}$C during finish rolling.

Table 6.10 provides the project 10 comparison. Locations 1 and 2 were compacted in very favorable conditions; compaction began at these locations well before 120 $^{\circ}$C. It should again be noted that temperature effects on tenderness were not considered in the assessment. Location 3 was compacted in an unfavorable condition as the temperature was below 80 $^{\circ}$C for all rolling operations.

Table 6.10. Comparison of Project 10 Construction Conditions to PaveCool 2.4

ID	Conditions	Notes
10-1	Very Favorable (5)	Temperature was relatively high throughout compaction. Compaction was complete prior to the asphalt cooling to 120 ^{o}C.
10-2	Very Favorable (5)	Temperature was relatively high throughout compaction. Breakdown rolling was complete prior to the asphalt cooling to 120 ^{o}C.
10-3	Unfavorable (1)	All compaction occurred below 80 ^{o}C.

Table 6.11 provides the project 11 comparison. Conditions were generally somewhat favorable, with temperatures decreasing below 80 ^{o}C during intermediate rolling in all cases but location 1 and being below 80 ^{o}C for all finish rolling. Temperature profiles were generally below PaveCool 2.4 for locations 3 and 4.

Table 6.11. Comparison of Project 11 Construction Conditions to PaveCool 2.4

ID	Conditions	Notes
11-1	Favorable (4)	Temperatures were moderate during compaction and above 80 ^{o}C except for finish rolling.
11-2	Somewhat Favorable (3)	Temperatures were moderate for breakdown rolling but were below 80 ^{o}C for part of intermediate rolling and were approximately 60 ^{o}C during finish rolling.
11-3	Somewhat Favorable (3)	Temperatures were moderate during breakdown rolling and were below for parts of intermediate rolling and all of finish rolling.
11-4	Somewhat Favorable (3)	Temperatures were moderate during breakdown rolling and were below for parts of intermediate rolling and all of finish rolling.

Table 6.12 provides the project 12 comparison. Conditions were somewhat unfavorable to unfavorable. Mix temperatures and roller pattern timing did not align well for this project. The conditions encountered in this project did not lend themselves well to achieving high in place density.

Table 6.12. Comparison of Project 12 Construction Conditions to PaveCool 2.4

ID	Conditions	Notes
12-1	Somewhat Unfavorable (2)	Temperatures were moderate during breakdown rolling but below 60 ^{o}C during finish rolling.
12-2	Unfavorable (1)	Temperatures were just above 80 ^{o}C during breakdown rolling and well below 80 ^{o}C during finish rolling. Compaction did not begin until after the recommended cessation time.
12-3	Somewhat Unfavorable (2)	Temperatures were moderate during breakdown rolling but below 60 ^{o}C during finish rolling.

Five of the forty-four locations were rated either Unfavorable (1) or Somewhat Unfavorable (2). Three of these five locations were project 12. Other than project 12, it appears that the contractors placed the asphalt in a condition that is somewhat to very favorable. Location 5-2 was rated Somewhat Unfavorable and the air voids were 8.9%, which is between the air voids measured at the other two locations for that project (8.4 and 9.9%). Location 10-3 was compacted to 7.1% air voids. Project 12 air voids were 11 to 14%.

Using PaveCool 2.4 as a tool could enhance the ability of Mississippi contractors to develop rolling patterns. The tool is straightforward and calculations take only a few minutes. The software is available at no charge.

6.2.3   Observations from Scanning Electron Microscope Data

The primary motivation for collecting SEM images was to visually identify adhered fines and use this information in conjunction with other data to support or refute those findings. Multiple regression analysis presented later in this chapter shows that adhered fines ($P_{Adh(\%)-5711}$) was not a significant predictor of in place air voids or moisture susceptibility. This finding in conjunction with the results in Section 6.3.3 limited the usefulness of the SEM images.

6.3   Multiple Regression Predictions

6.3.1   Multiple Regression Methodology

Multiple regression predictions were performed to predict compactability and stripping potential using the techniques presented in this sub-section. Multiple regression techniques are described in numerous textbooks; Sincich et al. (2002) was used for this report. Equation 6.1 is the general form of the multiple regression model used.

$$y_p = \beta_0 + \beta_1(x_1) + \beta_2(x_2) + ... + \beta_k(x_k) + \varepsilon \qquad (6.1)$$

Where,

y_p is the dependent or predicted variable
β_0 is the constant
$\beta_1, \beta_2,... \beta_k$ determine the contribution of each independent variable
$x_1, x_2,..., x_k$ are independent variables
ε is the random error of the model

To evaluate the adequacy of the models developed, all β parameters except β_0 were evaluated simultaneously with the null hypothesis being all β terms are zero and the alternative hypothesis being that at least one of the β terms is nonzero. An ANOVA was performed and the F statistic used to determine if the model is useful for predicting y_p. If the p-value resulting from the ANOVA is less than the threshold value, it implies the model is useful for predicting y_p. For example, if 95% confidence is desired in the regression model, a p-value of 0.05 or less implies the model is useful. In a similar manner, each individual β_i was evaluated and when the p-value was below the threshold value (e.g. 0.05, 0.10) it implied the individual term contributed to the prediction model at that level of confidence (e.g. 95%, 90%, respectively).

The R^2 value was reported for each model, alongside the number of observations (n) and the number of independent variables (k) used. One test location provided one observation in this report. R^2_a was also reported as it accounts for the proportions of n and k. R^2 can be misleading in multiple regression models where n is not considerably larger than k. R^2 increases as more independent variables are added to the model, and R^2 is affected by the presence or removal of β_o. The Standard Error (S) was also reported for each model; the S value reported should not be confused with the standard error of y_p as it the sample estimate of the standard deviation of ε.

6.3.2 Multiple Regression Prediction of Final in Place Air Voids

Tables 6.13 and 6.14 provide regression model results where y_p was equal to the final in place air voids (V_a) measured with AASHTO T166. Each regression model was developed for a specific purpose and each has been given an equation number denoted Eq. in Tables 6.13 and 6.14. The equations are all in the form of Eq. 6.1 and the table is interpreted as follows. Eq. 6.2 has a β_o of 91.3, a β_1 of 0.55, and so on. The independent variable for β_1 is $x_1 = w_{CF-\%}$. The p-value for β_o is 0.05 and the p-value for β_1 is 0.26.

Eq. 6.2 was developed to have the highest R^2 value of all the models, which required using the most independent variables. Four of the sixteen independent variables were significant at a 95% confidence level. Adhered fines had the highest p-value of any term in Eq 6.2 indicating it may not have value in predicting compactability. The overall model had a p-value of 0.001 implying the model is useful for predicting V_a, though the number of independent variables required and some of their corresponding p-values would render this model less than optimal for some applications.

Eq. 6.3 was intended to maximize R^2_a, and eight independent variables were able to do so while all being significant at 95% confidence. An alternative version of Eq. 6.3 was considered that used nine independent variables, which were the eight variables already included alongside t/NMAS. R^2_a was 0.57 when t/NMAS was included and was 0.56 when t/NMAS was omitted. The p-value for t/NMAS was 0.17 for the nine variable model, and since t/NMAS was considerably less significant relative to the other terms, the slight R^2_a increase was not deemed enough to warrant its inclusion in Eq. 6.3.

Eq. 6.3 independent variables can be divided into categories as follows: 1) moisture content from cold feed belt entering the mixing drum ($w_{CF-\%}$); 2) amount and properties of clay (MBV_{SP} and SE); 3) construction conditions (T_F and ACP); and 4) mixture volumetrics (P_{AC}, SA_8, and FM). These categories of independent variables are not greatly different from those reported by Cooley and Williams (2009) in Eq. 2.3 when considering that these studies collected different information for different purposes. Fines content was used by Cooley and Williams (2009) but was not a considerable factor in the study (approximately 0.2% change in density when varying the fines content). Excessive fines increase the asphalt's apparent viscosity and make the mixture difficult to place and compact according to Kandhal (1981); note that neither Cooley and Williams (2009) nor this study encountered excessive fines. Cooley and Williams (2009) used t/NMAS but the term was not statistically significant at 95% confidence in

the regression models of this report. It should be noted that T_F considers pavement thickness and temperature as the denominator of the term is the recommended cessation time of PaveCool 2.4. Different volumetric terms were used in each model, but different information was collected for each study. Gradation and asphalt content were (directly or indirectly) detected by Cooley and Williams (2009) and Eq. 6.3.

Overall, Eq. 6.3 appears to be a reasonable model useful for providing compaction guidance for Mississippi materials where tenderness during compaction is a potential concern. The model had a *p*-value of 0.000. A key attribute identified by Eq. 6.3 is the relationship between the methylene blue test and entering cold feed moisture content. The methylene blue test may have value in limiting moisture contents to manageable values.

Eq. 6.4 through Eq. 6.7 build on the observations from Eq. 6.3 and developed models relating one of the two measured methylene blue terms (MBV_{SP} or MBV_{CF}) to one of the two measured moisture content terms ($w_{Mix-\%}$ or $w_{CF-\%}$). One unique combination of the these four terms is included in each equation alongside material properties, mix design volumetrics, and design parameters that would be known to the user without investing any additional funds to collect additional information. The only additional effort required to use any of these four equations would be to measure the appropriate methylene blue value as cold feed and asphalt mixture moisture content measurement is likely a part of most producers' quality control programs.

Several of the *p*-values are high for individual terms in Eq. 6.4 through 6.7, but all four models have overall *p*-values well below 0.05. R^2_a values are marginal for all four models at 0.32 to 0.36, so they should not be considered highly accurate. They could, however, be useful for quality control in situations where density problems arise on a project. Interestingly, the predictions were not greatly different in terms of *p*-value or R^2_a regardless of the moisture or methylene blue term used.

Eq. 6.8 through Eq. 6.11 use minimal gradation terms in conjunction with MBV_{SP} and $w_{CF-\%}$ to predict behavior for each gravel source. MBV_{SP} and $w_{CF-\%}$ were chosen since they would be the easiest of the combinations investigated in Eq. 6.4 through 6.7 to implement and all these combinations predicted behavior essentially the same. Eq. 6.8 through 6.11 used as few independent variables as possible since only 11 locations were available. Interestingly, two of the four sources (Crystal Springs and Zeiglerville) showed a significant relationship between MBV_{SP}, $w_{CF-\%}$, and V_a while the other two sources did not. The *p*-value for the regression model was well below 0.05 for Crystal Springs and Zeiglerville but above 0.05 for Hazlehurst and Scribner. The same trend of *p*-values was observed for MBV_{SP} and $w_{CF-\%}$ individually, with values below 0.05 for Crystal Springs and Zeiglerville and above 0.05 for Hazlehurst and Scribner. R^2_a values were 0.85 and 0.88 for Crystal Springs and Zeiglerville while they were considerably lower for Hazlehurst and Scribner.

Figures 6.2 and 6.3 plot measured air voids versus air voids predicted with the aforementioned multiple regression models. In a few instances, data fell a considerable distance from the equality line shown on all Figure 6.2 plots. These data points were examined as discussed in the following paragraph. Figure 6.3 clearly shows the

difference in predictability for Crystal Springs and Zeiglerville as opposed to Hazlehurst and Scribner.

An attempt was made to identify any outliers in each of the regression equations presented. Possible outliers were identified by distance from the line of equality. Each possible outlier was examined based upon PaveCool 2.4 plots, construction type, and mixture properties. However, justification for eliminating only one mixture from one regression equation was found. The mixture was not removed from the analysis because doing so would not have had a noticeable effect on the overall results. If several points would have been identified as being outliers, the researchers would have removed those mixtures and performed another iteration of the analysis.

Gradation effects on compactability were investigated graphically using Figures 6.4 to 6.6 to provide additional insight on the regression models developed. The average gradation of plant mix and core specimens was plotted for each location. As Figure 6.2 shows, most 9.5 mm mixtures evaluated were coarse-graded with similar gradation shape and $P_{0.075}$. Project 11, however, was fine-graded with higher $P_{0.075}$. Figure 6.3 shows that most 12.5 mm mixtures also had similar gradation shape and $P_{0.075}$. Project 6 mixtures had coarser gradations compared to other 12.5 mm mixtures but had similar $P_{0.075}$. Project 10 was the only 19.0 mm mixture evaluated and had the lowest $P_{0.075}$ of all mixtures included in the study. The $P_{0.075}$ for all mixtures ranged from 2.4 to 8.3 percent with an average of 5.3 percent. Approximately 77 percent of mixtures evaluated had $P_{0.075}$ between 4.1 and 6.5 percent.

Table 6.13. Multiple Regression Summaries for Predicting Final in Place Air Voids (V_a)

Eq.		0	1	2	3	4	5	6	7	8	9	10	11	12	13	14	15	16
6.2	β	91.3	0.55	24.2	-0.20	-0.43	0.026	0.69	-2.48	-29.6	-10.0	-0.44	0.19	0.36	-0.002	$4.1e^{-4}$	-0.067	0.029
	x	---	$W_{CF-\%}$	$W_{Mix-\%}$	MBV_{CF}	MBV_{SP}	T_F	t/NMAS	P_{AC}	SA_8	FM	$P_{Adh(\%)-5711}$	FAA	$P_{0.075}$	C_1/C_2	ACP	SE	GVL
	p-value	0.05	0.26	0.26	0.25	0.00	0.10	0.11	0.05	0.07	0.04	0.92	0.42	0.35	0.70	0.04	0.12	0.54
6.3	β	121.1	0.73	-0.33	0.024	-2.44	-33.9	-0.068	$-3.8e^{-4}$	-12.8	---	---	---	---	---	---	---	---
	x	---	$W_{CF-\%}$	MBV_{SP}	T_F	P_{AC}	SA_8	SE	ACP	FM	---	---	---	---	---	---	---	---
	p-value	0.00	0.05	0.00	0.02	0.00	0.00	0.02	0.00	0.00	---	---	---	---	---	---	---	---
6.4	β	166.4	0.35	-4.02	-0.08	-0.22	-0.17	-0.19	-1.26	-38.8	-23.7	0.06	0.33	0.41	-0.35	0.03	---	---
	x	---	$W_{CF-\%}$	SA	FF_2	MBV_{SP}	Δ_8	t/NMAS	P_{AC}	SA_8	FM	D_R	FAA	$P_{0.075}$	P_{be}	GVL	---	---
	p-value	0.01	0.49	0.02	0.31	0.02	0.18	0.60	0.43	0.03	0.00	0.40	0.22	0.76	0.84	0.49	---	---
6.5	β	66.5	0.47	-0.81	-0.45	-0.09	-0.03	-0.22	1.37	-25.0	-8.1	-0.001	0.21	1.06	-2.04	0.06	---	---
	x	---	$W_{CF-\%}$	SA	MBV_{CF}	FF_2	Δ_8	t/NMAS	P_{AC}	SA_8	FM	D_R	FAA	$P_{0.075}$	P_{be}	GVL	---	---
	p-value	0.27	0.38	0.63	0.04	0.23	0.84	0.56	0.29	0.17	0.31	0.99	0.43	0.44	0.27	0.17	---	---
6.6	β	154.6	28.0	-4.23	-0.06	-0.37	-0.20	0.04	-1.12	-35.5	-23.6	0.08	0.48	0.21	-0.54	0.04	---	---
	x	---	$W_{Mix-\%}$	SA	FF_2	MBV_{SP}	Δ_8	t/NMAS	P_{AC}	SA_8	FM	D_R	FAA	$P_{0.075}$	P_{be}	GVL	---	---
	p-value	0.01	0.27	0.01	0.41	0.02	0.11	0.93	0.46	0.05	0.00	0.25	0.06	0.87	0.75	0.30	---	---
6.7	β	104.2	-1.56	-13.73	-0.39	-0.10	-0.06	-0.25	1.10	-33.7	-13.6	0.02	0.29	0.87	-1.88	0.06	---	---
	x	---	SA	$W_{Mix-\%}$	MBV_{CF}	FF_2	Δ_8	t/NMAS	P_{AC}	SA_8	FM	D_R	FAA	$P_{0.075}$	P_{be}	GVL	---	---
	p-value	0.13	0.39	0.38	0.08	0.17	0.68	0.51	0.44	0.08	0.13	0.79	0.25	0.52	0.32	0.19	---	---
6.8	β	-71.3	2.44	0.70	11.42	10.84	0.00	---	---	---	---	---	---	---	---	---	---	---
	x	---	$W_{CF-\%}$	MBV_{SP}	SA_8	FM	Δ_8	---	---	---	---	---	---	---	---	---	---	---
	p-value	0.13	0.01	0.04	0.48	0.08	0.95	---	---	---	---	---	---	---	---	---	---	---
6.9	β	618.3	-0.01	1.50	-260.5	-76.0	-0.06	---	---	---	---	---	---	---	---	---	---	---
	x	---	$W_{CF-\%}$	MBV_{SP}	SA_8	FM	Δ_8	---	---	---	---	---	---	---	---	---	---	---
	p-value	0.16	1.00	0.46	0.15	0.17	0.79	---	---	---	---	---	---	---	---	---	---	---
6.10	β	-91.6	0.09	-0.97	90.8	-4.09	-2.71	---	---	---	---	---	---	---	---	---	---	---
	x	---	$W_{CF-\%}$	MBV_{SP}	SA_8	FM	Δ_8	---	---	---	---	---	---	---	---	---	---	---
	p-value	0.81	0.98	0.37	0.69	0.89	0.32	---	---	---	---	---	---	---	---	---	---	---
6.11	β	-66.8	-2.82	-0.23	57.4	7.36	0.10	---	---	---	---	---	---	---	---	---	---	---
	x	---	$W_{CF-\%}$	MBV_{SP}	SA_8	FM	Δ_8	---	---	---	---	---	---	---	---	---	---	---
	p-value	0.08	0.02	0.03	0.05	0.08	0.66	---	---	---	---	---	---	---	---	---	---	---

Table 6.14. Statistical Summaries for V$_a$ Predicting Regression Models

Eq.	Description	n	k	p-value	R^2	R^2_a	S
6.2	Highest R^2	44	16	0.001	0.71	0.54	1.63
6.3	Highest R^2_a	44	8	0.000	0.64	0.56	1.61
6.4	Limit w$_{CF-\%}$ With MBV$_{SP}$	44	14	0.013	0.56	0.35	1.95
6.5	Limit w$_{CF-\%}$ With MBV$_{CF}$	44	14	0.021	0.54	0.32	1.99
6.6	Limit w$_{Mix-\%}$ With MBV$_{SP}$	44	14	0.010	0.57	0.36	1.93
6.7	Limit w$_{Mix-\%}$ With MBV$_{CF}$	44	14	0.021	0.54	0.32	1.99
6.8	Crystal Springs Only	11	5	0.007	0.93	0.85	0.36
6.9	Hazlehurst Only	11	5	0.072	0.81	0.61	1.80
6.10	Scribner Only	11	5	0.354	0.59	0.17	1.77
6.11	Zeiglerville Only	11	5	0.004	0.94	0.88	0.58
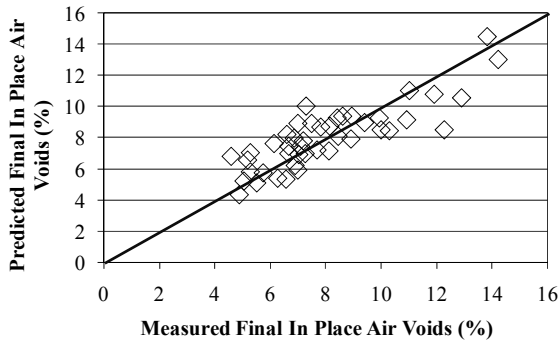
a) Equation 6.2
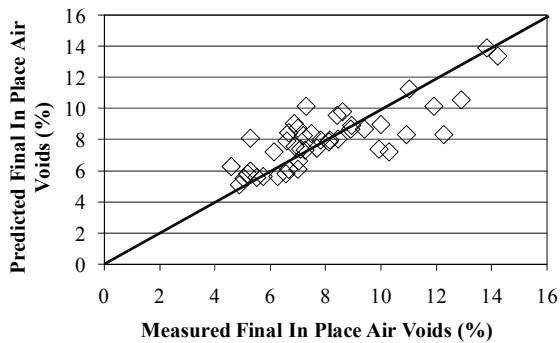
b) Equation 6.3
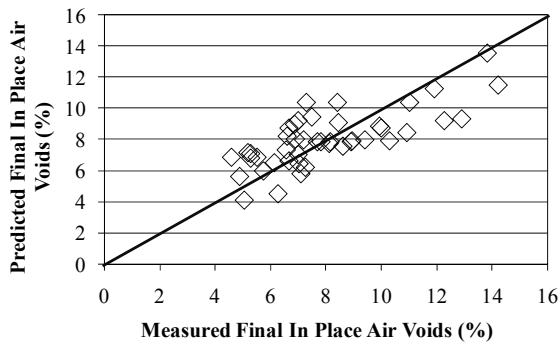
c) Equation 6.4
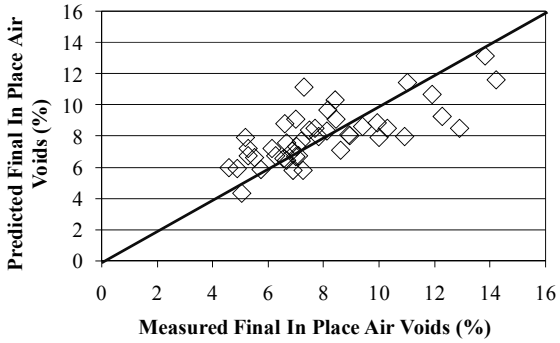
d) Equation 6.5
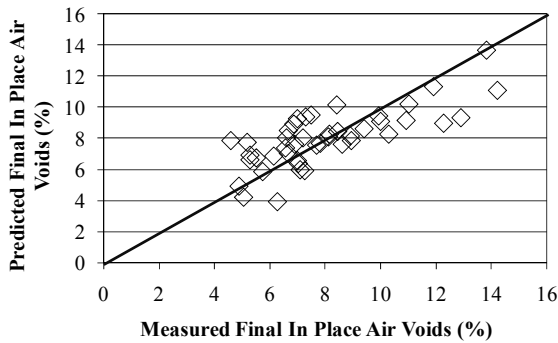
e) Equation 6.6
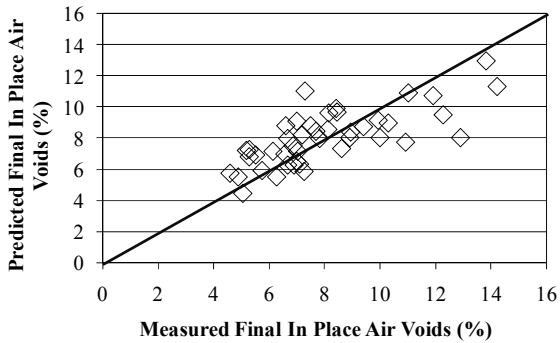
f) Equation 6.7

Figure 6.2. Measured Versus Predicted Plots for Equations 6.2 to 6.7
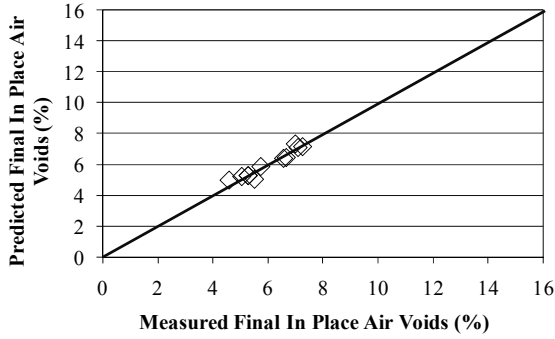
a) Crystal Springs (Eq. 6.8)
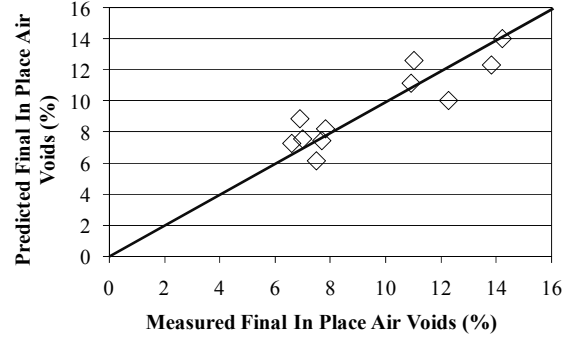
b) Hazlehurst (Eq. 6.9)
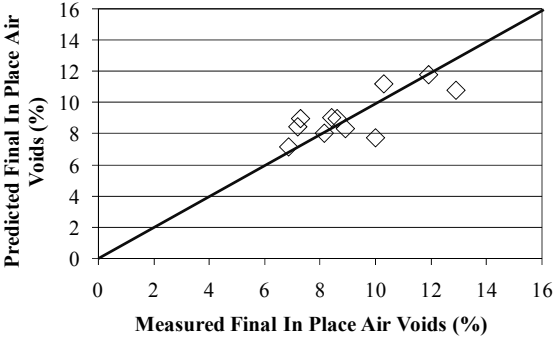
c) Scribner (Eq. 6.10)
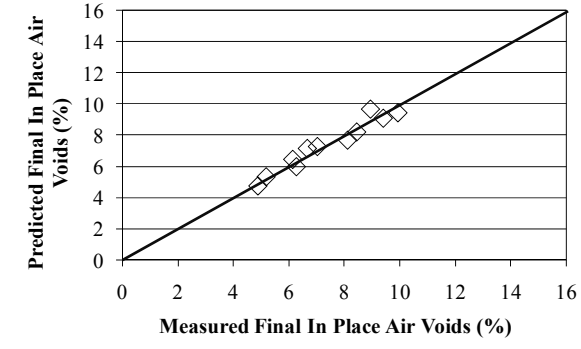
d) Zeiglerville (Eq. 6.11)

Figure 6.3. Measured Versus Predicted Plots for Equations 6.8 to 6.11
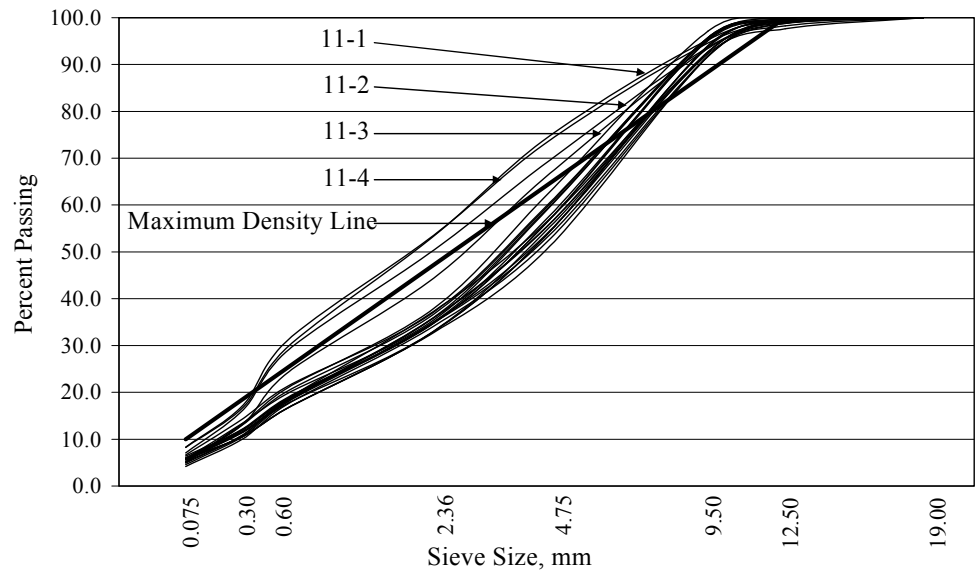
Figure 6.4. Comparison of 9.5mm Mixture Gradations

83
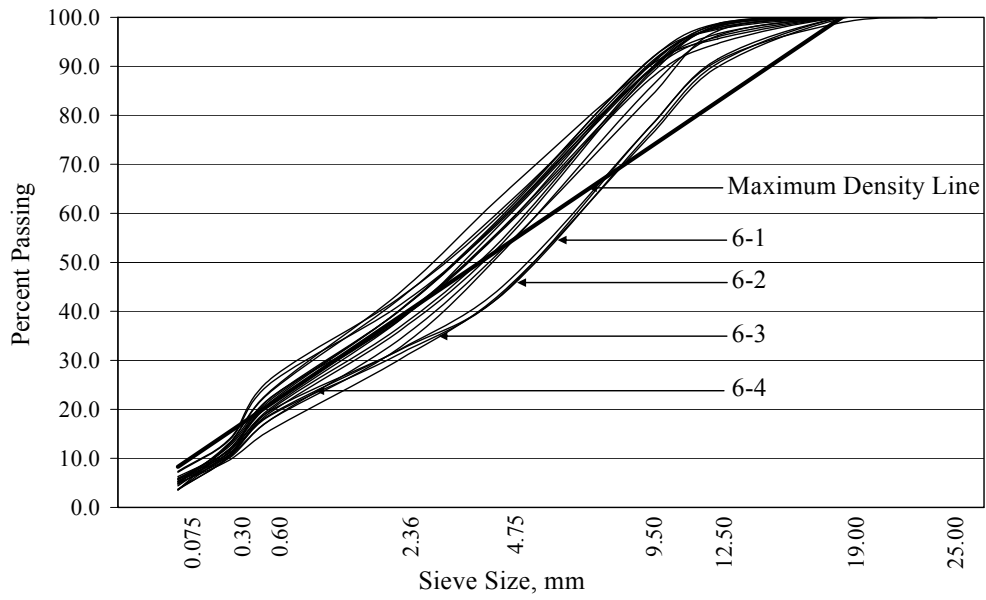
Figure 6.5. Plot of 12.5mm Mixture Gradations
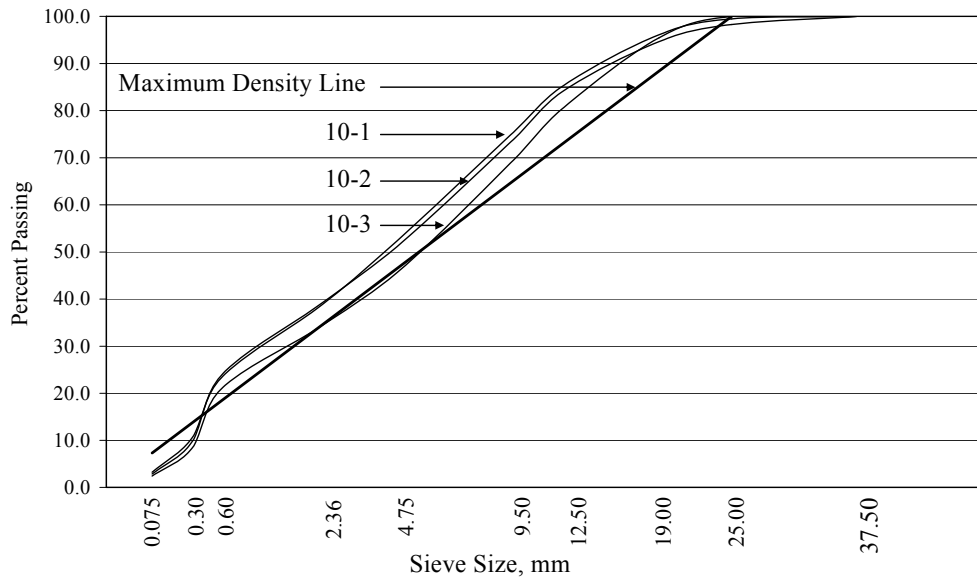
Figure 6.6. Plot of 19.0mm Mixture Gradations

6.3.3 Multiple Regression Prediction of Moisture Susceptibility

Tables 6.15 and 6.16 provide regression model results where y_p was equal to the TSR value measured on roadway cores or SGC compacted field mix. Interpretation of Tables 6.15 and 6.16 is the same as described in Section 6.3.2, and the models were developed as described in Section 6.3.1. TSR was the only parameter modeled due to boil and Hamburg test results. Boil test results indicated all mixes would be resistant to moisture damage. Hamburg test results indicated mixes were resistant to stripping as rut depths were moderate and stripping occurred during the test in minimal instances.

Table 6.15. Multiple Regression Summaries for Predicting TSR

Eq.		0	1	2	3	4
6.12	β	-13.02	4.31	-10.60	2.01	16.36
	x	---	V_a	$w_{CF-\%}$	MBV_{SP}	P_{AC}
	p-value	0.77	0.00	0.01	0.00	0.03
6.13	β	47.33	1.15	-0.80	0.44	4.95
	x	---	V_a	$w_{CF-\%}$	MBV_{SP}	P_{AC}
	p-value	0.03	0.09	0.67	0.11	0.15

Table 6.16. Statistical Summaries for TSR Predicting Regression Models

Eq.	Description	n	k	p-value	R^2	R^2_a	S
6.12	Roadway Cores	31	4	0.012	0.38	0.29	15.9
6.13	SGC Compacted Field Mix	40	4	0.279	0.13	0.03	8.7

Aggregate and compactability terms were largely absent when performing multiple regressions to develop Eq. 6.12 and 6.13 since they can be captured by including in place air voids in the models. Adhered fines had no benefit for TSR prediction for roadway cores or SGC compacted field mix. A model was developed for roadway cores (Eq. 6.12) that incorporated terms also used in Eq. 6.3. In Eq. 6.3 and 6.12 all terms had p-values at or below 0.05 within a model having an overall p-value well below 0.05. The Eq. 6.12 model has a low R^2_a value and its usefulness should be questioned in absence of further long term data and sensitivity analysis. Interestingly, SGC compacted field mix did not produce a model with useable p-values. The data presented in this paper brings into question the usefulness of TSR results from SGC compacted specimens conditioned as in this report.

Figures 6.7 and 6.8 compare dry tensile strength and TSR values for SGC compacted field mix and roadway cores. Figure 6.7 clearly shows SGC specimens to have higher tensile strength than roadway cores, and that there is no correlation between the two values. Figure 6.8 clearly shows no correlation between TSR values between SGC compacted field mix and roadway cores. These figures agree with the questionable nature of TSR testing of SGC specimens conditioned as in this report.
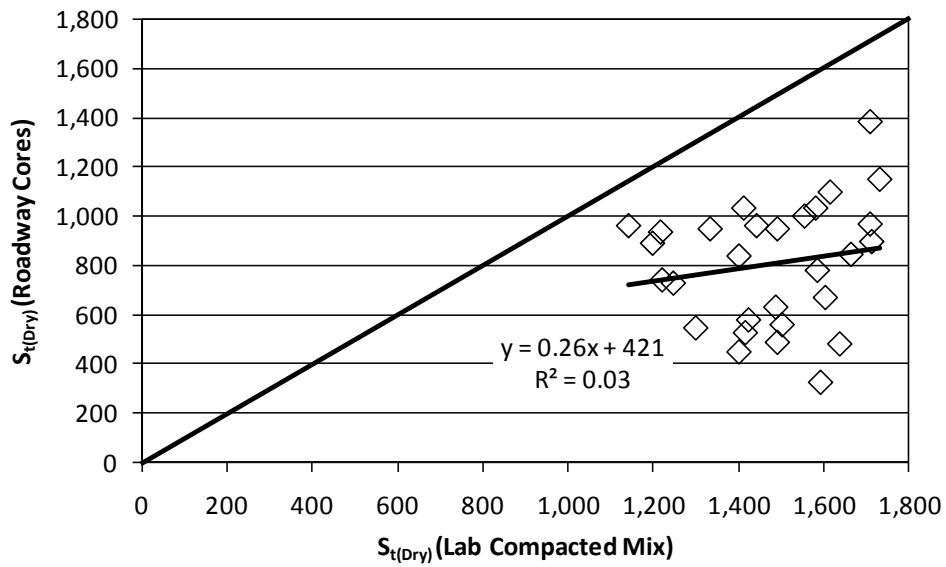
Figure 6.7. Comparison of Laboratory and Field Compacted $S_{t(Dry)}$ (kPa)
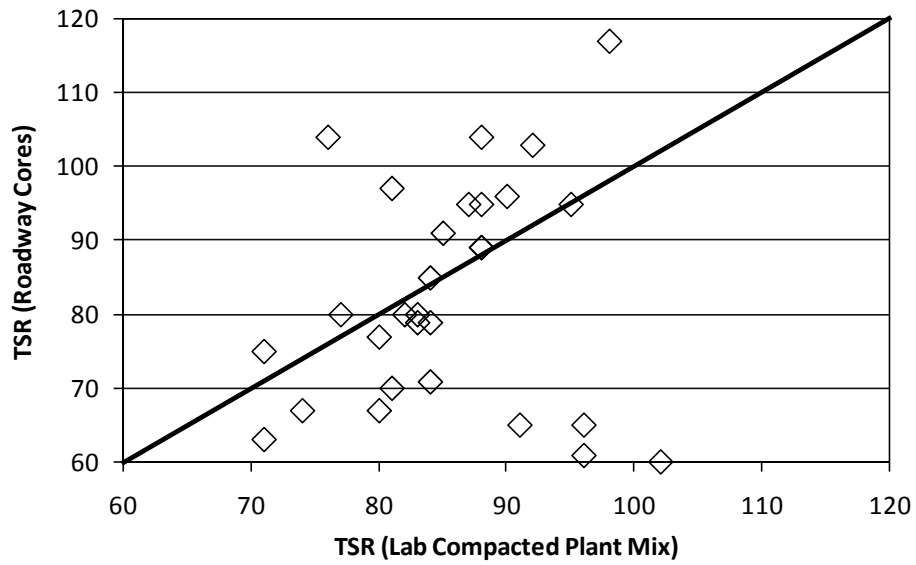
Figure 6.8. Comparison of Laboratory and Field Compacted TSR Values

CHAPTER 7 – CONCLUSIONS AND RECOMMENDATIONS

7.1   Conclusions

The overall conclusion from the research was that compactability appeared to be predicted in a reasonable manner while moisture susceptibility did not.   Multiple regression equations were developed that predicted final in place air voids with p-values below 0.05 and respectable R^2_a values. Moisture susceptibility data was not conclusive in terms of whether or not the mixes investigated will be damaged over time. Specific conclusions are as follows.

- Measurement of adhered fines did not provide useful information for predicting compactability or moisture susceptibility based on the multiple regressions performed in this report.
- The methylene blue test showed promise for use as a tool with mixes that exhibit undesirable compaction characteristics. Methylene blue values coupled with measured moisture contents could be an efficient means of improving density in some conditions.
- Overall, comparisons of measured construction conditions to PaveCool 2.4 showed Mississippi contractors placed asphalt in condition that is somewhat to very favorable for compaction.
- Using PaveCool 2.4 as a tool could enhance the ability of Mississippi contractors to develop rolling patterns. The tool is straightforward and calculations take only a few minutes. The software is available at no charge.
- The categories of independent variables that had p-values below 0.05 in Eq. 6.3 were not greatly different than those in Eq. 2.3 of Cooley and Williams (2009) considering the current study investigated compactability and moisture susceptibility while Cooley and Williams (2009) focused solely on lift thickness. The reasonable agreement of these efforts is promising as Eq. 6.3 may be a useful tool for the Mississippi DOT and its asphalt producers to assist with compaction where tenderness during compaction is a potential concern.
- Eq. 6.4 through 6.7 predicted similar trends when belt moisture and mix moisture were interchanged. This is noteworthy as methods to measure moisture content in asphalt concrete have been a source of debate in some situations.
- Eq. 6.4 through 6.7 may prove useful tools for limiting cold feed or mix moisture content, though the statistical summaries of these equations do not indicate the equations will be highly accurate. These equations use currently measured terms with exception of methylene blue values, so their use would not come with excessive expense.
- Compaction prediction by gravel source had varied results. Crystal Springs and Zeiglerville showed a significant relationship (p-value below 0.05) between

stockpile methylene blue values and cold feed moisture contents, while Hazlehurst and Scribner did not.

- Roadway core TSR values could be correlated somewhat to asphalt content, air voids, cold feed moisture, and stockpile methylene blue values.
- SGC compacted field mix TSR values could not be correlated to anything, bringing the usefulness of TSR results from SGC compacted specimens conditioned as in this report into question.

7.2 Recommendations

Recommendations from this project include suggestions for additional research and recommended methods to use the information learned from this study. Specific recommendations are as follows.

- Asphalt contractors in Mississippi should consider using PaveCool 2.4 as a tool to assist in developing roller patterns. The software is available at no cost and can be used with minimal effort.
- The Mississippi DOT and/or asphalt contractors should consider using the multiple regression equations developed for compactability over a period of time and compare the predicted results to actual in place air voids. Minimal effort would be required to do so and if the equations are useful for even a small portion of the producers in the state, a considerable increase in pavement quality will occur due to increased in place density.
- A sensitivity analysis should be performed for the regression equations developed in this report.
- The methylene blue test should be conducted for most (if not all) gravel aggregate sources used in Mississippi. The test was very promising in this research and it should be investigated in more detail in a follow on study.
- Methods to produce asphalt in the laboratory with retained moisture should be explored. In conjunction with this effort, improved methods to measure moisture content of asphalt mixtures should also be explored. These tools are needed for a variety of reasons, one of which is the likely shortcoming of TSR testing as it is currently performed.
- The field projects studied in this report should be monitored over a period of time to see if any stripping occurs in the field. Cores should be cut from some of the test locations at reasonably spaced intervals (e.g. one year) and tested for evidence of moisture damage. Eight cores taken at each location would allow tensile strength evaluation, Hamburg testing, and evaluation of binder properties.

CHAPTER 8 - REFERENCES

Aschenbrener, T. (1992). *Comparison of Colorado Component Hot Mix Asphalt Materials with Some European Specifications*. Report No. CDOT-DTD-R-92-14, Colorado Department of Transportation, pp.11-38.

Aschenbrener, T. (1995). "Evaluation of the Hamburg Wheel-Tracking Device to Predict Moisture Damage in Hot Mix Asphalt." *Transportation Research Record: Journal of the Transportation Research Board,* No. 1492, pp. 193-201.

Azari, H. (2010). *Precision Estimates of AASHTO T 283: Resistance of Compacted Hot Mix Asphalt (HMA) to Moisture-Induced Damage.* HCHRP Web-Only Document 166, Contractor's Final Task Report for NCHRP Project 9-26A.

Brown, E.R. (1984). "Experiences of Corps of Engineers in Compaction of Hot Asphalt Mixtures." *Placement and Compaction of Asphalt, ASTM STP 829,* pp. 67-79.

Brown, E.R., Lord, B., Decker, D., Newcomb, D. (2000). *Hot Mix Asphalt Tender Zone*. NCAT Report 00-02, National Center for Asphalt Technology, Auburn, AL, pp. 6.

Brown, E.R., Hainin, M.R., Cooley, A., and Hurley, G. (2004). *Relationship of Air Voids, Lift Thickness, and Permeability in Hot Mix Asphalt Pavements.* National Cooperative Highway Research Program (NCHRP) Report 531, Transportation Research Board, pp. 37.

Buchanan, M.S., and Cooley Jr., L.A. (2003). "Investigation of Tender Zone in Compaction of Coarse-Graded Superpave® Hot-Mix Asphalt Mixtures," *Transportation Research Record: Journal of the Transportation Research Board,* 1861, 29-36.

Buchanan, M.S., and Moore, V.M. (2005). *Laboratory Accelerated Stripping Simulator for Hot Mix Asphalt.* Report No. FHWA/MS-DOT-RD-04-167, Mississippi Department of Transportation, pp. 40-92.

Chadboum, B.A., Newcomb, D.E., Voller, V.R., DeSombre, R.A., Louma, J.A., and Timm, D.A. (1998). *An Asphalt Paving Tool for Adverse Conditions.* Report No. MN/RC-1998-18, Minnesota Department of Transportation, pp. 145.

Cooley Jr., L.A., Kandhal, P.S., Buchanan, M.S., Fee, F. and Epps, A. (2000). *Loaded Wheel Testers in the United States: State of the Practice.* E-Circular No. E-C016, Transportation Research Board, pp. 6-14.

Cooley Jr., L.A., and Williams, K.L. (2009). *Evaluation of Hot Mix Asphalt (HMA) Lift Thickness*. Report No. MS-DOT-RD-09-193, Mississippi Department of Transportation.

Finn, F.N., and Epps, J.A. (1980). *Compaction of Hot Mix Asphalt Concrete.* TTI Report 214-21, Texas Transportation Institute, Texas A&M University, College Station, TX.

Hicks, R.G., Santucci, L., and Aschenbrener, T. (2003). "Introduction and Seminar Objectives." *Moisture Sensitivity of Asphalt Pavements A National Seminar*, Transportation Research Board, pp. 15-16.

Huber, G.A., Peterson, R.L., Scherocman, J.A., D'Angelo, J., Anderson, R.M., and Buncher, M.S. (2002). "Determination of Moisture in Hot-Mix Asphalt and Relationship with Tender Mixture Behavior in the Laboratory." *Transportation Research Record: Journal of the Transportation Research Board*, No. 1813, pp. 95-101.

Izzo, R.P., and Tahmoressi, M. (1999). "Evaluation of the Use of the Hamburg Wheel-Tracking Device for Moisture Susceptibility of Hot Mix Asphalt." *Transportation Research Record: Journal of the Transportation Research Board*, No. 1681, pp. 76-85.

Kandhal, P.S. (1981). "Evaluation of Baghouse Fines in Bituminous Paving Mixtures." *Proceedings of the Association of Asphalt Paving Technologists,* Vol. 50, pp. 150-210.

Kandhal, P.S. (1992). *Moisture Susceptibility of HMA Mixes: Identification of Problem and Recommended Solutions.* NCAT Report 92-01, National Center for Asphalt Technology, Auburn, AL, pp.35-54.

Kandhal, P.S., and Parker Jr., F. (1998). *Aggregate Tests Related to Asphalt Concrete Performance in Pavements.* National Cooperative Highway Research Program, Report 405, Transportation Research Board, Washington D.C.

Kandhal, P.S., Lynn, C.Y., and Parker Jr., F. (1998). *Tests for Plastic Fines in Aggregates Related to Stripping in Asphalt Paving Mixtures.* NCAT Report No. 98-3, National Center for Asphalt Technology, Auburn, AL, pp. 1-15.

Kennedy, T.W., Roberts, F.L., and Lee, W.L. (1982). "Evaluation of Moisture Susceptibility of Asphalt Mixtures Using the Texas Freeze-Thaw Pedestal Test." *Proceedings of the Association of Asphalt Paving Technologists*, Vol. 51, pp.327-341.

Kennedy, T.W., Roberts, F.L., and McGennis, R.B. (1984). "Effects of Compaction Temperature and Effort on the Engineering Properties of Asphalt Concrete Mixtures." *Placement and Compaction of Asphalt, ASTM STP 829,* pp. 48-66.

Kennedy, T.W., and Huber, G.A. (1985). "Effect of Mixing Temperature and Stockpile Moisture on Asphalt Mixtures." *Transportation Research Record: Journal of the Transportation Research Board*, No. 1034, pp. 37-46.

Lee, D.Y., Guinn, J.A., Kandhal, P.S., and Dunning, R.L. (1990). *Absorption of Asphalt into Porous Aggregates.* Strategic Highway Research Program Report No. SHRP-A/UIR-90-009, National Research Council, Washington D.C.

Lee, D.Y. (1969). "The Relationship between Physical and Chemical Properties of Aggregates and Their Asphalt Absorption." *Proceedings of the Association of Asphalt Paving Technologists*, Vol. 38, pp. 243-271.

Leiva, F., and West, R.C. (2008). "Analysis of HMA Field Compactibility Using the Accumulated Compaction Pressure (ACP) Concept." *Transportation Research Board 87th Annual Meeting*, Paper No. 08-1222, pp. 3-8.

Little, D.N., and Jones IV, D.R. (2003). "Chemical and Mechanical Processes of Moisture Damage in Hot-Mix Asphalt Pavements." *Moisture Sensitivity of Asphalt Pavements A National Seminar*, Transportation Research Board, pp. 37.

Manandhar, C., Hossain, M., and Nelson, P. (2011). *Development of a Rapid Test to Determine Moisture Sensitivity of Hot Mix Asphalt (Superpave) Mixtures – Extended Study*. Report No. K-TRAN: KSU/KU-07-5P2, Kansas Department of Transportation, pp. 34-95.

Mississippi Department of Transportation Standard Operating Procedure No. TMD-11-59-00-000: Determination of Loss of Coating of HMA (Boiling Water Test), June 1, 2005.

Mississippi Department of Transportation Standard Operating Procedure No. TMD-11-63-00-000: Resistance of Bituminous Paving Mixtures to Stripping (Vacuum Saturation Method), June 1, 2005.

Mississippi Department of Transportation Standard Operating Procedure No. TMD-11-76-00-000: Microwave Method for Determining the Moisture Content of Hot Bituminous Mixtures, June 1, 2005.

NAPA (2001). *HMA Pavement Mix Type Selection Guide,* Information Series 128, National Asphalt Pavement Association, pp. 8.

Parker, F., and Gharaybeh, F.A. (1988). "Evaluation of Tests to Assess Stripping Potential of Asphalt Concrete Mixtures." *Transportation Research Record: Journal of the Transportation Research Board*, No.1171, pp. 18-26.

Sincich, T., Levine, D.M., and Stephan, D. (2002). *Practical Statistics by Example Using Microsoft® Excel and MINITAB®*. 2nd Edition, Prentice Hall, Upper Saddle River, NJ.

Tarrer, A.R and Wagh, V. (1991). *The Effect of the Physical and Chemical Characteristics of the Aggregate on Bonding.* Strategic Highway Research Program Report No. SHRP-A/UIR-91-507, National Research Council, Washington D.C.

US Army Corps of Engineers, (2000). *Hot-Mix Asphalt Paving Handbook*, Second Edition, pp. 202.

White, T.D., Haddock, J., and Rismantojo, E. (2006). *Aggregate Tests for Hot-Mix Asphalt Mixtures Used in Pavements.* National Cooperative Highway Research Program, Report 557, Transportation Research Board, Washington D.C.

Yildirim, Y., and Stokoe II, K.H. (2006). *Analysis of Hamburg Wheel-Tracking Device results in Relation to Field Performance.* Report No. FHWA/TX-06/0-4185-5, Texas Department of Transportation.

APPENDIX A

PaveCool 2.4 vs. MEASURED CONSTRUCTION DATA
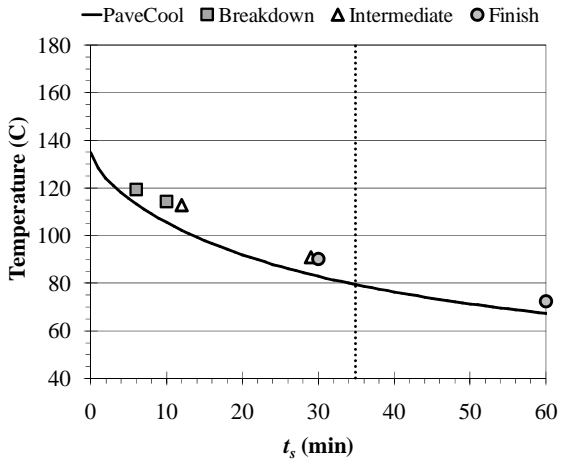
(a) Location 1
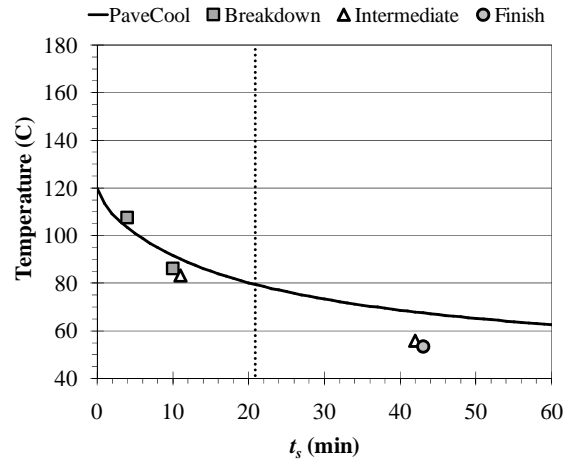
(b) Location 2
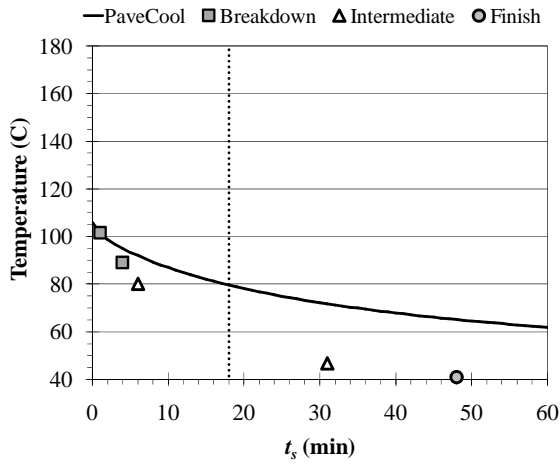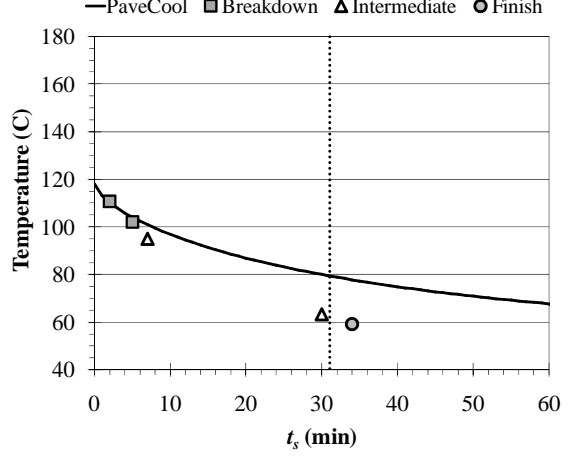
(c) Location 3

(d) Location 4

Figure A.1. PaveCool 2.4 vs. Measured Construction Data: Project 1

94
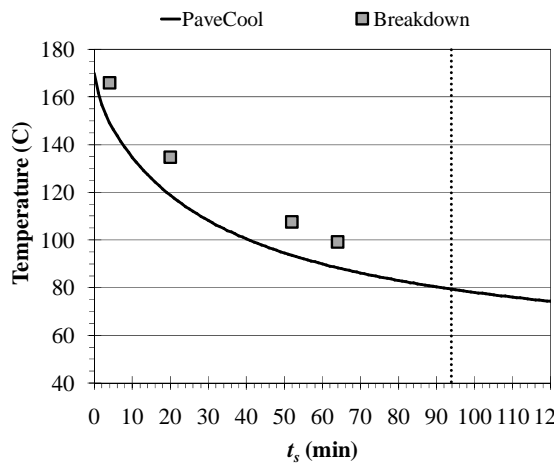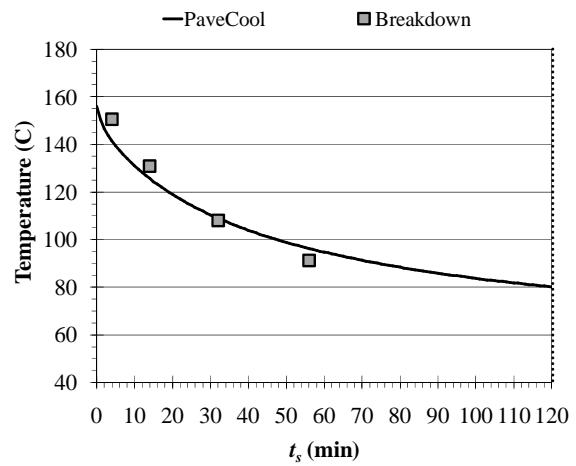
(a) Location 1
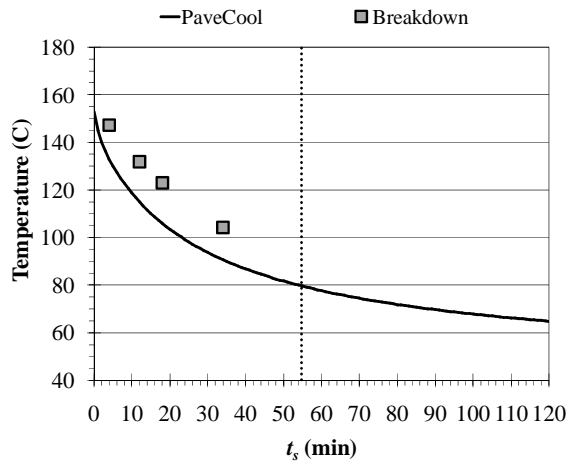
(b) Location 2
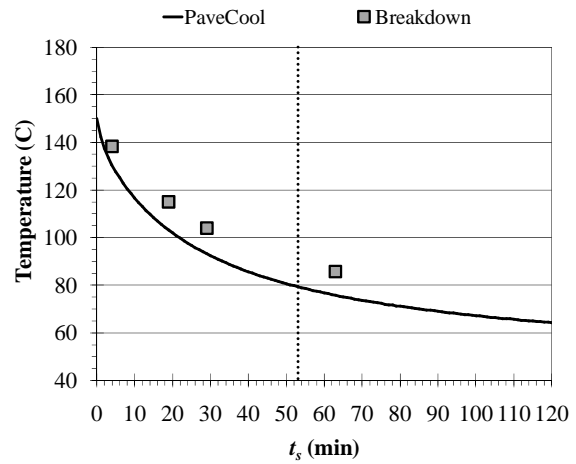
(c) Location 3

(d) Location 4

Note that four data points were presented for breakdown rolling in each plot since no intermediate or finish roller was used. The outer points denote beginning and ending of breakdown rolling.

Figure A.2. PaveCool 2.4 vs. Measured Construction Data: Project 2

95
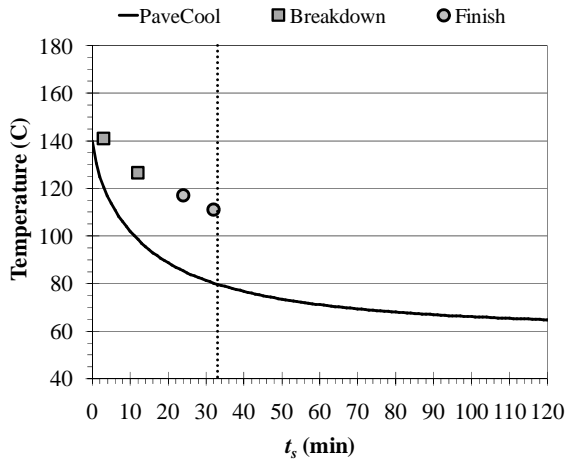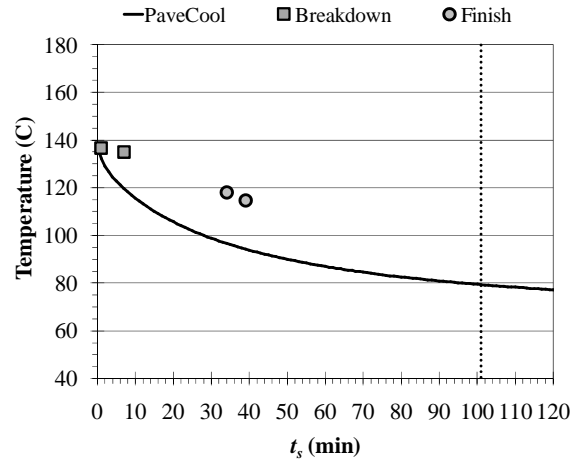
(a) Location 1
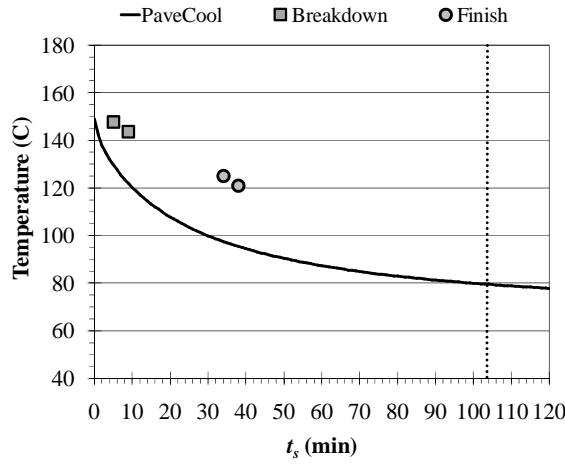
(b) Location 2
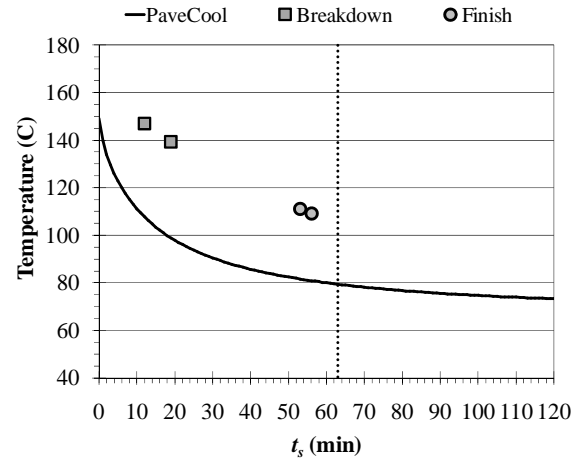
(c) Location 3

(d) Location 4

Figure A.3. PaveCool 2.4 vs. Measured Construction Data: Project 3
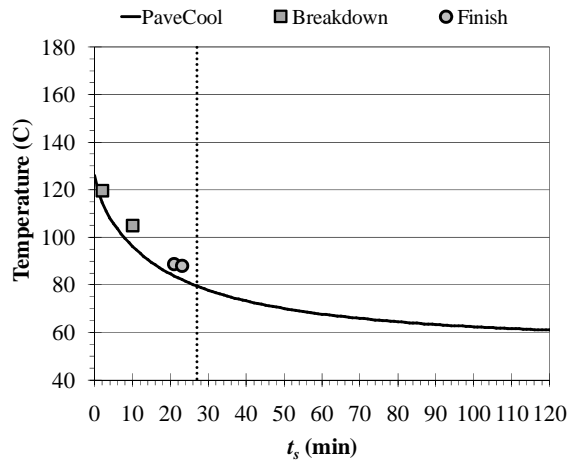
(a) Location 1
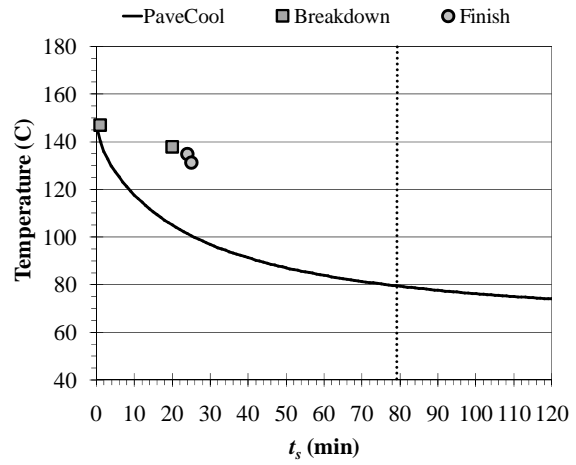
(b) Location 2
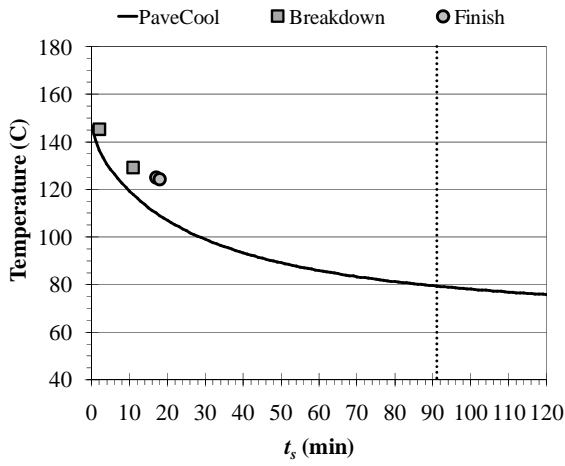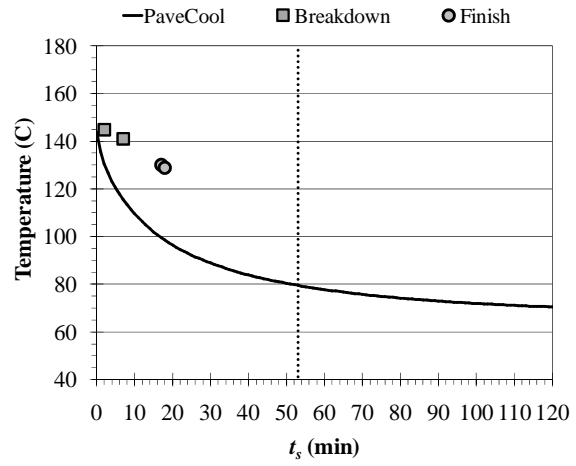
(c) Location 3

(d) Location 4

Figure A.4. PaveCool 2.4 vs. Measured Construction Data: Project 4

97

(a) Location 1

(b) Location 2

(c) Location 3

(d) Location 4

There was no location 4 at project 5

Figure A.5. PaveCool 2.4 vs. Measured Construction Data: Project 5
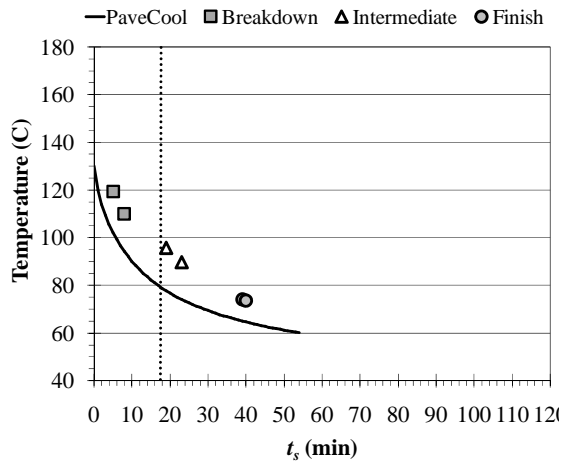
(a) Location 1
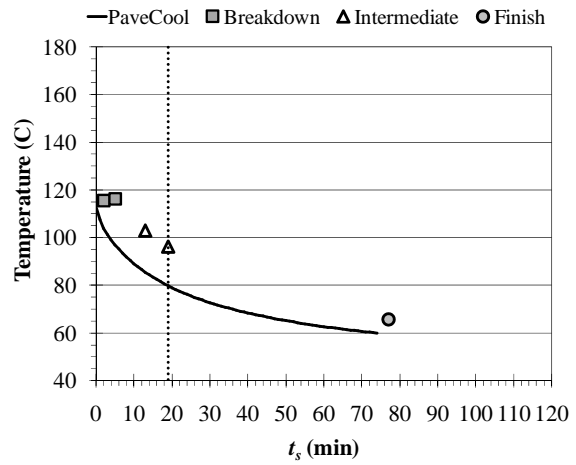
(b) Location 2
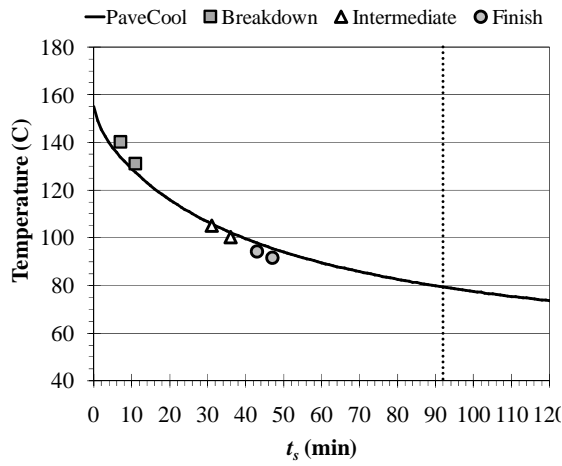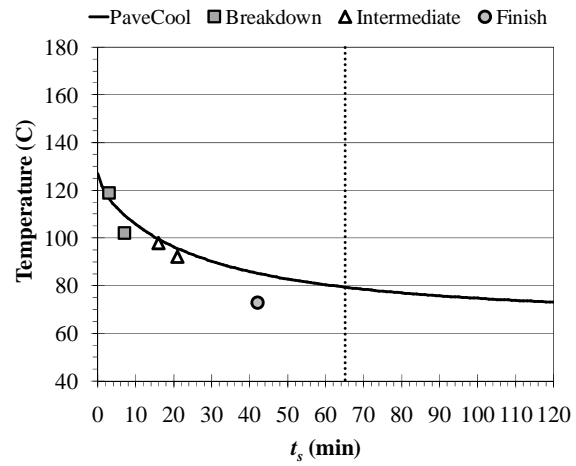
(c) Location 3

(d) Location 4

Figure A.6. PaveCool 2.4 vs. Measured Construction Data: Project 6
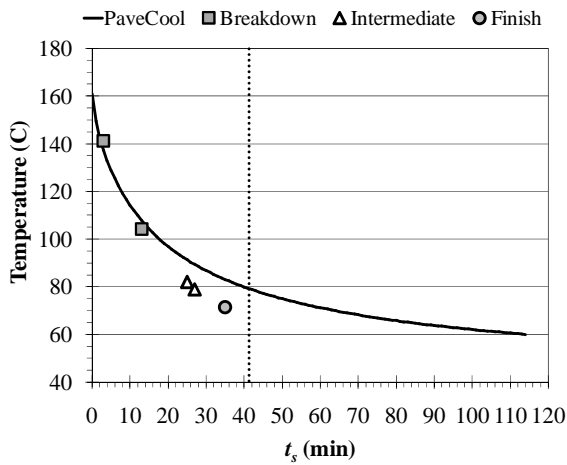
(a) Location 1
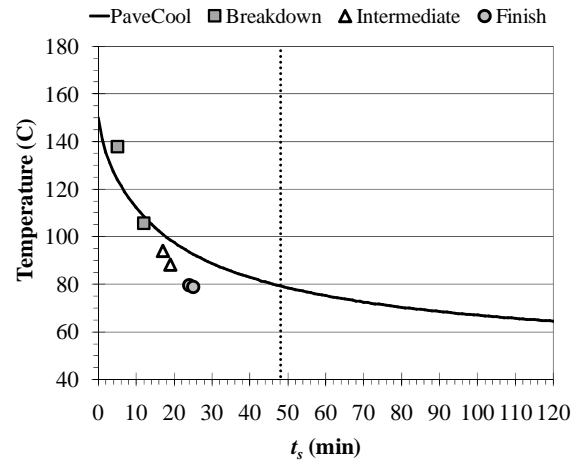
(b) Location 2
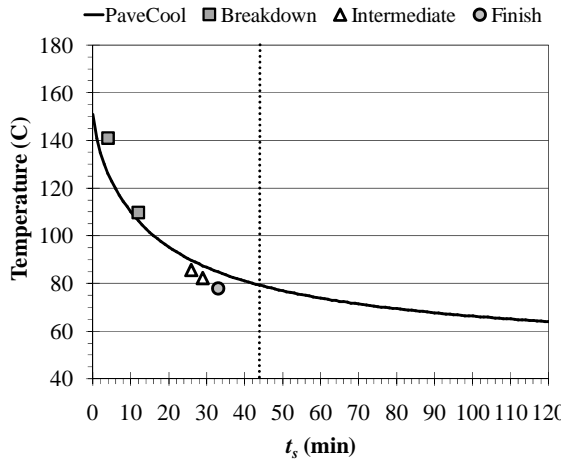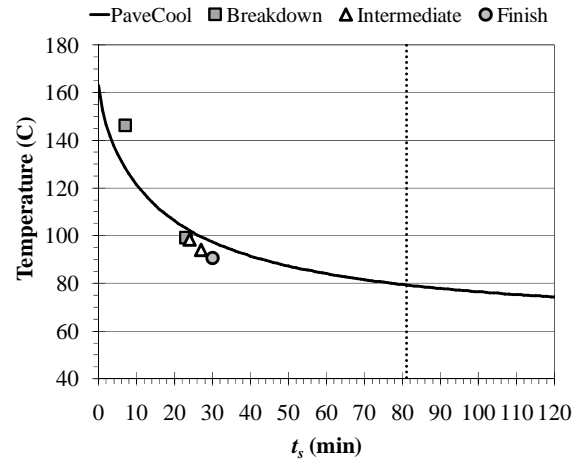
(c) Location 3

(d) Location 4

Figure A.7. PaveCool 2.4 vs. Measured Construction Data: Project 7

100

(a) Location 1

(b) Location 2

There was no location 4 at project 8

(c) Location 3

(d) Location 4

Figure A.8. PaveCool 2.4 vs. Measured Construction Data: Project 8
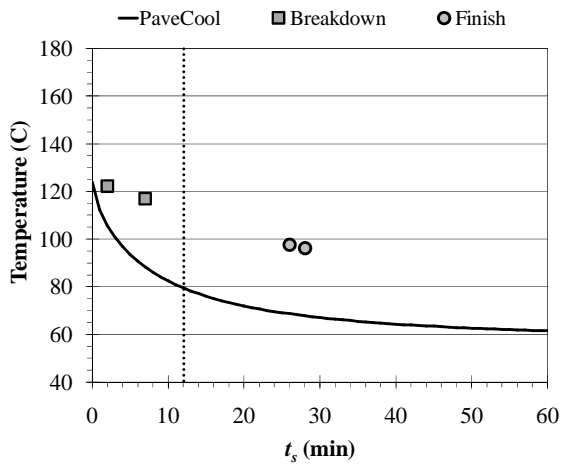
(a) Location 1
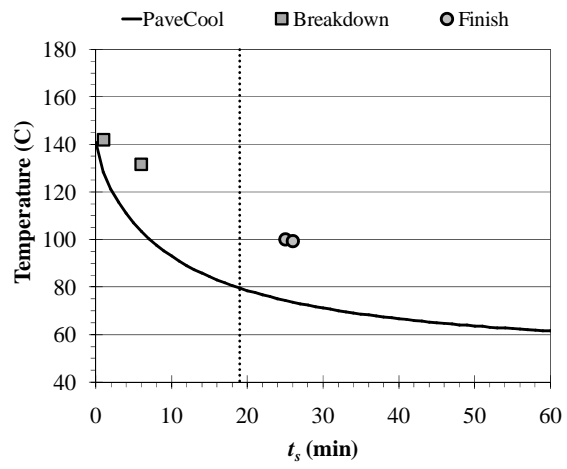
(b) Location 2
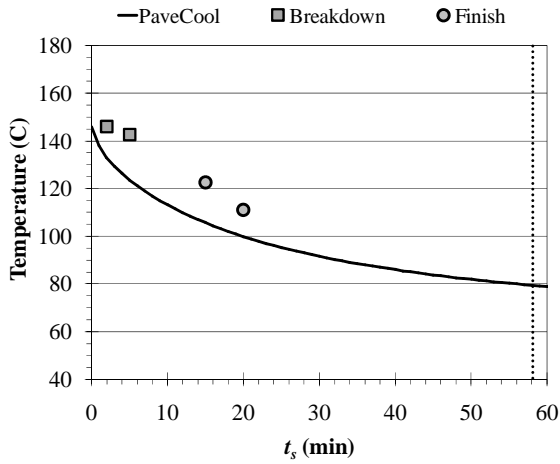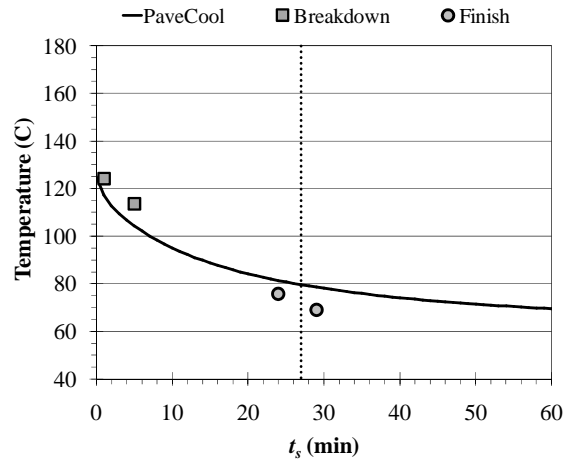
(c) Location 3

(d) Location 4

Figure A.9. PaveCool 2.4 vs. Measured Construction Data: Project 9

(a) Location 1

(b) Location 2

(c) Location 3

(d) Location 4

Figure A.10. PaveCool 2.4 vs. Measured Construction Data: Project 10
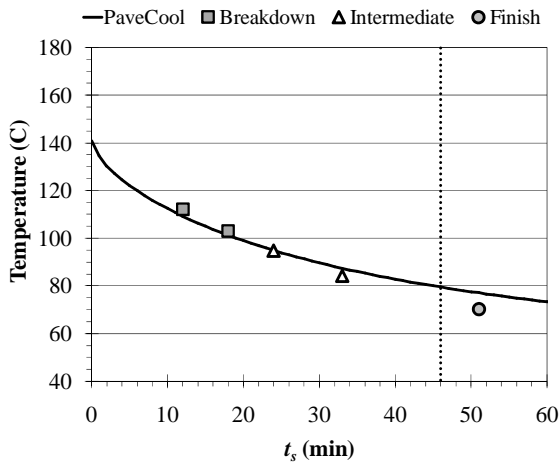
(a) Location 1
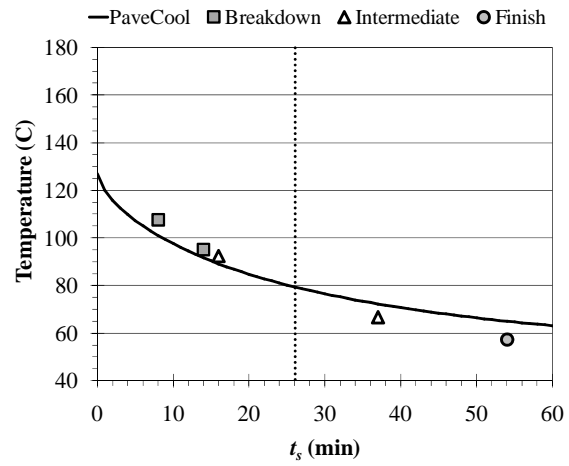
(b) Location 2
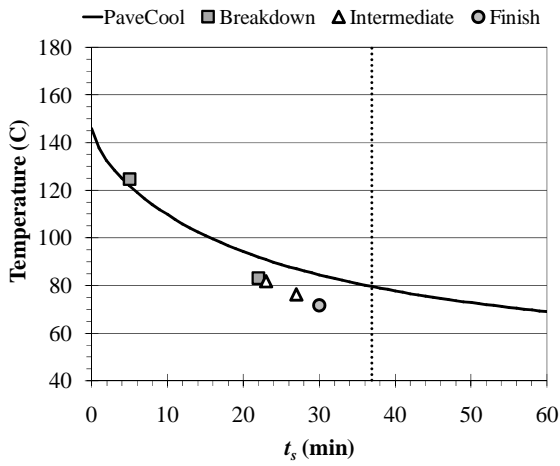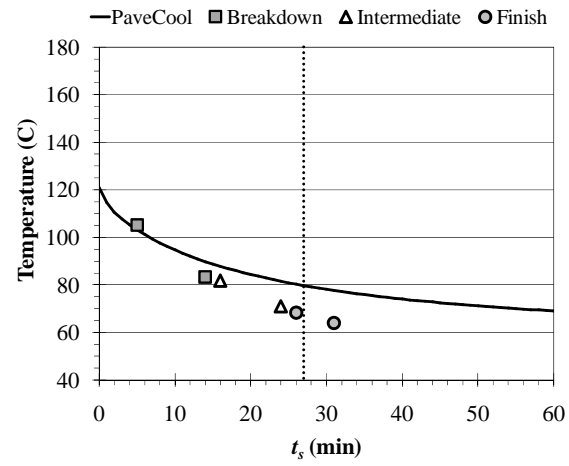
(c) Location 3

(d) Location 4

Figure A.11. PaveCool 2.4 vs. Measured Construction Data: Project 11

104
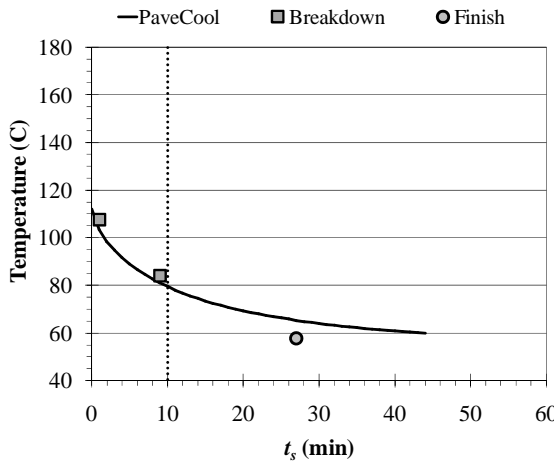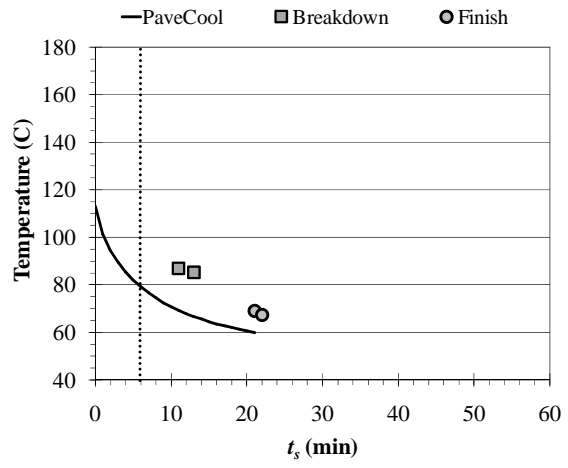
(a) Location 1
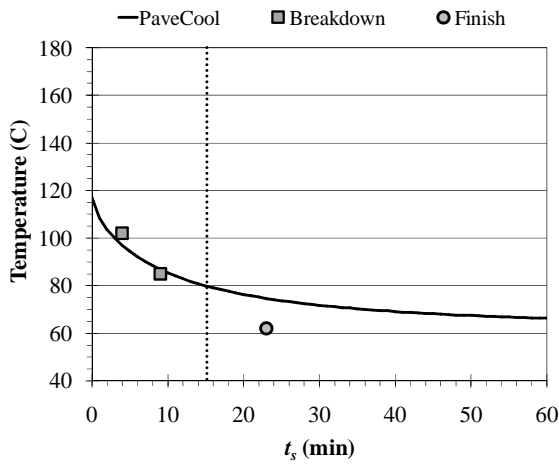
(b) Location 2

(c) Location 3

There was no location 4 at project 12

(d) Location 4

Figure A.12. PaveCool 2.4 vs. Measured Construction Data: Project 12

APPENDIX B

SCANNING ELECTRON MICROSCOPE (SEM) IMAGES
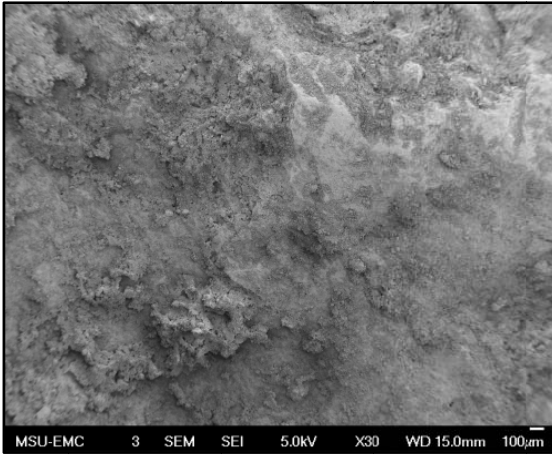
(a) Aggregate A
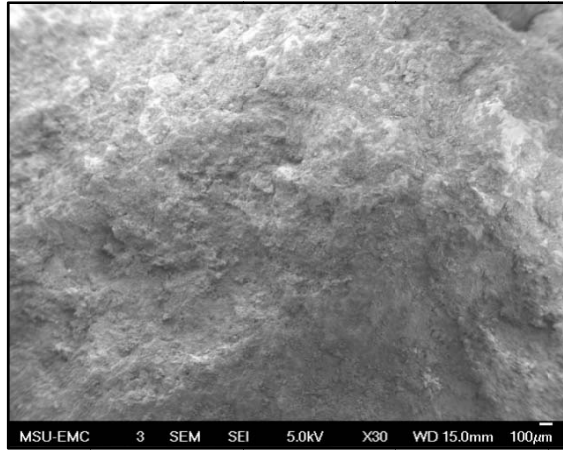
(b) Aggregate B
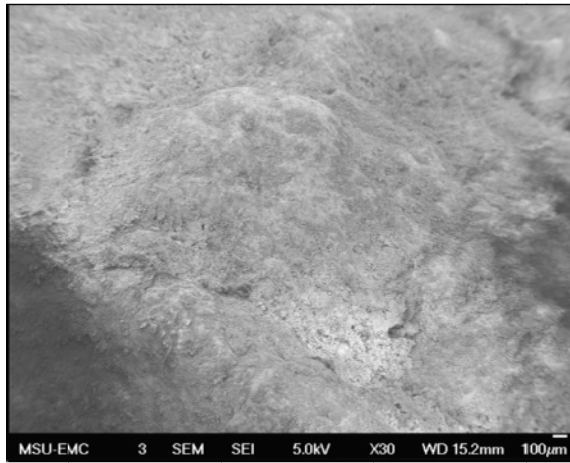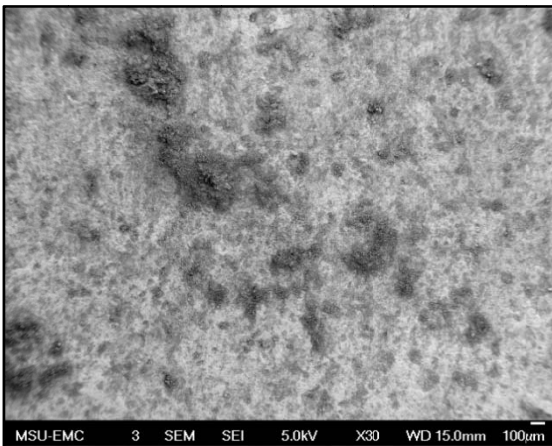

*(c) Aggregate C*
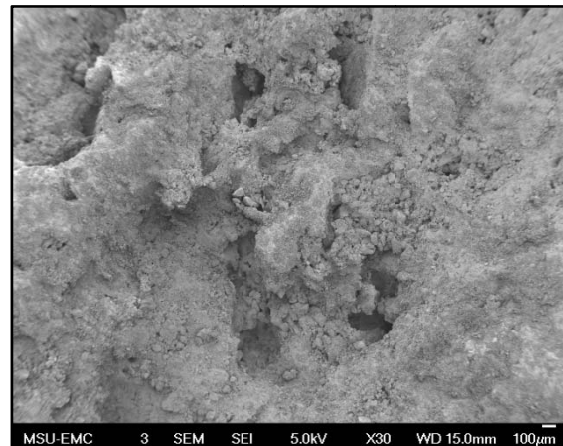
(d) Aggregate D

(e) Aggregate E

**Figure B.1. SEM Images of Sample 1, 9.5 mm Sieve, 30x**
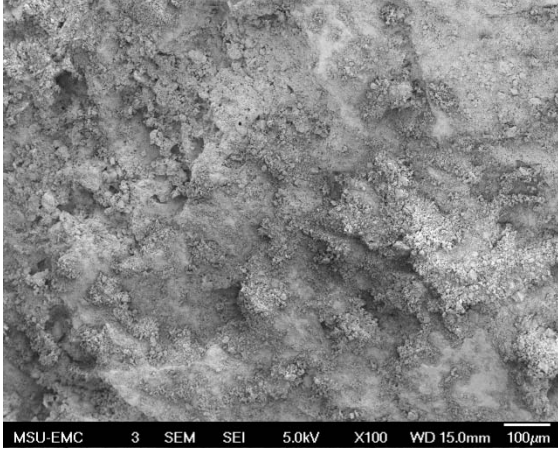
(a) Aggregate A
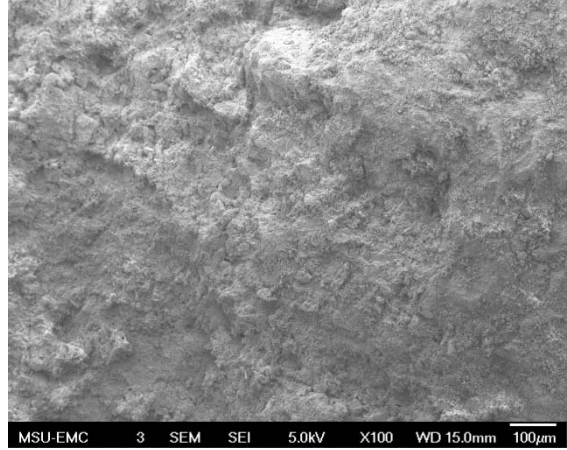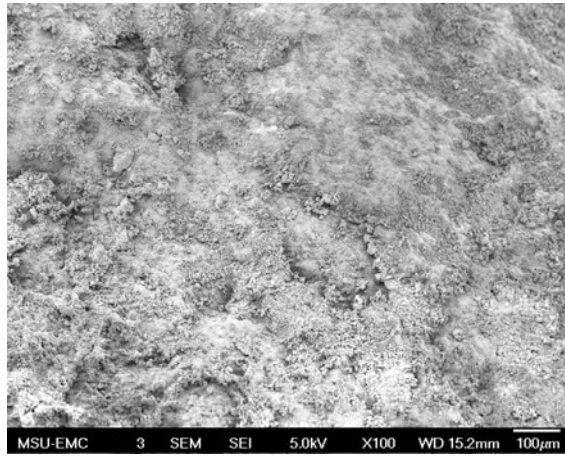
(b) Aggregate B
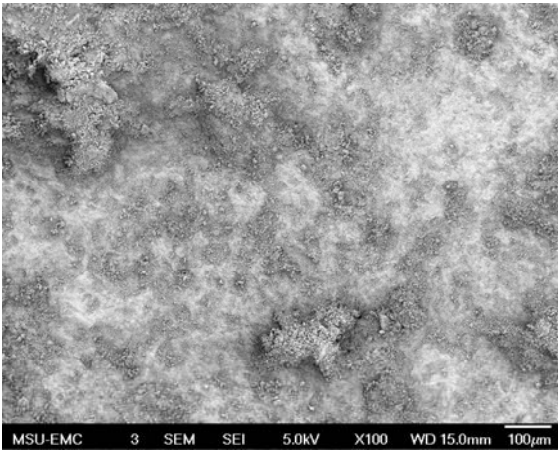
(c) Aggregate C
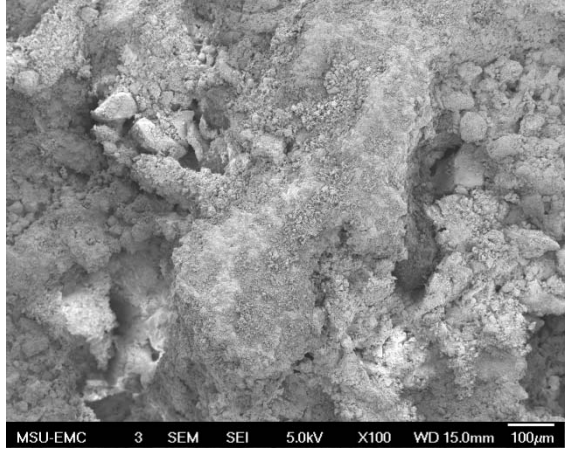
(d) Aggregate D

(e) Aggregate E

Figure B.2. SEM Images of Sample 1, 9.5 mm Sieve, 100x
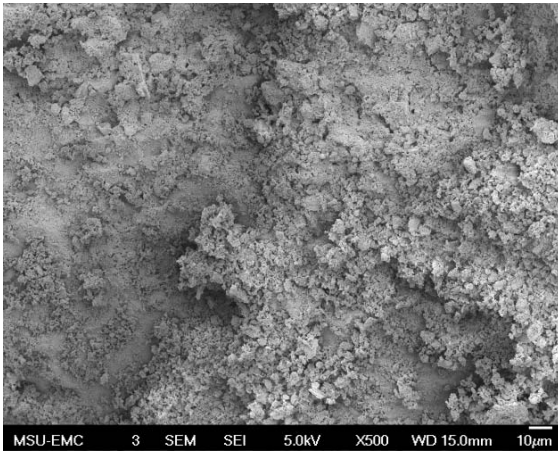
(a) Aggregate A
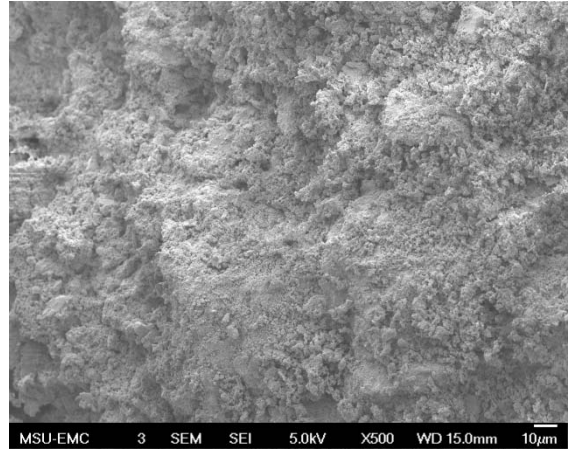
(b) Aggregate B
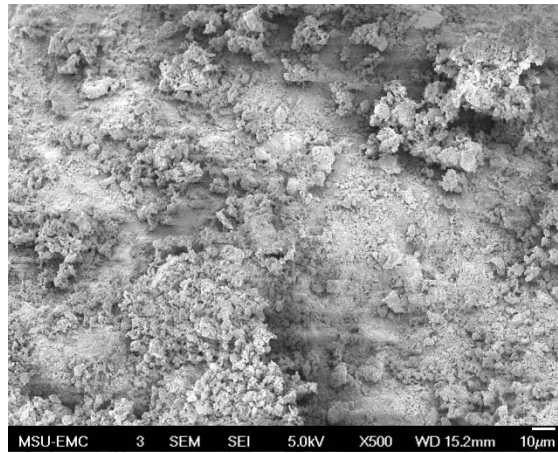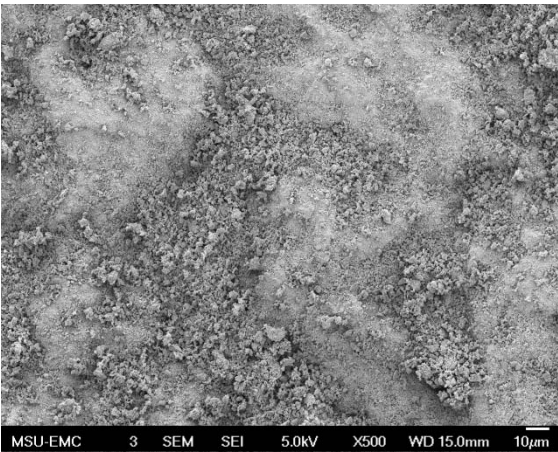
(c) Aggregate C
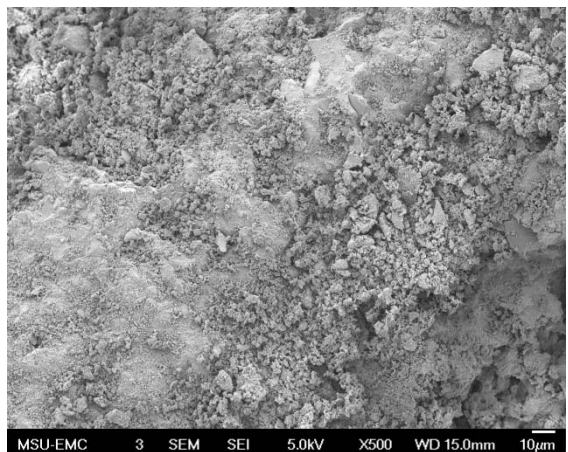
(d) Aggregate D

(e) Aggregate E

Figure B.3. SEM Images of Sample 1, 9.5 mm Sieve, 500x
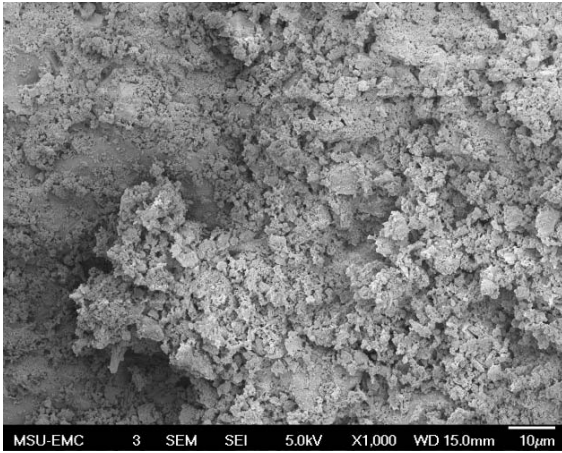
(a) Aggregate A
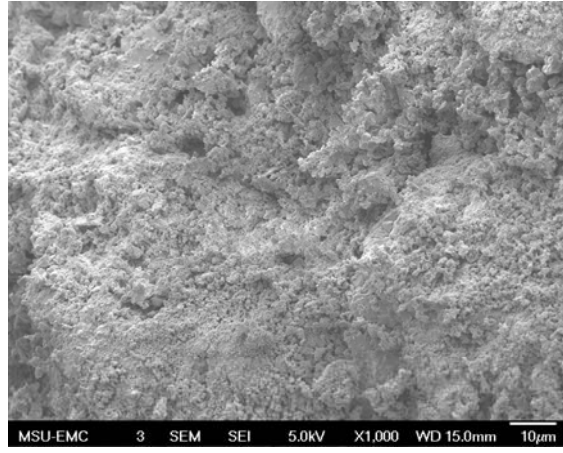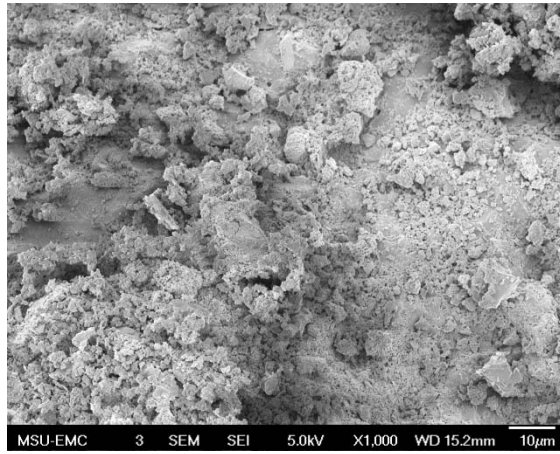
(b) Aggregate B
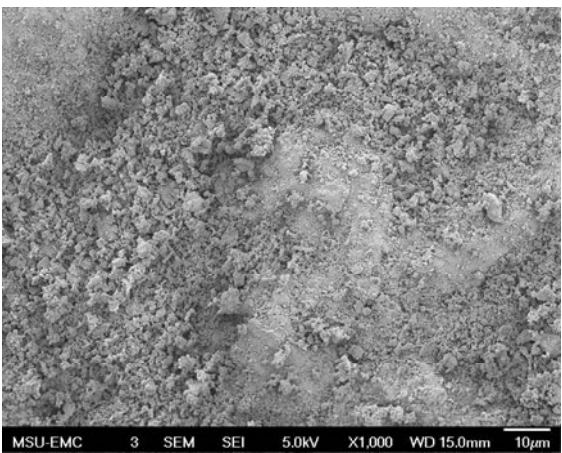
(c) Aggregate C
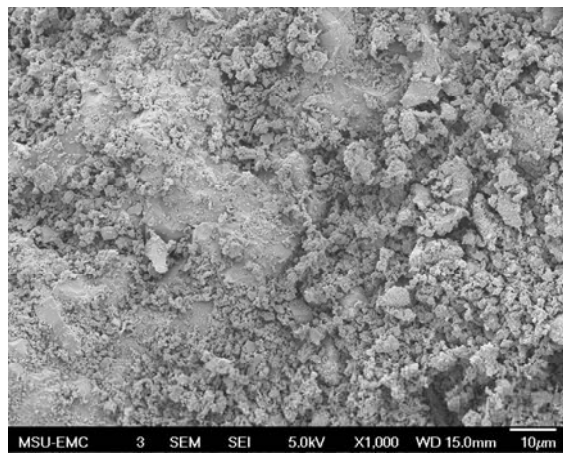
(d) Aggregate D

(e) Aggregate E

Figure B.4. SEM Images of Sample 1, 9.5 mm Sieve, 1000x
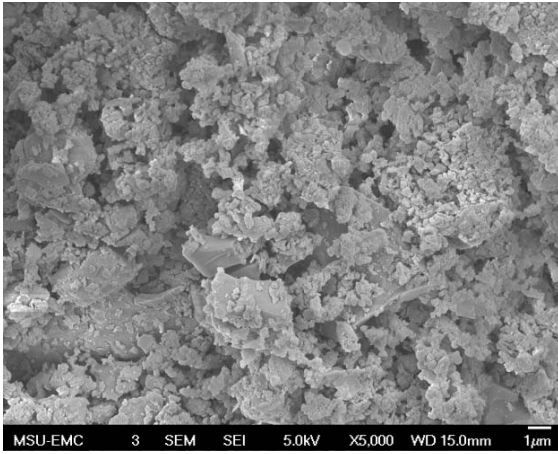
(a) Aggregate A
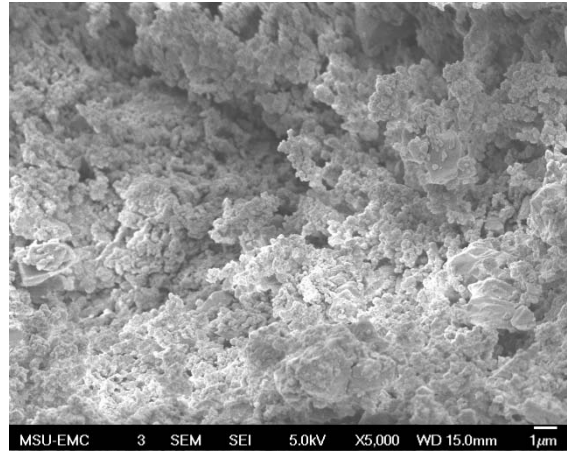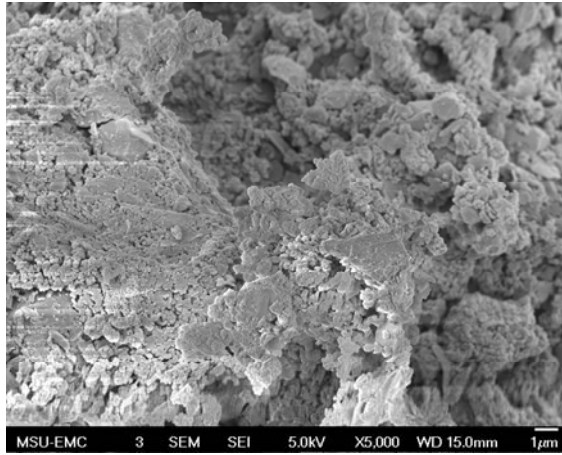
(b) Aggregate B
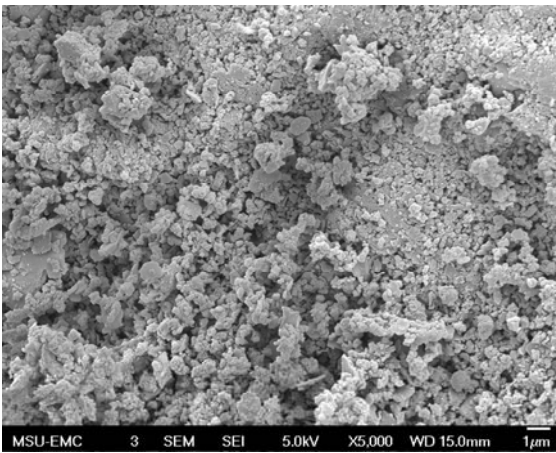
(c) Aggregate C
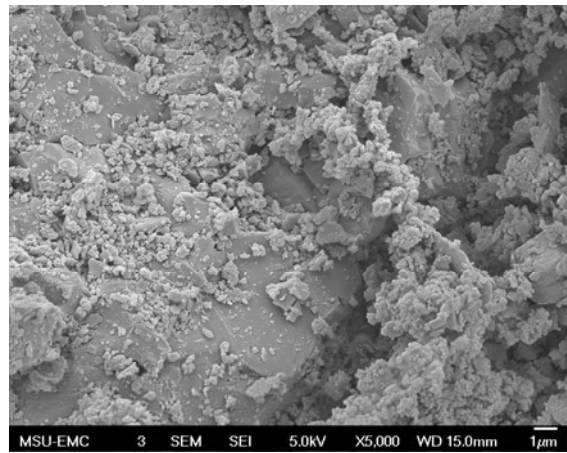
(d) Aggregate D

(e) Aggregate E

Figure B.5. SEM Images of Sample 1, 9.5 mm Sieve, 5000x
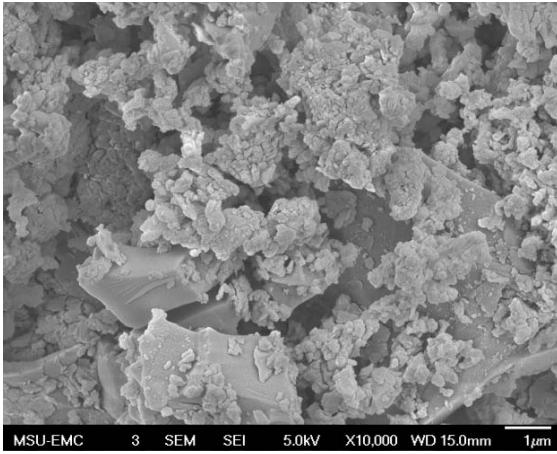
(a) Aggregate A
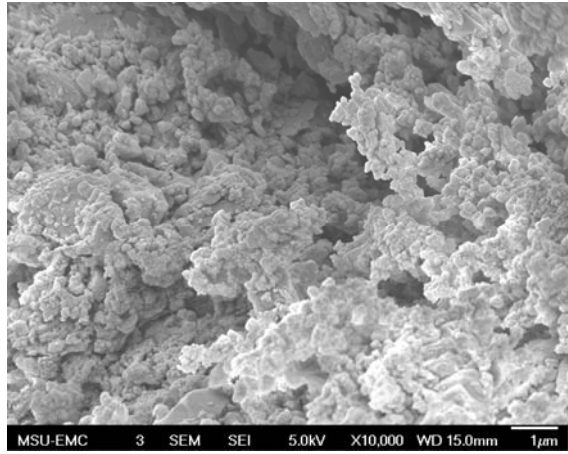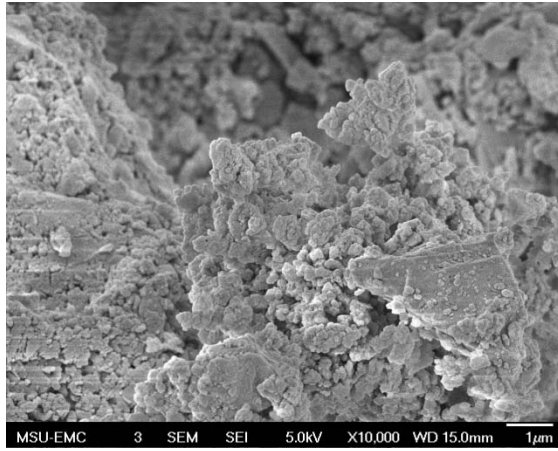
(b) Aggregate B
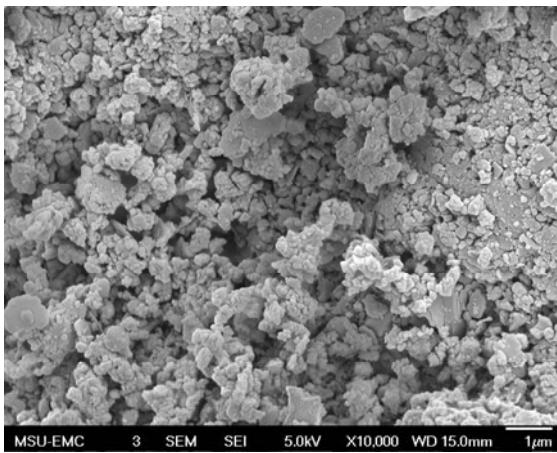
(c) Aggregate C
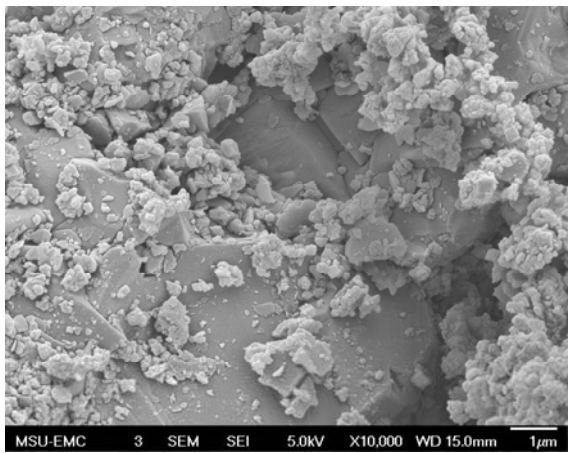
*(d) Aggregate D*

(e) Aggregate E

Figure B.6. SEM Images of Sample 1, 9.5 mm Sieve, 10000x
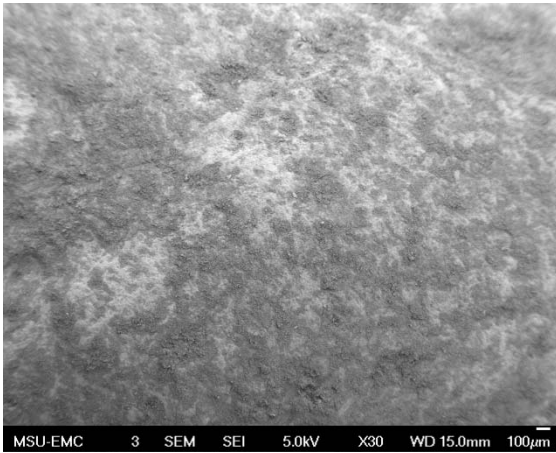
(a) Aggregate A
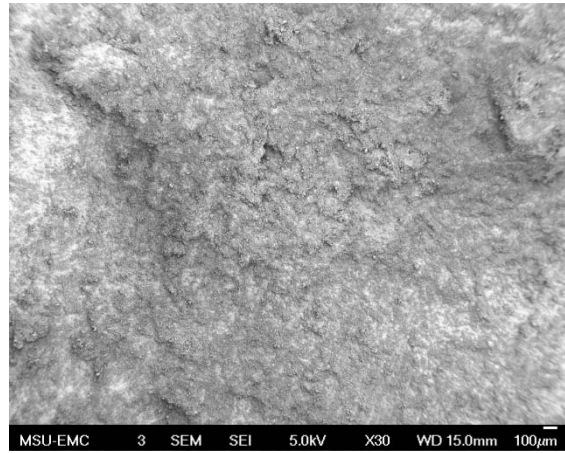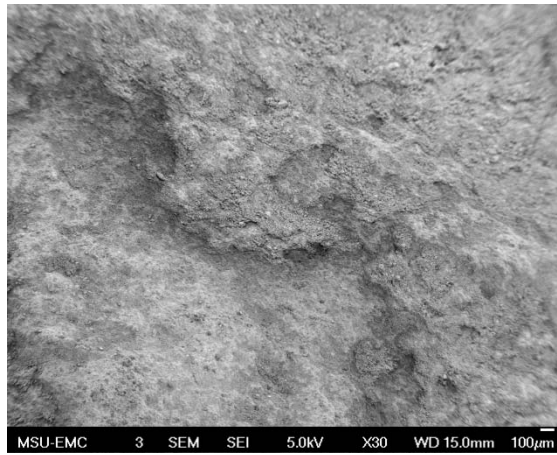
(b) Aggregate B
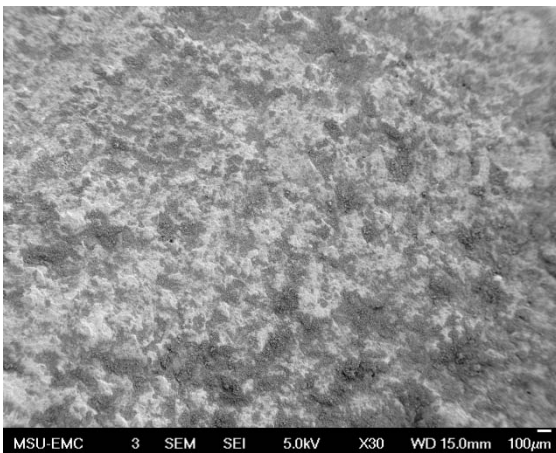
(c) Aggregate C
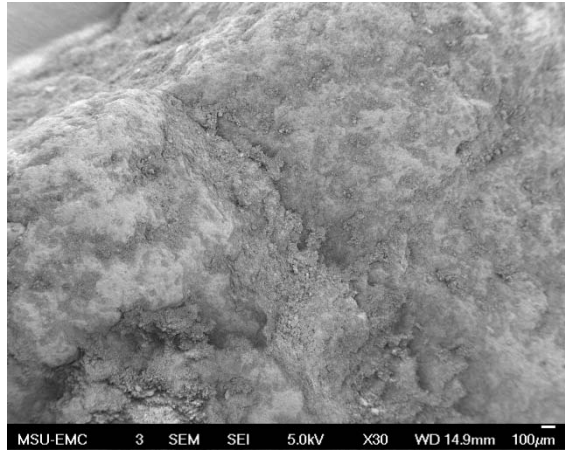
(d) Aggregate D

(e) Aggregate E

**Figure B.7. SEM Images of Sample 1, 4.75 mm Sieve, 30x**

113
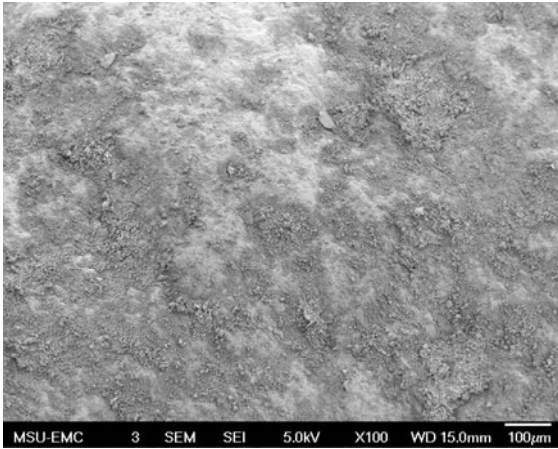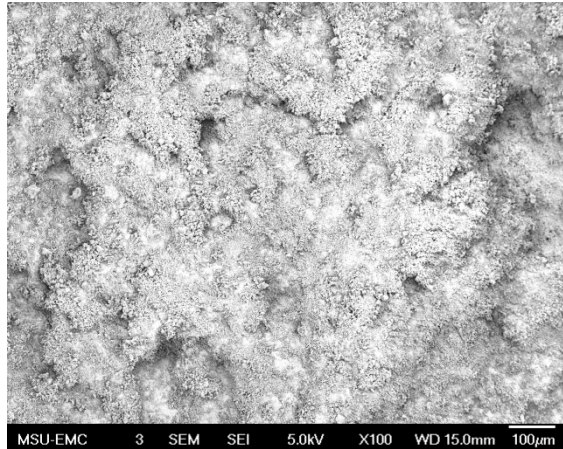
(a) Aggregate A
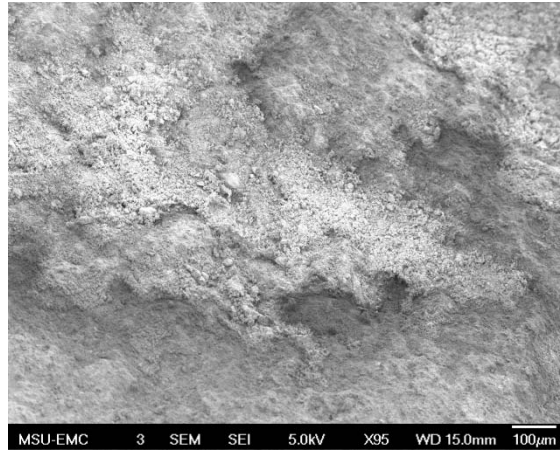
(b) Aggregate B
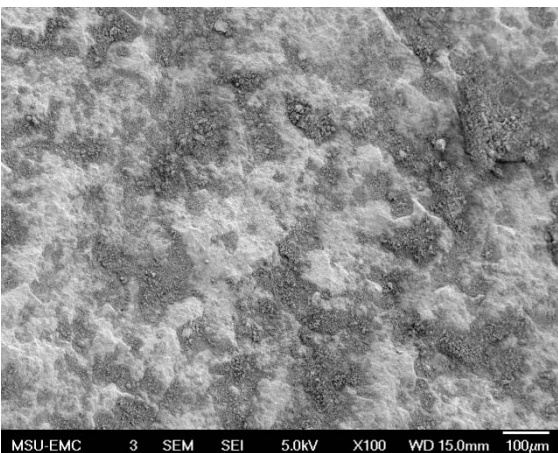
(c) Aggregate C
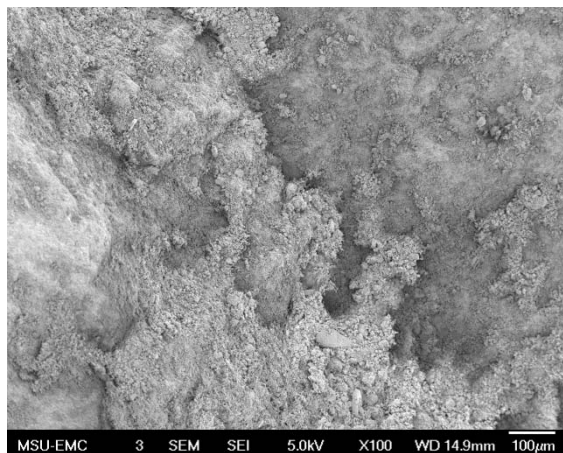
(d) Aggregate D

(e) Aggregate E

Figure B.8. SEM Images of Sample 1, 4.75 mm Sieve, 100x

114
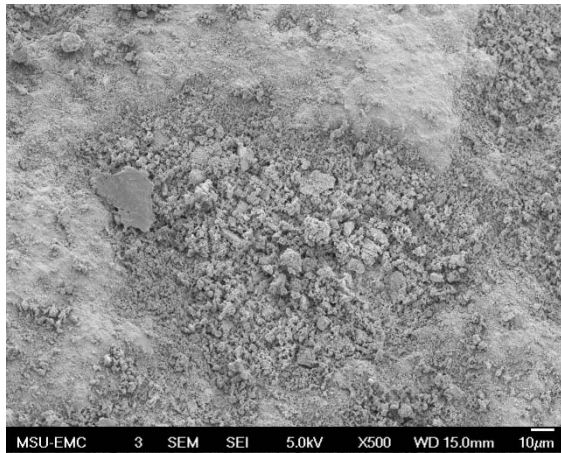
(a) Aggregate A

(b) Aggregate B

(c) Aggregate C

(d) Aggregate D

(e) Aggregate E

Figure B.9. SEM Images of Sample 1, 4.75 mm Sieve, 500x
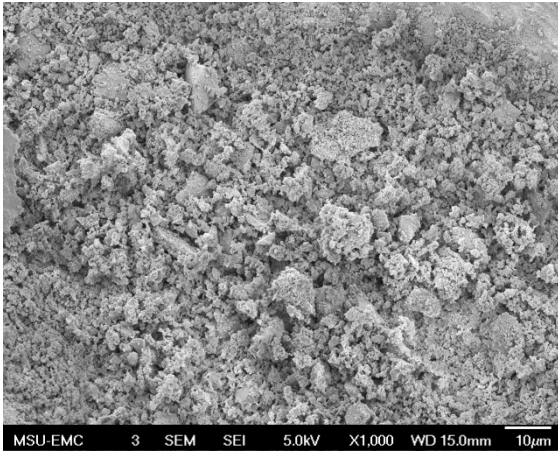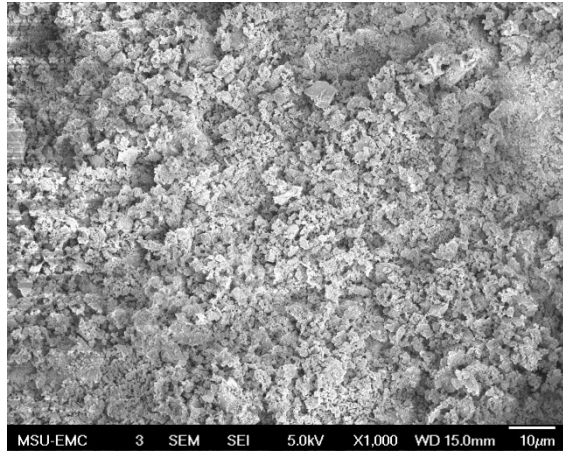
(a) Aggregate A
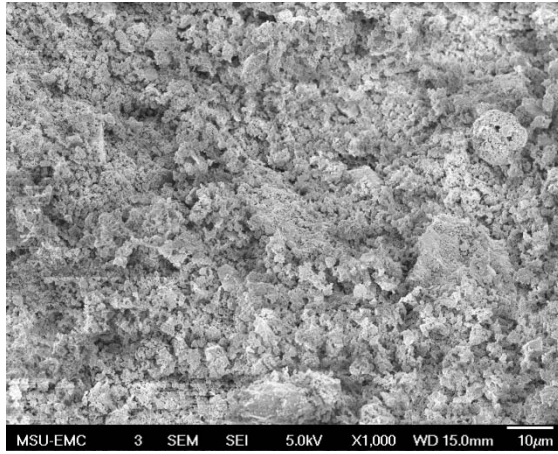
(b) Aggregate B
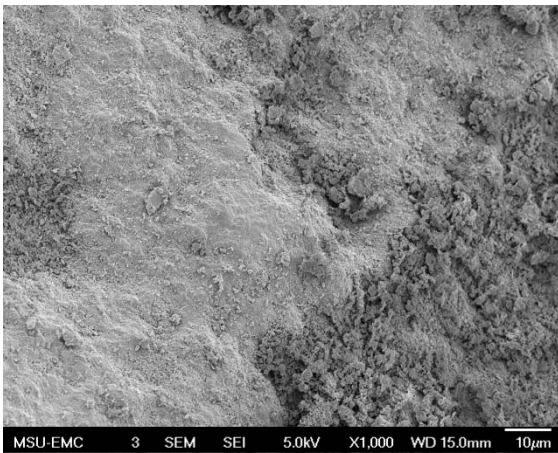
(c) Aggregate C
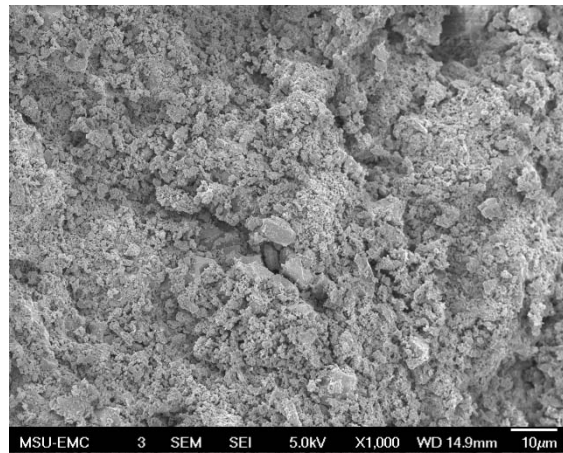
(d) Aggregate D

(e) Aggregate E

**Figure B.10. SEM Images of Sample 1, 4.75 mm Sieve, 1000x**
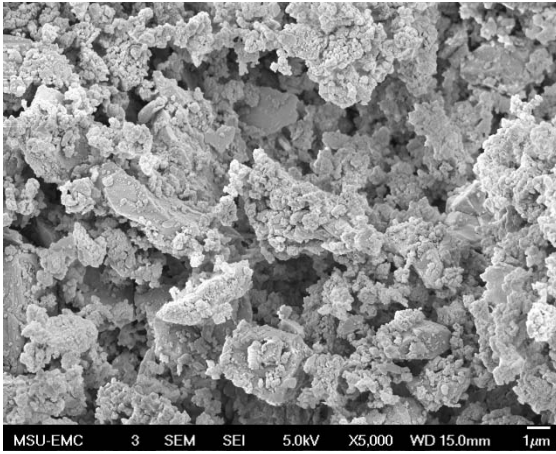
(a) Aggregate A
(b) Aggregate B
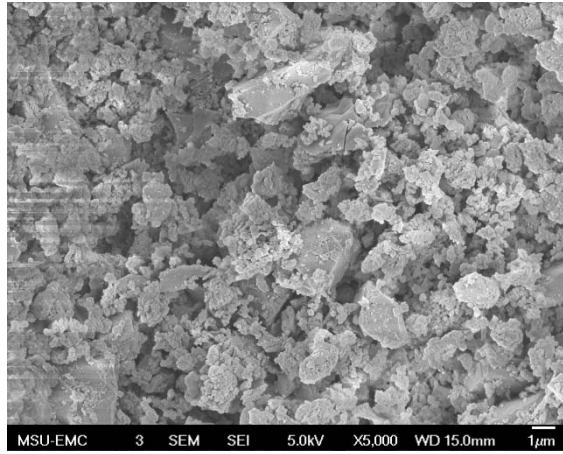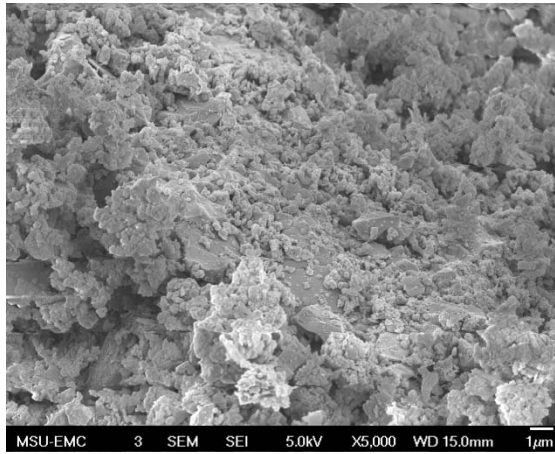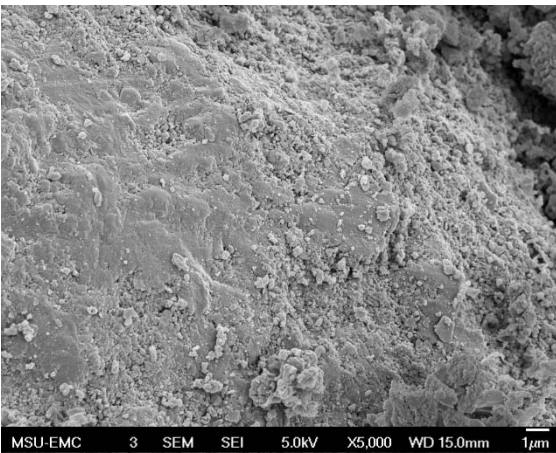
(c) Aggregate C

(d) Aggregate D
(e) Aggregate E

Figure B.11. SEM Images of Sample 1, 4.75 mm Sieve, 5000x
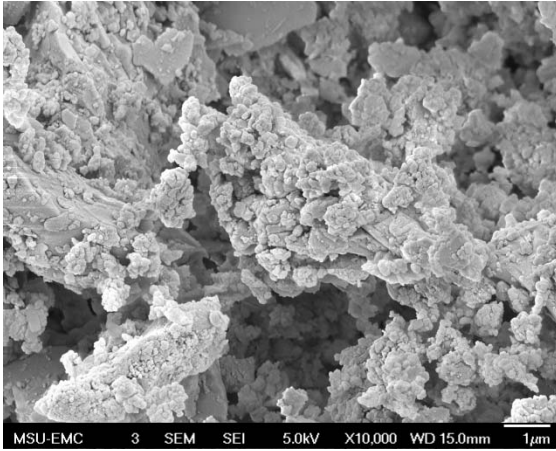
(a) Aggregate A
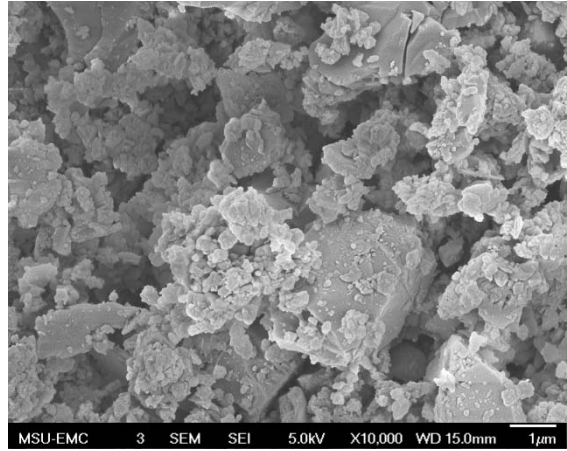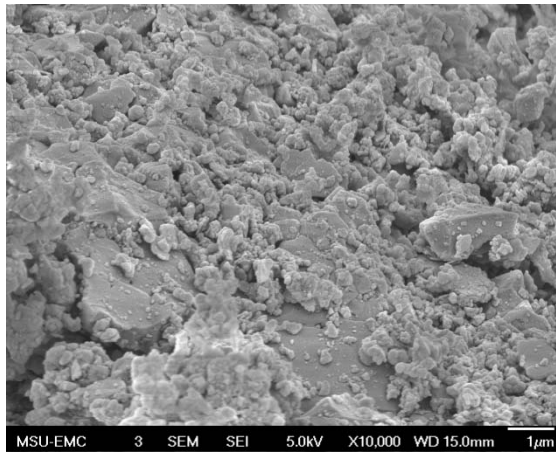
(b) Aggregate B
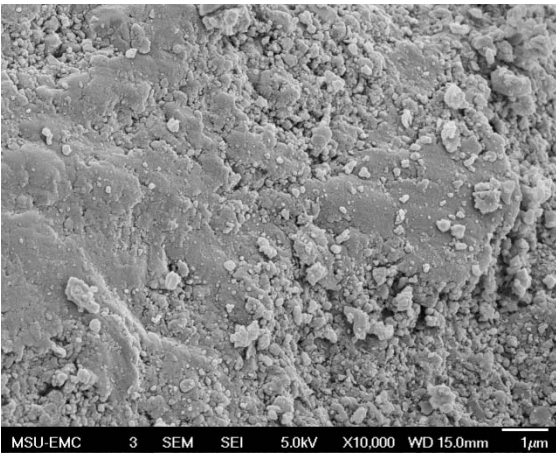
(c) Aggregate C
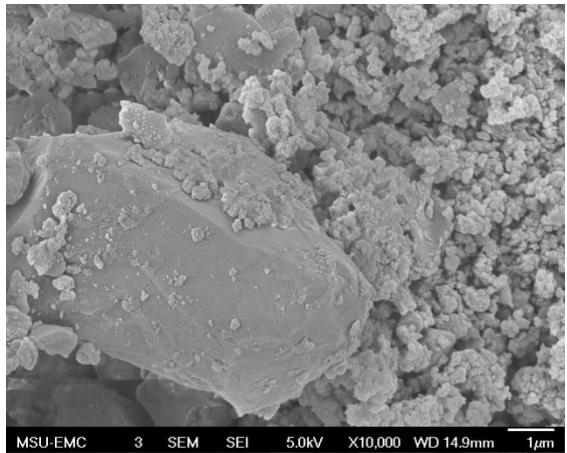
(d) Aggregate D

(e) Aggregate E

Figure B.12. SEM Images of Sample 1, 4.75 mm Sieve, 10000x

118
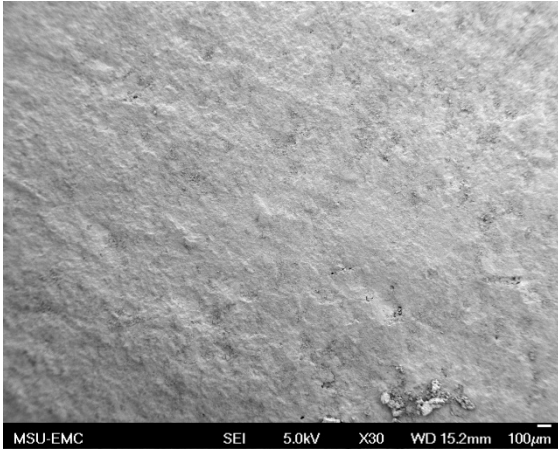
(a) Aggregate A

(b) Aggregate B

(c) Aggregate C

(d) Aggregate D

(e) Aggregate E

**Figure B.13. SEM Images of Sample 2, 4.75 mm Sieve, 30x**
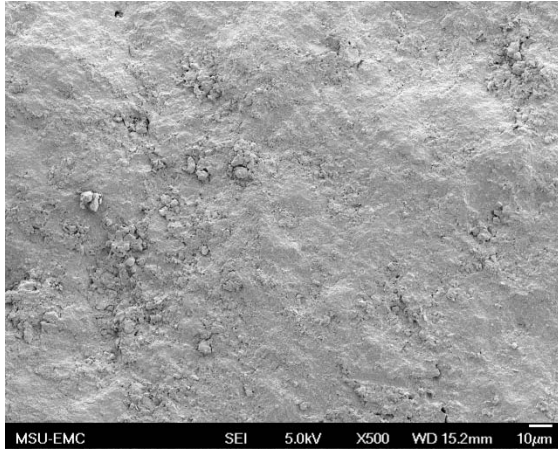
*(a) Aggregate A*
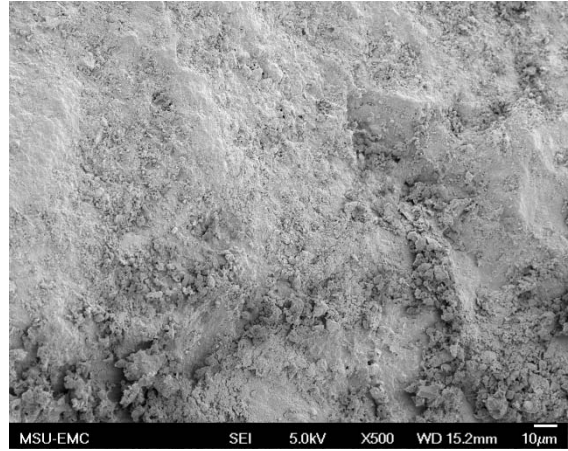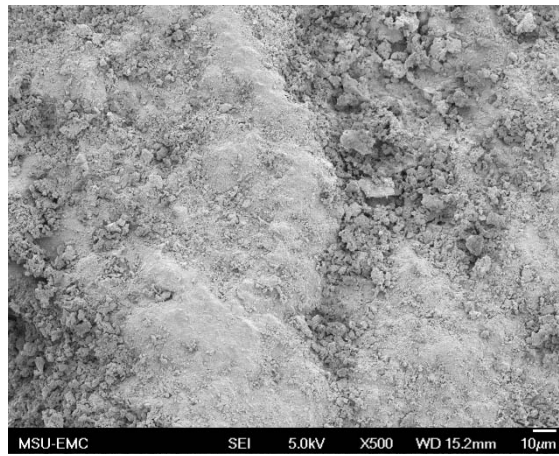
*(b) Aggregate B*
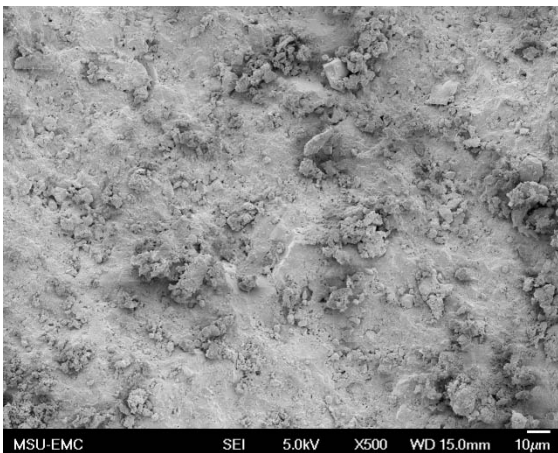
(c) Aggregate C
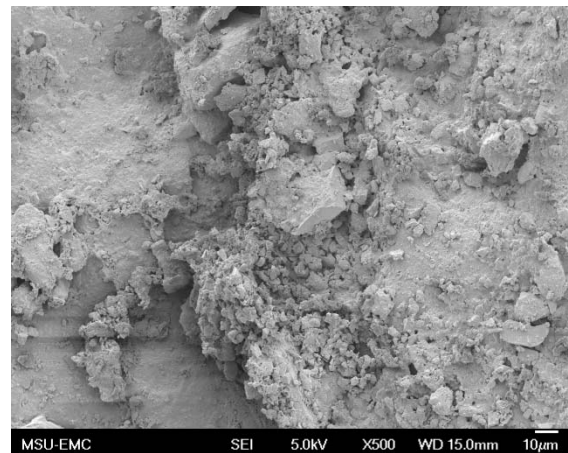

(d) Aggregate D

(e) Aggregate E

Figure B.14. SEM Images of Sample 2, 4.75 mm Sieve, 500x
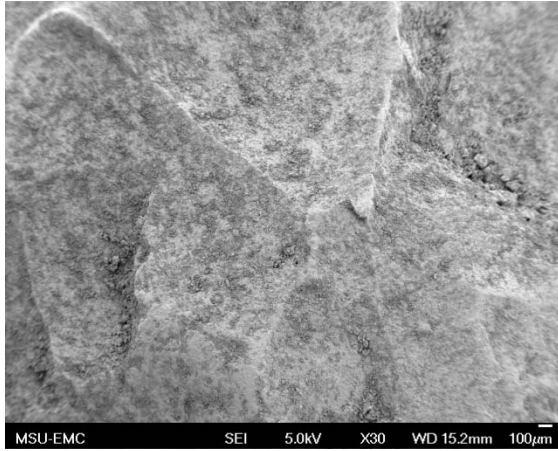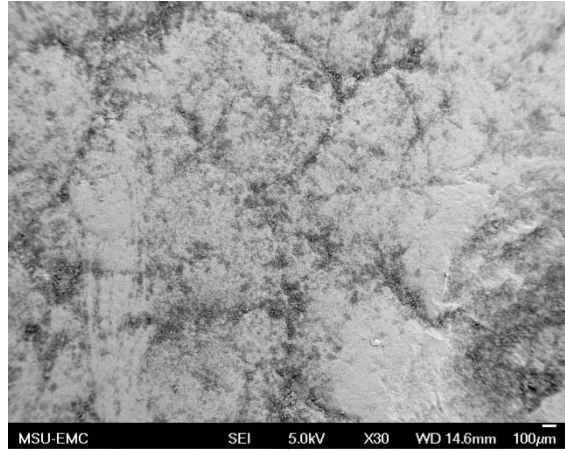
(a) Aggregate A
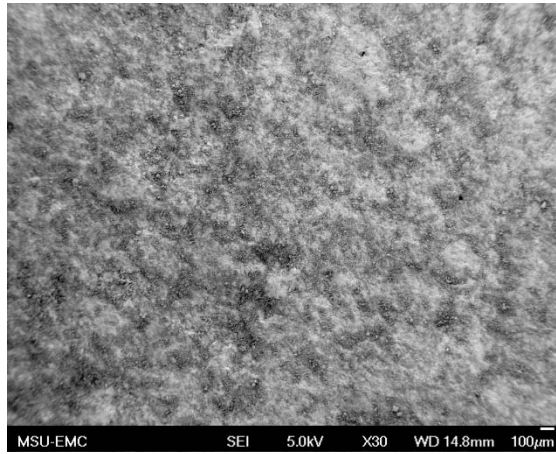
(b) Aggregate B
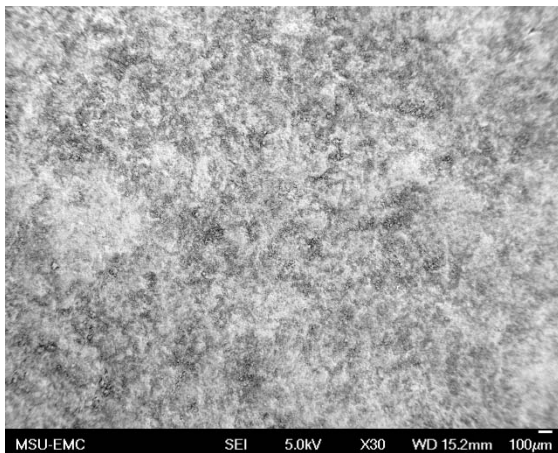
(c) Aggregate C
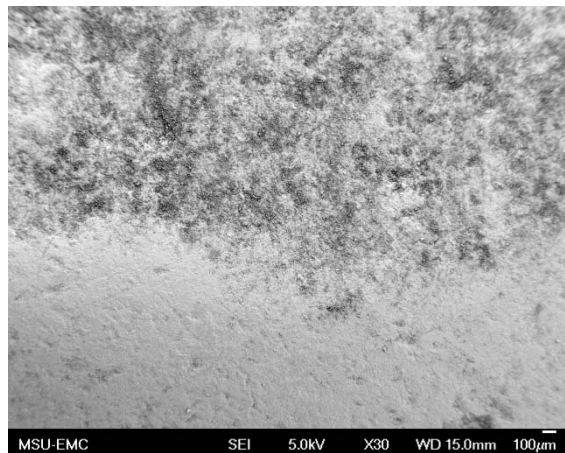
(d) Aggregate D

(e) Aggregate E

Figure B.15. SEM Images of Sample 3, 4.75 mm Sieve, 30x
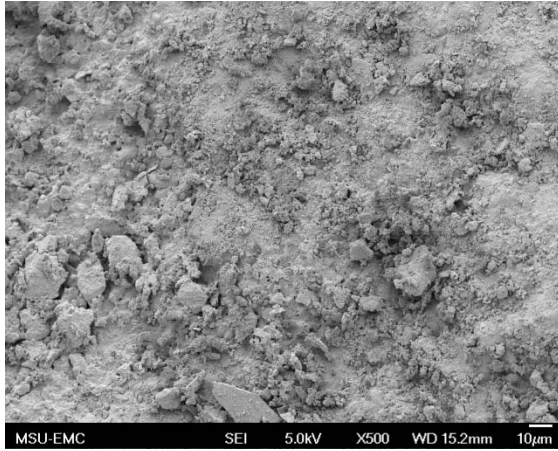
(a) Aggregate A
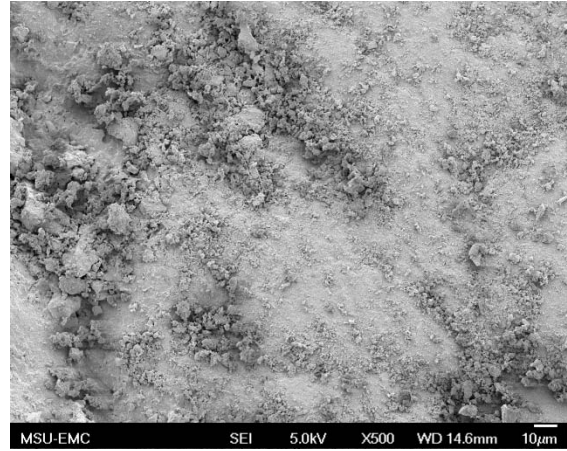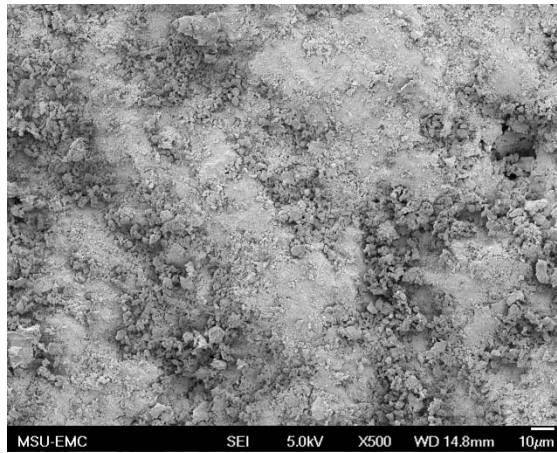
(b) Aggregate B
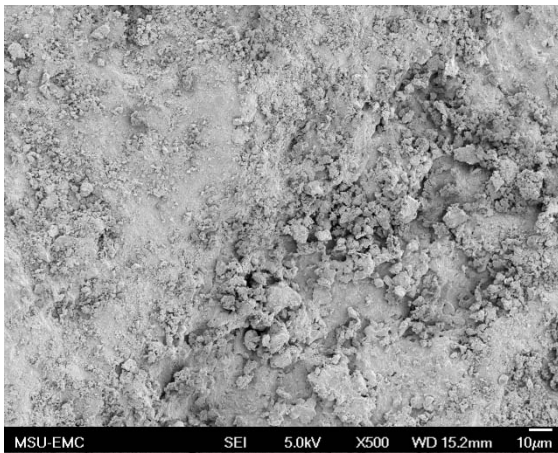
(c) Aggregate C
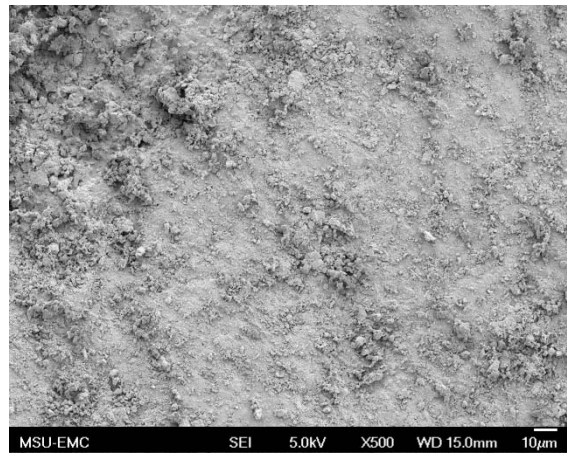
(d) Aggregate D

(e) Aggregate E

**Figure B.16. SEM Images of Sample 3, 4.75 mm Sieve, 500x**
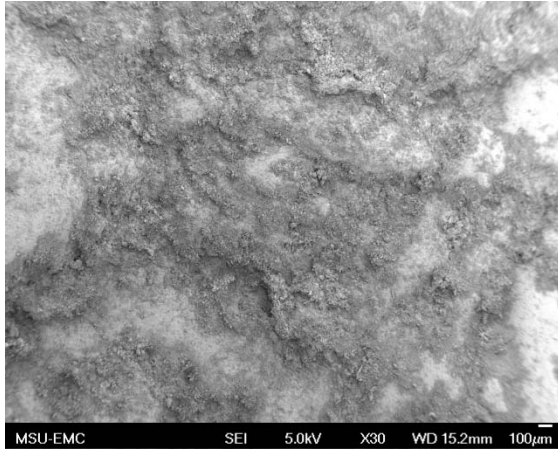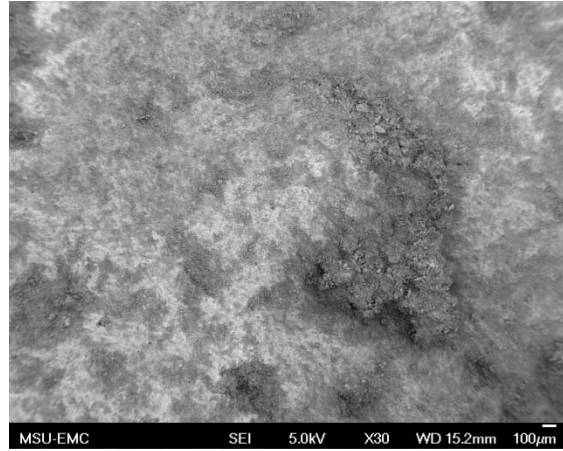
*(a) Aggregate A*
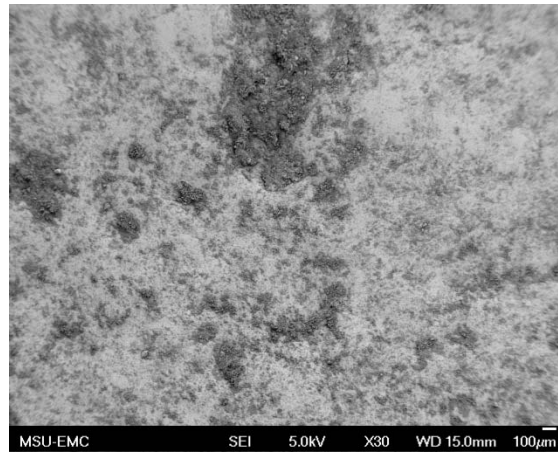
(b) Aggregate B
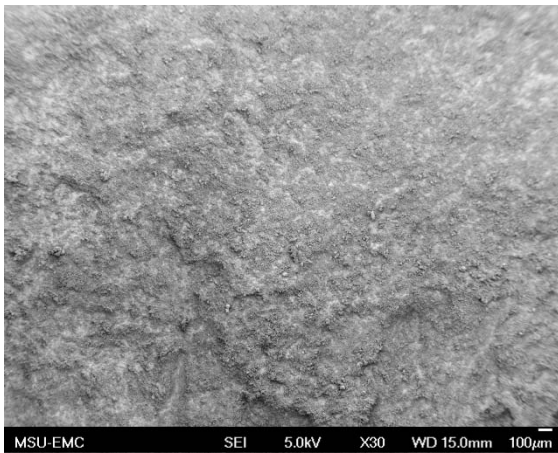
(c) Aggregate C
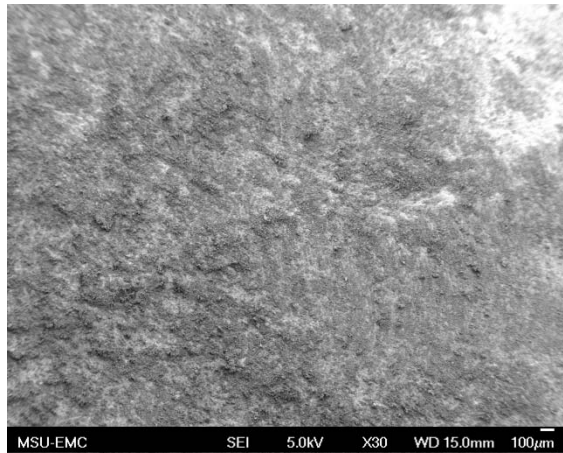
(d) Aggregate D

(e) Aggregate E

Figure B.17. SEM Images of Sample 4, 4.75 mm Sieve, 30x
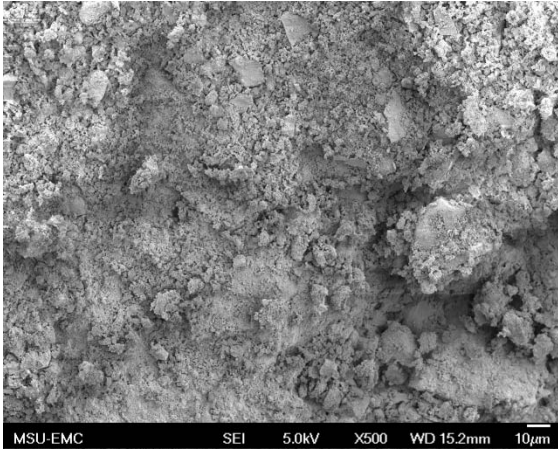
(a) Aggregate A
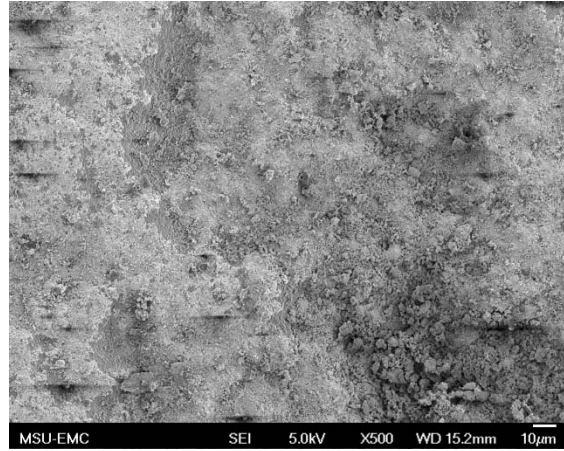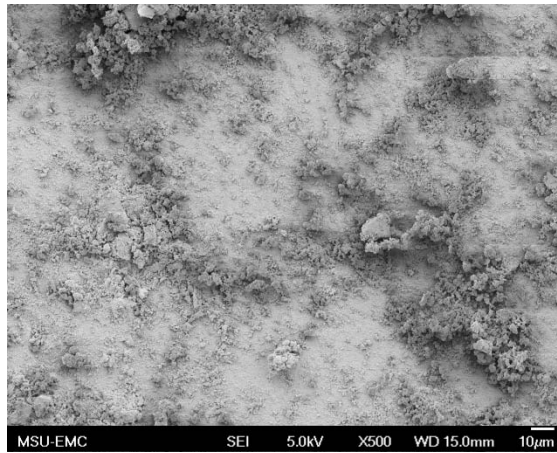
(b) Aggregate B
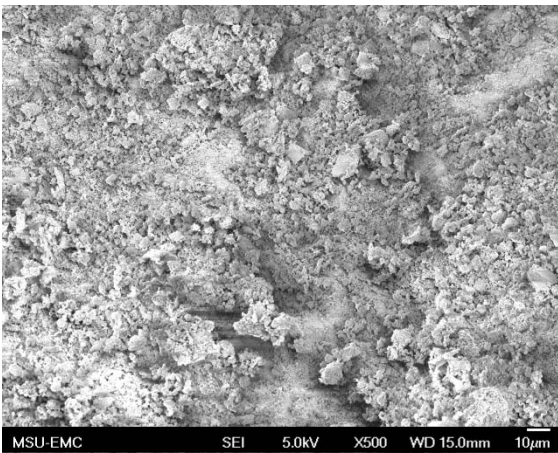
(c) Aggregate C
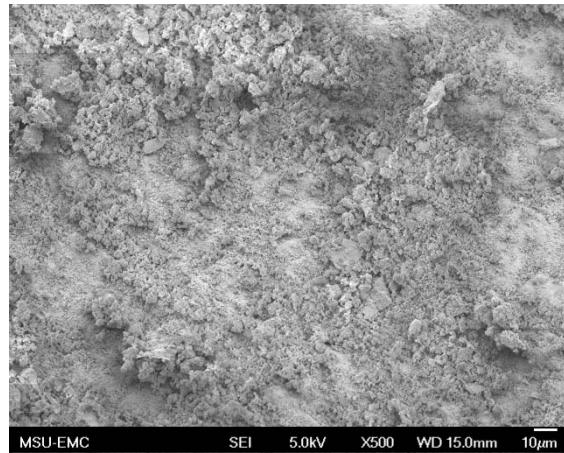
(d) Aggregate D

(e) Aggregate E

Figure B.18. SEM Images of Sample 4, 4.75 mm Sieve, 500x
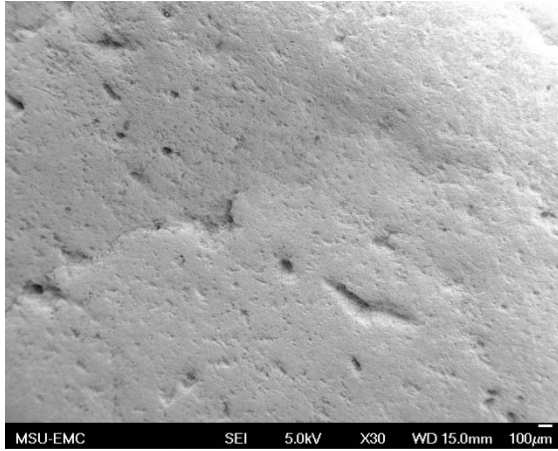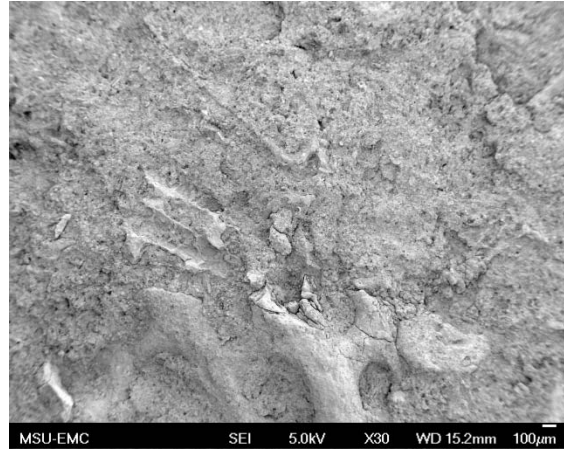
(a) Aggregate A
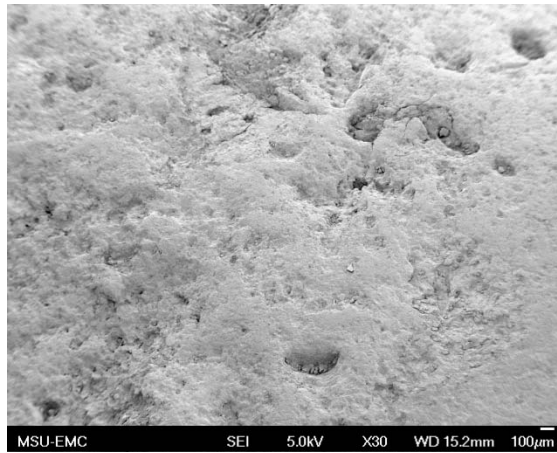
(b) Aggregate B
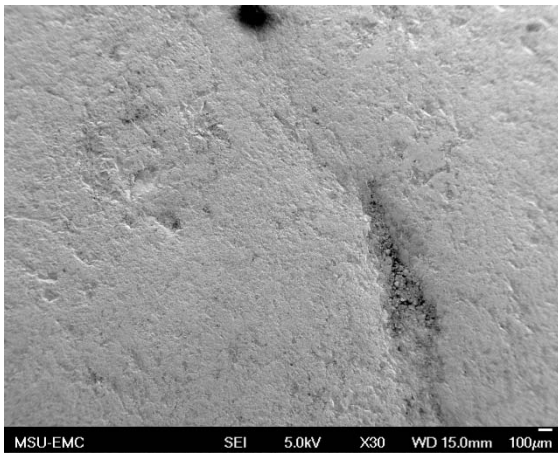
*(c) Aggregate C*
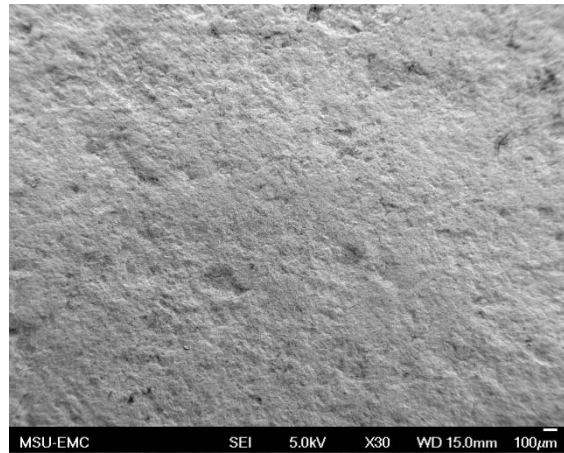

(d) Aggregate D

(e) Aggregate E

Figure B.19. SEM Images of Sample 4A, 4.75 mm Sieve, 30x
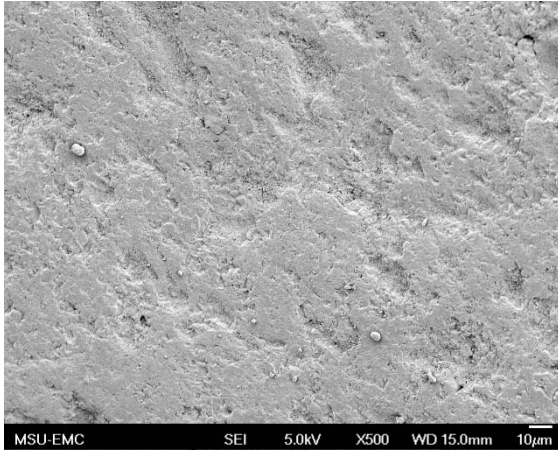
(a) Aggregate A
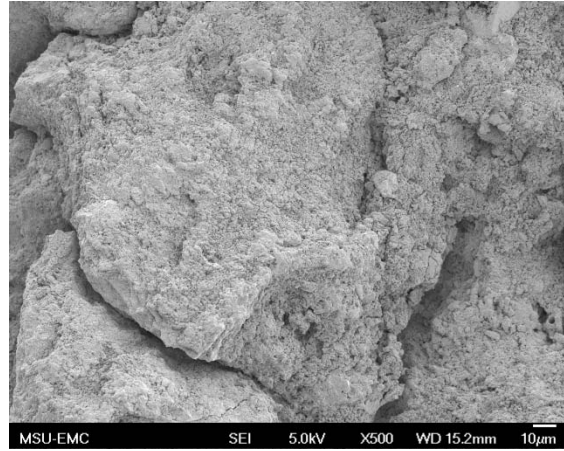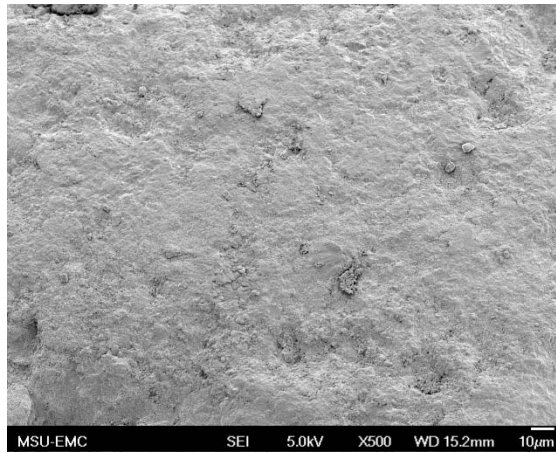
(b) Aggregate B
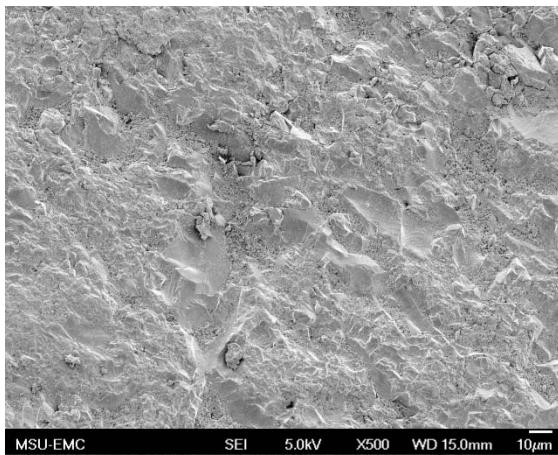
(c) Aggregate C
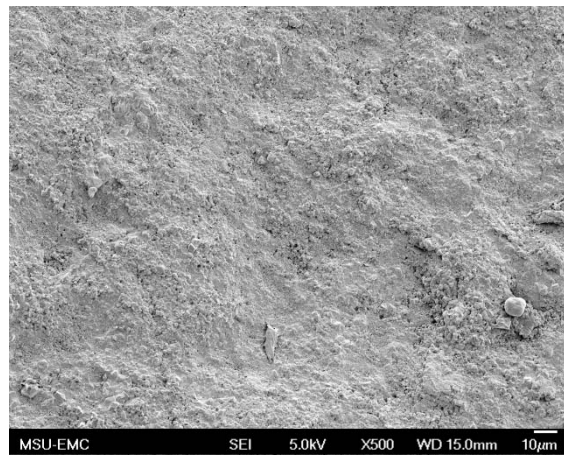
(d) Aggregate D

(e) Aggregate E

Figure B.20. SEM Images of Sample 4A, 4.75 mm Sieve, 500x
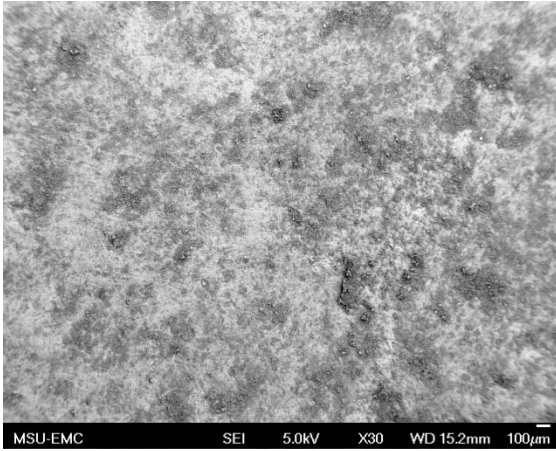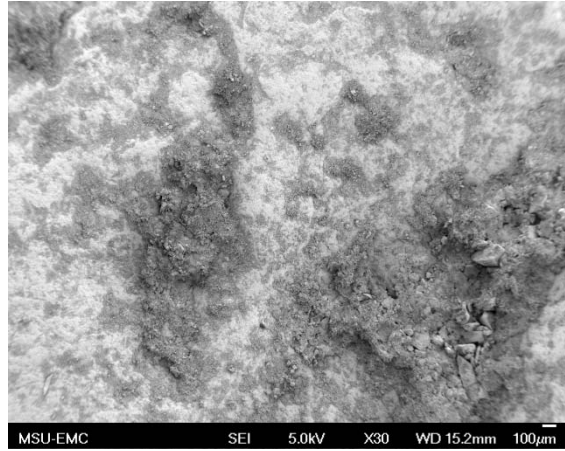
(a) Aggregate A
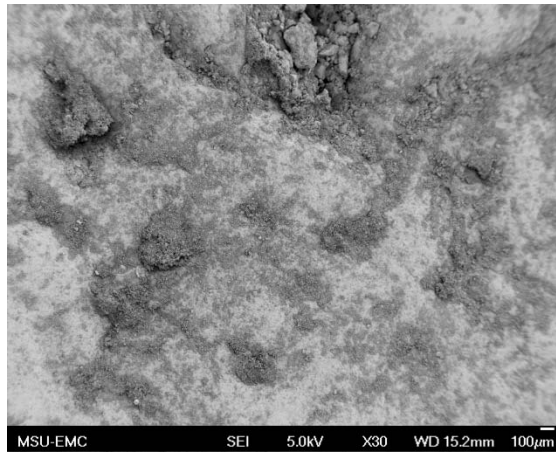
(b) Aggregate B
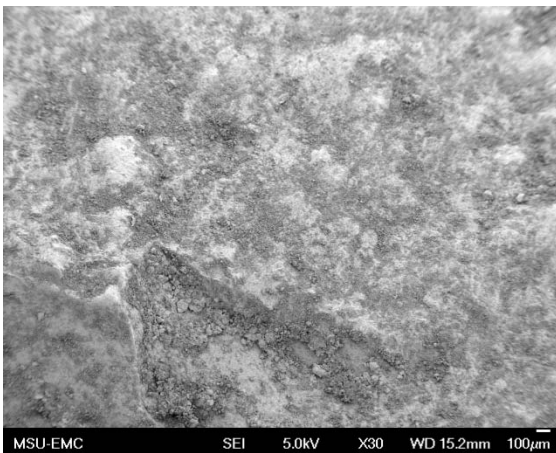
(c) Aggregate C
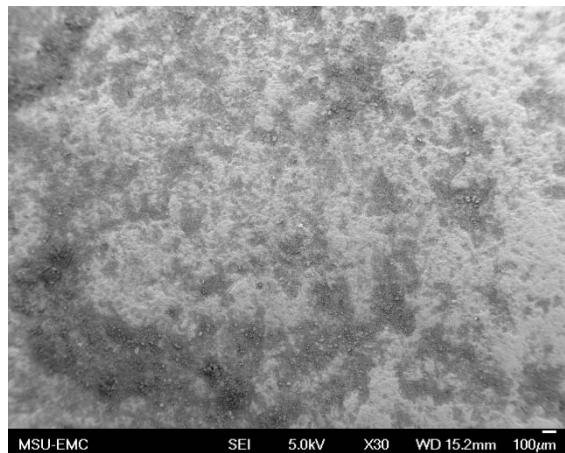
(d) Aggregate D

(e) Aggregate E

**Figure B.21. SEM Images of Sample 5, 4.75 mm Sieve, 30x**
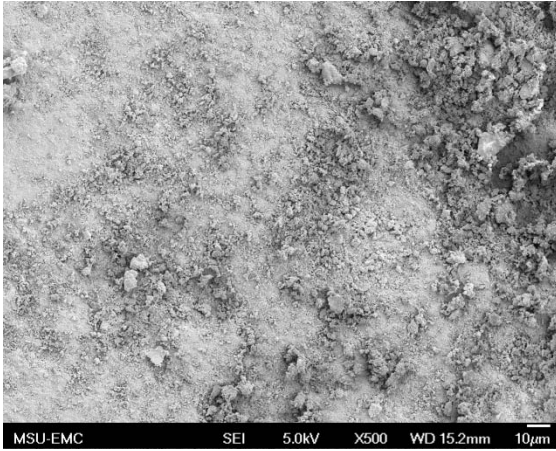
(a) Aggregate A
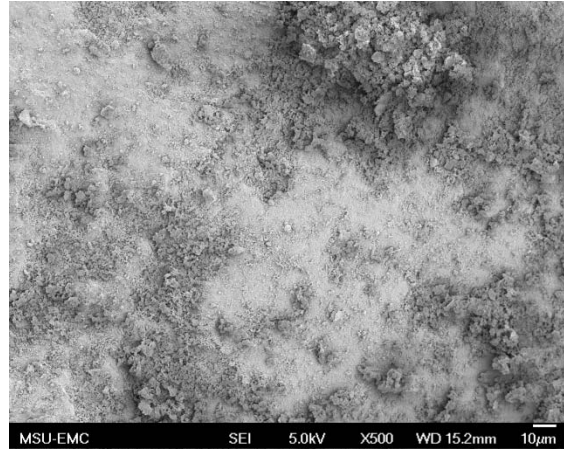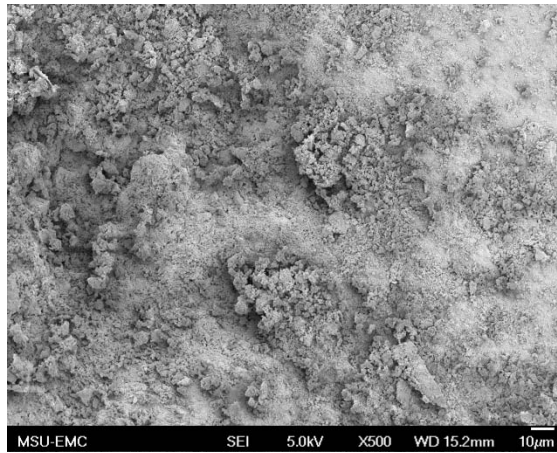
(b) Aggregate B
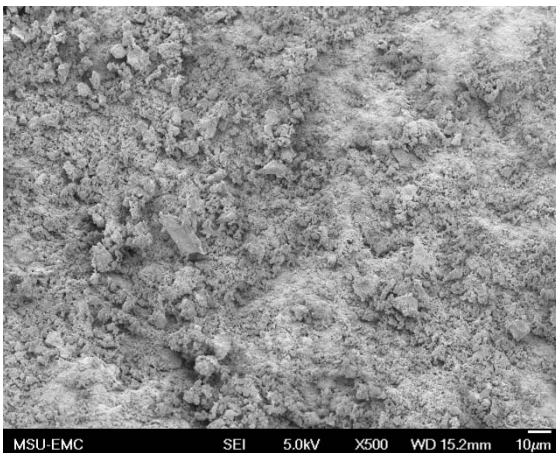
(c) Aggregate C

(d) Aggregate D

(e) Aggregate E

Figure B.22. SEM Images of Sample 5, 4.75 mm Sieve, 500x

128
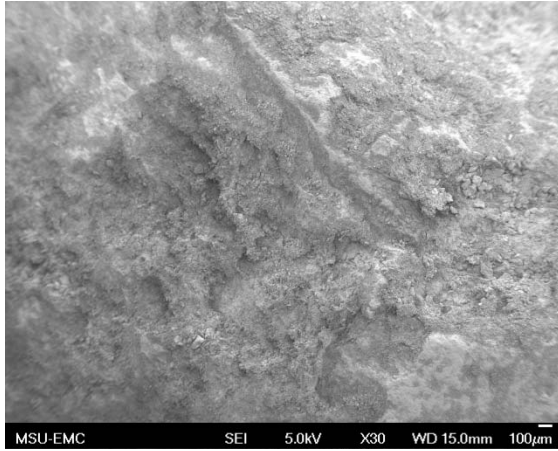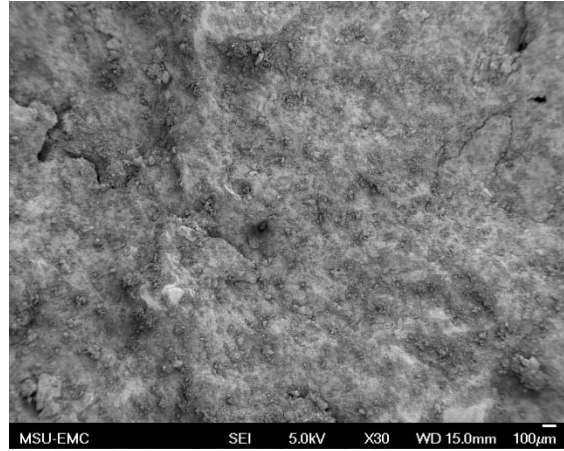
(a) Aggregate A
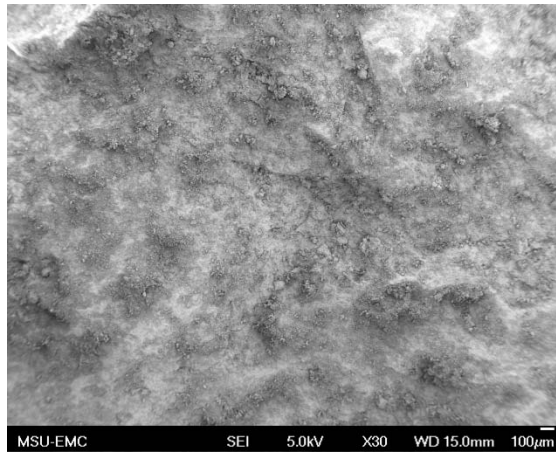
(b) Aggregate B
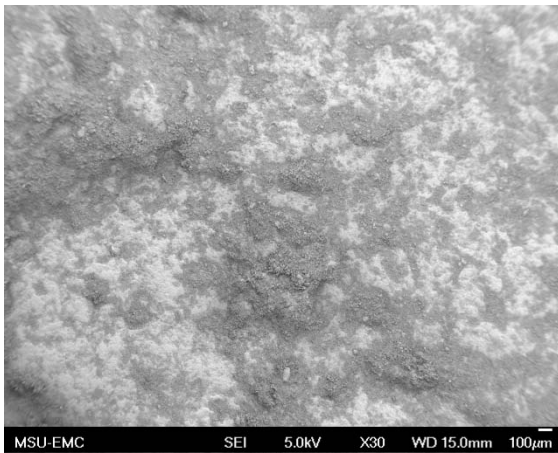
(c) Aggregate C
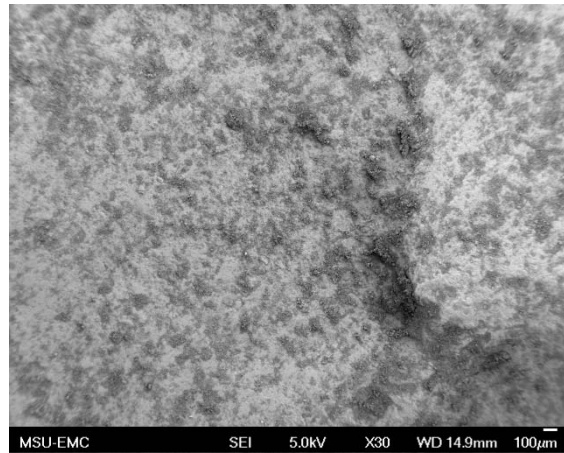
(d) Aggregate D

(e) Aggregate E

Figure B.23. SEM Images of Sample 6, 4.75 mm Sieve, 30x
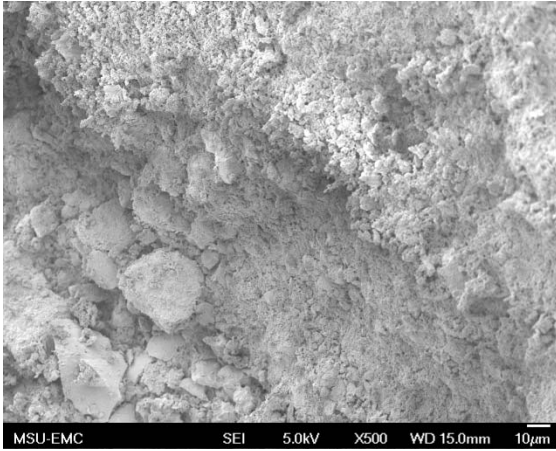
(a) Aggregate A
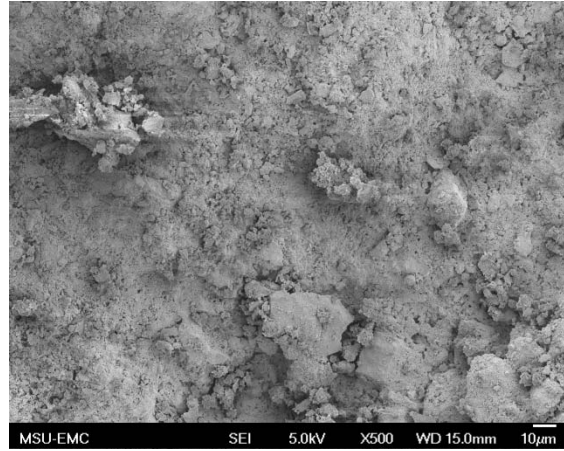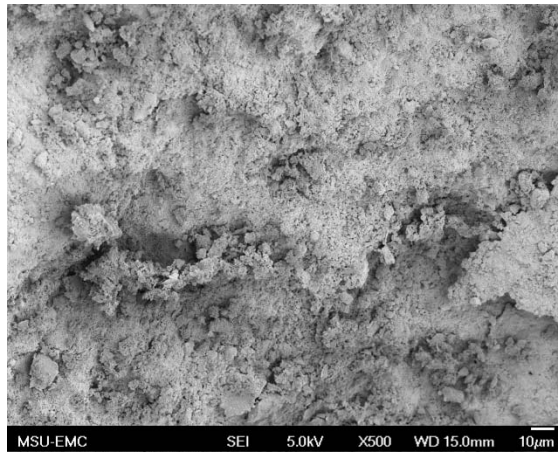

*(b) Aggregate B*
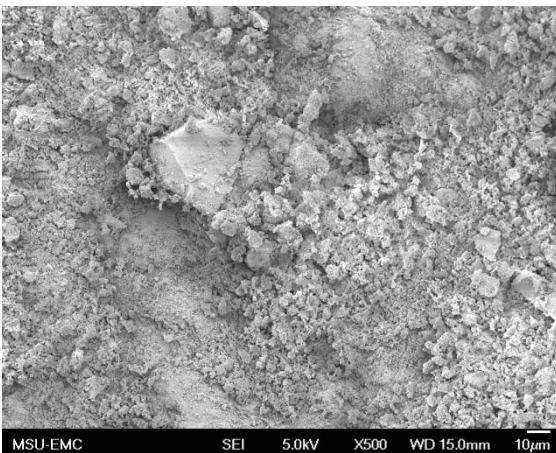
(c) Aggregate C
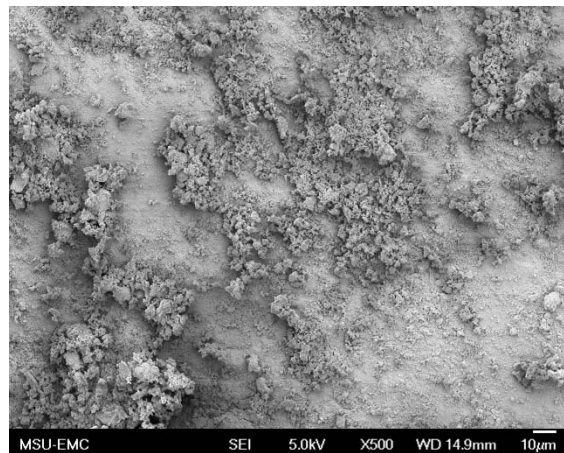

(d) Aggregate D

(e) Aggregate E

Figure B.24. SEM Images of Sample 6, 4.75 mm Sieve, 500x
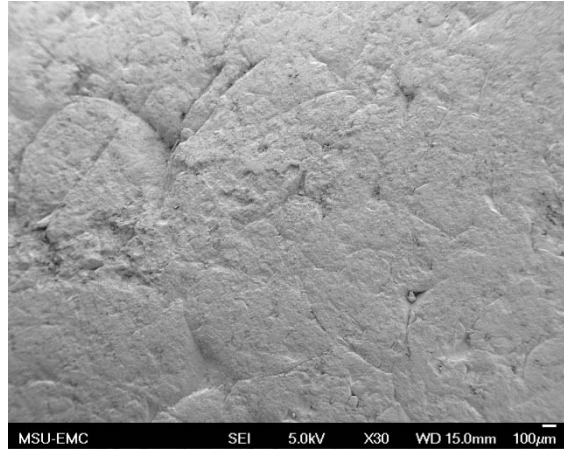
(a) Aggregate A
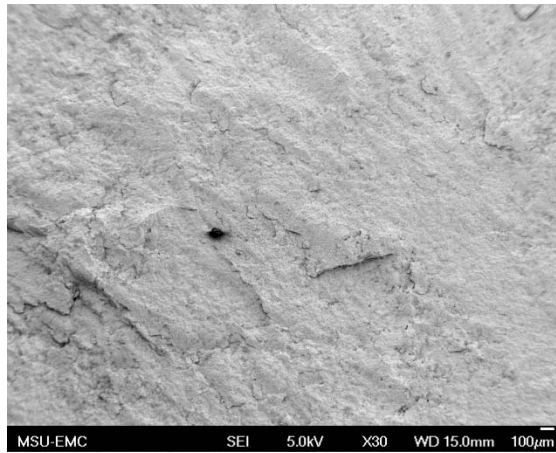
(b) Aggregate B
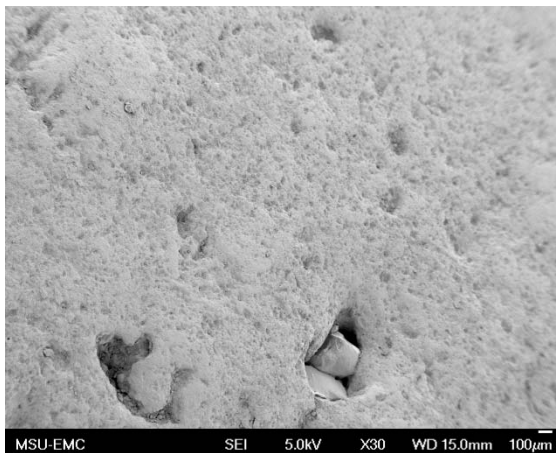
(c) Aggregate C
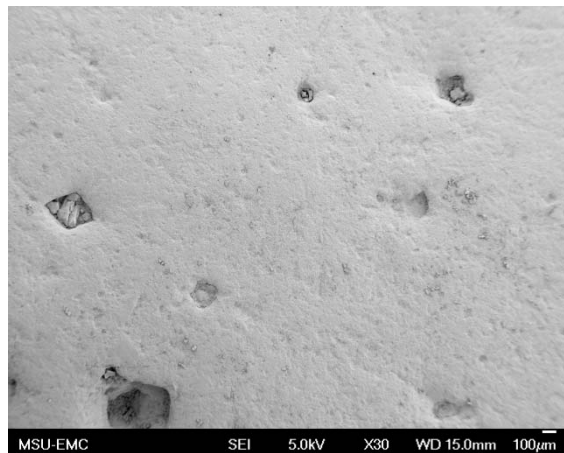
(d) Aggregate D

(e) Aggregate E

Figure B.25. SEM Images of Sample 6A, 4.75 mm Sieve, 30x
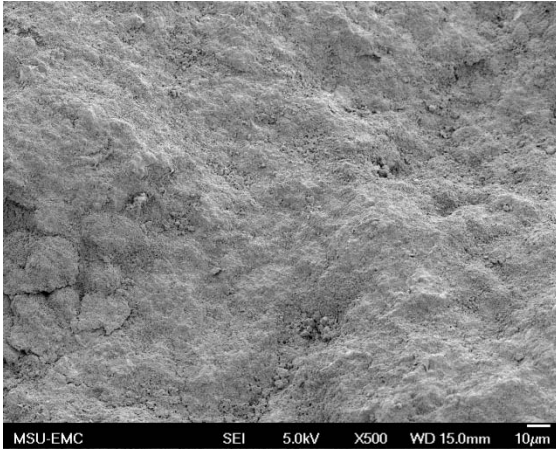
(a) Aggregate A
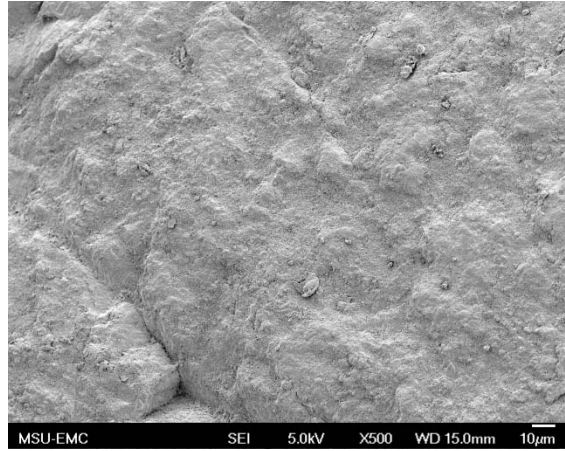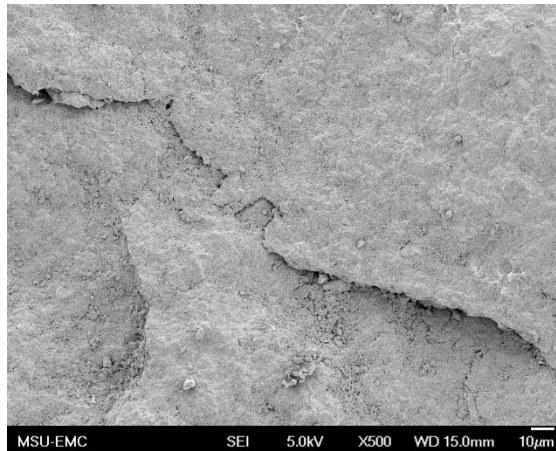
(b) Aggregate B
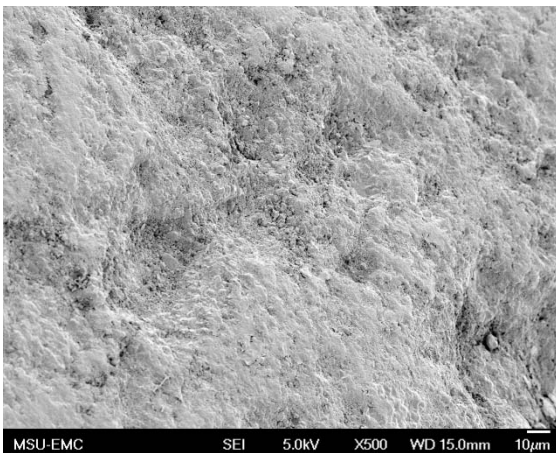
(c) Aggregate C
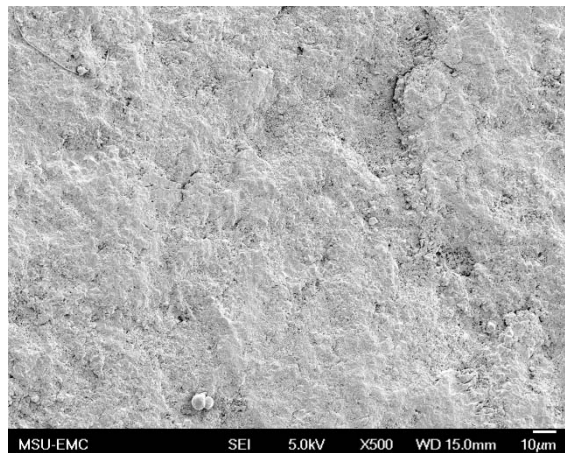
(d) Aggregate D

(e) Aggregate E

**Figure B.26. SEM Images of Sample 6A, 4.75 mm Sieve, 500x**
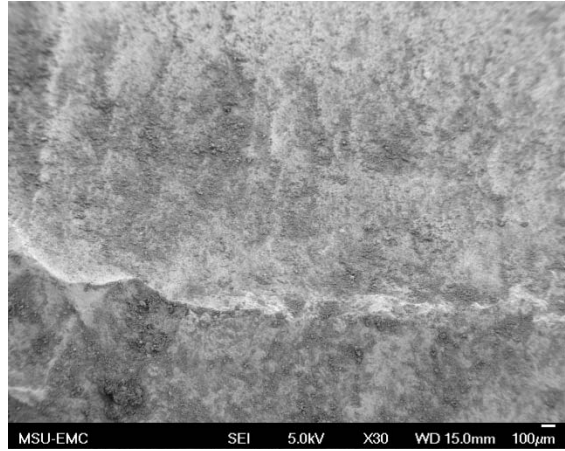
(a) Aggregate A
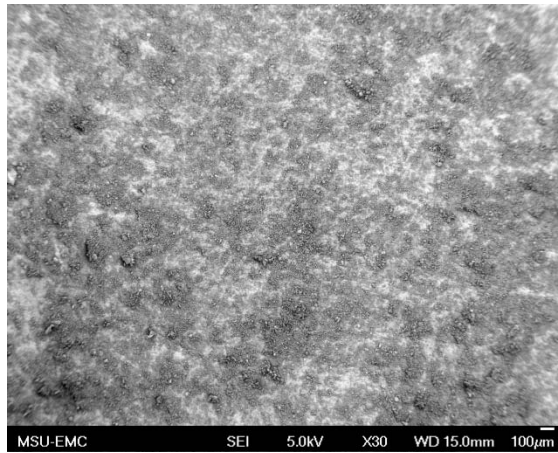
(b) Aggregate B
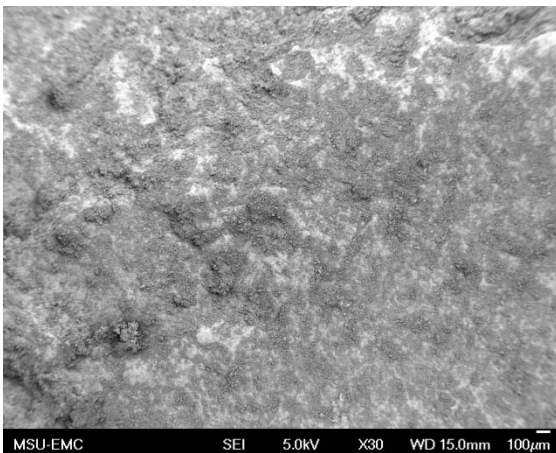
(c) Aggregate C
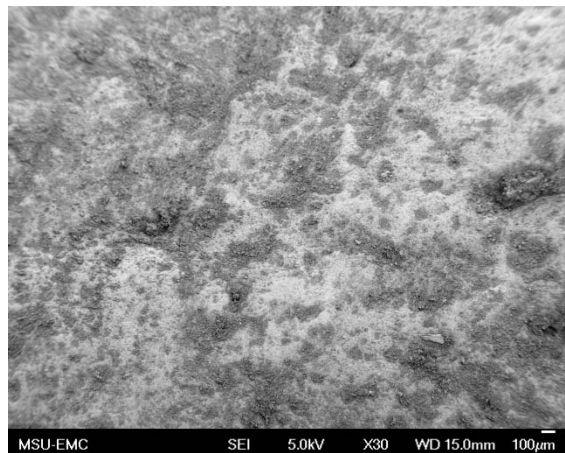
*(d) Aggregate D*

(e) Aggregate E

Figure B.27. SEM Images of Sample 7, 4.75 mm Sieve, 30x

133
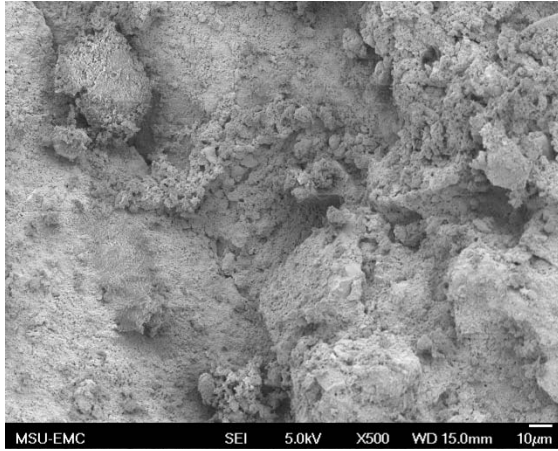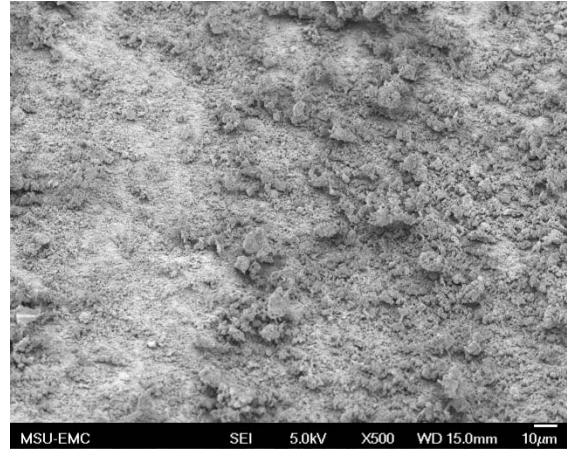
(a) Aggregate A
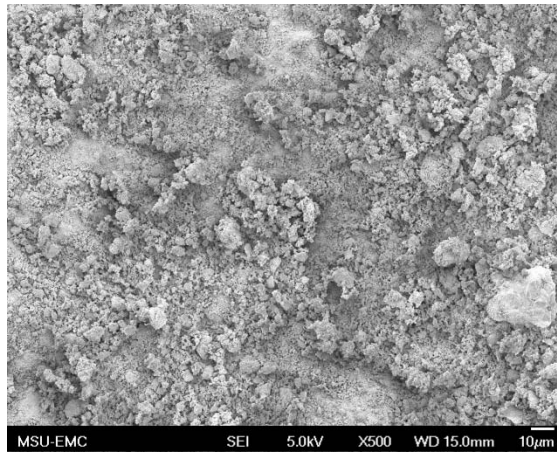
(b) Aggregate B
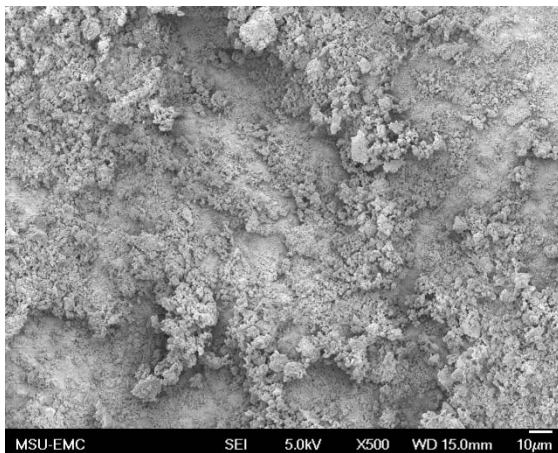
(c) Aggregate C
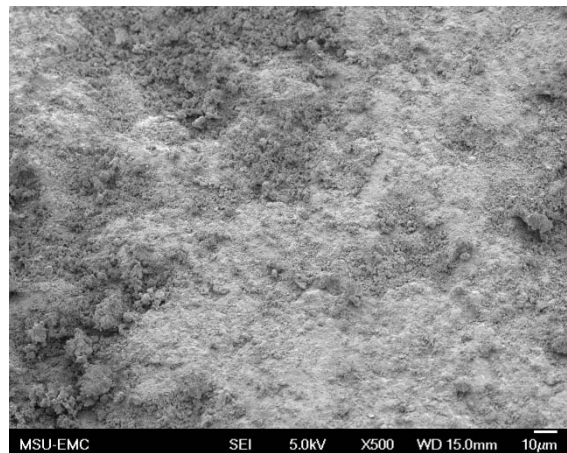
(d) Aggregate D

(e) Aggregate E

Figure B.28. SEM Images of Sample 7, 4.75 mm Sieve, 500x

134
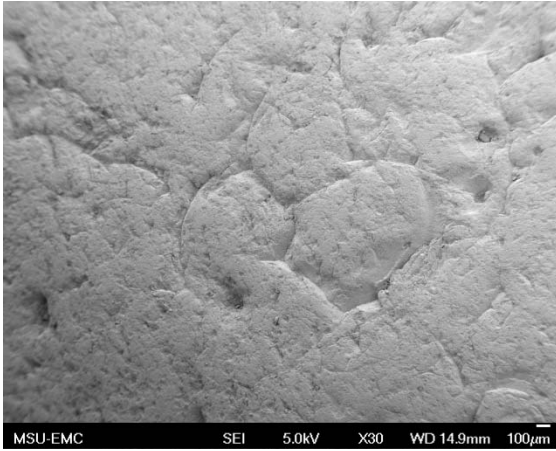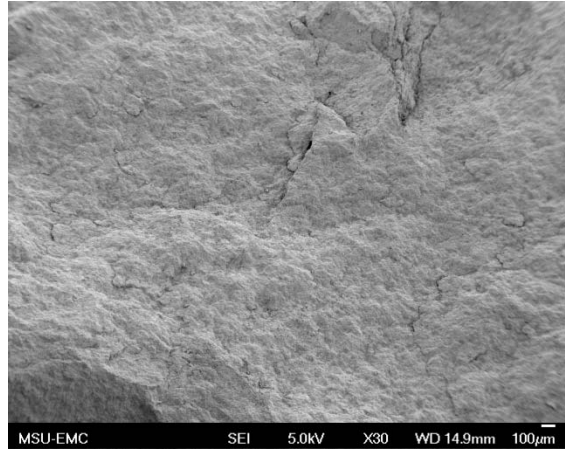
(a) Aggregate A
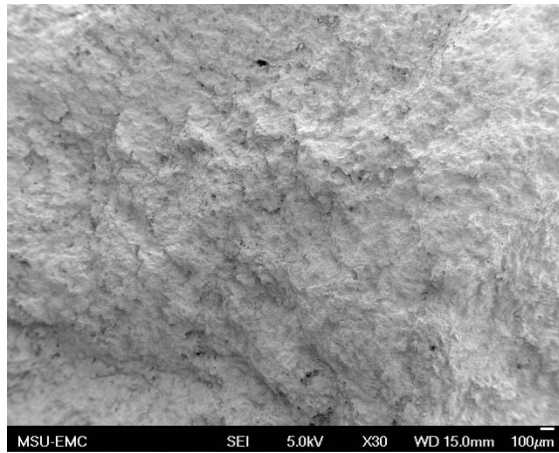
(b) Aggregate B
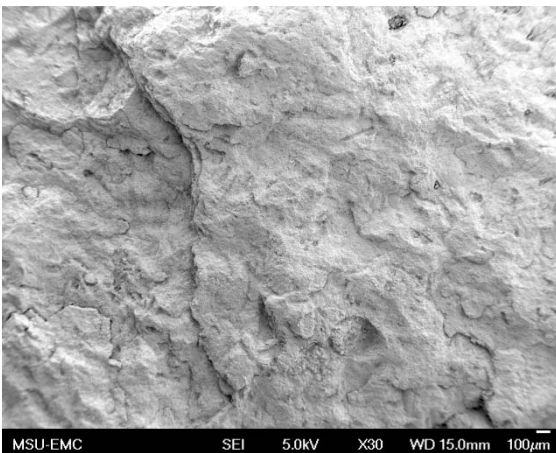
(c) Aggregate C
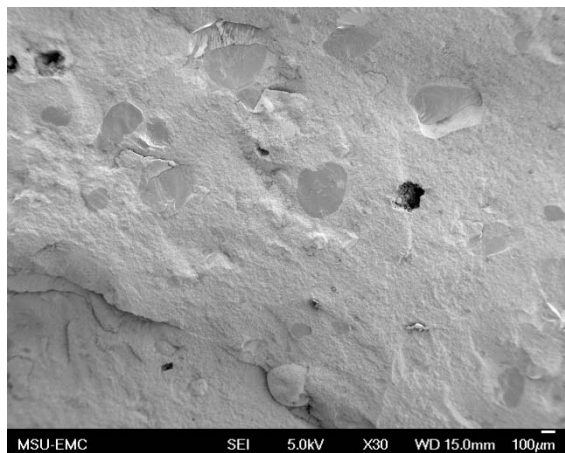
(d) Aggregate D

(e) Aggregate E

Figure B.29. SEM Images of Sample 7A, 4.75 mm Sieve, 30x
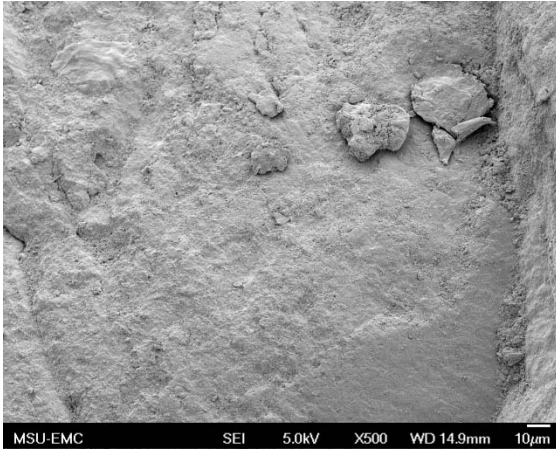
(a) Aggregate A
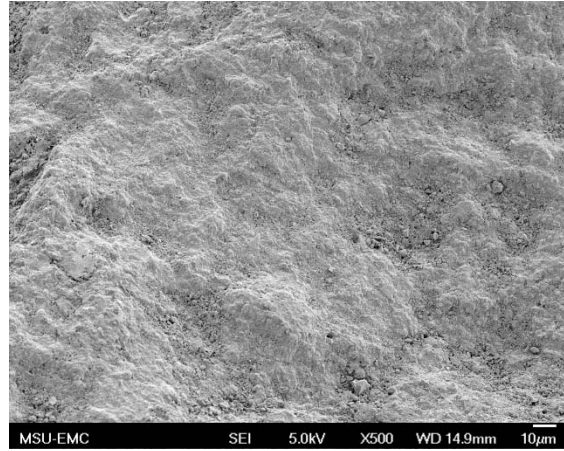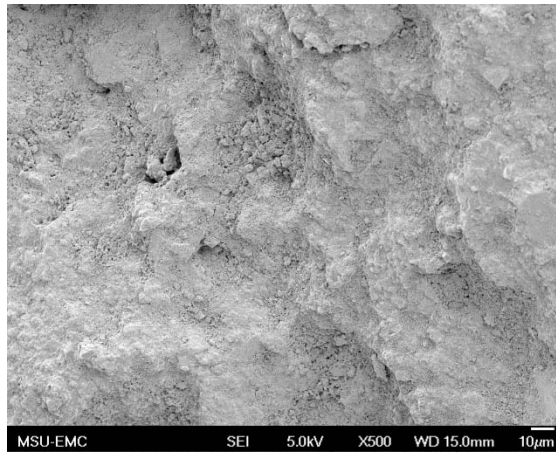
(b) Aggregate B
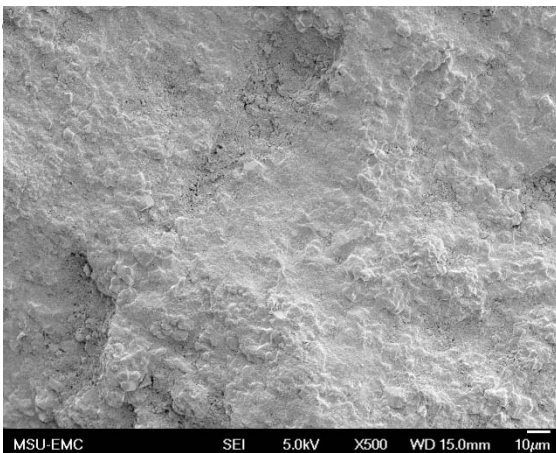
(c) Aggregate C
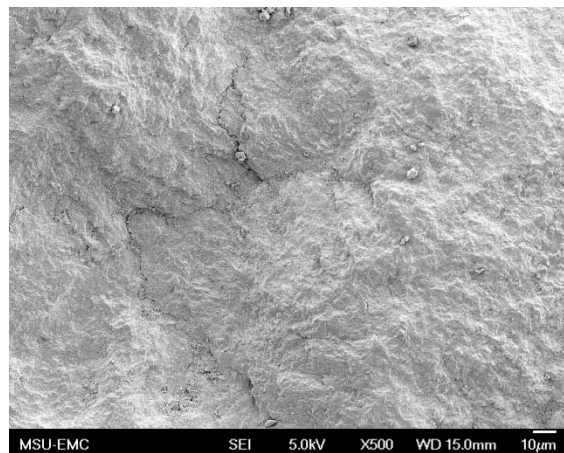
(d) Aggregate D

(e) Aggregate E

Figure B.30. SEM Images of Sample 7A, 4.75 mm Sieve, 500x
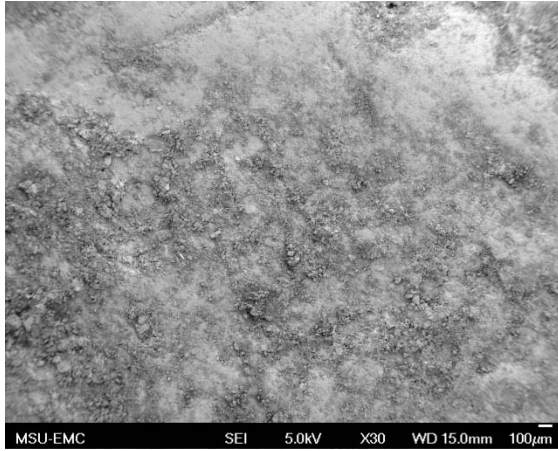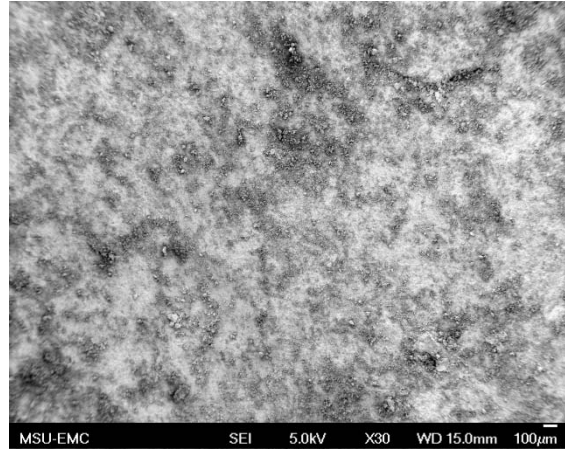
(a) Aggregate A
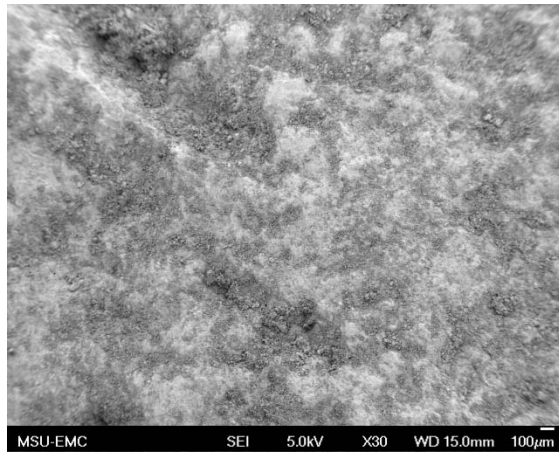
*(b) Aggregate B*
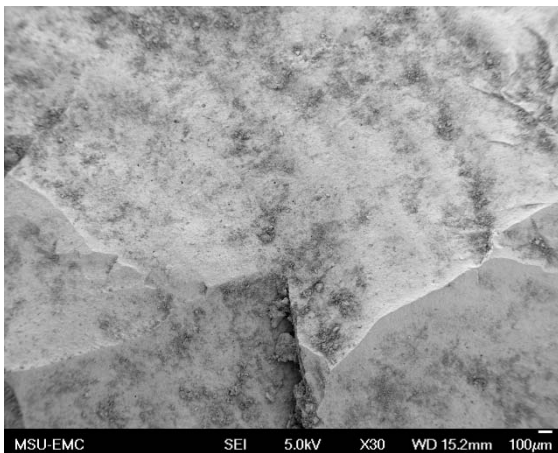
(c) Aggregate C
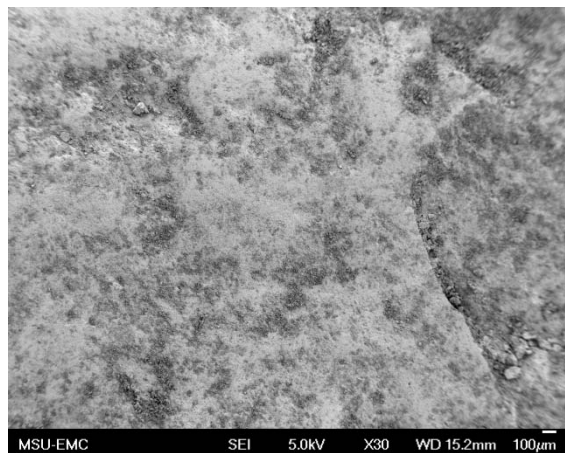
(d) Aggregate D

(e) Aggregate E

**Figure B.31. SEM Images of Sample 8, 4.75 mm Sieve, 30x**
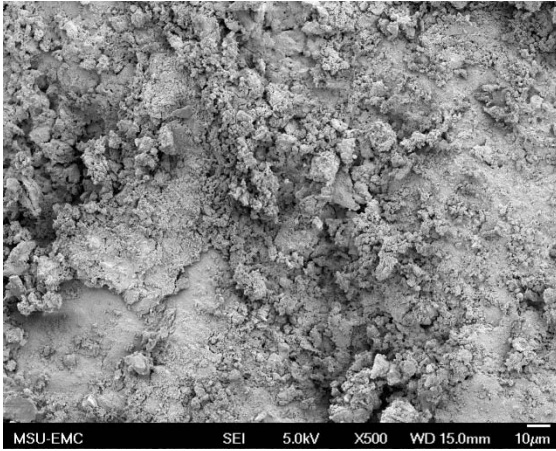
(a) Aggregate A
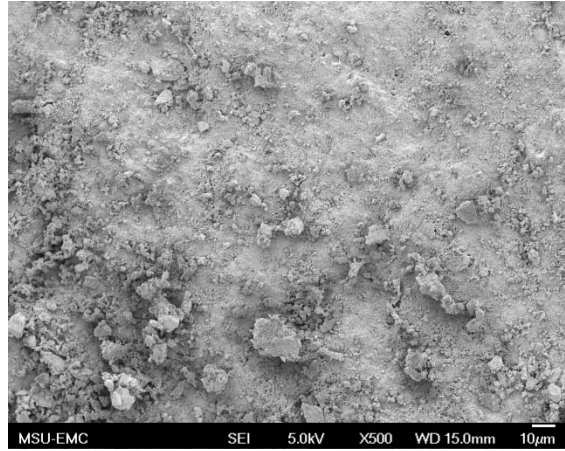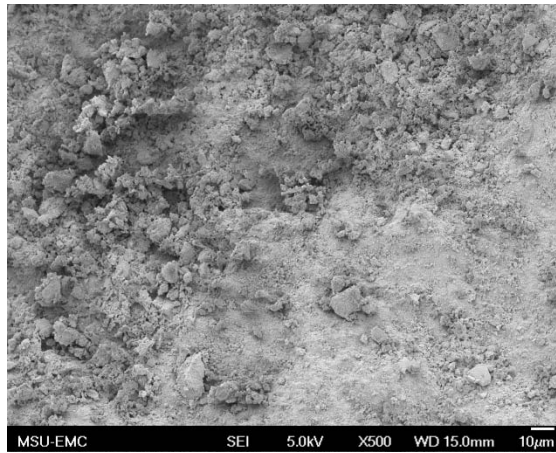
(b) Aggregate B
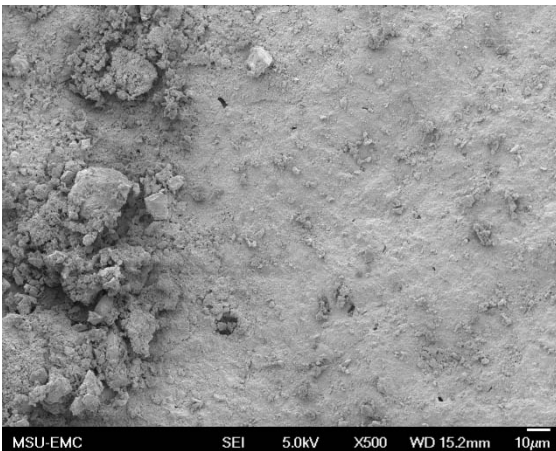
(c) Aggregate C
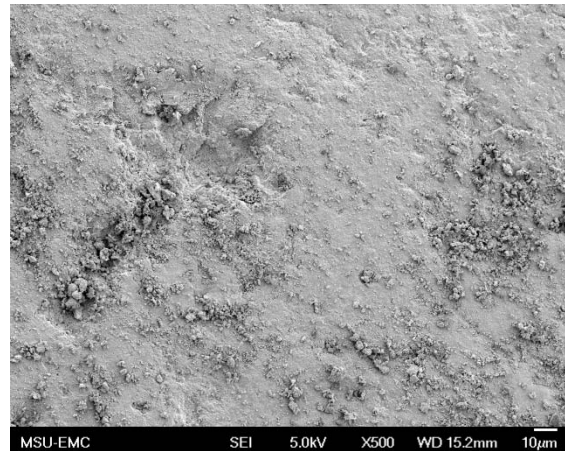
*(d) Aggregate D*

(e) Aggregate E

Figure B.32. SEM Images of Sample 8, 4.75 mm Sieve, 500x
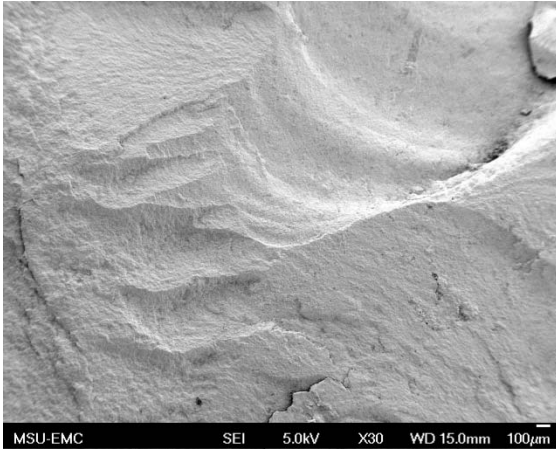
(a) Aggregate A
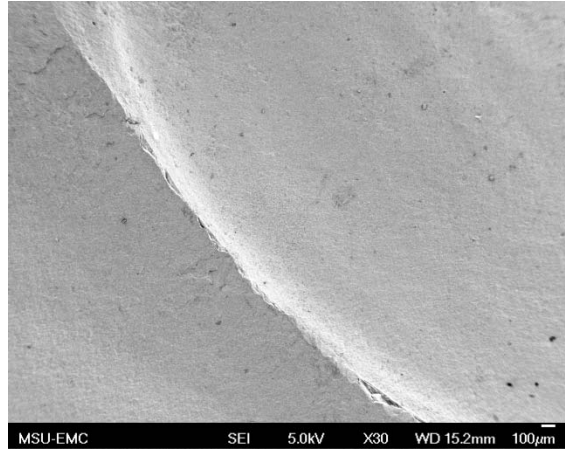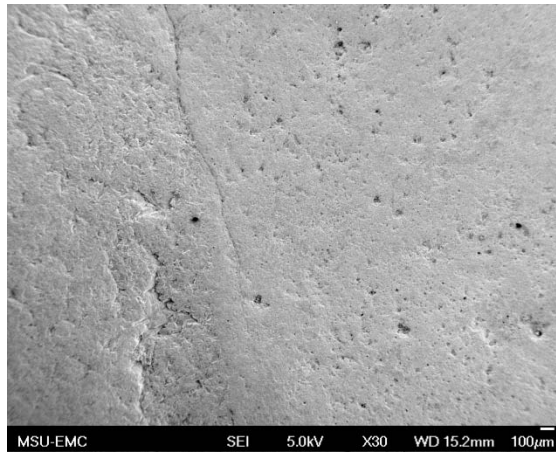
(b) Aggregate B
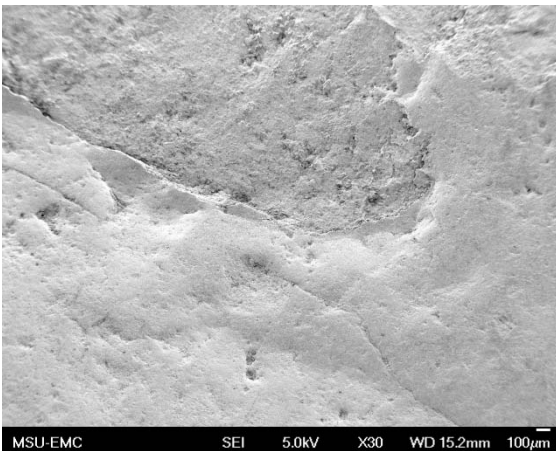
(c) Aggregate C
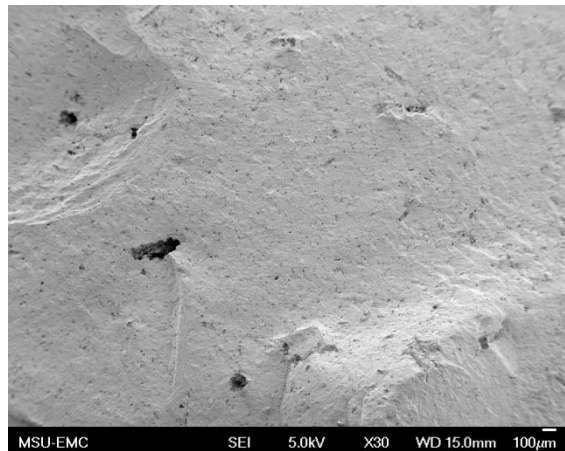
(d) Aggregate D

(e) Aggregate E

Figure B.33. SEM Images of Sample 8A, 4.75 mm Sieve, 30x
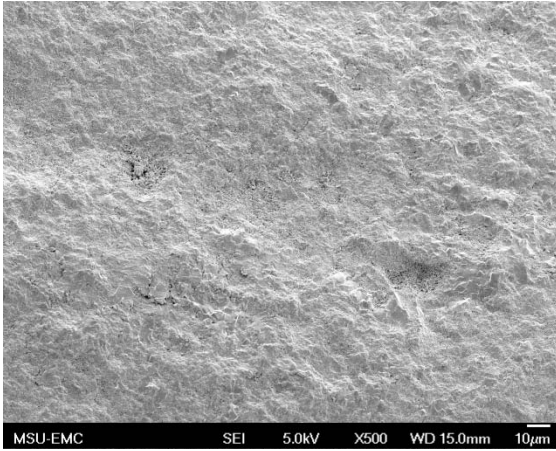
(a) Aggregate A
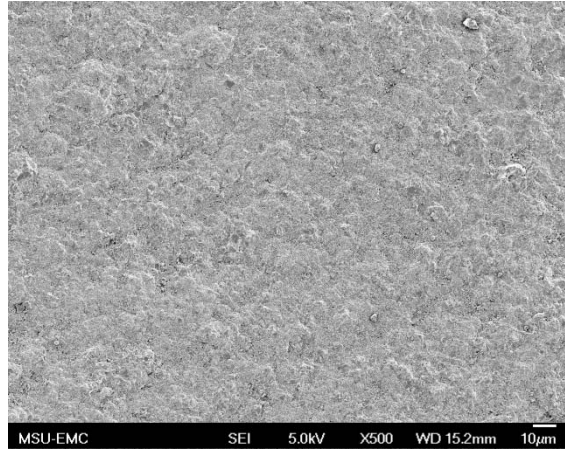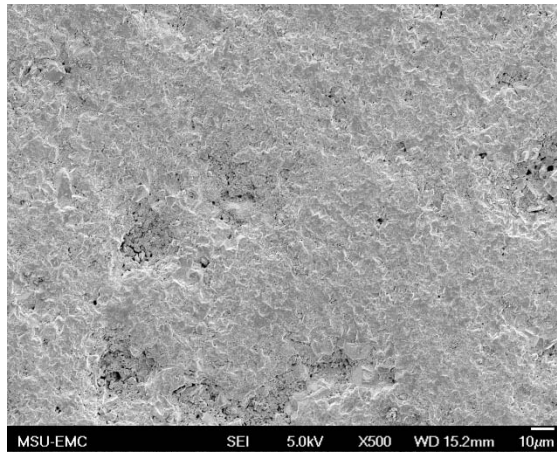
*(b) Aggregate B*
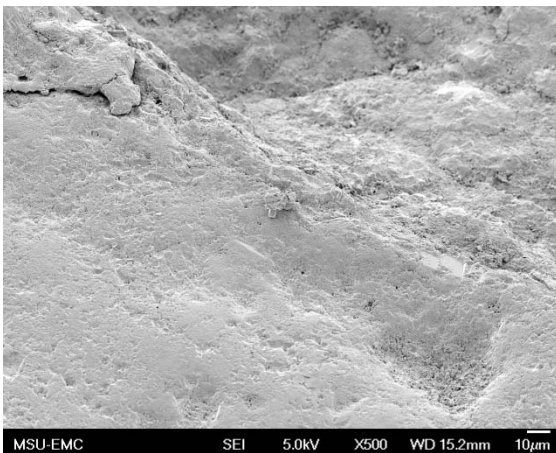
(c) Aggregate C
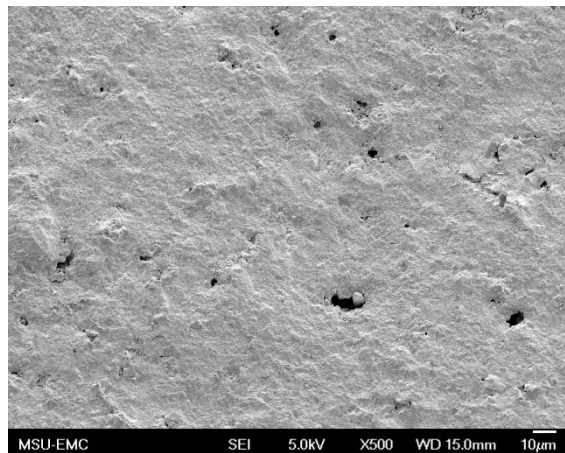
*(d) Aggregate D*

(e) Aggregate E

Figure B.34. SEM Images of Sample 8A, 4.75 mm Sieve, 500x
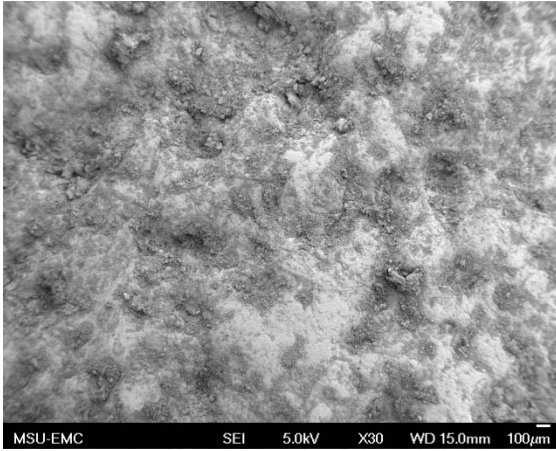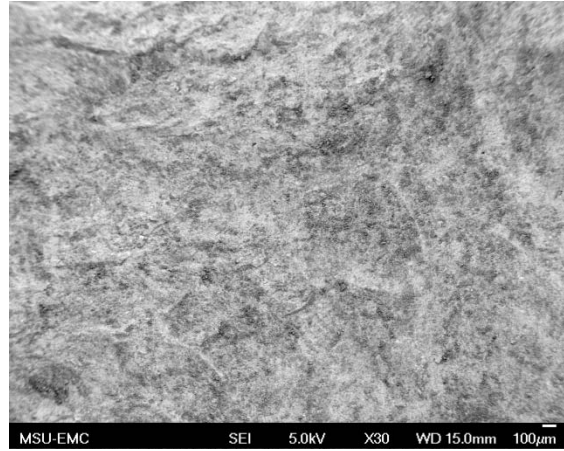
(a) Aggregate A
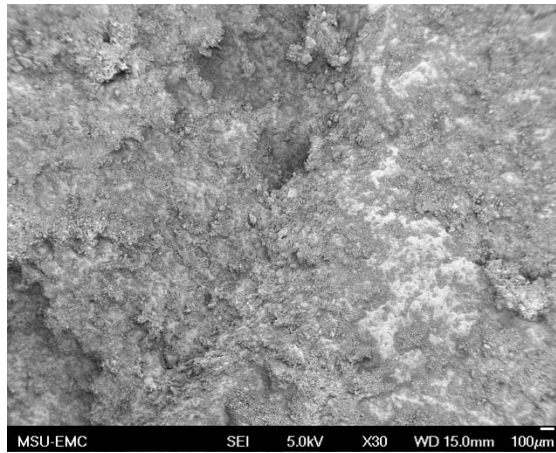
(b) Aggregate B
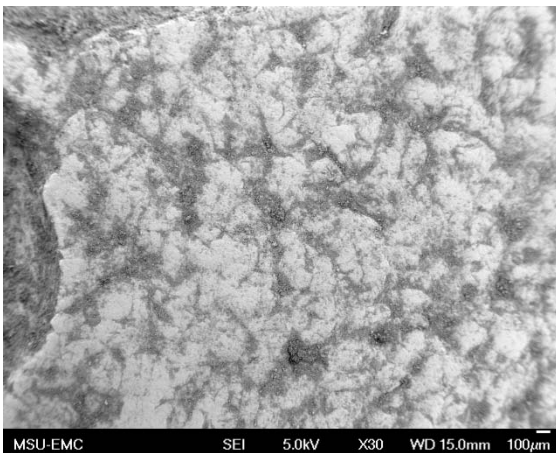
(c) Aggregate C
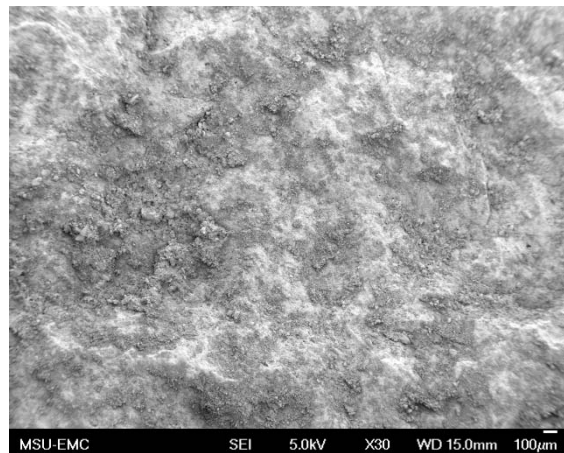
(d) Aggregate D

(e) Aggregate E

Figure B.35. SEM Images of Sample 9, 4.75 mm Sieve, 30x
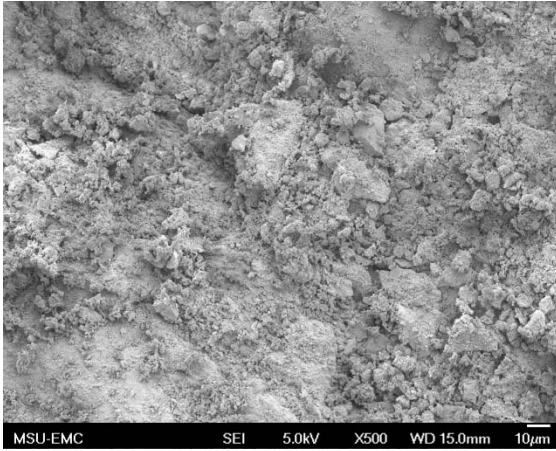
(a) Aggregate A
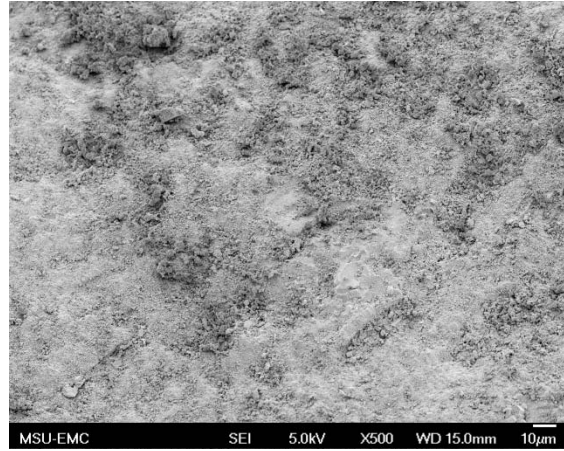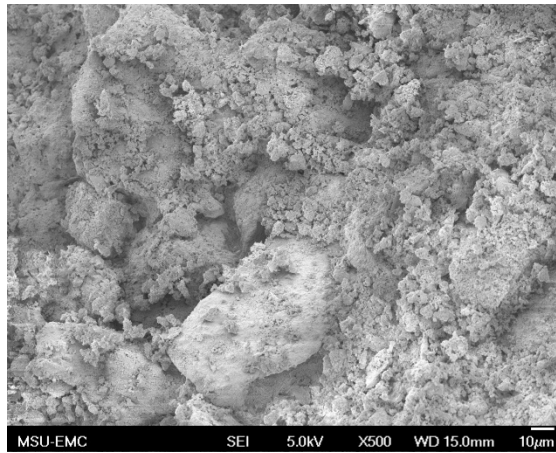
(b) Aggregate B
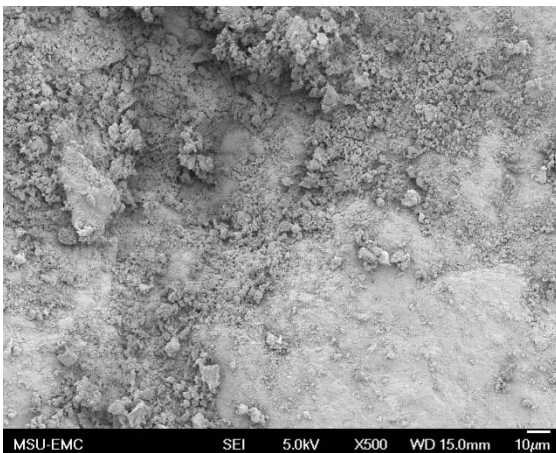
(c) Aggregate C
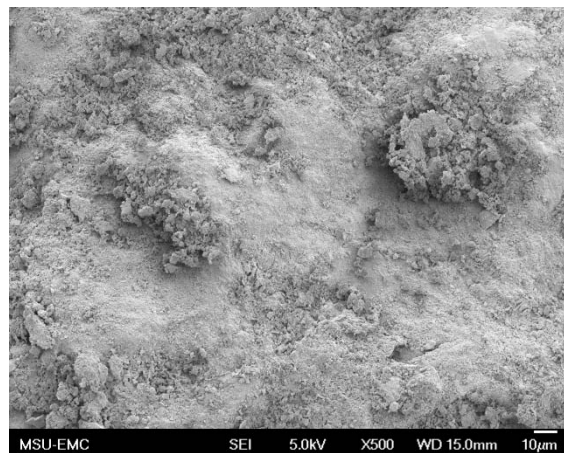
(d) Aggregate D

(e) Aggregate E

**Figure B.36. SEM Images of Sample 9, 4.75 mm Sieve, 500x**
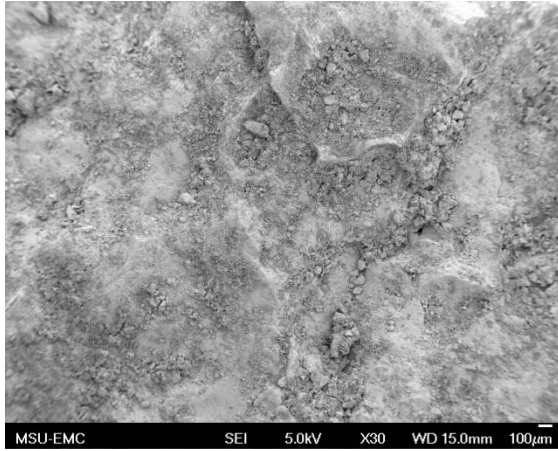
(a) Aggregate A
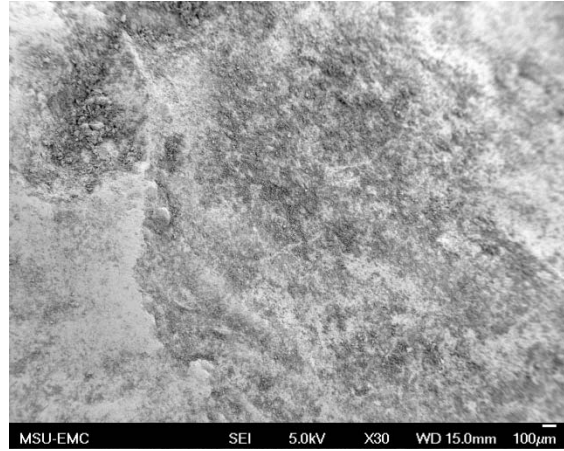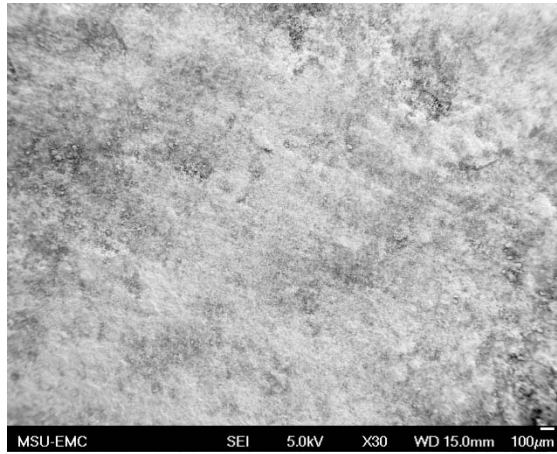
(b) Aggregate B
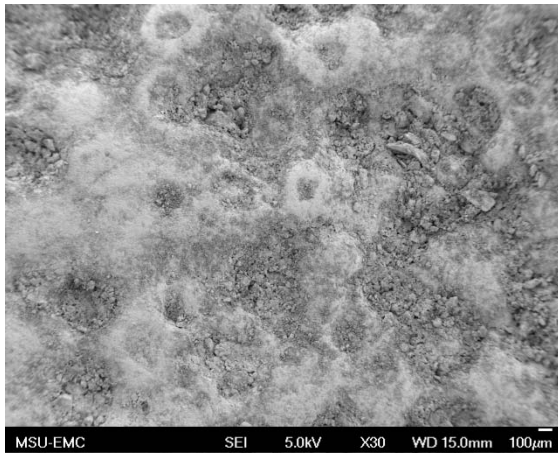
(c) Aggregate C
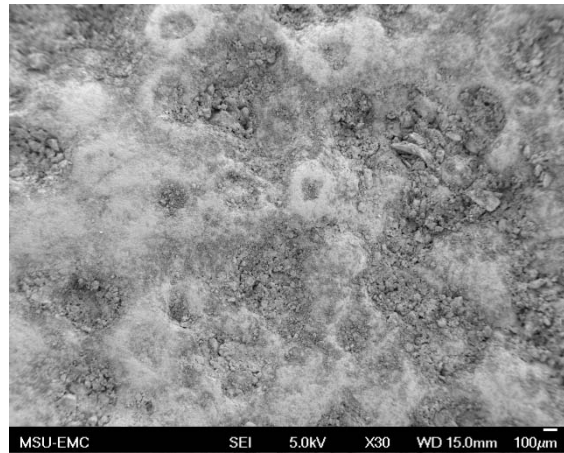
(d) Aggregate D

(e) Aggregate E

Figure B.37. SEM Images of Sample 10, 4.75 mm Sieve, 30x
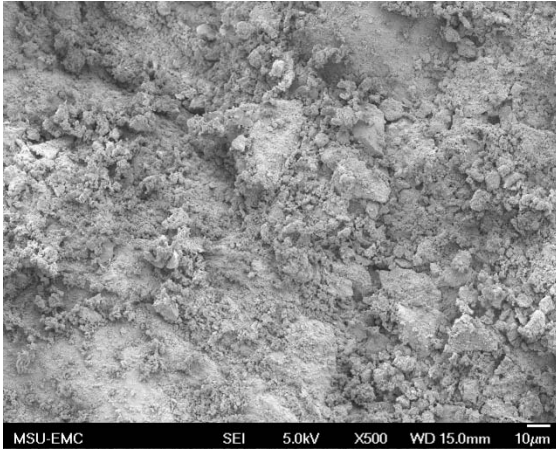
(a) Aggregate A
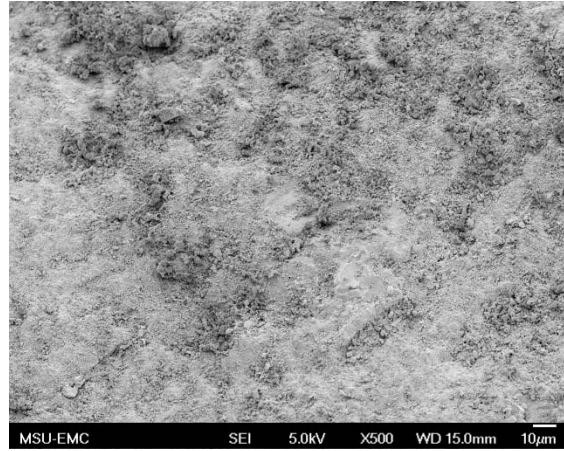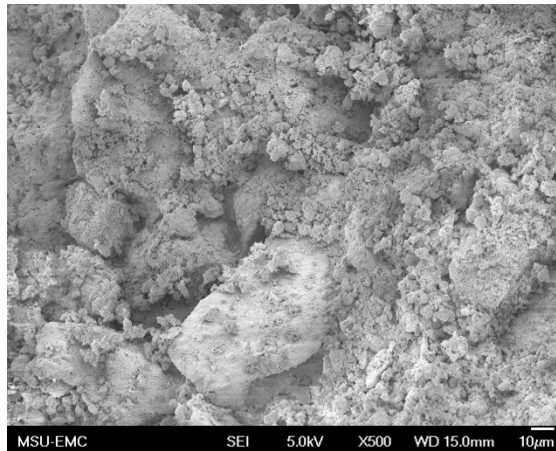
(b) Aggregate B
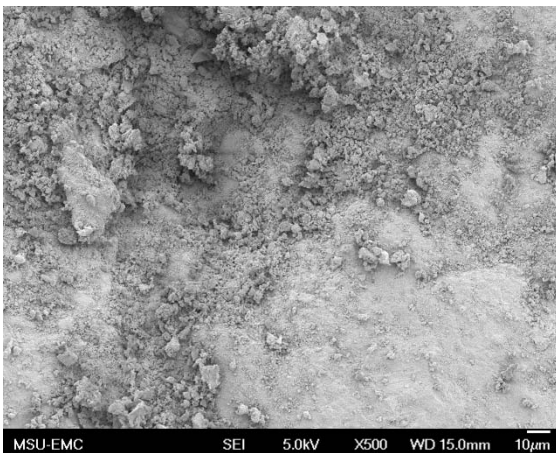
(c) Aggregate C
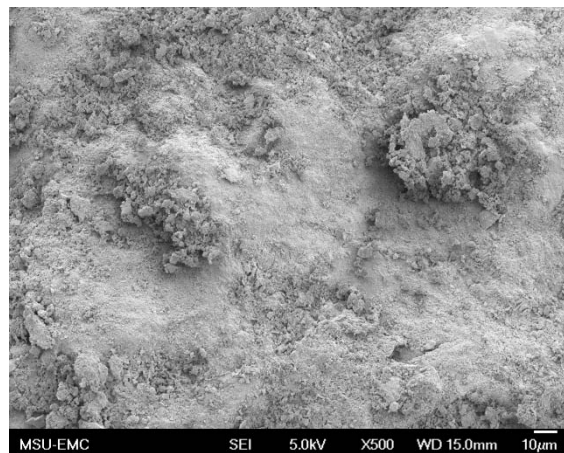
(d) Aggregate D

(e) Aggregate E

Figure B.38. SEM Images of Sample 10, 4.75 mm Sieve, 500x
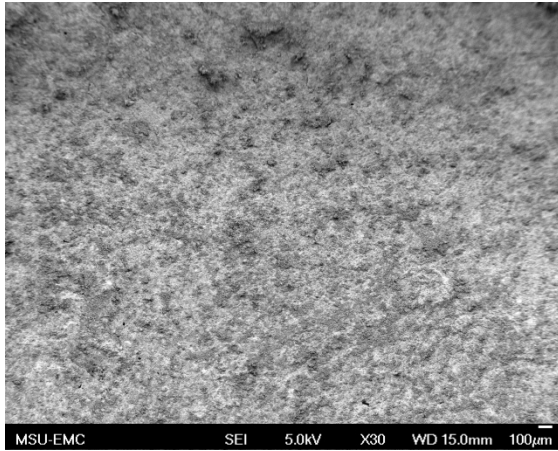
(a) Aggregate A
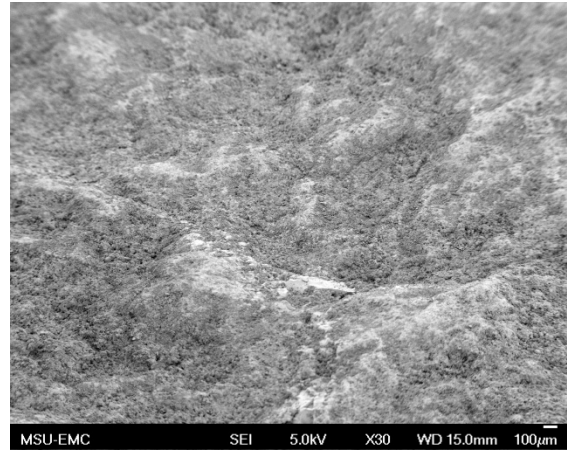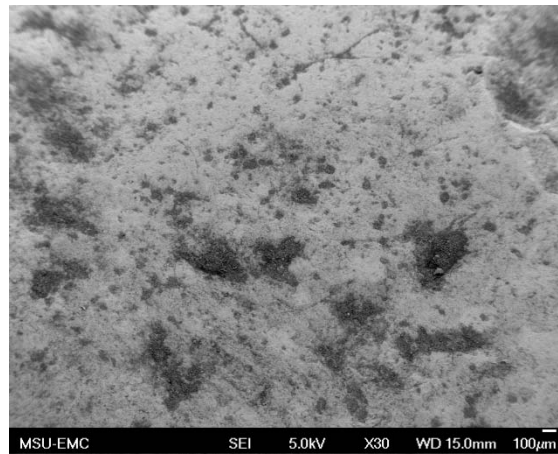
*(b) Aggregate B*
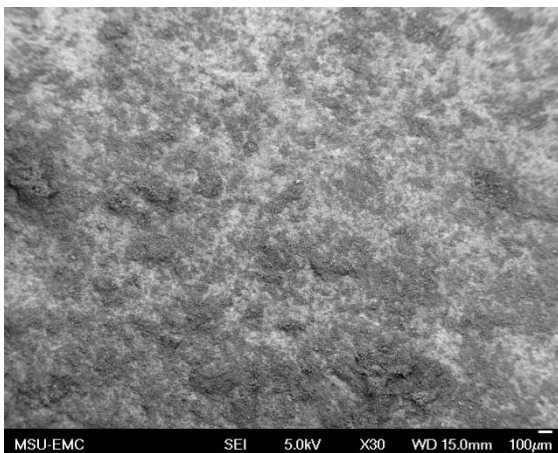
(c) Aggregate C
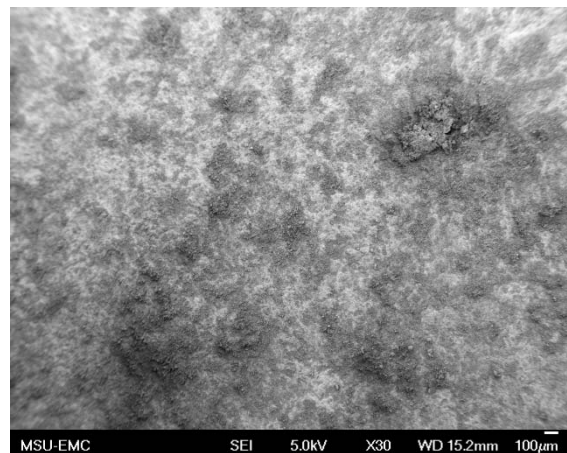
(d) Aggregate D

(e) Aggregate E

Figure B.39. SEM Images of Sample 11, 4.75 mm Sieve, 30x

145
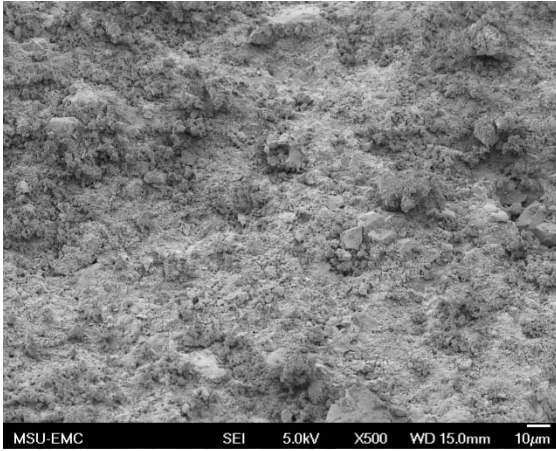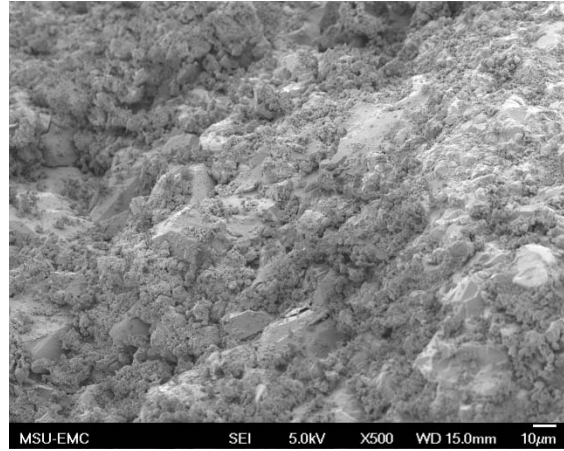
(a) Aggregate A
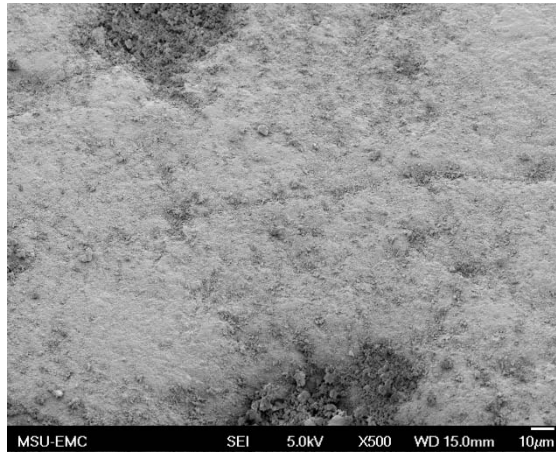
(b) Aggregate B
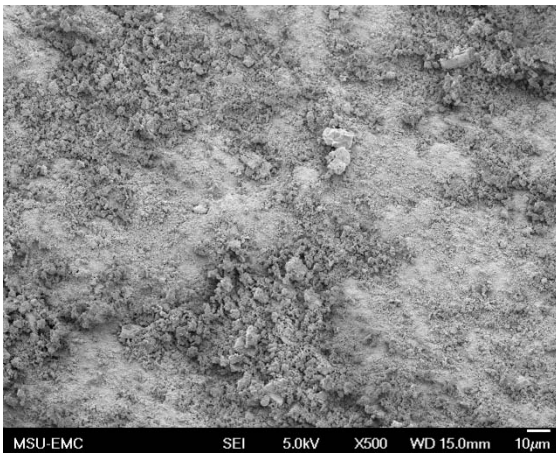
(c) Aggregate C
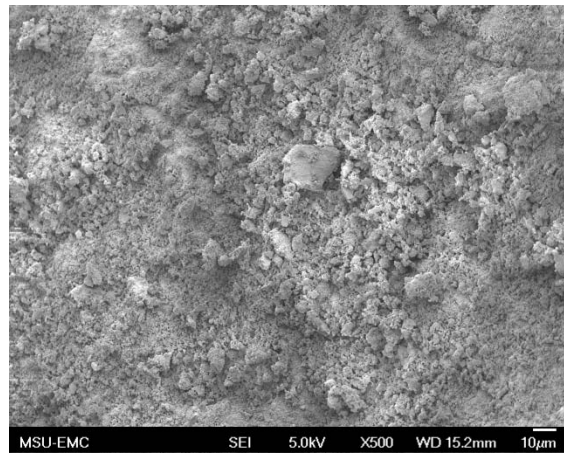

(d) Aggregate D

(e) Aggregate E

Figure B.40. SEM Images of Sample 11, 4.75 mm Sieve, 500x
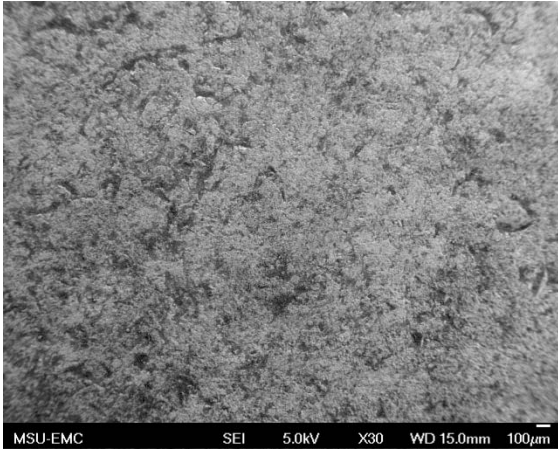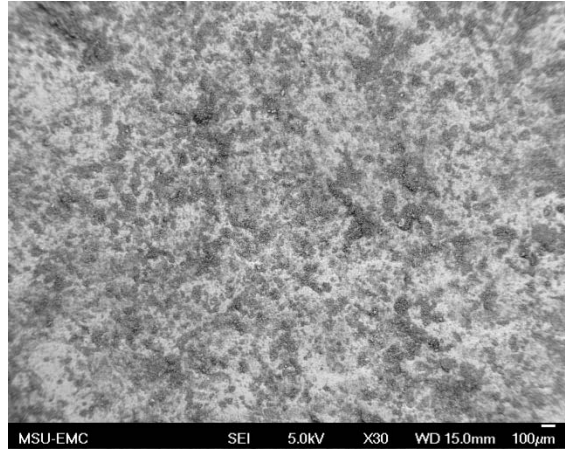
(a) Aggregate A
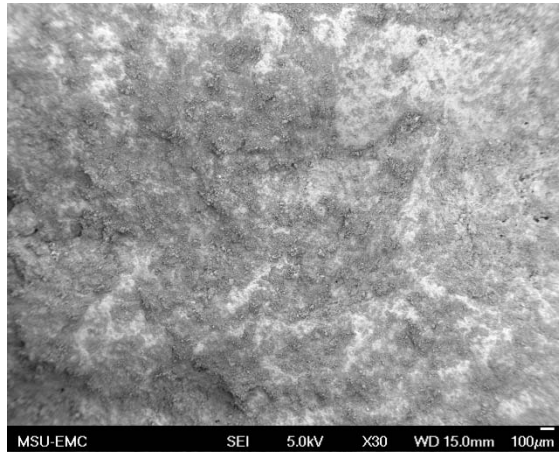
(b) Aggregate B
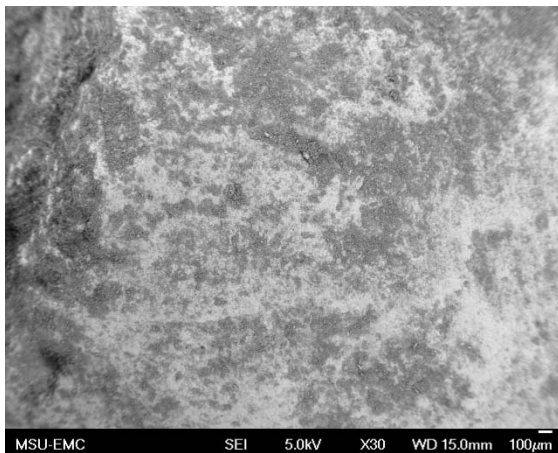
(c) Aggregate C
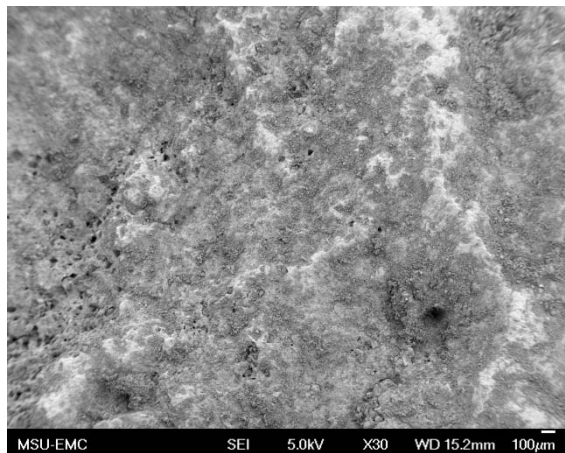
(d) Aggregate D

(e) Aggregate E

Figure B.41. SEM Images of Sample 12, 4.75 mm Sieve, 30x

147
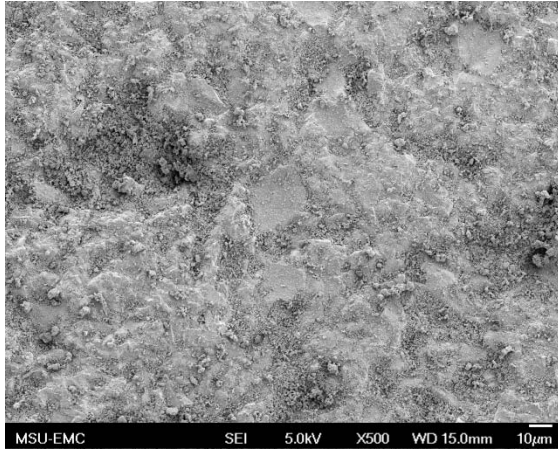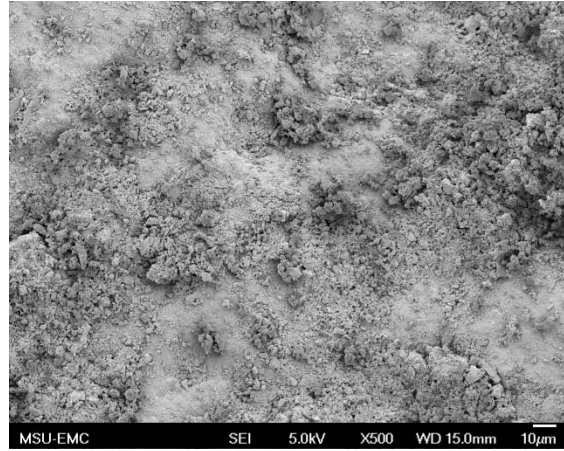
(a) Aggregate A
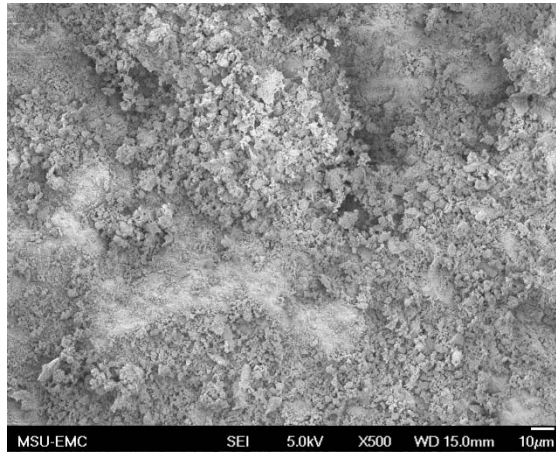
(b) Aggregate B
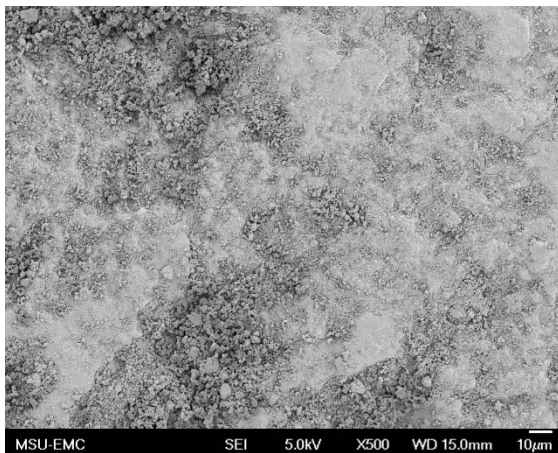
(c) Aggregate C
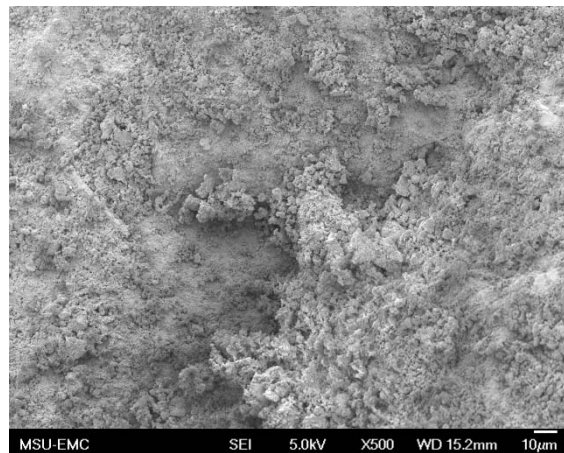
(d) Aggregate D

(e) Aggregate E

Figure B.42. SEM Images of Sample 12, 4.75 mm Sieve, 500x
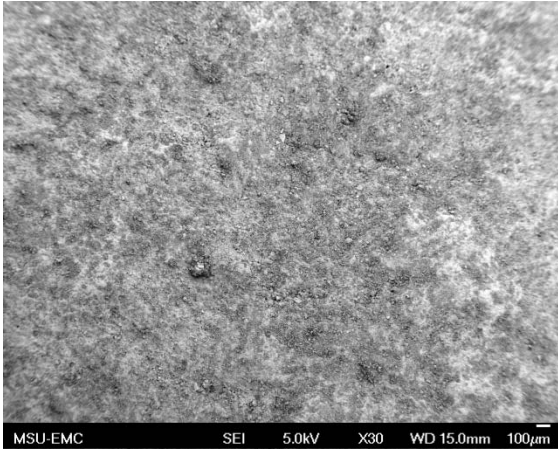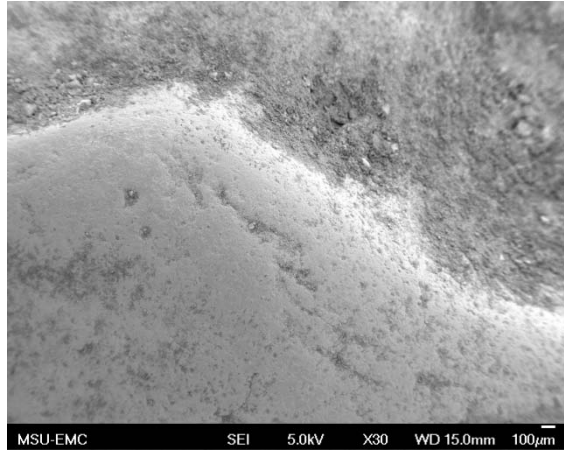
(a) Aggregate A
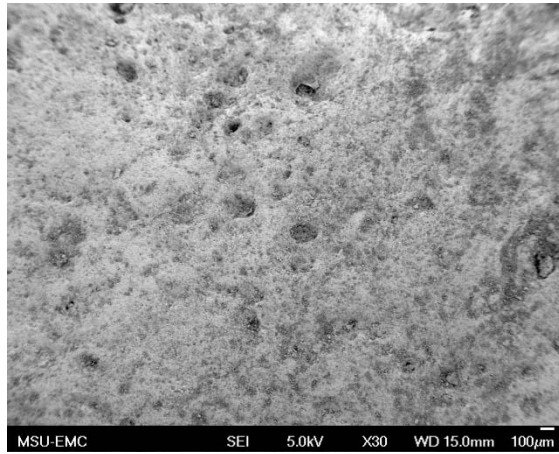
(b) Aggregate B
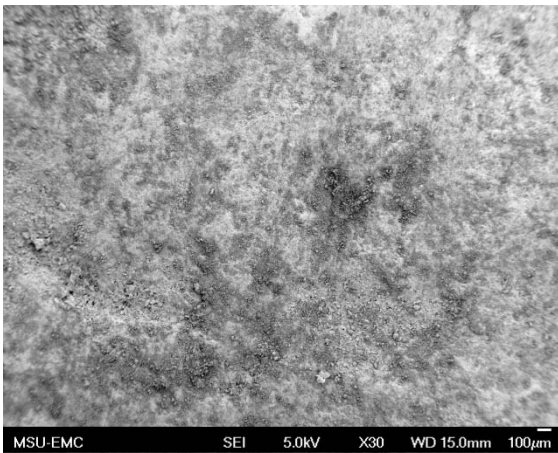
(c) Aggregate C
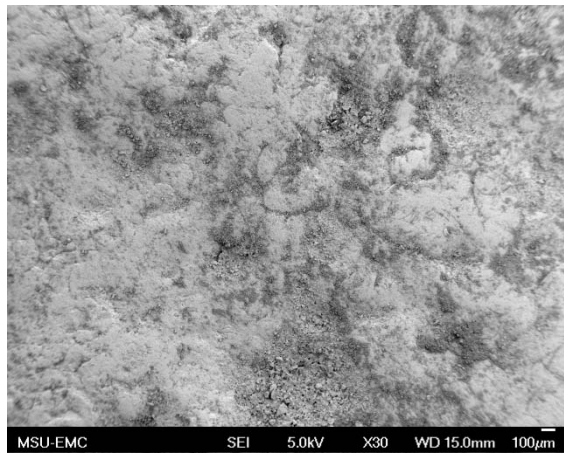
(d) Aggregate D

(e) Aggregate E

Figure B.43. SEM Images of Sample 13, 4.75 mm Sieve, 30x
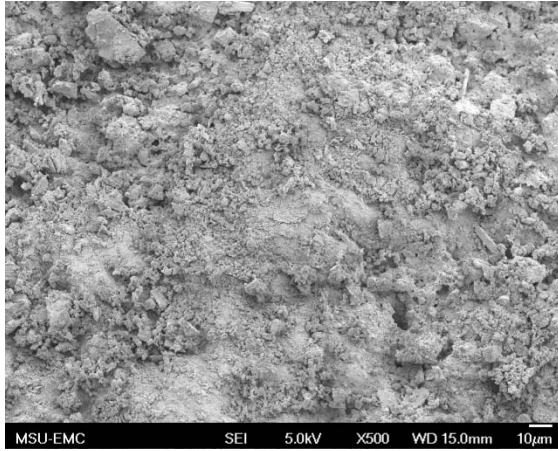
(a) Aggregate A
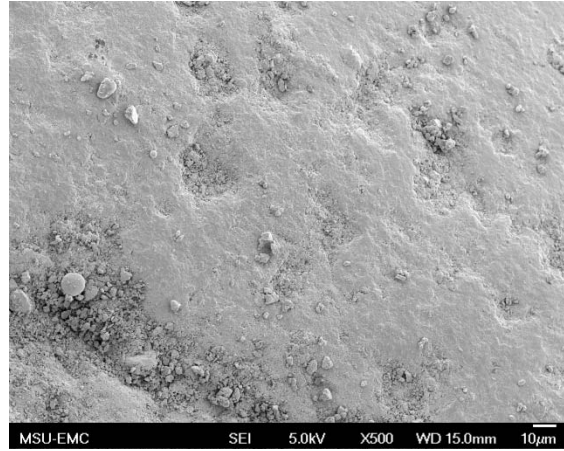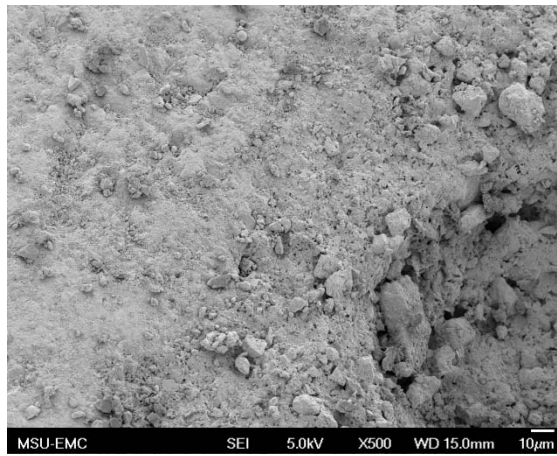
*(b) Aggregate B*
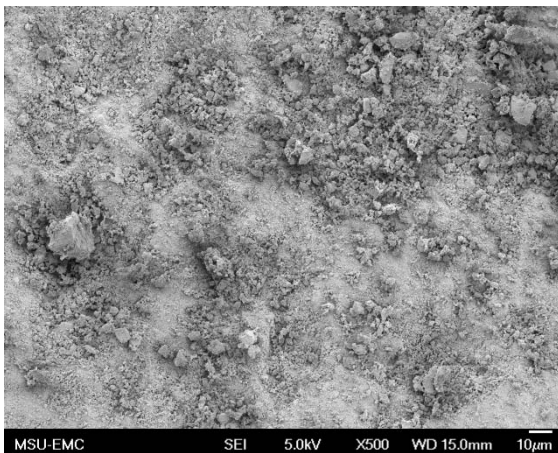
(c) Aggregate C
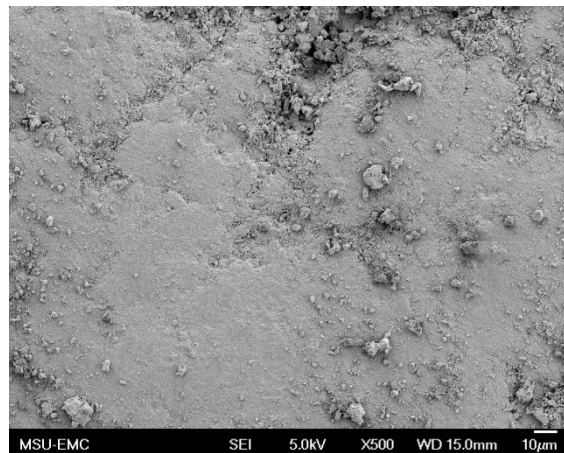
(d) Aggregate D

(e) Aggregate E

Figure B.44. SEM Images of Sample 13, 4.75 mm Sieve, 500x
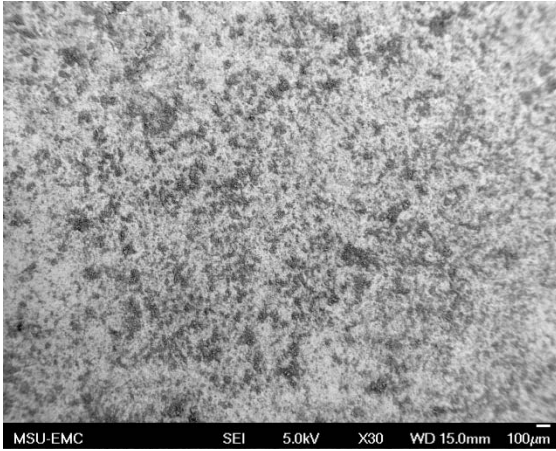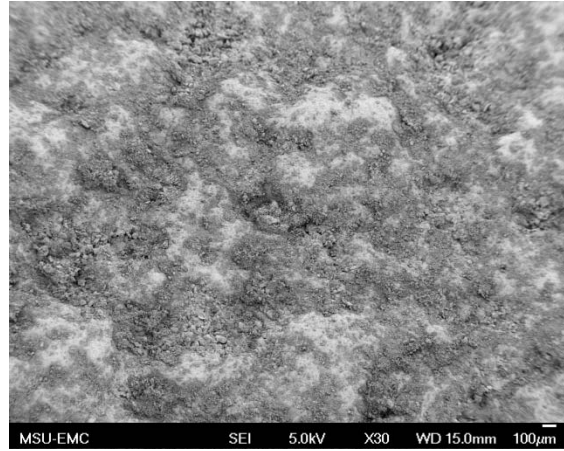
(a) Aggregate A
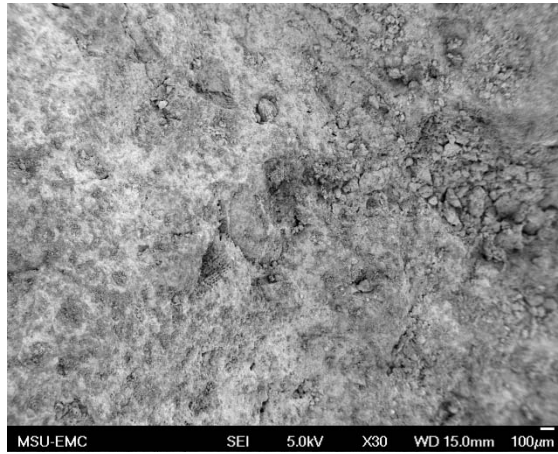
(b) Aggregate B
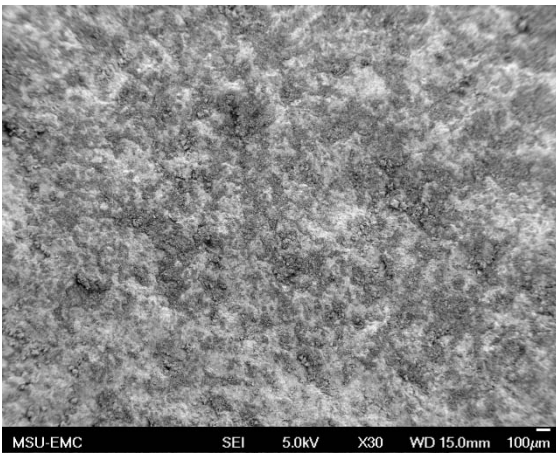
(c) Aggregate C
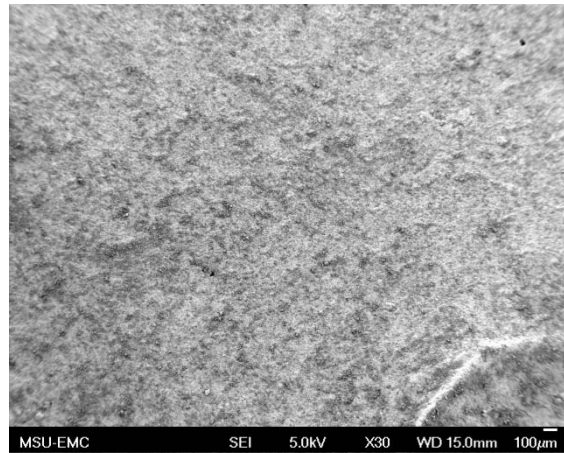
(d) Aggregate D

(e) Aggregate E

Figure B.45. SEM Images of Sample 14, 4.75 mm Sieve, 30x
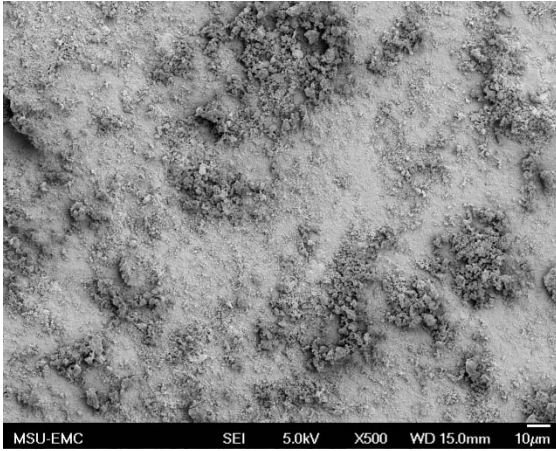
(a) Aggregate A
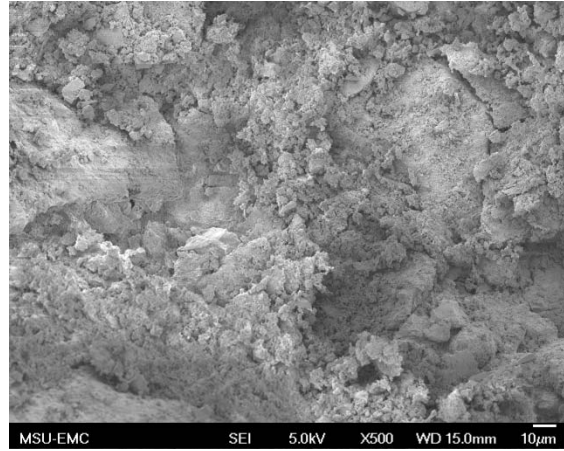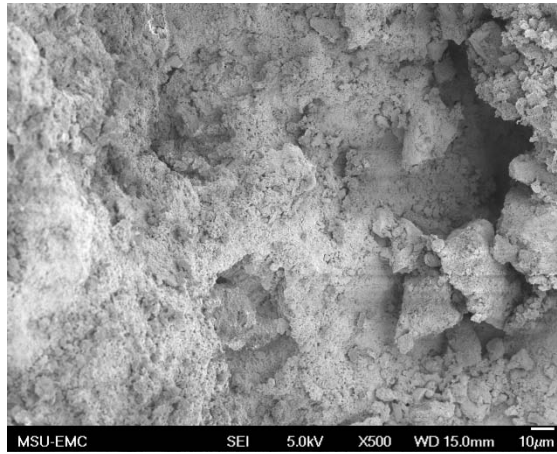
(b) Aggregate B
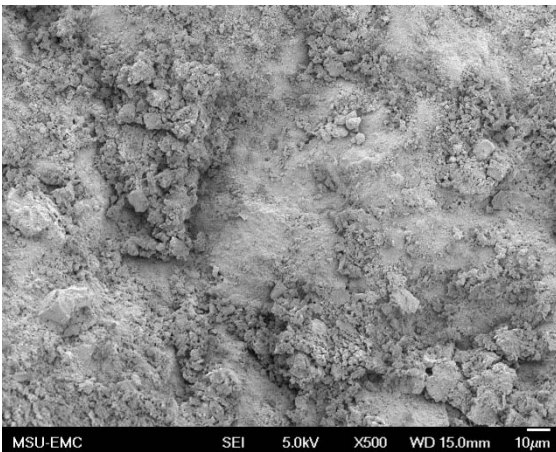
(c) Aggregate C

(d) Aggregate D

(e) Aggregate E

**Figure B.46. SEM Images of Sample 14, 4.75 mm Sieve, 500x**
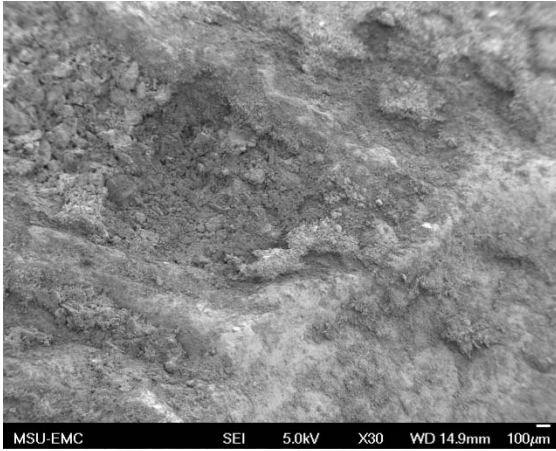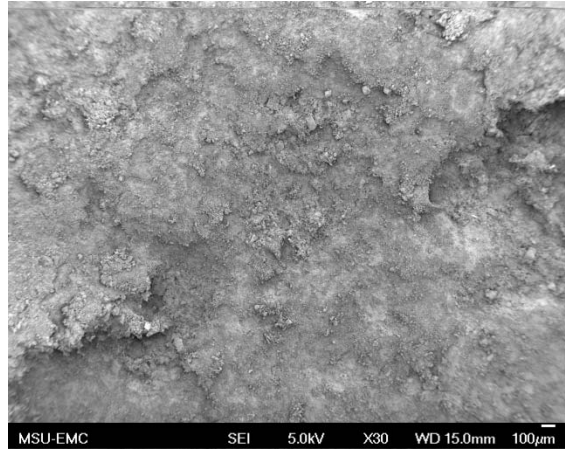
*(a) Aggregate A*
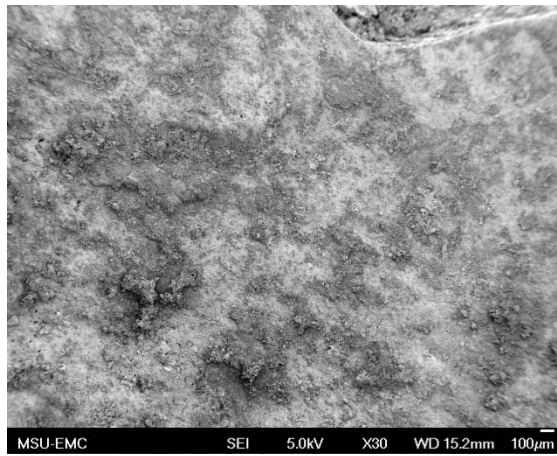
(b) Aggregate B
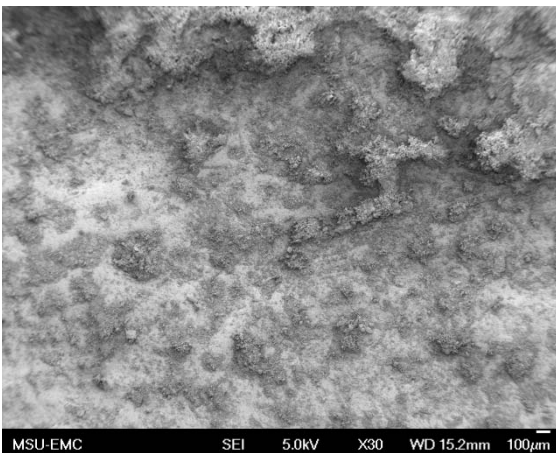
(c) Aggregate C
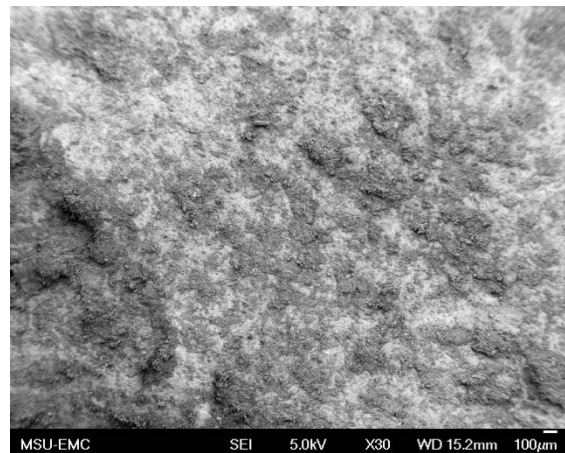
(d) Aggregate D

(e) Aggregate E

Figure B.47. SEM Images of Sample 15, 4.75 mm Sieve, 30x
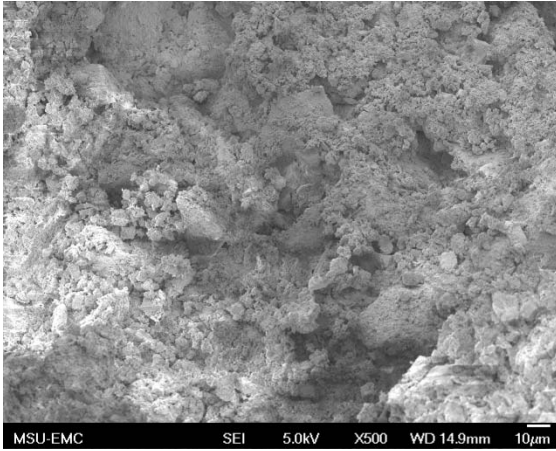
(a) Aggregate A
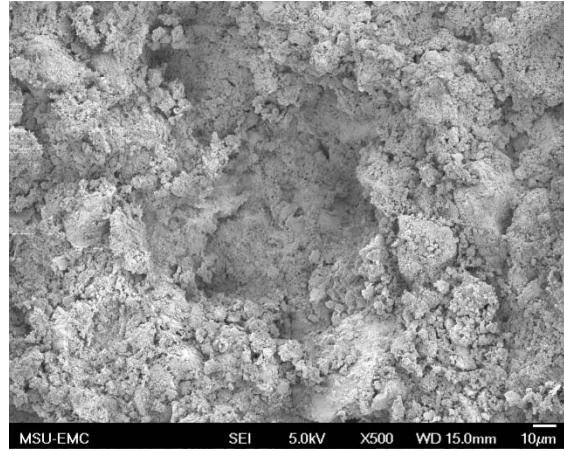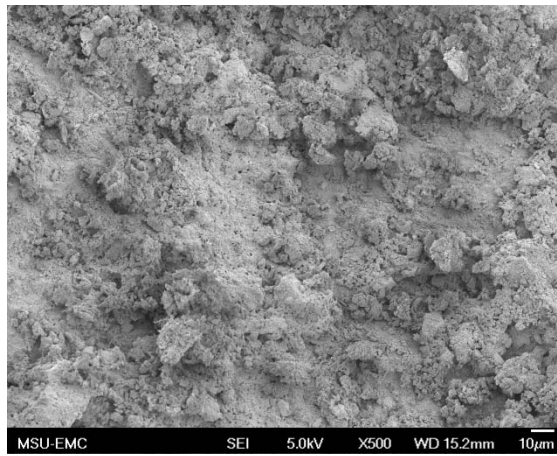
(b) Aggregate B
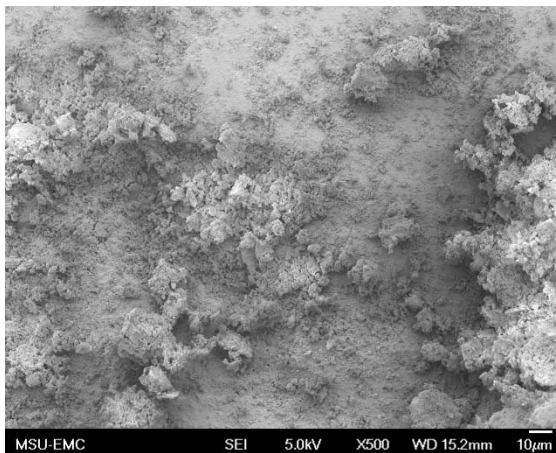
(c) Aggregate C
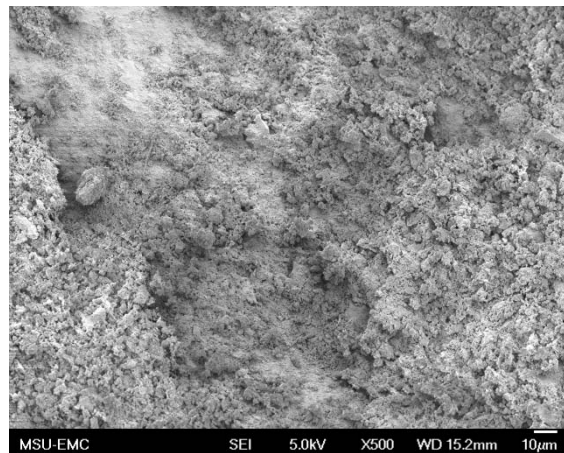
(d) Aggregate D

(e) Aggregate E

Figure B.48. SEM Images of Sample 15, 4.75 mm Sieve, 500x
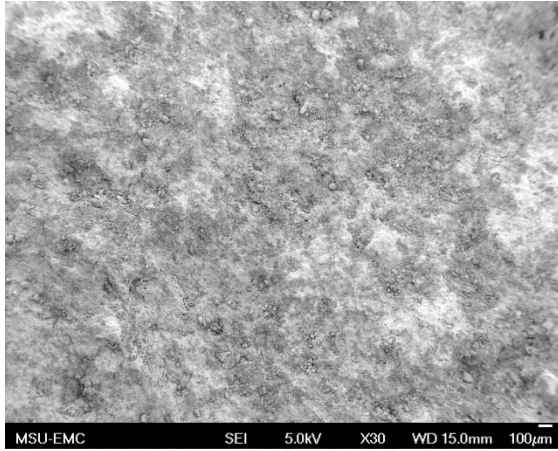
(a) Aggregate A
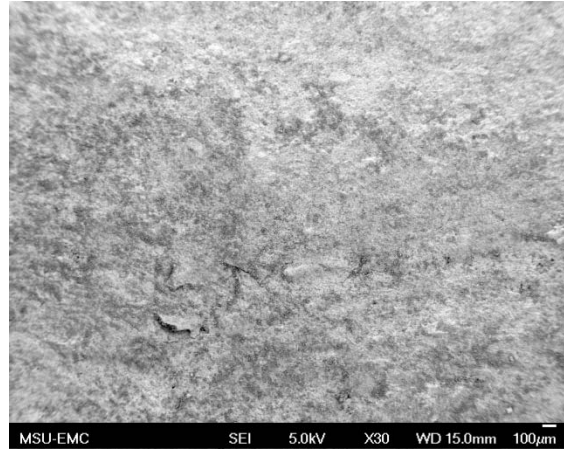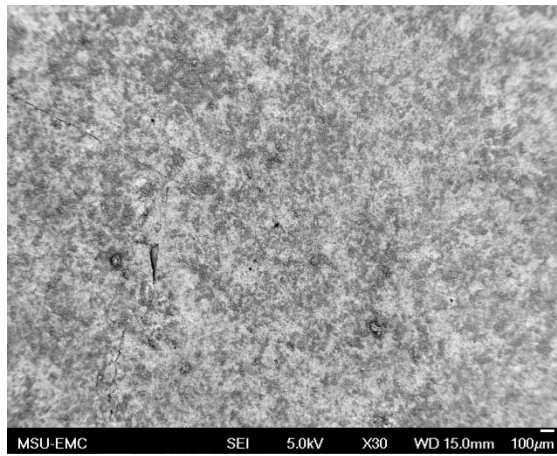
*(b) Aggregate B*
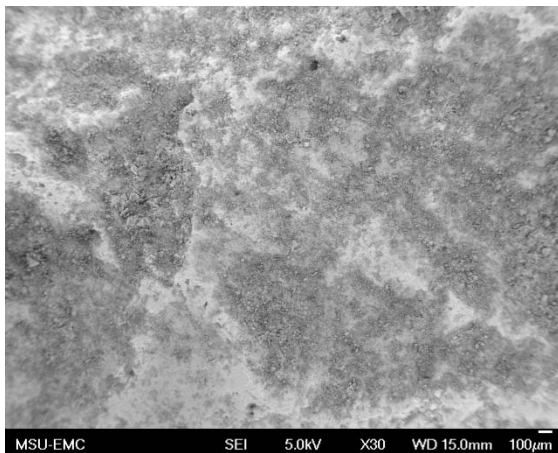
(c) Aggregate C
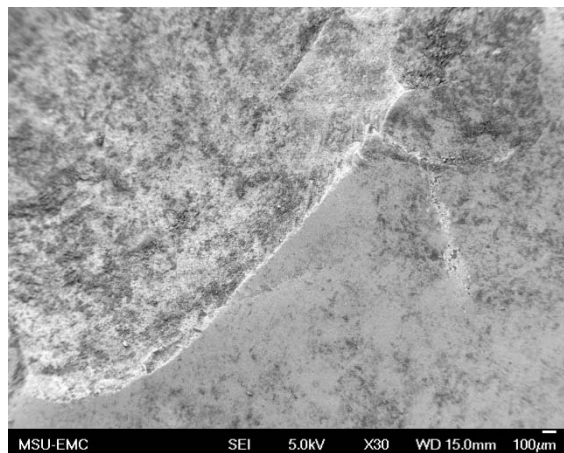
(d) Aggregate D

(e) Aggregate E

Figure B.49. SEM Images of Sample 16, 4.75 mm Sieve, 30x
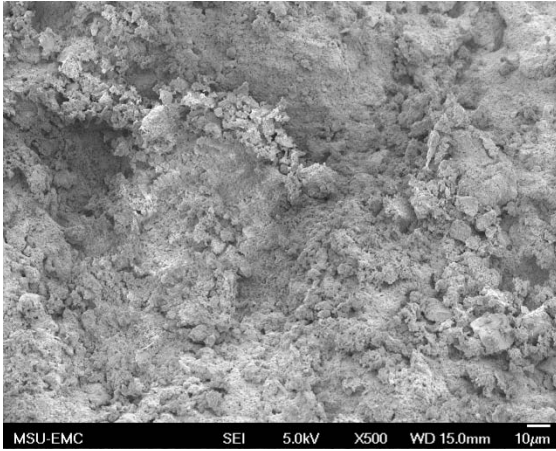
(a) Aggregate A
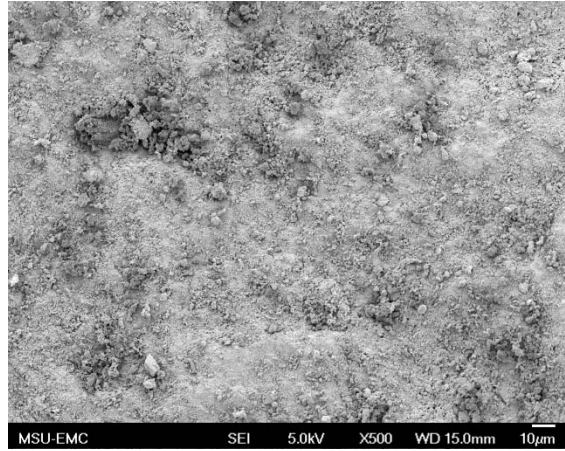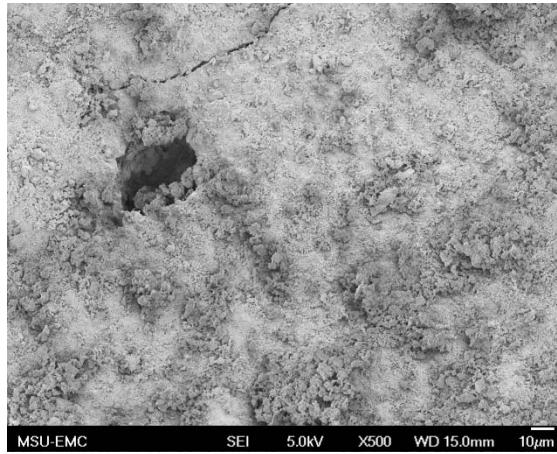
(b) Aggregate B
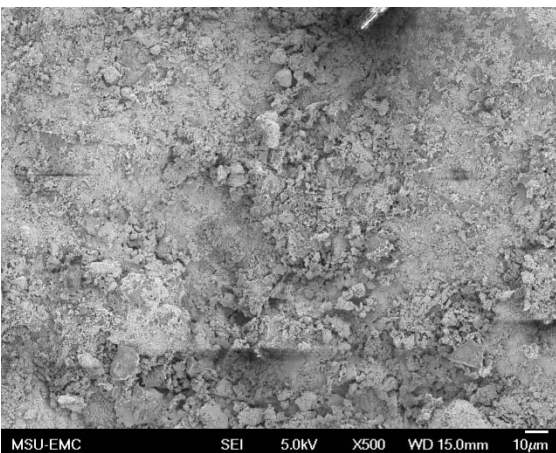
(c) Aggregate C
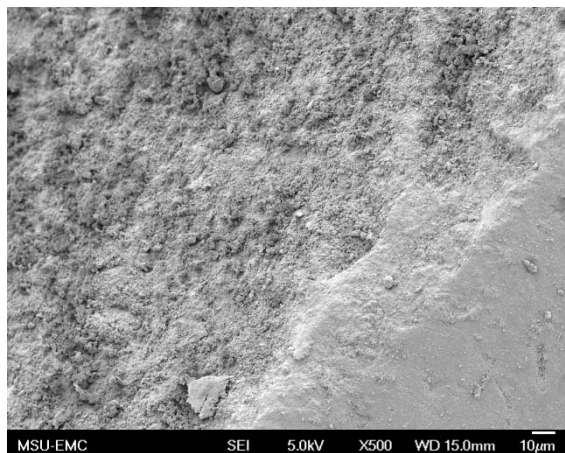
(d) Aggregate D

(e) Aggregate E

Figure B.50. SEM Images of Sample 16, 4.75 mm Sieve, 500x
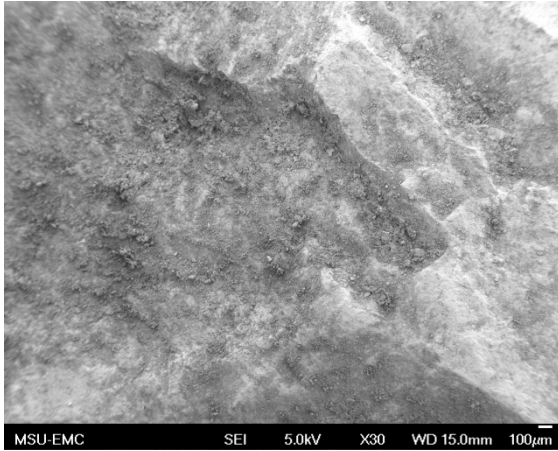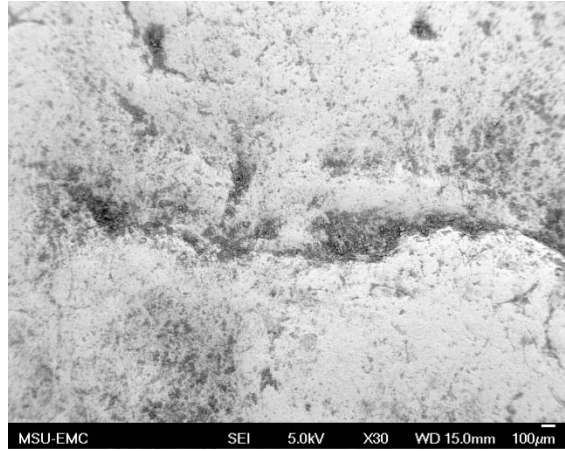
(a) Aggregate A
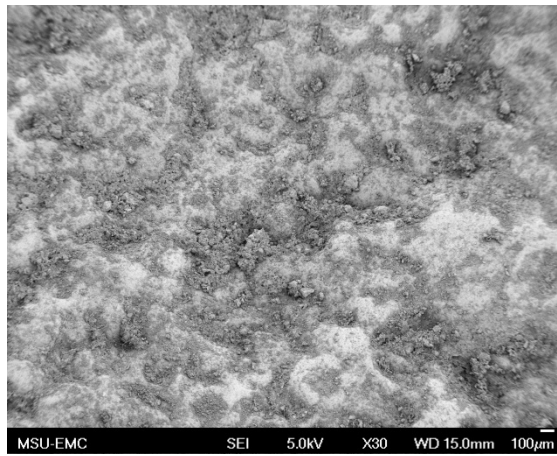
(b) Aggregate B
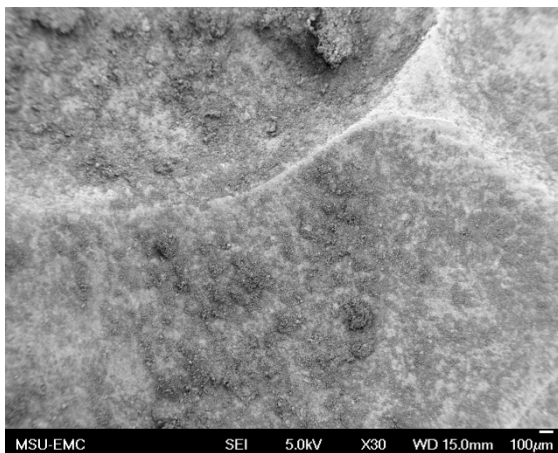
(c) Aggregate C
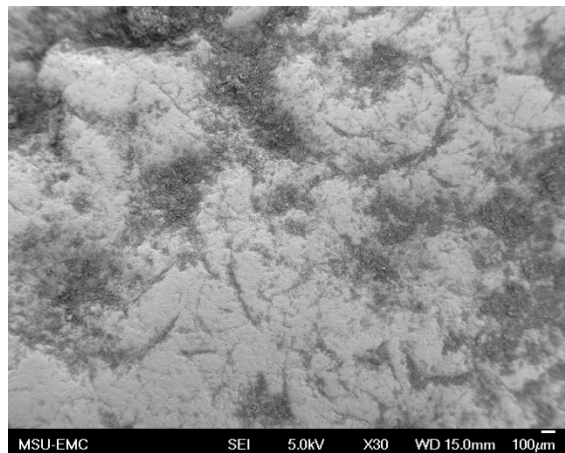
(d) Aggregate D

(e) Aggregate E

Figure B.51. SEM Images of Sample 17, 4.75 mm Sieve, 30x
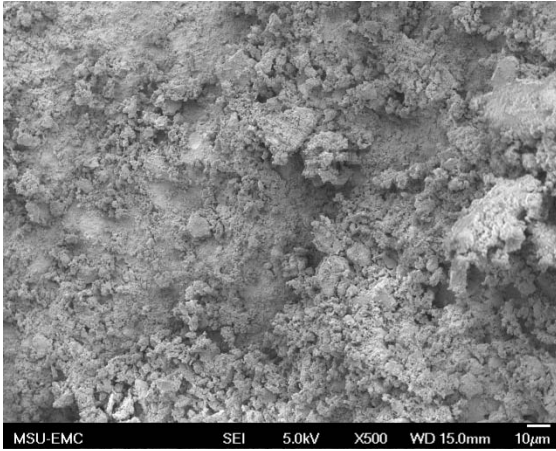
(a) Aggregate A
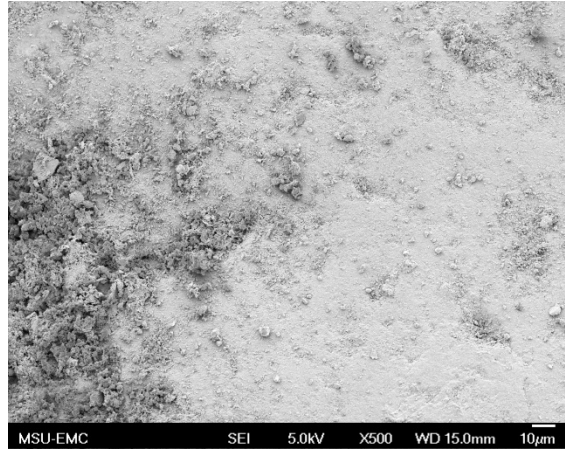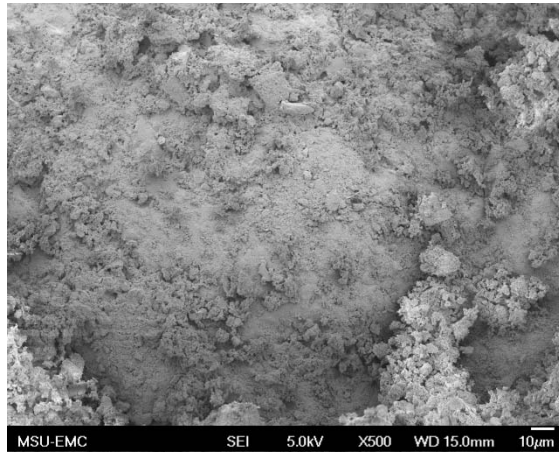
(b) Aggregate B
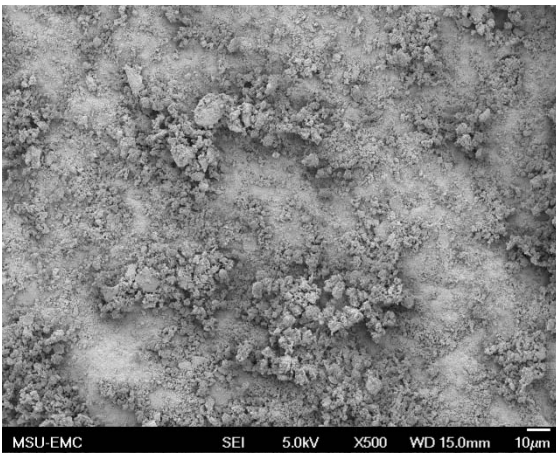
*(c) Aggregate C*
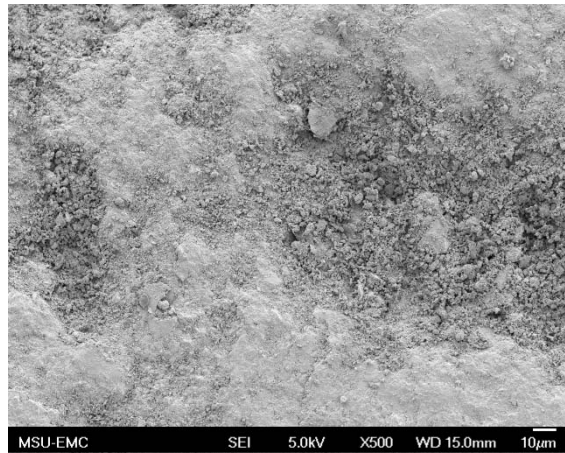
*(d) Aggregate D*

(e) Aggregate E

Figure B.52. SEM Images of Sample 17, 4.75 mm Sieve, 500x